

---

**The Adenoma-Carcinoma Sequence in Colorectal  
Cancer: scratching the surface**

**Paola Alberici**



---

# **The Adenoma-Carcinoma Sequence in Colorectal Cancer: scratching the surface**

**De adenoom-carcinoom sequentie in dikke darmkanker:  
"scratching the surface"**

## **Proefschrift**

ter verkrijging van de graad van doctor aan de  
Erasmus Universiteit Rotterdam  
op gezag van de rector magnificus

Prof.dr. S.W.J. Lamberts

en volgens besluit van het College voor Promoties

De openbare verdediging zal plaatsvinden op  
vrijdag 20 april 2007 om 13.30 uur

door

**Paola Alberici**

geboren te Milaan, Italië

**Promotiecommissie:**

**Promotor:** Prof. dr. R.Fodde

**Overige leden:** Prof. dr. L.H.J. Looijenga  
Prof. dr. C.P.Verrijzer  
Dr. H.R. Delwel

Cover: Photograph from the series "Cancer in our life" by Tee A. Corinne (1943-2006). Reprint with permission from the Library of the University of Oregon.

Printed by: PrintPartners Ipskamp, Enschede, The Netherlands

The studies described in this thesis were performed at the Department of Human and Clinical Genetics, Leiden University Medical Center, Leiden and at the Department of Pathology-Josephine Nefkens Institute, Erasmus University Medical Center, Rotterdam, The Netherlands.

Financial support for the printing cost of this thesis was kindly provided by Erasmus University, Department of Pathology-Josephine Nefkens Institute and Maag Lever Darm Stichting.



## Table of contents

<b>Aims and Outline of this thesis</b>	8
<b>Chapter 1. Introduction</b>	11
1.1. Introduction to cancer	13
1.2 Histopathology of colorectal cancer development	13
1.3 Genetic events along the adenoma–carcinoma sequence	16
1.4 The Role of APC Tumor Suppressor in Chromosomal Instability. <i>Genome and Disease, Genome Dynamics. 2006; 1:149-170</i>	21
<b>Chapter 2.</b> <i>APC</i> and oncogenic <i>KRAS</i> are synergistic in enhancing Wnt signaling in intestinal tumor formation and progression. <i>Gastroenterology. 2006;131:1096-109.</i>	45
<b>Chapter 3.</b> Aneuploidy arises at early stages of <i>Apc</i> -driven intestinal tumorigenesis and pinpoints conserved chromosomal loci of allelic imbalance between mouse and human. <i>Am J Pathol. 2007;170:377-87.</i>	61
<b>Chapter 4.</b> <i>Smad4</i> haploinsufficiency in mouse models for intestinal cancer. <i>Oncogene. 2006;25:1841-51.</i>	75
<b>Chapter 5.</b> <i>Smad4</i> haploinsufficiency results in partial inhibition of TGF- $\beta$ /BMP signal transduction and in differential regulation of a subset of dosage-dependent downstream targets <i>Submitted</i>	89
<b>Chapter 6. Discussion</b>	115
6.1. CIN in the adenoma-carcinoma sequence	117
6.2. Accommodating haploinsufficiency of tumor suppressor genes in the adenoma-carcinoma sequence	120

6.3. Signal transductions cross talk	125
<b>References</b>	137
<b>Summary</b>	145
<b>Samenvatting</b>	149
<b>Curriculum vitae</b>	153
<b>List of publications</b>	155
<b>Aknowledgments</b>	157
<b>Appendix and Colour Figures</b>	159
I Wnt/Beta catenin signaling	161
II TGF- $\beta$ superfamily of signalings	162
III RAS/ RTK pathways	163

## **Aims and Outline of the Thesis**

Colorectal cancer is the second leading cause of cancer-related death in the Western industrialized world. Already more than 15 years ago, Fearon and Vogelstein formulated a genetic model for colorectal tumorigenesis, the so-called adenoma-carcinoma sequence, that nowadays still represents the paradigm and the basis of our understanding of the molecular and genetic basis of this disease. By exploiting the possibility to recognize different histological stages of tumor development in the colon, each progression step has been related to specific genetic “hits” in defined oncogenes and tumor suppressor genes. The genetic mutations accumulated during tumor development are responsible for the deregulation of key signal transduction pathways like Wnt, TGF- $\beta$  and receptor tyrosine kinase (RTK) pathways responsible for uncontrolled cell growth, inhibition of apoptosis, and immortalisation. Still, little is known about the multiple interactions and mutual influences of these defective pathways and on the mechanisms responsible for the ‘just-right’ level of genetic instability that contributes to the establishment of the multiple genetic defects necessary to promote tumor progression and malignancy. In this thesis, I have made an attempt to the molecular and cellular analysis of the major genes mutated along the adenoma-carcinoma sequence (*APC*, *KRAS*, and *SMAD4*) and the cross-talk of the signalling pathways they regulate (Wnt, RTK, and TGF- $\beta$ ) in particular with regard to their role in the onset and malignant behaviour of the intestinal tumor cell. The first part of the introduction encompassed in **Chapter 1** describes in details the adenoma-carcinoma sequence as the experimental model of choice for the studies enclosed in my thesis, followed by an overview of the different genetic defects underlying tumor initiation and progression. The second part of the introduction is a review on the mechanism of chromosomal instability in CRC and the involvement of the *APC* tumor suppressor gene in this form of genetic instability in intestinal tumor initiation and progression.

Forty to fifty percent of colorectal carcinomas carry activating mutations in the *KRAS* proto-oncogene, usually in association with poor prognosis. The generation

and molecular analysis of the  $Apc^{+/1638N}/pVillin-KRAS^{V12G}$  compound mutant mouse model and the corresponding *in vitro* model systems as described in **Chapter 2**, enabled us to address whether the concomitant activation of the *KRAS* and Wnt pathways in colorectal tumors results in enhanced tumor onset and accelerated adenoma-carcinoma progression through a cumulative or synergistic interaction between the two signalling cascades.

In the study included in **Chapter 3**, we assessed the contribution of genes frequently mutated during the adenoma-carcinoma progression, namely *APC*, *KRAS* and *p53*, to chromosomal instability, measured as tumor-specific aneuploid changes by BAC arrayCGH. The identification of chromosomal aberrations in early intestinal lesions from  $Apc^{+/1638N}$  mice supports a model where loss of APC function causes mitotic spindle defects and thus abnormal chromosomal segregation. As discussed, the integration of genomic and expression profiling data from mouse and human intestinal tumors represents a powerful tool for the mapping and identification of conserved chromosomal loci and candidate genes involved in malignant progression.

In **Chapter 4** the analysis of  $Smad4^{+/E6sad}$  mouse intestinal tumors revealed that the somatic loss of the wild type *Smad4*, a key element for the transduction of TGF- $\beta$  signals, occurs only at later stages of tumor development thus demonstrating that haploinsufficiency underlies *Smad4*-driven tumor initiation in the GI tract. Furthermore, the generation and detailed phenotypic and molecular analysis of two distinct *Apc/Smad4* compound heterozygous mouse models, either in the *cis* (CAS) or *trans* (TAS) allelic phases, enabled us to dissect the differential roles of TGF- $\beta$  signaling in distinct steps of tumor initiation and progression, and provided a unique *in vivo* model to study the concomitant effects of Wnt and TGF- $\beta$  signaling.

The further characterization of *Smad4* haploinsufficiency presented in **Chapter 5**, demonstrates that the ~50% reduction in protein expression observed in the heterozygous  $Smad4^{+/-}$  cells leads to a correspondent decrease in TGF- $\beta$  and BMP signal transduction pathways, as measured by specific reporter assays. Also, the expression profiling analysis of hetero- ( $Smad4^{+/-}$ ) and homozygous ( $Smad4^{-/-}$ ) ES cells led to the identification of a subset of dosage-dependent target genes

involved in different cellular pathways and functions. The validation by quantitative RT-PCR of these transcripts on intestinal tissues from *Smad4*<sup>+/*E6sad*</sup> animals confirms that *Smad4* haploinsufficiency results in a broad spectrum of downstream transcriptional defects that may promote the tumorigenesis process in intestinal cells.

---

## **Chapter 1.**

### **Introduction**



### **1.1. Introduction to cancer**

Cancer is, in essence, a genetic disease that originates through a multistep process. In this model, the first stage, the initiation, is caused by the acquisition in a cell of a mutation that can provide a growth advantage and/or irreversible alterations in cellular homeostasis and differentiation. The next step, the promotion, can be a potentially reversible or interruptible clonal expansion of the initiated cell by a combination of growth stimulation and inhibition of apoptosis. Further progression steps occur upon clonal expansion of the initial cells and accumulation of a sufficient number of mutations and epigenetic alterations to acquire growth stimulus-independency and resistance to growth inhibitors and apoptosis, ultimately leading to an unlimited replicative potential. The acquisition of the ability to invade the surrounding tissue defines the malignant character of cancer cells, while the process through which cells can migrate to distal organs and acquire the potential to form metastasis represents the achievement of a full malignant cancerous phenotype.

Colorectal cancer represents an ideal model to investigate and elucidate the genetic alterations involved in tumor onset and progression, mainly because it arises and progresses through a series of well-defined histopathological changes, the so-called adenoma-carcinoma sequence.

### **1.2 Histopathology of colorectal cancer development**

The digestive surface of the human large intestine is characterized by a monolayer of specialized epithelial cells that forms invaginations called crypts. At the base of each crypt 4-6 intestinal stem cells are located from which the four cellular types that constitute the intestinal layer originate: columnar absorptive cells, the mucus-secreting goblet cells, the neuroepithelial cells and the Paneth cells. By asymmetrical division, these stem cells are able to renew the complete layer in 3-8 days.

The first recognisable manifestation of epithelial alteration during colorectal tumor development are the Aberrant Crypt Foci (ACF), small hyper- or dysplastic lesions characterized by: (1) bigger size than the normal crypts; (2) increased pericryptal

space that separates them from the normal crypts; (3) a thicker layer of epithelial cells that often stains darker compared with normal crypts; (4) generally oval rather than circular openings. The ACF can be observed as single altered crypts or as a group of altered crypts that appears to form a single unit or focus. They frequently are microscopically elevated above the mucosa but also may be depressed, i.e., they usually are not in the same focal plane as the surrounding normal crypts. (McLellan & Bird, 1988).

From a practical perspective, although only a small number of ACF will ultimately progress to CRC, larger ACF with altered morphology, dysplastic histology and associated gene mutations remain high-risk candidates for adenoma and CRC formation (Hurlstone & Cross, 2005).

Upon increase of birth/loss ratio among epithelial cell, their progressive accumulation results in a benign tumor mass or polyp (i.e. any abnormal accumulation of cells). In the intestine, a tumor is clinically recognized as a protrusion into the lumen from the wall. From an histological perspective, there are at least two major types of polyps: the hyperplastic or non-neoplastic polyp and the dysplastic or adenomatous polyp. Whether the first kind of lesion consists of large number of cells with a normal morphology that line up in a single row, the adenomatous polyp is represented by abnormal cells which show intracellular and intercellular irregularities, with disruption of normal tissue architecture. The nuclei of these cells are often hyperchromatic and larger in size than in normal intestinal cells, with irregular positioning along the crypt-villus axis due to loss of cell polarity and nuclear stratification. Several layers of these abnormal cells form on the lamina propria, occasionally giving rise to branching glands. According to their architecture, adenomas may be divided in tubular, when coarsely lobulated and pedunculated, or villous, when sessile, covering a broad area directly onto the *muscularis mucosae* (the muscle layer underlying the epithelial lining) and submucosa (the underlying stromal layer). Villous adenomas are thought to have higher risk of malignant progression (Takata et al., 2003).

When an adenoma progresses, more undifferentiated cells appear, with a marked pleomorphism (variation in size and shape) and a nuclear:cytoplasm ratio close to

1. Moreover, tumor cells show aberrant orientations and grow in disorganized fashion. These lesions are can also be referred to as carcinoma *in situ*, i.e. advanced high dysplastic lesions still confined within the epithelial layer. Finally, malignant adeno-carcinomas are characterized by the ability to invade the surrounding tissues through the muscularis mucosae and into the stromal compartment, and migrate to distal organs (e.g. the liver) where they can form metastasis (Vinay Kumar, 2004) .

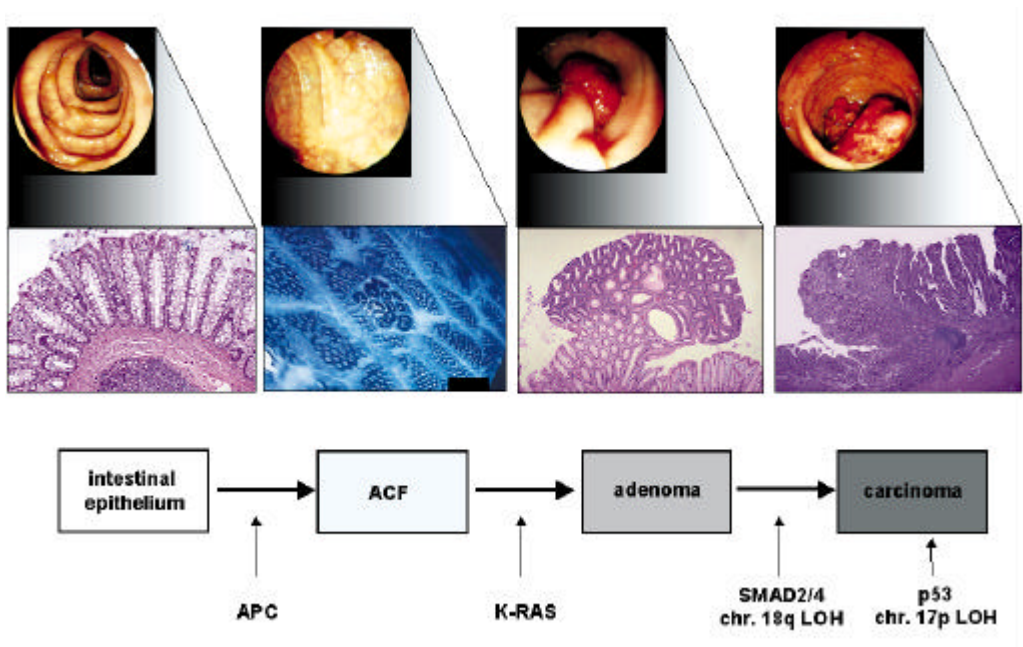


**Figure 1.** The adenoma-carcinoma sequence: a stepwise progression from normal epithelium to carcinoma due to a series of genetic changes. Macro- and microscopical representations of the progression changes are depicted. See text for details.

The development of carcinoma from adenomatous lesions is substantiated by a number of observations: first, the peak of incidence of adenomatous polyps precedes by some years that of colorectal cancer; secondly, small carcinomatous foci are found within advanced adenomatous polyps. Also, cancer risk is directly

related to the number of adenomas, as shown by the very high incidence of carcinoma in patients with >100 polyps such familial adenomatous polyposis (FAP) (Vinay Kumar, 2004).

### **1.3 Genetic events along the adenoma–carcinoma sequence**

The stepwise progression from normal to dysplastic epithelium and to carcinoma is earmarked by specific genetic alterations at known oncogenes and tumor suppressor genes. This molecular pathway to colorectal cancer is triggered within a single cell that acquires a genetic alteration that provides it with a specific type of growth survival advantage. Loss of function mutations at the *APC* tumor suppressor gene on chromosome 5q21 occur in over 80% of colon adenocarcinoma (Smith et al., 1993; Kinzler & Vogelstein, 1996), thus representing the earliest and rate-limiting genetic event in colorectal tumor initiation (Powell et al., 1992). Indeed, *APC* mutations are present already at the ACF stage and they are related with the degree of dysplasia of these early lesions (Jen et al., 1994b; Smith et al., 1994). The *APC* protein has multiple functions as discussed in paragraph 1.4 of this introduction. It has been shown that *APC*'s main tumor suppressor activity resides in its capacity to regulate intracellular levels of  $\beta$ -catenin (Korinek et al., 1997; Morin et al., 1997; Smits et al., 1999), a key member of the Wnt signal transduction pathway. In fact, mutations of members of the Wnt pathways, including  $\beta$ -catenin, Axin-1 and Conductin (Axin-2) have also found in colorectal cancer (Sparks et al., 1998; Satoh et al., 2000; Clevers, 2000). The inactivation of both alleles of the *APC* gene can be detected in most of the intestinal tumors at early stages of development (Powell et al., 1992; Miyoshi et al., 1992), in agreement with Knudson's two hit hypothesis. However, *APC* second mutational hits are not randomly selected, but distributed according to the resulting levels of residual  $\beta$ -catenin down-regulating activity (Lamlum et al., 1999; Albuquerque et al., 2002). In the situation in which a germline mutation is inherited or spontaneously occurred as in the FAP syndrome, the rate of initiation of colonic polyps is dramatically increased with the development of thousands of colorectal

adenomas and the inevitable progression of some of these into carcinoma, unless the intestine is not surgically resected (Kinzler & Vogelstein, 1996).

Activation of the *KRAS* oncogene represents the second step in the evolution towards intestinal cancer. The proto-oncogene *KRAS* encodes a 21 kD protein that binds guanine nucleotides and is localized on the inner cell membrane. The identification of *KRAS* mutations has been the first major breakthrough in the molecular genetic analysis of colorectal cancer (Forrester et al., 1987). *KRAS* mutations are found in at least 50% of colorectal adenomas larger than 1 cm and in carcinomas but are infrequent in adenomas smaller than 1 cm in size (Vogelstein et al., 1988), indicating a role in adenoma progression rather than initiation. Alternatively, mutations in other oncogenes like *BRAF* encoding for members of the same RAS pathway, are often found among adenomas (Beach et al., 2005). *KRAS* mutations affect only specific codons (12-13,59-61) relevant for the endogenous guanine triphosphatase activity, leading to the constitutive activation of the Ras/Raf/MEK/ERK signal transduction pathway. Activation of this signaling pathway results in the transduction from the surface receptors to the nucleus of signals for the transcriptional activation of target genes involved in cell proliferation and apoptosis inhibition like Cyclin-dependent kinases, Cyclins and Bcl-2 (Kim & Lance, 1997) and thus malignant transformation.

Further malignant progression towards the carcinoma stage is accompanied by loss of all or part of the long arm of chromosome 18 (18q). At least 50% of large adenomas and 75% of carcinomas show LOH at chr. 18q (Vogelstein et al., 1988; Vogelstein et al., 1989; Jen et al., 1994a). The first candidate tumor suppressor gene in this chromosomal interval, the "deleted in colorectal cancer" gene (*DCC*), has now been identified as a component of a receptor complex that mediates axon guidance in neurons (Keino-Masu et al., 1996). However *DCC* mutations are rarely found in colorectal cancers (Cho et al., 1994). Other tumor suppressor genes have been subsequently identified in this region and, among others, two intracellular mediators of the TGF- $\beta$  signal transduction pathway *SMAD2* and *SMAD4*.

Binding of TGF- $\beta$  to the TGFBR2 receptor promotes the formation of heterodimer with the TGFBR1 receptor and phosphorylation of members of the SMAD family of

intracellular mediators like SMAD2. Activated SMAD2 binds SMAD4 with its consequent nuclear translocation where the complex activates the transcription of genes responsible for a broad spectrum of cellular functions such as cellular growth inhibition, apoptosis, differentiation, and matrix production (Heldin et al., 1997; Duff & Clarke, 1998). Thus, when *SMAD2* or *SMAD4* are mutated, TGF- $\beta$  signal is not transduced into the nucleus of the cell. *TGFBR2* mutations are also frequently found to affect TGF- $\beta$  signaling in CRC, mainly among microsatellite instable (MSI) tumors but also in approximately 55% of microsatellite stable (MMS) tumors (Grady et al., 1999) (For more details on the types of genetic instabilities in colorectal cancer see Chapter 1.4, page 25). Overall, there is convincing mutational evidence for the major role of TGF- $\beta$  pathway inactivation in the adenoma-carcinoma transition and, more in general, as primary tumor suppressor in human colorectal carcinogenesis.

Most malignant colorectal tumors are also characterized by loss of the short arm of chromosome 17 (17p). LOH or cytogenetic alterations at this locus correlate with the transition from benign adenoma to invasive cancer (Vogelstein et al., 1988; Baker et al., 1989; Baker et al., 1990). The *TP53* gene, encoding for p53, maps to this chromosomal interval. p53 is a multifunctional protein essential to cell growth control (Lane, 1992) often regarded to as the "guardian of the genome" due to his ability to block cell proliferation via transcriptional activation of cyclin inhibitors, like p21, in the presence of DNA damage (Waldman et al., 1995). p53 also promotes apoptosis via transcriptional activation of genes such *BAX* in situations where the DNA repair machinery cannot cope with the DNA damage load (Burns & El-Deiry, 1999). P53 alterations, often measured as aberrant overexpression in immunohistochemical assays, by direct DNA sequencing or by 17p allelic loss, have been reported in 4-26% of adenomas, approx. 50% of in situ carcinomas, and in 50-75% of adenocarcinoma (Ohue et al., 1994; Yamaguchi et al., 1994; Kaklamanis et al., 1993; Kaserer et al., 2000; Boland et al., 1995). The latter is indicative of the central role of loss of p53 function in the adenoma to carcinoma transition.

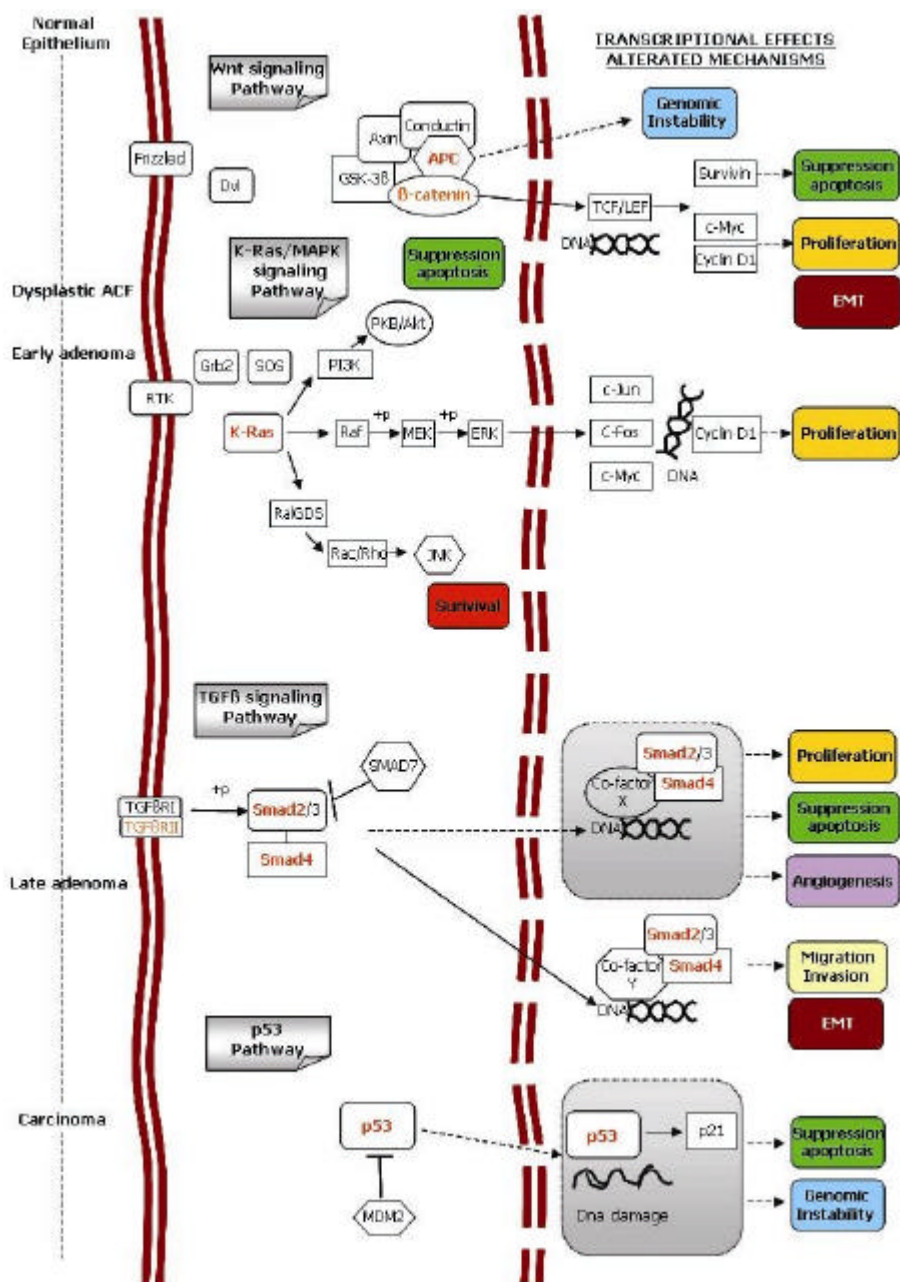


**Figure 2.** Schematic representation of the accumulation of alterations in different pathways along the adenoma-carcinoma sequence. In red are shown the genes frequently mutated in CRC. The different cellular alterations resulting from the accumulations of these signaling defects are listed in the right column.

In conclusion, the identification of stepwise acquisition of specific mutations in colorectal adenoma-carcinoma sequence has provided important clues relative to the cellular processes underlying tumorigenesis in the gastro-intestinal tract and has opened new avenues for tailor-made therapeutic approaches.

---

## **Chapter 1. 4**

**The Role of APC Tumor Suppressor in Chromosomal Instability.**

***Genome and Disease, Genome Dynamics. 2006; 1:149-170***



.....

# The Role of the APC Tumor Suppressor in Chromosomal Instability

*P. Alberici, R. Fodde*

Department of Pathology, Josephine Nefkens Institute, ErasmusMC,  
Rotterdam, The Netherlands

© Free Author  
Copy - for per-  
sonal use only

PLEASE NOTE THAT ANY  
DISTRIBUTION OF THIS AR-  
TICLE WITHOUT WRITTEN  
CONSENT FROM S. KARGER  
AG, BASEL IS A VIOLATION  
OF THE COPYRIGHT.

Upon request a written per-  
mission to distribute the PDF  
file will be granted against  
payment of a permission fee  
depending on the number of  
accesses required. Please  
contact Karger Publishers,  
Basel, Switzerland at  
permission@karger.ch

---

## Abstract

Colorectal cancer (CRC) still represents the model of choice to study the mechanisms underlying tumor initiation and progression. Accordingly, CRC has been central in the analysis of the role played by chromosomal instability (CIN) in tumor initiation and progression. Although loss of APC tumor suppressor function initiates the adenoma-carcinoma sequence in the vast majority of CRCs through constitutive activation of Wnt/ $\beta$ -catenin signaling, the *APC* gene also represents a candidate CIN gene in CRC. Accordingly, two studies published in 2001 showed that truncating *Apc* mutations can lead to both quantitative and qualitative ploidy changes in primary mouse cell lines, mainly due to kinetochore and centrosome abnormalities. Here, we review and discuss the more recent literature on APC's functional activities possibly related to its role in eliciting CIN in tumor initiation and progression. We propose a model where loss and/or truncation of APC cause mitotic spindle defects that, upon somatic inactivation of other putative CIN genes (e.g. spindle and cell cycle checkpoint genes, DNA repair, telomere maintenance, etc.) underlie aneuploidy as observed in the majority of CRCs.

---

Copyright © 2006 S. Karger AG, Basel

## Chromosomal Instability in Tumorigenesis

Genetic instability has long been postulated as an essential condition for tumors to develop and progress towards more malignant stages. Chromosome number variations and loss of genome integrity in cancer have been observed since the very first cytological and molecular analyses, thus implying that cancer cells contain multiple gene mutations [1, 2]. Nevertheless, the majority of chromosomal abnormalities are not tumor-specific, which may indicate that genetic instability is an intrinsic feature of cancer cells [3]. The concept according to

which tumors develop through the accumulation of genetic alterations in oncogenes and tumor suppressor genes is widely accepted [4]. However, normal mutation rates are likely to be too low to allow the multiplicity of mutations observed in cancer cells. Hence, defects that increase mutation rates are essential to account for the large numbers of abnormalities observed in human tumors [3, 5, 6]. From this perspective, genetic instability, here referred to as an increased dynamic rate of changes, is likely to represent an essential prerequisite to accumulate the large number of alterations that occur during the tumorigenic process. The latter is supported by different mathematical models [7, 8]. However, alternative models indicate that the clonal evolution model is still in agreement with the concept of selection being the main driving force behind tumor initiation and progression [9, 10]. Colorectal cancer (CRC) has been instrumental in this debate as its different histological stages allow the dissection of the genetic events underlying tumor initiation and progression [11].

### **Chromosomal Instability in Colorectal Cancer**

Colorectal tumor initiation and progression towards malignancy occur through well-defined histopathological and molecular steps, the so-called adenoma-carcinoma sequence [12]. Two main types of genetic instability have been recognized in human CRC, microsatellite instability (MSI or MIN) and chromosomal instability (CIN) [3]. MSI results from loss of mismatch repair (MMR) function and is earmarked by tumor-specific frame-shift mutations in stretches of short repetitive DNA sequences (microsatellite repeats) distributed throughout the genome [13, 14]. Notably, MIN tumors have increased nucleotide mutation rates when compared with normal cells but share near-diploid chromosomal contents [15–17]. Germline defects in MMR genes account for the hereditary non-polyposis colorectal cancer syndrome (HNPCC), an autosomal dominant predisposition to colorectal, uro-genital and skin cancers [18]. MSI and/or somatic defects in the same MMR genes are found in approximately 15% of sporadic colon cancers.

The first indication of the presence of specific genetic alterations underlying changes in tumor histology came from cytogenetics. Karyotype analyses of colorectal cancers have revealed characteristic patterns of chromosomal abnormalities [19–21]. In fact, the vast majority of CRCs are characterized by abnormal chromosomal contents with a heterogeneous and broad spectrum of both numerical and structural changes such as inversions, deletions, duplications and translocations [22]. These abnormalities define aneuploidy. Experimental evidence indicates that aneuploidy arises in these cancers as a result of CIN, here defined as the accelerated rate of gains or losses of entire chromosomes or

part of them [22, 23]. Clones from various colorectal cancer cell lines, expanded through a given number of passages and then analyzed by fluorescent in situ hybridization (FISH) with centromeric DNA probes of each individual chromosome, indicated that, whereas MSI cell lines are mostly near-diploid, microsatellite stable (MSS) colorectal cancer cells showed an increased frequency of chromosomal gains and losses at each cell division. CIN may provide additional growth advantage to the cancer cell by accelerating the rate of loss of heterozygosity at tumor suppressor loci and/or by amplifying chromosomal regions encompassing oncogenes. CIN may also represent a mechanism by which the cancer cell can fine-tune its growth characteristics to meet changes in the environment, thus possibly underlying therapeutic failures.

Over 90% of all CRCs show chromosomal aberrations, some of which are recurrent and represent key chromosomal changes underlying colorectal cancer initiation and progression, e.g. loss of chromosome 18, gain of chromosome 7, and other structural rearrangements, e.g. at chromosomes 1 p and 17 p. However, conventional cytogenetic analysis is limited by its low-resolution. In more recent years, the introduction of techniques like comparative genomic hybridization (CGH) and FISH, has allowed the high-resolution detection of chromosomal aberrations throughout the progression from low-grade adenoma to carcinoma [24]. By means of array CGH, Hermsen and colleagues showed evidence for the presence of specific subsets of chromosomal gains and losses strongly associated with adenoma-carcinoma progression [25].

To assess more functional aspects of genomic instability, colorectal cancer is often the experimental tumor of choice as it offers a well-defined model of step-wise progression, tissue samples from different stages are available from gastroenterology and surgical units for molecular analysis, and because a large number of well-characterized cell lines have been established from several CIN and MIN tumors. Analysis of CRC-derived cell lines that do not harbor MMR defects showed high rates of chromosome gain and loss, with acquisition of chromosomal changes at rates 10–100 times faster than in MMR-deficient cells [22]. These experiments also indicated that MSI and CIN may be mutually exclusive pathways of genetic instability in colorectal cancer [3]. However, the existence of a subgroup of colorectal cancers with apparently stable, near-diploid chromosomes and stable microsatellites (MACS) was more recently reported [26].

To date, many potential mechanisms have been shown to play a role in CIN by contributing to aneuploidy: mitotic and cell cycle checkpoints, telomere shortening and telomerase expression, centrosome number regulation, double-strand break repair, kinetochore function, and chromatid segregation [3, 27] (table 1). In particular, mutations at the mitotic checkpoint genes *BUB1* and *BUBR1* [28, 29], the cyclin E regulator *CDC4* [30], and the *TP53* tumor suppressor [31] have been implicated as rate-limiting events in eliciting CIN in CRC. However,

**Table 1.** Possible mechanisms of chromosomal instability in tumors and a selection of genes involved

Cell structural defect	Mechanisms leading to CIN	Genes implicated	References
Centrosome	Segregation defect	p53 pathway, <i>ATR</i> , <i>BRCA1</i> , <i>BRCA2</i> , <i>XRCC2/3</i> , <i>RAD6</i> , Aurora-A, Survivin	31; 125–133
Mitosis check point	Chromosome missegregation	<i>BUB1/BUBR1</i> , <i>MAD2</i>	28; 29; 134; 135
DNA damage check point	Enhanced/aberrant mitotic recombination	<i>ATM</i> , <i>ATR</i> , <i>BML</i> , <i>BRCA2</i> , <i>FANCA-L</i> , <i>NBS1</i>	136–142
Microtubules and spindle dynamics	Spindle defects	<i>APC</i> , <i>GSK3-β</i>	35; 36; 69; 97; 98; 143; 144
Kinetochores assembly	Premature anaphase	<i>HEC1</i>	145
Chromatin cohesion and chromosome condensation	Disjunction failure	Securin/ <i>PTTG</i>	146; 147
Cell cycle control	Cell cycle disturbance	<i>TP53</i> , <i>CDC4</i> , <i>CCNE1</i>	30; 148–150
Telomeres	Chromosome fusion	<i>PINX1</i> , <i>TERC</i> , <i>TERF1/PIN2</i>	151
Cytokinesis	Multinucleate cells	<i>BRCA2</i>	123

mutations in these alleged CIN genes are relatively rare [28, 29], and occur at late stages of the adenoma-carcinoma sequence [4], whereas aneuploid changes have been observed already at early adenoma stages [32–34]. More recently, we and others have found that mutations in *APC* give rise to polyploid and aneuploid chromosomal changes in mouse primary cell lines and may therefore trigger CIN at the very start of the adenoma-carcinoma sequence [35, 36]. Here, we will review the functional aspects of the APC tumor suppressor protein with respect to chromosomal stability at mitosis and its role in CIN in CRC.

### **Functional Aspects of the APC Tumor Suppressor Protein**

Inactivation of the adenomatous polyposis coli (*APC*) tumor suppressor gene represents the very first and rate-limiting step of the adenoma-carcinoma sequence in CRC. Notwithstanding its well-known multi-functionality [37], APC's main tumor suppressing function resides in its capacity to regulate Wnt signaling as elegantly shown by the identification of  $\beta$ -catenin (*CTNNB1*) gene mutations in sporadic colorectal cancers with an intact *APC* gene [38, 39].  $\beta$ -catenin is the main intracellular signaling protein of the canonical Wnt pathway and its cellular level is regulated by a 'destruction' complex composed by several proteins among which there is APC (see below). Loss of APC function or oncogenic  $\beta$ -catenin mutations that make it resistant to APC-driven proteolytic degradation, result in the constitutive activation of the Wnt signal transduction pathway that regulates epithelial homeostasis along the intestinal villus-crypt axis [11, 40]. Notwithstanding the latter, the *APC* gene encodes a 312 kDa protein encompassing multiple and diverse functional motifs that, upon APC truncation and/or complete loss of function, may play additional roles in tumor progression and malignant transformation [37] (fig. 1).

The N-terminus of APC contains several regions of heptad repeats responsible for the formation of coiled-coil domains and often involved in oligodimerization [41–43]. Whereas the N-terminal 55 amino acids of APC form a dimeric coiled-coil [41], residues 129–250 can result in an intramolecular coiled-coil [44]. The N-terminus of APC also encompasses two nuclear export sequences (NES), both required for shuttling APC between nucleus and cytoplasm [45, 46]. Seven armadillo (ARM) repeats, a motif first found in the fruit fly  $\beta$ -catenin homolog Armadillo, are also found in the N-terminal region of APC [47]. Additional binding motifs for the protein phosphatase PP2A, the guanine nucleotide exchange factor (GEF) Asef, and Kap3, a linker protein for kinesins [48–50], partially overlap with the ARM repeats. Although it is not clear how these complex interactions occur and are regulated at specific phases of the cell

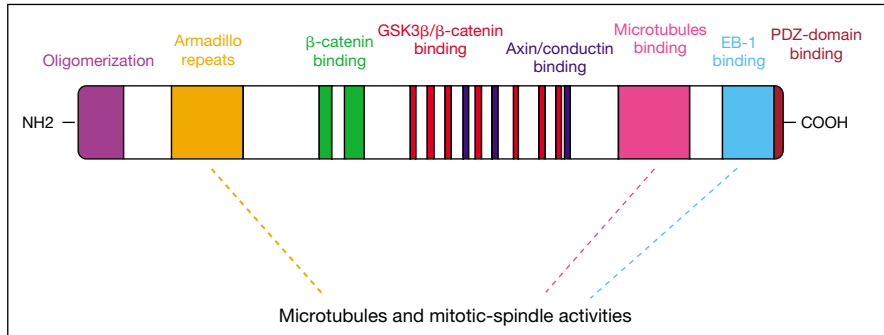


**Fig. 1.** Schematic representation of the APC protein with its functional motifs.

cycle and in specific cellular types, it is important to point out that truncated APC proteins encompassing the N-terminus positively affect GEF activity and cell motility by Asef when compared with full length APC [51]. The latter is consistent with the alleged dominant-negative effect exerted by truncating *APC* mutations on apoptosis, cell motility and cytoskeletal organization [52, 53]. The recent report of the putative interaction between the N-terminal third of APC and its C-terminal region may support this hypothesis [54].

The middle region of the APC protein encompasses the domains responsible for  $\beta$ -catenin regulation in Wnt signaling. Three 15 a.a. and seven 20 a.a. repeats mediate binding and downregulation of  $\beta$ -catenin, respectively. Three Ser-Ala-Met-Pro repeats (SAMP) are interspersed among the 20 amino acid repeats and allow interaction with the scaffold proteins axin/conductin [47].

APC regulates Wnt signaling by catalyzing the formation of a multi-protein complex, the so-called ‘destruction complex’, comprehensive of the scaffolding proteins axin and conductin, the glycogen synthase kinase 3 $\beta$  (GSK3 $\beta$ ) and casein kinase (CKI), and APC itself [55–58]. In the absence of the Wnt ligand, the destruction complex is formed which results in Ser/Thr-phosphorylation of  $\beta$ -catenin and its subsequent proteosomal degradation [59–61]. In the presence of the Wnt ligand, Dishevelled (Dsh) inactivates GSK3 $\beta$ , thus resulting in the intracellular stabilization of  $\beta$ -catenin and its nuclear translocation. Once in the nucleus,  $\beta$ -catenin binds to DNA-binding proteins of the T-cell factor (TCF) family, to serve as an essential co-activator of transcription [62, 63]. The activity of TCF is tightly controlled, as TCFs are complexed with potent co-repressors such as Groucho in the absence of Wnt signaling [64].

Finally, the C-terminal third of the APC protein, the least conserved throughout evolution, encompasses distinct domains that mediate interactions with several cytoskeletal proteins. A stretch of approximately 200 amino acids, enriched

in positive charges, is responsible for the interaction of APC with microtubules (MT) [65–67]. The C-terminal 170 amino acids of APC bind the end binding protein 1 (EB1), a small microtubule end-binding protein [68], whereas the very last 15 residues encompass the binding site for PDZ domains [69, 70].

Although previous reports indicated active nuclear-cytoplasmic shuttling of APC [71] and its putative role in transcriptional regulation via its ability to bind DNA [72], to date there is no evidence that APC directly acts as a transcriptional regulator. Moreover, a recent study questioned the specificity of many commonly used anti-APC antibodies and showed that both wild-type and truncated APC were primarily cytoplasmic in colon cancer cells, but increased in the nucleus after leptomycin B treatment, consistent with CRM1-dependent nuclear export [73]. The predominantly cytoplasmic subcellular localization of APC possibly reflects its physical interaction with the cytoskeleton. APC can bind both directly and indirectly to microtubules [66, 67], and clusters at the distal tips (the ‘plus ends’) of microtubules in cellular protrusion of migrating cells [74]. The association with the plasma membrane is highly dynamic and requires an intact actin cytoskeleton [75]. In highly polarized cells from the inner ear, APC localizes at the plus end of microtubules oriented towards the basal membrane [76]. The observation that truncated APC proteins lacking the MT binding site fail to interact with the microtubules though retaining KAP3 binding, suggests that the relation of APC with the cytoskeleton is due to a combination of direct and indirect interactions that possibly modulate its subcellular distribution [50]. APC has been shown to promote microtubule polymerization *in vitro* [66, 77]. Also, microtubules bound to APC are more stable under depolymerizing conditions both *in vivo* and *in vitro* [78]. Notably, Cdc42-dependent phosphorylation of GSK3 $\beta$  occurs specifically at the leading edge of migrating cells, and induces the interaction of APC with the plus ends of microtubules, essential to promote cell polarization and control the direction of cell protrusion [79]. The latter suggests that interaction of APC with the cytoskeleton, similar to its interaction with  $\beta$ -catenin, is regulated by binding to GSK3 $\beta$ . Accordingly, binding of APC to microtubules is modulated by phosphorylation [78], suggesting that APC is alternatively employed as scaffolding protein in the regulation of Wnt/ $\beta$ -catenin signaling and as microtubule-stabilizing protein in the regulation of cell polarity and migration.

Truncated APC proteins lacking the N-terminal ARM repeats or the C-terminal MT-binding site fail to form proper aggregates at the plus ends of the microtubules, thus affecting their subcellular distribution pattern [80].

An additional interaction between microtubules and APC occurs through EB1. EB1, initially isolated by a two-hybrid screen as a protein binding to the C-terminus of APC [81], is highly conserved throughout evolution, from yeast to mammals. EB1-like proteins have been shown to be involved in almost all the

microtubule-based processes including maintenance of cell polarity, anchorage to nucleation sites, and the regulation of spindle formation and chromosome segregation at mitosis [82, 83]. The C-terminal domain of the EB1 protein interacts with the C-terminus of APC [84–86], and this APC/EB1 complex has been described to stabilize microtubule ends in vivo [87]. However, in colon cancer cell lines carrying truncated APC not encompassing the EB1-binding site, endogenous EB1 localization is unchanged, suggesting that EB1 can bind to microtubule tips independently of APC [88, 89]. Also, CRC cell lines transfected with several different GFP-mutant APC show that the interaction with EB1 is responsible for directing APC to the tip of microtubules. In fact only the mutant APC that express the EB1 binding motif show localization at the plus ends of microtubules [68].

A more recent study [90] suggests that the major EB1 interaction site in APC involves the dipeptide segment 2805–2806 and that the same interaction is negatively regulated by cyclin-dependent mitotic kinase Cdc2 phosphorylation of the Ser2789 residue of APC. Thus, C-terminal phosphorylation of APC appears to play a key role in the regulation of its interaction with EB1 throughout the cell cycle and in particular during mitosis [68].

Although the majority of *APC* mutations in human tumors encode truncated proteins lacking the EB1 binding domain [91, 92], no cancer-associated mutations in the *EB1* gene have been found to date [93]. Moreover, mice carrying targeted *Apc* truncations that remove the EB1-binding motif without affecting its capacity to regulate Wnt/ $\beta$ -catenin signaling, do not develop tumors [94]. However, the possibility remains that loss of EB1-APC binding plays a role in tumor progression by affecting cell migration, polarity and/or chromosomal segregation (see below).

### **A Role for APC in Chromosomal Instability**

During mitosis, APC clusters at the plus-ends of the spindle microtubules and co-localizes with the kinetochore, the attachment site of the mitotic spindle to the newly duplicated chromosomes [35, 36] (fig. 2). These observations strongly suggest a role for APC in mitotic spindle formation and chromosome segregation. Multicolor FISH analysis of mouse embryonic stem (ES) cell lines homozygous for the *Min* allele, lacking the C-terminal third of the protein, revealed ploidy defects and structural chromosomal aberrations. Genetic evidence that the observed chromosomal abnormalities do not result from Wnt signaling defects but from deletion of the C-terminal APC functional domains was provided by the confirmation of the aneuploid and polyploid changes in ES lines homozygous for the *Apc1638T* targeted mutation, previously shown to retain wild type  $\beta$ -catenin

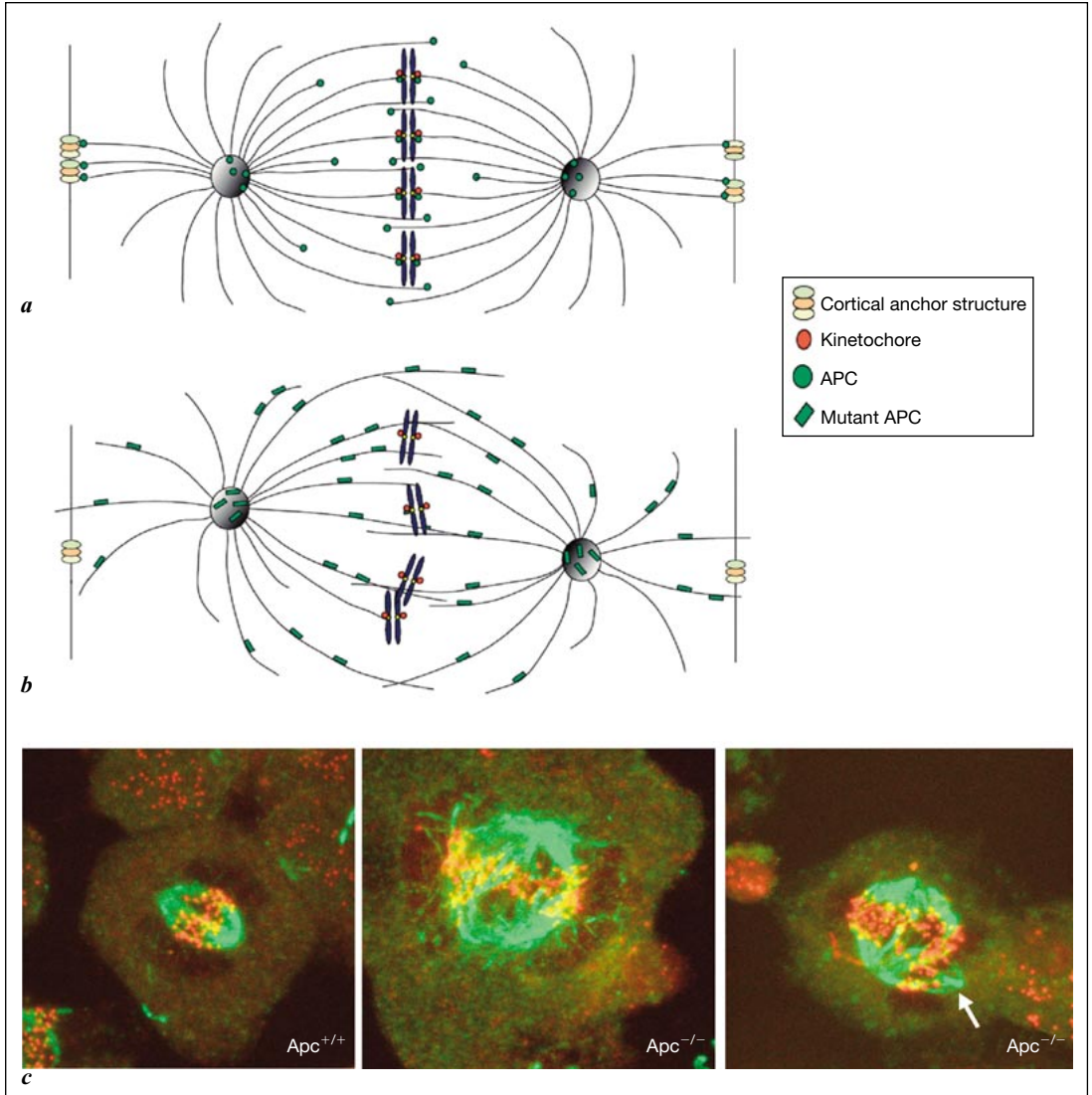


**Fig. 2.** Mitotic spindle defects in *Apc* mutant cells. In (a) a representation of a normal mitotic figure with localization of APC at the kinetochore and at the plus-ends of the microtubules is shown. The hypothetical binding of APC on astral microtubules to the cortical anchor structure allows to keep the mitotic spindle parallel to the epithelial plane. In (b) there is represented a mitosis in an *Apc* mutant cell with defects in the spindle organization and the failure of the APC binding to the kinetochore and to the cortical anchor structure. In (c) examples of spindles formed in *Apc* wild type and mutant ES cells lines are shown. In green the  $\beta$ -tubulin staining marks the spindle, whereas in red the CREST/kinetochore structure is stained. Note in the *Apc* mutants the spindle abnormalities with most of the microtubules projecting in a chaotic manner in the cytoplasm. In the right *Apc*<sup>-/-</sup> picture, the white arrow designates an extra centrosome.

regulatory function [35, 94]. The co-localization of APC at the kinetochore of the metaphase chromosomes is abolished by colcemid treatment, an agent that selectively depolymerizes microtubules. Microtubule staining of *Apc* mutant ES cells shows a disorganized mitotic spindle with most microtubules projecting randomly into the cytoplasm in contrast with the properly aligned spindles observed in wild-type cells (fig. 2). Also, *Apc*-mutant ES lines showed high incidence of mono- and multicentric spindles and supernumerary centrosomes at mitosis when compared with wild type ES cells [35, 36]. Notably, APC and EB1 co-localize with the centrosome in both mammalian and *Xenopus* mitotic cells, and are thus likely to play a role in centrosomally driven spindle formation by anchoring cytoplasmic MT minus ends to the centriole [35, 36, 69, 95, 96]. However, the latter could also represent a consequence of APC's role in directly supporting spindle formation and stability in vivo, as suggested by the observation of microtubule-resistance against nocodazole treatment in cells expressing full-length or C-terminal APC [78]. Moreover, APC acts, possibly within a protein complex together with EB1 and the formin mDia, a component of the Rho-GTPase pathway, to selectively stabilize microtubules in fibroblasts [87].

Another observation of APC involvement in CIN comes from an experiment in which the overexpression of a dominant-negative C-terminal APC fragment encompassing the EB1-binding domain in the APC-proficient and near-diploid HTC116 CRC cell line resulted in a 2.5–5 fold increase in the frequency of numerical chromosomal aberrations [97].

Since these first reports, additional studies have provided additional insights on the role of loss and/or truncation of APC in eliciting CIN. Green and Kaplan [98] have shown that CIN tumor cells exhibit inefficient microtubule plus-end attachments during mitosis, accompanied by impairment of chromosome alignment at metaphase. These abnormalities correlate with the *APC* mutational status. Notably, it was also found that a single truncating mutation in APC acts dominantly to interfere with microtubule plus-end attachments and causes a dramatic increase in mitotic abnormalities [98]. Consistent with the latter, N-terminal APC fragments expressed in HCT-116, a near diploid colon cancer cell line with two wild-type *APC* alleles, result in spindle checkpoint defect and aneuploidy [97]. Although these alleged dominant-negative effects of truncated APC need to be confirmed by additional in vitro and in vivo studies with knock-in and inducible *APC* mutations to exclude artifacts due to changes in the expression levels and subcellular localization of the transfected recombinant proteins, they may have important implications for the further elucidation of APC-driven tumorigenesis. In a previous study by somatic cell fusion analysis, MSI was shown to behave as a recessive trait, whereas CIN appeared to be dominant [22]. However, complete loss of APC function also results in spindle abnormalities similar to those observed in cells with truncated APC: depletion

of APC from *Xenopus* extracts leads to a decrease in microtubule density and changes in tubulin distribution in spindles and asters [69].

Notably, it has also been observed that the level of Bub1p was enriched at kinetochores during metaphase in cells transfected with the truncated APC construct [98]. Similarly, kinetochore-bound BubR1 is also significantly increased in HTC-116 expressing a mutant N-terminal APC fragment [97]. This is of interest in view of a previous study showing that the dissociation of Bub1 and BubR1 from the kinetochores of aligned chromosomes depends on microtubule attachment and tension, respectively [99]. The observed stabilization of checkpoint proteins at the kinetochore during metaphase may indeed result from the dominant-negative effects exerted by truncated APC on kinetochore-microtubule attachment and tension.

In mitotic cells, APC and Bub3 are juxtaposed in prometaphase and metaphase along kinetochore microtubules, as also confirmed by co-immunoprecipitation [36]. These observations, together with the fact that Bub1-Bub3 and BubR1-Bub3 complexes can phosphorylate APC in vitro with high specificity, are suggestive of a role for APC phosphorylation by Bub kinases in the regulation of kinetochore-microtubule attachment through the different stages of mitosis.

An additional function of APC in spindle formation and stabilization possibly related to its capacity to elicit CIN when mutated, lies in its microtubule-capture activity at the cell-cortex, homologous to the yeast cortical microtubule capture site composed by Bim1 (homolog of mammalian EB1) and Kar9 [100, 101]. In yeast, Kar9 represents a central link between the actin cytoskeleton and microtubules in establishing correct spindle orientation [102, 103]. Although Kar9 does not seem to be conserved throughout evolution, functional similarities can be observed between Kar9 and the C-terminus of APC encompassing the EB1-binding site [104]. Recently, APC has been described to be distributed in a punctuated fashion along the path of microtubule growth and, in addition, to localize at the basal cortex of mammalian cells where it provides attachment for growing microtubules thus contributing to the organization and stabilization of the microtubule network at the cortex [101]. Interestingly, a direct APC-EB1 interaction is not required for either APC or EB1 localization to the microtubules at the basal cortex [101].

Hence, APC, like Kar9, is a component of the cortical template and may act in mammalian cells as a guide to capture microtubules at specific sites along the plasma membrane. Whether this anchor function also ensures the correct position of the mitotic spindle and thus chromosomal segregation during mitosis is a fascinating though yet to be demonstrated hypothesis.

In summary, the above data indicate that, during mitosis, APC contributes both to spindle formation radiating from the centrosome, and to the proper

attachment of the growing ends of microtubules to the kinetochore (either directly and/or through EB1). Hence, *APC* mutations are likely to affect several structural complexes and pathways (kinetochore, microtubules, centrosomes, and spindle checkpoints) known to be implicated in both numerical and structural CIN [105] (fig. 2). Accordingly, both tetraploidy and aneuploidy were found to represent the main chromosomal defects in mouse primary *Apc*-mutant cell lines [35, 36].

### **In vivo Consequences of APC Mutations on Chromosomal Instability**

Although loss of APC-mediated regulation of Wnt/ $\beta$ -catenin signaling represents the main initiating event in colorectal tumorigenesis, it is safe to assume that *APC* mutation affects a multitude of additional cellular functions thus providing the nascent tumor with additional selective advantages likely to play important roles in progression towards malignancy. The latter is also suggested by the observation according to which tumors with oncogenic  $\beta$ -catenin mutations are usually smaller and less aggressive than those with *APC* mutations [106]. Accordingly, additional defects in cell migration, apoptosis, and differentiation have been reported in mouse cells carrying *Apc* truncating mutations [53, 107, 108].

Whether loss of APC function directly results in CIN is at present still a matter of debate. In general, aneuploidy has been reported in larger adenomas, suggesting its increase with tumor progression [25, 32]. Shih and colleagues [34] demonstrated allelic imbalance (AI), indicative of losses or gains of defined chromosomal regions, in small benign colorectal tumors thus suggesting that CIN occurs at very early stages during colorectal neoplasia. On the other hand, Sieber et al. [109] failed to detect any chromosomal changes in the majority of *APC*-mutant adenomas analyzed. These apparent discrepancies may be explained by the different detection sensitivity of the methods employed in the two studies, namely digital PCR vs. a combination of flow cytometry and conventional CGH and LOH analyses [34, 109]. In a more recent study, we have shown aneuploid changes at specific chromosomal regions (Cardoso et al., submitted) in a small but significant fraction of FAP adenomas with established *APC* mutations by array CGH. This approach allows to measure relative DNA abundances with a sensitivity that theoretically ranges from abnormalities affecting complete chromosome arms to few megabases. Digital PCR, when employed to assess AI, is even more sensitive than array CGH to detect gain and loss events affecting chromosomal regions <1 Mb. Both digital PCR and array CGH are also likely to detect ploidy changes present in subpopulations of

neoplastic cells that only become completely clonal at later stages of tumorigenesis. In contrast, although flow-cytometry is the method of choice when analyzing ploidy status of tumor samples, aneuploid changes below specific thresholds are likely to go undetected. Therefore, based on the above functional and observational studies, we hypothesize that loss of the MT- and EB1-binding functions of APC, triggers a broad spectrum of mitotic spindle defects that may elicit a subtle but significantly increased rate of CIN. As truncated APC proteins may act in a dominant-negative fashion in eliciting similar mitotic defects [53, 97, 98], CIN may even precede the rate-limiting somatic hit at the wild type *APC* allele.

## Discussion

CIN in CRC has been previously associated with mitotic spindle checkpoint defects [28]. Cells with defective spindle checkpoint prematurely exit mitosis after colcemid treatment. However, these findings contrast with the report by Tighe and colleagues that CIN cells do undergo mitotic arrest in response to spindle damage and have a robust checkpoint [110]. *Apc*-mutant ES cells also fail to show differences in mitotic index in comparison to wild type line [35], whereas analysis of *Mad2*- or *Bub3*-mutant embryonic cells revealed a dramatic drop in mitotic index levels [111, 112], due to the mitotic arrest upon microtubule depolymerization. Mutations in known spindle checkpoint genes are found in human cancers, though at overall low frequencies [27–29, 113].

It seems plausible that loss of APC function is necessary but insufficient to result in full-blown CIN. In *APC*-mutant aberrant crypt foci and small adenomas, a subtle but significant defect in microtubule dynamics and mitotic spindle assembly may occasionally lead to ploidy changes. Additional mutations in different categories of genes involved in mitotic and cell cycle checkpoints, telomere shortening and telomerase expression, centrosome number regulation, and double-strand break repair [3, 27] may work synergistically with the kinetochore and chromosome segregation defects caused by *APC* mutation in eliciting CIN. In fact, CIN may initially be suppressed by active cell cycle and mitotic checkpoints. Experimental evidence for the latter was provided by studies in *Apc<sup>Min/+</sup>/BubR1<sup>+/-</sup>* compound mutant mice [114]. While *BubR1<sup>+/-</sup>* animals do not develop colonic tumors, compound *Apc<sup>Min/+</sup>/BubR1<sup>+/-</sup>* mice are affected by increased intestinal tumor multiplicity and progression towards advanced stages when compared with *Apc<sup>Min/+</sup>* animals. Mouse embryonic fibroblasts (MEFs) derived from *Apc<sup>Min/+</sup>/BubR1<sup>+/-</sup>* embryos show enhanced mitotic slippage in the presence of nocodazole and exhibit a higher rate of genomic instability than that of wild type or *BubR1<sup>+/-</sup>* or *Apc<sup>Min/+</sup>* MEFs, as indicated by

premature separation of sister chromatids, increased rates of micronuclei formation and aneuploid metaphases. It is therefore likely that even haploinsufficiency at spindle checkpoint genes like *BubR1* may elicit CIN in the presence of the mitotic spindle assembly defect caused by *APC* mutation.

Notwithstanding the above, the spectrum of genes that may act synergistically with *APC* in eliciting CIN in CRC is likely to extend beyond those implicated in checkpoint functions. Supporting evidence for the existence of specific CIN-genes able to synergize with *APC* to exert genomic instability has been provided by studies with *Apc*-mutant mouse models. Expression of *CDX2*, a homeodomain transcriptional factor involved in the development, differentiation and physiology of the intestinal epithelial lining, is markedly reduced in the later stages of human colorectal carcinogenesis, namely, high grade dysplasia and invasive carcinoma [115, 116]. Compound heterozygous *Apc*<sup>+/ $\Delta$ 716</sup>/*Cdx2*<sup>+/-</sup> mice show a marked increase in colonic polyp formation when compared with the single mutant animals, with lesions frequently characterized by an increased anaphase bridge index (ABI), indicative of CIN [117]. Notably, normal colonic epithelium from compound heterozygous animals shows an increased ABI when compared to single mutant littermates, indicative of a putative synergism between *APC* and *CDX2* mutations in eliciting CIN.

In general, telomere abnormalities are known to be associated with promotion of epithelial cancer [118, 119], and genes related to telomere maintenance may co-operate with *APC* to exert CIN in CRC. Indeed, progressive telomere dysfunction increases intestinal tumor multiplicity in the second and third generation *Apc*<sup>Min/+</sup>/*Terc*<sup>-/-</sup> mice, when telomere shortening becomes critical [120]. Notably, these tumors are characterized by high ABI incidence leading to the formation of dicentric chromosomes and high rate of chromosome loss. Also, the presence of short telomeres in colorectal carcinoma [121, 122], together with the increase of anaphase bridges at the adenoma-carcinoma transition [120] points to a role for defective telomere dynamics in genomic instability during colorectal carcinoma progression.

Recently, it has been reported that loss of the *BRCA2* tumor suppressor gene causes a cytokinesis defect, i.e. an impairment of the completion of cell separation upon mitosis [123]. As for *APC*, *BRCA2* was already known to cause both qualitative (aneuploidy) and quantitative (polyploidy) chromosomal changes. Whereas the first can be explained by the failure to repair double strand DNA breaks by mutant *BRCA2*, the latter appears now to result from impeded cell separation accompanied by abnormalities in myosin organization during late stages of cytokinesis. Accordingly, *BRCA2* was shown to localize to the cytokinetic midbody [123]. Though no evidence to date has been reported for a role of *APC* in cytokinesis, tetraploidy is a main feature of *APC*-mutant cells [35, 36] and it may represent the primary consequence of the loss of its

multiple functional roles in mitosis (attachment of the mitotic spindle to the kinetochore, centrosome and cell cortex) and a first step towards aneuploidy. The subtlety of this initial and random CIN defect might represent the ‘just-right’ type of genetic instability [124] as it allows the occasional generation of cells carrying specific genetic defects on which clonal selection operates without excessive accumulation of genetic damage above viability thresholds. Additional somatic mutations in different categories of genes will act in a cumulative and/or synergistic fashion to progressively elicit increasing levels of CIN along the adenoma-carcinoma sequence.

## Acknowledgements

We thank J. Kuipers and H. Clevers for the photographic material of figure 2. This work was supported by grants from the Dutch cancer Society (KWF/NKB), the Netherlands Organization for Scientific Research (NWO VICI-grant 918.36.636), and the Center of Medical System Biology (CMSB) established by the Netherlands Genomics Initiative (NGI) and NWO.

## References

- 1 Boveri T: Zur Frage der Entstehung maligner Tumoren. Gustav Fisher Verlag, Jena, 1914.
- 2 Loeb LA, Springgate CF, Battula N: Errors in DNA replication as a basis of malignant changes. *Cancer Res* 1974;34:2311–2321.
- 3 Lengauer C, Kinzler KW, Vogelstein B: Genetic instabilities in human cancers. *Nature* 1998;396: 643–649.
- 4 Vogelstein B, Fearon ER, Hamilton SR, Kern SE, Preisinger AC, Leppert M, Nakamura Y, White R, Smits AM, Bos JL: Genetic alterations during colorectal-tumor development. *N Engl J Med* 1988;319:525–532.
- 5 Loeb LA: Mutator phenotype may be required for multistage carcinogenesis. *Cancer Res* 1991;51: 3075–3079.
- 6 Loeb LA, Loeb KR, Anderson JP: Multiple mutations and cancer. *Proc Natl Acad Sci USA* 2003;100:776–781.
- 7 Michor F, Iwasa Y, Nowak MA: Dynamics of cancer progression. *Nat Rev Cancer* 2004;4:197–205.
- 8 Michor F, Iwasa Y, Vogelstein B, Lengauer C, Nowak MA: Can chromosomal instability initiate tumorigenesis? *Semin Cancer Biol* 2005;15:43–49.
- 9 Tomlinson IP, Novelli MR, Bodmer WF: The mutation rate and cancer. *Proc Natl Acad Sci USA* 1996;93:14800–14803.
- 10 Tomlinson I, Bodmer W: Selection, the mutation rate and cancer: ensuring that the tail does not wag the dog. *Nat Med* 1999;5:11–12.
- 11 Fodde R, Smits R, Clevers H: APC, signal transduction and genetic instability in colorectal cancer. *Nat Rev Cancer* 2001;1:55–67.
- 12 Fearon ER, Vogelstein B: A genetic model for colorectal tumorigenesis. *Cell* 1990;61:759–767.
- 13 Ionov Y, Peinado MA, Malkhosyan S, Shibata D, Perucho M: Ubiquitous somatic mutations in simple repeated sequences reveal a new mechanism for colonic carcinogenesis. *Nature* 1993;363: 558–561.
- 14 Thibodeau SN, Bren G, Schaid D: Microsatellite instability in cancer of the proximal colon [see comments]. *Science* 1993;260:816–819.

- 15 Parsons R, Li GM, Longley MJ, Fang WH, Papadopoulos N, Jen J, de la Chapelle A, Kinzler KW, Vogelstein B, Modrich P: Hypermutability and mismatch repair deficiency in RER+ tumor cells. *Cell* 1993;75:1227–1236.
- 16 Bhattacharyya NP, Skandalis A, Ganesh A, Groden J, Meuth M: Mutator phenotypes in human colorectal carcinoma cell lines. *Proc Natl Acad Sci USA* 1994;91:6319–6323.
- 17 Eshleman JR, Casey G, Kochera ME, Sedwick WD, Swinler SE, Veigl ML, Willson JK, Schwartz S, Markowitz SD: Chromosome number and structure both are markedly stable in RER colorectal cancers and are not destabilized by mutation of p53. *Oncogene* 1998;17:719–725.
- 18 Lynch HT, Lynch J: Lynch syndrome: genetics, natural history, genetic counseling, and prevention. *J Clin Oncol* 2000;18:19S–31S.
- 19 Mitelman F: *Catalog of Chromosome Aberrations in Cancer*. Wiley-Liss, New York, 1991.
- 20 Muleris M, Delattre O, Olschwang S, Dutrillaux AM, Remvikos Y, Salmon RJ, Thomas G, Dutrillaux B: Cytogenetic and molecular approaches of polyploidization in colorectal adenocarcinomas. *Cancer Genet Cytogenet* 1990;44:107–118.
- 21 Bardi G, Sukhikh T, Pandis N, Fenger C, Kronborg O, Heim S: Karyotypic characterization of colorectal adenocarcinomas. *Genes Chromosomes Cancer* 1995;12:97–109.
- 22 Lengauer C, Kinzler KW, Vogelstein B: Genetic instability in colorectal cancers. *Nature* 1997;386:623–627.
- 23 Thiagalingam S, Laken S, Willson JK, Markowitz SD, Kinzler KW, Vogelstein B, Lengauer C: Mechanisms underlying losses of heterozygosity in human colorectal cancers. *Proc Natl Acad Sci USA* 2001;98:2698–2702.
- 24 Ried T, Knutzen R, Steinbeck R, Blegen H, Schrock E, Heselmeyer K, du Manoir S, Auer G: Comparative genomic hybridization reveals a specific pattern of chromosomal gains and losses during the genesis of colorectal tumors. *Genes Chromosomes Cancer* 1996;15:234–245.
- 25 Hermesen M, Postma C, Baak J, Weiss M, Rapallo A, Sciotto A, Roemen G, Arends JW, Williams R, Giaretti W, De Goeij A, Meijer G: Colorectal adenoma to carcinoma progression follows multiple pathways of chromosomal instability. *Gastroenterology* 2002;123:1109–1119.
- 26 Chan TL, Curtis LC, Leung SY, Farrington SM, Ho JW, Chan AS, Lam PW, Tse CW, Dunlop MG, Wyllie AH, Yuen ST: Early-onset colorectal cancer with stable microsatellite DNA and near-diploid chromosomes. *Oncogene* 2001;20:4871–4876.
- 27 Wang Z, Cummins JM, Shen D, Cahill DP, Jallepalli PV, Wang TL, Parsons DW, Traverso G, Awad M, Silliman N, Ptak J, Szabo S, Willson JK, Markowitz SD, Goldberg ML, Karess R, Kinzler KW, Vogelstein B, Velculescu VE, Lengauer C: Three classes of genes mutated in colorectal cancers with chromosomal instability. *Cancer Res* 2004;64:2998–3001.
- 28 Cahill DP, Lengauer C, Yu J, Riggins GJ, Willson JK, Markowitz SD, Kinzler KW, Vogelstein B: Mutations of mitotic checkpoint genes in human cancers. *Nature* 1998;392:300–303.
- 29 Shichiri M, Yoshinaga K, Hisatomi H, Sugihara K, Hirata Y: Genetic and epigenetic inactivation of mitotic checkpoint genes *hBUB1* and *hBUBR1* and their relationship to survival. *Cancer Res* 2002;62:13–17.
- 30 Rajagopalan H, Jallepalli PV, Rago C, Velculescu VE, Kinzler KW, Vogelstein B, Lengauer C: Inactivation of hCDC4 can cause chromosomal instability. *Nature* 2004;428:77–81.
- 31 Fukasawa K, Choi T, Kuriyama R, Rulong S, Vande Woude GF: Abnormal centrosome amplification in the absence of p53. *Science* 1996;271:1744–1747.
- 32 Giaretti W: A model of DNA aneuploidization and evolution in colorectal cancer. *Lab Invest* 1994;71:904–910.
- 33 Bardi G, Parada LA, Bomme L, Pandis N, Willen R, Johansson B, Jeppsson B, Beroukas K, Heim S, Mitelman F: Cytogenetic comparisons of synchronous carcinomas and polyps in patients with colorectal cancer. *Br J Cancer* 1997;76:765–769.
- 34 Shih IM, Zhou W, Goodman SN, Lengauer C, Kinzler KW, Vogelstein B: Evidence that genetic instability occurs at an early stage of colorectal tumorigenesis. *Cancer Res* 2001;61:818–822.
- 35 Fodde R, Kuipers J, Rosenberg C, Smits R, Kielman M, Gaspar C, van Es JH, Breukel C, Wiegant J, Giles RH, Clevers H: Mutations in the *APC* tumour suppressor gene cause chromosomal instability. *Nat Cell Biol* 2001;3:433–438.
- 36 Kaplan KB, Burds AA, Swedlow JR, Bekir SS, Sorger PK, Nathke IS: A role for the adenomatous polyposis coli protein in chromosome segregation. *Nat Cell Biol* 2001;3:429–432.

- 37 Fodde R: The multiple functions of tumour suppressors: it's all in APC. *Nat Cell Biol* 2003;5: 190–192.
- 38 Morin PJ, Sparks AB, Korinek V, Barker N, Clevers H, Vogelstein B, Kinzler KW: Activation of beta-catenin-Tcf signaling in colon cancer by mutations in beta-catenin or APC. *Science* 1997;275:1787–1790.
- 39 Sparks AB, Morin PJ, Vogelstein B, Kinzler KW: Mutational analysis of the APC/beta-catenin/Tcf pathway in colorectal cancer. *Cancer Res* 1998;58:1130–1134.
- 40 Gaspar C, Fodde R: APC dosage effects in tumorigenesis and stem cell differentiation. *Int J Dev Biol* 2004;48:377–386.
- 41 Day CL, Alber T: Crystal structure of the amino-terminal coiled-coil domain of the APC tumor suppressor. *J Mol Biol* 2000;301:147–156.
- 42 Joslyn G, Richardson DS, White R, Alber T: Dimer formation by an N-terminal coiled coil in the APC protein. *Proc Natl Acad Sci USA* 1993;90:11109–11113.
- 43 Lupas A, Van Dyke M, Stock J: Predicting coiled coils from protein sequences. *Science* 1991;252:1162–1164.
- 44 Tickenbrock L, Cramer J, Vetter IR, Muller O: The coiled coil region (amino acids 129–250) of the tumor suppressor protein adenomatous polyposis coli (APC). Its structure and its interaction with chromosome maintenance region 1 (Crm-1). *J Biol Chem* 2002;277:32332–32338.
- 45 Henderson BR: Nuclear-cytoplasmic shuttling of APC regulates beta-catenin subcellular localization and turnover. *Nat Cell Biol* 2000;2:653–660.
- 46 Neufeld KL, Nix DA, Bogerd H, Kang Y, Beckerle MC, Cullen BR, White RL: Adenomatous polyposis coli protein contains two nuclear export signals and shuttles between the nucleus and cytoplasm. *Proc Natl Acad Sci USA* 2000;97:12085–12090.
- 47 Polakis P: The adenomatous polyposis coli (APC) tumor suppressor. *Biochim Biophys Acta* 1997;1332:F127–F147.
- 48 Seeling JM, Miller JR, Gil R, Moon RT, White R, Virshup DM: Regulation of beta-catenin signaling by the B56 subunit of protein phosphatase 2A. *Science* 1999;283:2089–2091.
- 49 Kawasaki Y, Senda T, Ishidate T, Koyama R, Morishita T, Iwayama Y, Higuchi O, Akiyama T: Asef, a link between the tumor suppressor APC and G-protein signaling. *Science* 2000;289: 1194–1197.
- 50 Jimbo T, Kawasaki Y, Koyama R, Sato R, Takada S, Haraguchi K, Akiyama T: Identification of a link between the tumour suppressor APC and the kinesin superfamily. *Nat Cell Biol* 2002;4:323–327.
- 51 Kawasaki Y, Sato R, Akiyama T: Mutated APC and Asef are involved in the migration of colorectal tumour cells. *Nat Cell Biol* 2003;5:211–215.
- 52 Hughes SA, Carothers AM, Hunt DH, Moran AE, Mueller JD, Bertagnolli MM: Adenomatous polyposis coli truncation alters cytoskeletal structure and microtubule stability in early intestinal tumorigenesis. *J Gastrointest Surg* 2002;6:868–874; discussion 875.
- 53 Mahmoud NN, Boolbol SK, Bilinski RT, Martucci C, Chadburn A, Bertagnolli MM: *Apc* gene mutation is associated with a dominant-negative effect upon intestinal cell migration. *Cancer Res* 1997;57:5045–5050.
- 54 Li Z, Nathke IS: Tumor-associated NH<sub>2</sub>-terminal fragments are the most stable part of the adenomatous polyposis coli protein and can be regulated by interactions with COOH-terminal domains. *Cancer Res* 2005;65:5195–5204.
- 55 Hart MJ, de los Santos R, Albert IN, Rubinfeld B, Polakis P: Downregulation of beta-catenin by human Axin and its association with the APC tumor suppressor, beta-catenin and GSK3 beta. *Curr Biol* 1998;8:573–581.
- 56 Behrens J, Jerchow BA, Wurtele M, Grimm J, Asbrand C, Wirtz R, Kuhl M, Wedlich D, Birchmeier W: Functional interaction of an axin homolog, conductin, with beta-catenin, APC, and GSK3beta. *Science* 1998;280:596–599.
- 57 Fagotto F, Jho E, Zeng L, Kurth T, Joos T, Kaufmann C, Costantini F: Domains of axin involved in protein-protein interactions, Wnt pathway inhibition, and intracellular localization. *J Cell Biol* 1999;145:741–756.
- 58 Kishida M, Koyama S, Kishida S, Matsubara K, Nakashima S, Higano K, Takada R, Takada S, Kikuchi A: Axin prevents Wnt-3a-induced accumulation of beta-catenin. *Oncogene* 1999;18: 979–985.

- 59 Ikeda S, Kishida M, Matsuura Y, Usui H, Kikuchi A: GSK-3beta-dependent phosphorylation of adenomatous polyposis coli gene product can be modulated by beta-catenin and protein phosphatase 2A complexed with Axin. *Oncogene* 2000;19:537–545.
- 60 Jiang J, Struhl G: Regulation of the Hedgehog and Wntless signalling pathways by the F-box/WD40-repeat protein Slimb. *Nature* 1998;391:493–496.
- 61 Marikawa Y, Elinson RP: Beta-TrCP is a negative regulator of Wnt/beta-catenin signaling pathway and dorsal axis formation in *Xenopus* embryos. *Mech Dev* 1998;77:75–80.
- 62 Behrens J, von Kries JP, Kuhl M, Bruhn L, Wedlich D, Grosschedl R, Birchmeier W: Functional interaction of beta-catenin with the transcription factor LEF-1. *Nature* 1996;382:638–642.
- 63 Molenaar M, van de Wetering M, Oosterwegel M, Peterson-Maduro J, Godsave S, Korinek V, Roose J, Destree O, Clevers H: XTcf-3 transcription factor mediates beta-catenin-induced axis formation in *Xenopus* embryos. *Cell* 1996;86:391–399.
- 64 Roose J, Molenaar M, Peterson J, Hurenkamp J, Brantjes H, Moerer P, van de Wetering M, Destree O, Clevers H: The *Xenopus* Wnt effector XTcf-3 interacts with Groucho-related transcriptional repressors. *Nature* 1998;395:608–612.
- 65 Deka J, Kuhlmann J, Muller O: A domain within the tumor suppressor protein APC shows very similar biochemical properties as the microtubule-associated protein tau. *Eur J Biochem* 1998;253:591–597.
- 66 Munemitsu S, Souza B, Muller O, Albert I, Rubinfeld B, Polakis P: The APC gene product associates with microtubules in vivo and promotes their assembly in vitro. *Cancer Res* 1994;54: 3676–3681.
- 67 Smith KJ, Levy DB, Maupin P, Pollard TD, Vogelstein B, Kinzler KW: Wild-type but not mutant APC associates with the microtubule cytoskeleton. *Cancer Res* 1994;54:3672–3675.
- 68 Askham JM, Moncur P, Markham AF, Morrison EE: Regulation and function of the interaction between the APC tumour suppressor protein and EB1. *Oncogene* 2000;19:1950–1958.
- 69 Dikovskaya D, Newton IP, Nathke IS: The adenomatous polyposis coli protein is required for the formation of robust spindles formed in CSF *Xenopus* extracts. *Mol Biol Cell* 2004;15: 2978–2991.
- 70 Matsumine A, Ogai A, Senda T, Okumura N, Satoh K, Baeg GH, Kawahara T, Kobayashi S, Okada M, Toyoshima K, Akiyama T: Binding of APC to the human homolog of the *Drosophila* discs large tumor suppressor protein. *Science* 1996;272:1020–1023.
- 71 Henderson BR, Fagotto F: The ins and outs of APC and beta-catenin nuclear transport. *EMBO Rep* 2002;3:834–839.
- 72 Deka J, Herter P, Sprenger-Haussels M, Koosch S, Franz D, Muller KM, Kuhnen C, Hoffmann I, Muller O: The APC protein binds to A/T rich DNA sequences. *Oncogene* 1999;18:5654–5661.
- 73 Brocardo M, Nathke IS, Henderson BR: Redefining the subcellular location and transport of APC: new insights using a panel of antibodies. *EMBO Rep* 2005;6:184–190.
- 74 Nathke IS, Adams CL, Polakis P, Sellin JH, Nelson WJ: The adenomatous polyposis coli tumor suppressor protein localizes to plasma membrane sites involved in active cell migration. *J Cell Biol* 1996;134:165–179.
- 75 Rosin-Arbesfeld R, Ihrke G, Bienz M: Actin-dependent membrane association of the APC tumour suppressor in polarized mammalian epithelial cells. *EMBO J* 2001;20:5929–5939.
- 76 Mogensen MM, Tucker JB, Mackie JB, Prescott AR, Nathke IS: The adenomatous polyposis coli protein unambiguously localizes to microtubule plus ends and is involved in establishing parallel arrays of microtubule bundles in highly polarized epithelial cells. *J Cell Biol* 2002;157:1041–1048.
- 77 Schuyler SC, Pellman D: Microtubule ‘plus-end-tracking proteins’: the end is just the beginning. *Cell* 2001;105:421–424.
- 78 Zumbrunn J, Kinoshita K, Hyman AA, Nathke IS: Binding of the adenomatous polyposis coli protein to microtubules increases microtubule stability and is regulated by GSK3beta phosphorylation. *Curr Biol* 2001;11:44–49.
- 79 Etienne-Manneville S, Hall A: Cdc42 regulates GSK-3beta and adenomatous polyposis coli to control cell polarity. *Nature* 2003;421:753–756.
- 80 Barth AI, Siemers KA, Nelson WJ: Dissecting interactions between EB1, microtubules and APC in cortical clusters at the plasma membrane. *J Cell Sci* 2002;115:1583–1590.
- 81 Su LK, Burrell M, Hill DE, Gyuris J, Brent R, Wiltshire R, Trent J, Vogelstein B, Kinzler KW: APC binds to the novel protein EB1. *Cancer Res* 1995;55:2972–2977.

- 82 Tirnauer JS, Bierer BE: EB1 proteins regulate microtubule dynamics, cell polarity, and chromosome stability. *J Cell Biol* 2000;149:761–766.
- 83 Galjart N, Perez F: A plus-end raft to control microtubule dynamics and function. *Curr Opin Cell Biol* 2003;15:48–53.
- 84 Berrueta L, Tirnauer JS, Schuyler SC, Pellman D, Bierer BE: The APC-associated protein EB1 associates with components of the dynactin complex and cytoplasmic dynein intermediate chain. *Curr Biol* 1999;9:425–428.
- 85 Mimori-Kiyosue Y, Shiina N, Tsukita S: The dynamic behavior of the APC-binding protein EB1 on the distal ends of microtubules. *Curr Biol* 2000;10:865–868.
- 86 Bu W, Su LK: Characterization of functional domains of human EB1 family proteins. *J Biol Chem* 2003;278:49721–49731.
- 87 Wen Y, Eng CH, Schmoranzler J, Cabrera-Poch N, Morris EJ, Chen M, Wallar BJ, Alberts AS, Gundersen GG: EB1 and APC bind to mDia to stabilize microtubules downstream of Rho and promote cell migration. *Nat Cell Biol* 2004;6:820–830.
- 88 Berrueta L, Kraeft SK, Tirnauer JS, Schuyler SC, Chen LB, Hill DE, Pellman D, Bierer BE: The adenomatous polyposis coli-binding protein EB1 is associated with cytoplasmic and spindle microtubules. *Proc Natl Acad Sci USA* 1998;95:10596–10601.
- 89 Morrison EE, Wardleworth BN, Askham JM, Markham AF, Meredith DM: EB1, a protein which interacts with the APC tumour suppressor, is associated with the microtubule cytoskeleton throughout the cell cycle. *Oncogene* 1998;17:3471–3477.
- 90 Honnappa S, John CM, Kostrewa D, Winkler FK, Steinmetz MO: Structural insights into the EB1-APC interaction. *EMBO J* 2005;24:261–269.
- 91 Powell SM, Zilz N, Beazer-Barclay Y, Bryan TM, Hamilton SR, Thibodeau SN, Vogelstein B, Kinzler KW: APC mutations occur early during colorectal tumorigenesis. *Nature* 1992;359:235–237.
- 92 Su LK, Johnson KA, Smith KJ, Hill DE, Vogelstein B, Kinzler KW: Association between wild type and mutant APC gene products. *Cancer Res* 1993;53:2728–2731.
- 93 Jais P, Sabourin JC, Bombled J, Rougier P, Lasser P, Duvillard P, Benard J, Bressac-de Paillerets B: Absence of somatic alterations of the EB1 gene adenomatous polyposis coli-associated protein in human sporadic colorectal cancers. *Br J Cancer* 1998;78:1356–1360.
- 94 Smits R, Kielman MF, Breukel C, Zurcher C, Neufeld K, Jagmohan-Changur S, Hofland N, van Dijk J, White R, Edelmann W, Kucherlapati R, Khan PM, Fodde R: Apc1638T: a mouse model delineating critical domains of the adenomatous polyposis coli protein involved in tumorigenesis and development. *Genes Dev* 1999;13:1309–1321.
- 95 Olmeda D, Castel S, Vilaro S, Cano A: Beta-catenin regulation during the cell cycle: implications in G<sub>2</sub>/M and apoptosis. *Mol Biol Cell* 2003;14:2844–2860.
- 96 Louie RK, Bahmanyar S, Siemers KA, Votin V, Chang P, Stearns T, Nelson WJ, Barth AI: Adenomatous polyposis coli and EB1 localize in close proximity of the mother centriole and EB1 is a functional component of centrosomes. *J Cell Sci* 2004;117:1117–1128.
- 97 Tighe A, Johnson VL, Taylor SS: Truncating APC mutations have dominant effects on proliferation, spindle checkpoint control, survival and chromosome stability. *J Cell Sci* 2004;117:6339–6353.
- 98 Green RA, Kaplan KB: Chromosome instability in colorectal tumor cells is associated with defects in microtubule plus-end attachments caused by a dominant mutation in APC. *J Cell Biol* 2003;163:949–961.
- 99 Taylor SS, Hussein D, Wang Y, Elderkin S, Morrow CJ: Kinetochores localisation and phosphorylation of the mitotic checkpoint components Bub1 and BubR1 are differentially regulated by spindle events in human cells. *J Cell Sci* 2001;114:4385–4395.
- 100 Bloom K: It's a kar9ochore to capture microtubules. *Nat Cell Biol* 2000;2:E96–E98.
- 101 Reilein A, Nelson WJ: APC is a component of an organizing template for cortical microtubule networks. *Nat Cell Biol* 2005;7:463–473.
- 102 Beach DL, Thibodeaux J, Maddox P, Yeh E, Bloom K: The role of the proteins Kar9 and Myo2 in orienting the mitotic spindle of budding yeast. *Curr Biol* 2000;10:1497–1506.
- 103 Liakopoulos D, Kusch J, Grava S, Vogel J, Barral Y: Asymmetric loading of Kar9 onto spindle poles and microtubules ensures proper spindle alignment. *Cell* 2003;112:561–574.
- 104 Bienz M: The subcellular destinations of APC proteins. *Nat Rev Mol Cell Biol* 2002;3:328–338.
- 105 Doxsey S: The centrosome – a tiny organelle with big potential. *Nat Genet* 1998;20:104–106.

- 106 Samowitz WS, Powers MD, Spirio LN, Nollet F, van Roy F, Slattery ML: Beta-catenin mutations are more frequent in small colorectal adenomas than in larger adenomas and invasive carcinomas. *Cancer Res* 1999;59:1442–1444.
- 107 Mahmoud NN, Bilinski RT, Churchill MR, Edelmann W, Kucherlapati R, Bertagnolli MM: Genotype-phenotype correlation in murine *Apc* mutation: differences in enterocyte migration and response to sulindac. *Cancer Res* 1999;59:353–359.
- 108 Sansom OJ, Reed KR, Hayes AJ, Ireland H, Brinkmann H, Newton IP, Batlle E, Simon-Assmann P, Clevers H, Nathke IS, Clarke AR, Winton DJ: Loss of *Apc* in vivo immediately perturbs Wnt signaling, differentiation, and migration. *Genes Dev* 2004;18:1385–1390.
- 109 Sieber OM, Heinemann K, Gorman P, Lamlum H, Crabtree M, Simpson CA, Davies D, Neale K, Hodgson SV, Roylance RR, Phillips RK, Bodmer WF, Tomlinson IP: Analysis of chromosomal instability in human colorectal adenomas with two mutational hits at *APC*. *Proc Natl Acad Sci USA* 2002;99:16910–16915.
- 110 Tighe A, Johnson VL, Albertella M, Taylor SS: Aneuploid colon cancer cells have a robust spindle checkpoint. *EMBO Rep* 2001;2:609–614.
- 111 Dobles M, Liberal V, Scott ML, Benezra R, Sorger PK: Chromosome missegregation and apoptosis in mice lacking the mitotic checkpoint protein *Mad2*. *Cell* 2000;101:635–645.
- 112 Kalitsis P, Earle E, Fowler KJ, Choo KH: *Bub3* gene disruption in mice reveals essential mitotic spindle checkpoint function during early embryogenesis. *Genes Dev* 2000;14:2277–2282.
- 113 Imai Y, Shiratori Y, Kato N, Inoue T, Omata M: Mutational inactivation of mitotic checkpoint genes, *hsMAD2* and *hBUB1*, is rare in sporadic digestive tract cancers. *Jpn J Cancer Res* 1999;90: 837–840.
- 114 Rao CV, Yang YM, Swamy MV, Liu T, Fang Y, Mahmood R, Jhanwar-Uniyal M, Dai W: Colonic tumorigenesis in *BubR1*<sup>+/-</sup>*Apc*<sup>Min/+</sup> compound mutant mice is linked to premature separation of sister chromatids and enhanced genomic instability. *Proc Natl Acad Sci USA* 2005;102: 4365–4370.
- 115 Ee HC, Erler T, Bhathal PS, Young GP, James RJ: Cdx-2 homeodomain protein expression in human and rat colorectal adenoma and carcinoma. *Am J Pathol* 1995;147:586–592.
- 116 Mallo GV, Rechreche H, Frigerio JM, Rocha D, Zweibaum A, Lacasa M, Jordan BR, Dusetti NJ, Dagorn JC, Iovanna JL: Molecular cloning, sequencing and expression of the mRNA encoding human *Cdx1* and *Cdx2* homeobox. Down-regulation of *Cdx1* and *Cdx2* mRNA expression during colorectal carcinogenesis. *Int J Cancer* 1997;74:35–44.
- 117 Aoki K, Tamai Y, Horiike S, Oshima M, Taketo MM: Colonic polyposis caused by mTOR-mediated chromosomal instability in *Apc*<sup>+/-</sup>*Delta716 Cdx2*<sup>+/-</sup> compound mutant mice. *Nat Genet* 2003;35:323–330.
- 118 Artandi SE, DePinho RA: A critical role for telomeres in suppressing and facilitating carcinogenesis. *Curr Opin Genet Dev* 2000;10:39–46.
- 119 Hanahan D, Weinberg RA: The hallmarks of cancer. *Cell* 2000;100:57–70.
- 120 Rudolph KL, Millard M, Bosenberg MW, DePinho RA: Telomere dysfunction and evolution of intestinal carcinoma in mice and humans. *Nat Genet* 2001;28:155–159.
- 121 Hastie ND, Dempster M, Dunlop MG, Thompson AM, Green DK, Allshire RC: Telomere reduction in human colorectal carcinoma and with ageing. *Nature* 1990;346:866–868.
- 122 Engelhardt M, Drullinsky P, Guillem J, Moore MA: Telomerase and telomere length in the development and progression of premalignant lesions to colorectal cancer. *Clin Cancer Res* 1997;3: 1931–1941.
- 123 Daniels MJ, Wang Y, Lee M, Venkitaraman AR: Abnormal cytokinesis in cells deficient in the breast cancer susceptibility protein *BRCA2*. *Science* 2004;306:876–879.
- 124 Cahill DP, Kinzler KW, Vogelstein B, Lengauer C: Genetic instability and darwinian selection in tumours. *Trends Cell Biol* 1999;9:M57–M60.
- 125 Carroll PE, Okuda M, Horn HF, Biddinger P, Stambrook PJ, Gleich LL, Li YQ, Tarapore P, Fukasawa K: Centrosome hyperamplification in human cancer: chromosome instability induced by p53 mutation and/or *Mdm2* overexpression. *Oncogene* 1999;18:1935–1944.
- 126 Fuchs E, Cleveland DW: A structural scaffolding of intermediate filaments in health and disease. *Science* 1998;279:514–519.

- 127 Schliwa M, Euteneuer U, Graf R, Ueda M: Centrosomes, microtubules and cell migration. *Biochem Soc Symp* 1999;65:223–231.
- 128 Piel M, Nordberg J, Euteneuer U, Bornens M: Centrosome-dependent exit of cytokinesis in animal cells. *Science* 2001;291:1550–1553.
- 129 Griffin CS, Simpson PJ, Wilson CR, Thacker J: Mammalian recombination-repair genes *XRCC2* and *XRCC3* promote correct chromosome segregation. *Nat Cell Biol* 2000;2:757–761.
- 130 Shekhar MP, Lyakhovich A, Visscher DW, Heng H, Kondrat N: Rad6 overexpression induces multinucleation, centrosome amplification, abnormal mitosis, aneuploidy, and transformation. *Cancer Res* 2002;62:2115–2124.
- 131 Hinchcliffe EH, Sluder G: Centrosome reproduction in *Xenopus* lysates. *Methods Cell Biol* 2001;67:269–287.
- 132 Piel M, Bornens M: Centrosome reproduction in vitro: mammalian centrosomes in *Xenopus* lysates. *Methods Cell Biol* 2001;67:289–304.
- 133 Tomonaga T, Matsushita K, Ishibashi M, Nezu M, Shimada H, Ochiai T, Yoda K, Nomura F: Centromere protein H is up-regulated in primary human colorectal cancer and its overexpression induces aneuploidy. *Cancer Res* 2005;65:4683–4689.
- 134 Li GQ, Li H, Zhang HF: Mad2 and p53 expression profiles in colorectal cancer and its clinical significance. *World J Gastroenterol* 2003;9:1972–1975.
- 135 Michel L, Benezra R, Diaz-Rodriguez E: MAD2 dependent mitotic checkpoint defects in tumorigenesis and tumor cell death: a double edged sword. *Cell Cycle* 2004;3:990–992.
- 136 Shiloh Y: ATM and related protein kinases: safeguarding genome integrity. *Nat Rev Cancer* 2003;3:155–168.
- 137 Casper AM, Nghiem P, Arlt MF, Glover TW: ATR regulates fragile site stability. *Cell* 2002;111:779–789.
- 138 Smith L, Liu SJ, Goodrich L, Jacobson D, Degnin C, Bentley N, Carr A, Flaggs G, Keegan K, Hoekstra M, Thayer MJ: Duplication of ATR inhibits MyoD, induces aneuploidy and eliminates radiation-induced G<sub>1</sub> arrest. *Nat Genet* 1998;19:39–46.
- 139 Kuhn EM: Localization by Q-banding of mitotic chiasmata in cases of Bloom's syndrome. *Chromosoma* 1976;57:1–11.
- 140 Goss KH, Risinger MA, Kordich JJ, Sanz MM, Straughen JE, Slovek LE, Capobianco AJ, German J, Boivin GP, Groden J: Enhanced tumor formation in mice heterozygous for *Blm* mutation. *Science* 2002;297:2051–2053.
- 141 Moynahan ME, Pierce AJ, Jasin M: BRCA2 is required for homology-directed repair of chromosomal breaks. *Mol Cell* 2001;7:263–272.
- 142 Davies AA, Masson JY, McIlwraith MJ, Stasiak AZ, Stasiak A, Venkiteraman AR, West SC: Role of BRCA2 in control of the RAD51 recombination and DNA repair protein. *Mol Cell* 2001;7: 273–282.
- 143 Sanchez C, Perez M, Avila J: GSK3beta-mediated phosphorylation of the microtubule-associated protein 2C (MAP2C) prevents microtubule bundling. *Eur J Cell Biol* 2000;79:252–260.
- 144 Goold RG, Owen R, Gordon-Weeks PR: Glycogen synthase kinase 3beta phosphorylation of microtubule-associated protein 1B regulates the stability of microtubules in growth cones. *J Cell Sci* 1999;112 (Pt 19):3373–3384.
- 145 Chen Y, Riley DJ, Chen PL, Lee WH: HEC, a novel nuclear protein rich in leucine heptad repeats specifically involved in mitosis. *Mol Cell Biol* 1997;17:6049–6056.
- 146 Pei L, Melmed S: Isolation and characterization of a pituitary tumor-transforming gene (PTTG). *Mol Endocrinol* 1997;11:433–441.
- 147 Yu R, Lu W, Chen J, McCabe CJ, Melmed S: Overexpressed pituitary tumor-transforming gene causes aneuploidy in live human cells. *Endocrinology* 2003;144:4991–4998.
- 148 Ekholm-Reed S, Spruck CH, Sangfelt O, van Drogen F, Mueller-Holzner E, Widschwendter M, Zetterberg A, Reed SI: Mutation of hCDC4 leads to cell cycle deregulation of cyclin E in cancer. *Cancer Res* 2004;64:795–800.
- 149 Baker SJ, Markowitz S, Fearon ER, Willson JK, Vogelstein B: Suppression of human colorectal carcinoma cell growth by wild-type p53. *Science* 1990;249:912–915.

- 150 Spruck CH, Won KA, Reed SI: Deregulated cyclin E induces chromosome instability. Nature 1999;401:297–300.
- 151 O’Hagan RC, Chang S, Maser RS, Mohan R, Artandi SE, Chin L, DePinho RA: Telomere dysfunction provokes regional amplification and deletion in cancer genomes. Cancer Cell 2002;2: 149–155.

Riccardo Fodde  
Dept. of Pathology  
Josephine Nefkens Institute  
ErasmusMC, PO Box 1738  
3000 DR Rotterdam (The Netherlands)  
Tel. +31 10 408 84 90, Fax +31 10 408 84 50, E-Mail r.fodde@erasmusmc.nl

**© Free Author  
Copy - for per-  
sonal use only**

PLEASE NOTE THAT ANY  
DISTRIBUTION OF THIS AR-  
TICLE WITHOUT WRITTEN  
CONSENT FROM S. KARGER  
AG, BASEL IS A VIOLATION  
OF THE COPYRIGHT.

Upon request a written per-  
mission to distribute the PDF  
file will be granted against  
payment of a permission fee  
depending on the number of  
accesses required. Please  
contact Karger Publishers,  
Basel, Switzerland at  
permission@karger.ch

---

## Chapter 2.

***APC* and oncogenic *KRAS* are synergistic in enhancing Wnt signaling in intestinal tumor formation and progression.**

***Gastroenterology. 2006;131:1096-109.***



## APC and Oncogenic KRAS Are Synergistic in Enhancing Wnt Signaling in Intestinal Tumor Formation and Progression

KLAUS-PETER JANSSEN,\*† PAOLA ALBERICI,§ HAFIDA FSIHI,\* CLAUDIA GASPAR,§ COR BREUKEL,|| PATRICK FRANKEN,§ CHRISTOPHE ROSTY,† MIGUEL ABAL,\* FATIMA EL MARJOU,\* RON SMITS,§ DANIEL LOUWARD,\* RICCARDO FODDE,§ and SYLVIE ROBINE\*

\*UMR144 Institut Curie, Paris, France; †Klinikum rechts der Isar, TUM, Munich, Germany; §Department of Pathology, Josephine Nefkens Institute, Erasmus UMC, Rotterdam, The Netherlands; ||Center for Human & Clinical Genetics, LUMC, Leiden, The Netherlands; and †Pathology Service, Institut Curie, Paris, France

**Background & Aims:** Synchronous activation of the Wnt signaling pathway, mostly because of loss of function of the APC tumor suppressor, and of the oncogenic KRAS-signaling pathway is very frequent in colorectal cancer and is associated with poor prognosis. **Methods:** We have generated a compound transgenic mouse model, *KRAS*<sup>V12G</sup>/*Apc*<sup>+ /1638N</sup>, to recapitulate the human disease and compared it with single transgenic littermates. **Results:** Compound mutant mice are characterized by a 10-fold increase in tumor multiplicity and by accelerated tumor progression, resulting in strongly enhanced morbidity and mortality. Tumors from compound mutant mice proliferate faster and show decreased levels of apoptosis. Several lines of evidence indicate that the observed increase in tumor multiplicity and malignant transformation is caused by the synergistic activation of Wnt signaling in cells with oncogenic KRAS and loss-of-function *Apc* mutations. Activated KRAS is known to induce tyrosine phosphorylation of  $\beta$ -catenin, leading to its release from E-cadherin at the adherens junction. This results in an increased  $\beta$ -catenin pool in the cytoplasm, its subsequent translocation to the nucleus, and the transcriptional activation of Wnt downstream target genes. Accordingly, intestinal tumors from *KRAS*<sup>V12G</sup>/*Apc*<sup>+ /1638N</sup> mice show a significant increase in cells with nuclear accumulation of  $\beta$ -catenin when compared with *Apc*<sup>+ /1638N</sup> animals. Moreover, *Apc*/*KRAS*-mutant embryonic stem cells show a significantly enhanced  $\beta$ -catenin/T-cell factor-mediated transcriptional activation, accompanied by increased  $\beta$ -catenin nuclear localization. **Conclusions:** This KRAS-induced increase in Wnt/ $\beta$ -catenin signaling may enhance the plasticity and self-renewal capacity of the tumor, thus resulting in the drastically augmented tumor multiplicity and malignant behavior in compound mutant animals.

Colorectal cancer (CRC) and in particular the adenoma-carcinoma sequence still represents a paradigm for the molecular and genetic mechanisms underlying tumor formation and progression.<sup>1,2</sup> Cancers of the colon and rectum are among the most frequent cause of morbidity and mortality among Western industrialized countries.<sup>3,4</sup> In the vast majority of sporadic CRC cases, mutations in genes known to play rate-limiting roles in the canonical Wnt/ $\beta$ -catenin signal transduction pathway such as the adenomatous polyposis coli (*APC*) tumor suppressor gene and the  $\beta$ -catenin (*CTNNB1*) oncogene trigger adenomatous polyp formation, the first step toward colorectal neoplasia.<sup>5</sup> Activating mutations of the *KRAS* oncogene accompany adenoma growth and progression, whereas

loss of heterozygosity (LOH) and mutations at the *SMAD4* and *TP53* tumor suppressor genes underlie malignant transformation at later stages.<sup>1</sup> Loss-of-function mutations at *APC* have been observed in more than 60% of colonic adenomas and carcinomas.<sup>6</sup> Also, germ-line *APC* mutations are responsible for familial adenomatous polyposis (FAP), an autosomal dominant predisposition to the development of multiple colorectal polyps.<sup>7</sup> Loss of *APC* function results in constitutive activation of Wnt signaling because of impaired  $\beta$ -catenin down-regulation, leading to its cytoplasmic accumulation and nuclear translocation.<sup>8,9</sup> In the nucleus, upon association with members of the T-cell factor (TCF) family of transcriptional activators,  $\beta$ -catenin differentially modulates the expression of Wnt downstream target genes implicated in cell proliferation, migration, differentiation, and apoptosis<sup>10</sup> (<http://www.stanford.edu/~rnusse/pathways/targets.html><sup>11</sup>). Approximately 50% of colorectal adenomas and carcinomas carry activating mutations of the *RAS* protooncogene.<sup>1,12</sup> The *KRAS* gene is an effective marker for molecular diagnosis and tumor progression in colorectal, pancreas, and lung cancer. Oncogenic *RAS* proteins are locked in their guanosine triphosphate (GTP)-bound (active) form and mediate their tumorigenic effects through multiple downstream effectors, the most prominent of which, the *RAS* effector RAF kinase, activates on its turn the extracellular signal-regulated kinase (ERK)-mitogen-activated protein (MAP) kinase (MAPK) cascade.<sup>13–15</sup> Activated MAP kinases phosphorylate downstream transcription factors, thus inducing the expression of regulatory genes required for entry into the S phase of the cell cycle.<sup>16,17</sup> Thus, activation of the Wnt as well as of the *RAS* signal transduction pathways plays a rate-limiting role in human CRC formation and progression. Both *APC* and *KRAS* mutations occur in aberrant crypt foci, microscopic precursor lesions that have been postulated to precede the development of adenomatous polyps.<sup>18</sup> *APC* mutations are associated with dysplasia in small precursor lesions, whereas *KRAS* mutations are more often found in nondysplastic lesions.<sup>19</sup> Also, synchronous detection of activated *KRAS* and of  $\beta$ -catenin nuclear accumulation, the hallmark of canonical Wnt-signaling activation, identifies a group of CRC patients with poor prognosis and

**Abbreviations used in this paper:** APC, adenomatous polyposis coli; CRC, colorectal cancer; CSC, cancer stem cell; ES, embryonic stem; GTP, guanosine triphosphate; LOH, loss of heterozygosity; MAPK, mitogen-activated protein kinase; TCF, T-cell factor; WT, wild-type.

© 2006 by the American Gastroenterological Association (AGA) Institute

0016-5085/06/\$32.00

doi:10.1053/j.gastro.2006.08.011

resistance to standard chemotherapy.<sup>20</sup> However, whether the frequent concurrent activation of *RAS* and the Wnt pathways in colorectal tumors is due to a cumulative effect or to a more synergistic interaction between the 2 signaling cascades is still largely unknown. To address this clinically relevant issue, we have generated a mouse model that carries both a targeted loss-of-function mutation at the endogenous *Apc* gene<sup>21</sup>, *Apc*<sup>1638N</sup>, and a transgene encoding for the activated form of the human *KRAS* oncogene, the pVillin-*KRAS*<sup>V12G</sup> (hereafter further referred to as *KRAS*<sup>V12G</sup>).<sup>22</sup> Compound animals are characterized by a striking increase in intestinal tumor multiplicity and progression, leading to high morbidity and mortality. Molecular analysis of these tumors and of primary cell lines carrying both mutations indicate that enhanced Wnt-signalling activity by oncogenic *KRAS* is likely to underlie the increased tumor initiation and progression toward malignancy in the compound *Apc/KRAS* animals.

## Materials and Methods

### Animal Models

All experiments on mice were performed in accordance with institutional and national guidelines and regulations. The *Apc*<sup>1638N</sup> mouse lineage in the inbred C57Bl/6J background<sup>21</sup> was bred with the transgenic model<sup>22</sup> pVillin-*KRAS*<sup>V12G</sup> in the genetic background B6D2 (C57Bl/6J × DBA/2). To control for genetic background effects, littermates were always used as controls. Mice were maintained under a 12-hour light-dark cycle and fed with standard diet and water ad lib. Genotyping was performed on DNA extracted from mouse tails as previously described.<sup>22,23</sup>

### Tumor Analysis and Tissue Processing

The median age of the analyzed animals was 5.5 months (*KRAS*<sup>V12G</sup>/*Apc*<sup>+1638N</sup>), 7 months (*Apc*<sup>+1638N</sup>), and 9 months (*KRAS*<sup>V12G</sup>). Animals were killed at the ages indicated or at the appearance of signs of distress, and the gross study of the tissues was carried out as described.<sup>22</sup> Macroscopically visible tumors were resected and embedded in paraffin according to standard procedures. Tumors were classified according to standard World Health Organization (WHO) histopathologic criteria by an experienced pathologist. In addition to the processing for histopathologic analysis, a subset of freshly isolated tumors was also snap frozen in liquid nitrogen and stored at -80°C. Frozen tumors were either used for DNA/RNA extraction (Qiagen, Hilden, Germany) or embedded in Tissue-Tek (Sakura B.V., Zoeterwoude, The Netherlands) and processed for cryosections. Kidneys, liver, and lungs of all animals were also investigated for the presence of metastases by macroscopic and, in a selected number of cases, microscopic analysis of serial sections. For protein analysis, snap-frozen mouse tissue or scrapings of intestinal mucosa were lysed in ice-cold lysis buffer (50 mmol/L Tris-HCl, pH 7.5, 150 mmol/L NaCl, 1 mmol/L benzamidine, 1 mmol/L PMSF, 1 mmol/L DTT, 2 mmol/L EGTA, 1% Triton X-100, 1% NP-40, Mammalian Protease Inhibitor Cocktail; Sigma Chemical Co, St. Louis, MO) using a 1-mL Dounce Homogenizer. After centrifugation (15,000g, 15 minutes, 4°C), supernatants were collected, and protein concentration was determined (Bio-Rad assay, Richmond, CA).

### LOH Analysis

LOH of the *Apc* and *Tp53* genes was determined by PCR amplification of dinucleotide repeat markers.<sup>22,24</sup> DNA was isolated from microdissected tumors and from normal intestinal tissue with an RNA/DNA extraction kit (Qiagen). Primer sequences were obtained from the Mouse Genome Database.<sup>22,25</sup> The following polymorphic markers were used for the *Apc* locus: D18Mit64, D18Mit111, D18Mit132, and D18Mit17 and for the *Tp53* locus: D11Mit4, D11Mit30, and D11Mit278. LOH was defined at *P* < .05 for 3 independent PCR reactions.<sup>22,26</sup> A functional assay previously described was used to validate the pathogenicity of molecular changes at the *Tp53* gene.<sup>22,26,27</sup>

### RT-PCR Analysis of Wnt Downstream Targets in Intestinal Tumors

C-myc and cyclin D1 messenger RNA (mRNA) expression levels were analyzed in normal mucosa and tumors (*n* = 5 mice/genotype). RNA was harvested from snap-frozen tissues using the RNeasy extraction kit (Qiagen). Up to 2 μg of total RNA was then subjected to reverse transcription using Superscript II Reverse Transcriptase (Invitrogen Life Technologies, Carlsbad, CA) and oligo dT primers (pd(N)6, Roche, Mannheim, Germany). Reactions were carried out in SybrGreen PCR Master mix (Applied Biosystems, Courtaboeuf Cedex, France) under recommended conditions, run on ABI PRISM 7900, and analyzed with Sequence Detector Software (Applied Biosystems). Relative quantities were calculated using the ddCT formula and normalized to the transcript levels of the housekeeping gene TATA binding protein (TBP). Assays were performed in triplicate. Primer sequences used were as follows: TBP: forward, CCACGGACAACCTGCGTTGAT; reverse, GGCTCAT-AGCTACTGAACTG. c-myc: forward, TAGTGCTGCATGAG-GAGACA; reverse, GGTGGCTCTTCTCCACAG. cyclinD1: forward, CACAACGCACCTTCTTCCAG; reverse, CGCAG-GCTTGACTCCAGAAG.

### Detection of Liver Micrometastases by RT-PCR

Mouse livers were dissected under sterile conditions to avoid contamination. Liver RNA was extracted from different tissues using the RNA Now Kit (Ozyme, St Quentin, France). RT-PCR reactions were performed as previously described.<sup>22,28</sup> Primers were used that amplify specifically the transgenic *KRAS*<sup>V12G</sup> gene under control of the villin promoter. The sense primer is specific to the villin promoter, CAAGCCTGGCTC-GACGGCC, and the antisense primer recognizes the coding sequence of the human *KRAS*<sup>V12G</sup> gene, ATTTGCGGCCGCTT-TACATAATTACACACT, yielding a fragment of 400 base pair. PCR reactions were repeated twice for each sample, and RNA was extracted twice from each tissue to confirm the result. Direct sequencing of the fragment confirmed the identity of the transgenic *KRAS*<sup>V12G</sup>.

### Western Blot Analysis

Equal amounts (40 μg) of protein lysate were separated on 13% polyacrylamide gels and further subjected to immunoblotting according to standard procedures. Primary antibodies used were as follows: anti-pan-Ras (Transduction

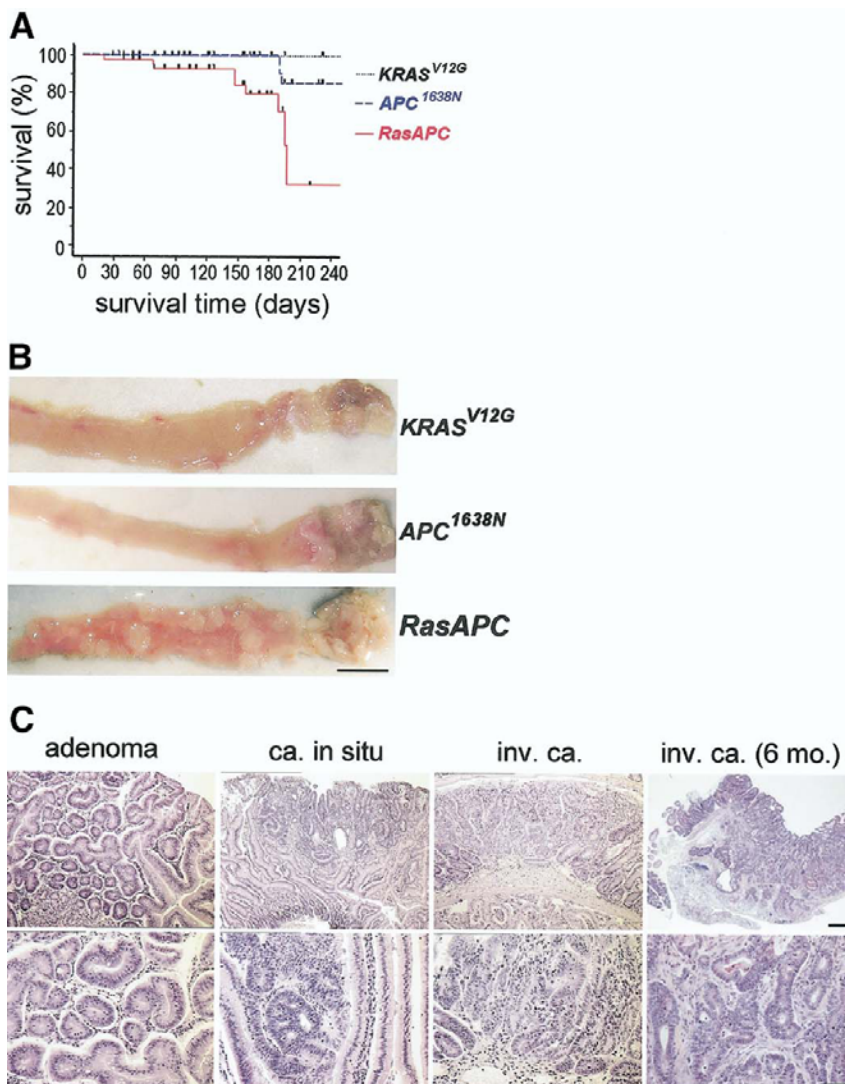


**Figure 1.** Increased tumor multiplicity and progression in  $KRAS^{V12G}/Apc^{+/1638N}$  mice (A) Kaplan–Meier survival analysis of  $KRAS^{V12G}/Apc^{+/1638N}$  mice and their single transgenic littermates.  $RasAPC$ , compound mutant mice ( $n = 50$  mice/genotype; intergroup difference at  $P < .001$ ). (B) Macroscopic view of longitudinally dissected small intestinal tissue specimens representative for 6 months of age. No tumors can be observed in  $KRAS^{V12G}$  mice at this age, and few (2–4) lesions in  $Apc^{+/1638N}$  mice.  $KRAS^{V12G}/Apc^{+/1638N}$  ( $RasAPC$ ) mice show abundant, multiple lesions throughout the upper GI tract. Scale bar = 1 cm. (C) H&E stained sections from  $KRAS^{V12G}/Apc^{+/1638N}$  animals. Left to right: benign adenoma at 3.5 months; in situ carcinoma at 3.5 months; invasive adenocarcinoma at 3.5 months; invasive carcinoma at 6 months. Scale bars = 200  $\mu$ m (upper row) and 50  $\mu$ m (lower row).

Laboratories, Lexington, KY), anti- $\beta$ -Actin (Sigma), anti- $\beta$ -catenin (Transduction Lab.), anti-E-cadherin, anti-phospho-(Thr202, Tyr204)-p44/42 MAPK, anti-p44/42 MAPK, anti-phospho-(Thr308)-Akt, anti-phospho-(Ser473)-Akt, anti-Akt (all Cell Signaling, New England Biolabs, Beverly, MA). Peroxidase-conjugated secondary antibodies (Jackson ImmunoResearch, West Grove, PA) were visualized with an ECL kit (Pierce, Rockford, IL).<sup>22</sup>

### GTPase Activity Assays

GTP-Ras pull-down assays were performed on mouse tissue lysates as previously described.<sup>22</sup> GTP-Ras pull-down assays on embryonic stem (ES) cells followed essentially the same protocol; the cells were first washed with ice-cold phosphate-buffered saline (PBS) and then incubated in lysis buffer.<sup>22,28</sup> Samples were run on 13% SDS-PAGE gels and trans-

**Table 1.** Incidence and Distribution of Intestinal Neoplasia in *KRAS*<sup>V12G</sup>/*Apc*<sup>+ /1638N</sup> Mice

Genotype	Median age (range)	Mice, n	Incidence n	Tumors/ animal mean ± SD	Tumor range (absolute no. of tumors)	Size distribution (S/M/L) (%)	Tumor localization
<i>KRAS</i> <sup>V12G</sup>	9 mo (4–16)	22	13/22 59%	1.9 ± 2.4	0–8	12/88/0	P: 4%; D: 32%; J: 55%; I: 23%; C: 0%
<i>Apc</i> <sup>+ /1638N</sup>	7 mo (4–20)	20	20/20 100%	4.3 ± 2.3	1–10	12/38/50	P: 88%; D: 100%; J: 38%; I: 0%; C: 19%
<i>KRAS</i> <sup>V12G</sup> / <i>Apc</i> <sup>+ /1638N</sup>	5 mo (4–7)	20	20/20 100%	29.5 ± 12.0	12–59	22/58/20	P: 58%; D: 100%; J: 100%; I: 41%; C: 41%

NOTE. Size distribution (diameter): small, <1 mm; medium, 1–3 mm; large, >3 mm. Tumor localization = incidence of lesions in periampullar region (P), duodenum (D), jejunum (J), ileum (I), colon (C).

ferred to membranes. Immunodetection was performed with anti-Ras antibody (Cell Signaling). The amount of GTP-bound GTPases was normalized to the total amount of GTPases present in whole cell lysates.

**Flow Cytometry**

Flow cytometry from mouse tissue was carried out essentially as described.<sup>22</sup> For each genotype, 2 mice were injected intraperitoneally with 0.01 mL/g body weight of a 6 mg/mL solution of 5-bromo-2'-deoxyuridine (BrdU; Sigma). Animals were killed 2 hours after bromodeoxyuridine (BrdU) injection and dissected. Bivariate distributions of BrdU content (FITC) vs DNA content (propidium iodide) were measured using a FACScan flow cytometer (Becton Dickinson, San Jose, CA). Doublets and clumps were excluded from the analysis by gating on a bivariate distribution of the propidium iodide area vs signal width.

**Immunohistochemistry Analysis of Tissue Sections**

Cryosections of Tissue-tek OCT (Sakura) embedded mouse tissues were cut at 5-µm thickness, air-dried, and fixed with 3% paraformaldehyde at room temperature for 20 minutes. The paraformaldehyde-fixed sections were treated with 50 mmol/L NH<sub>4</sub>Cl in PBS for 20 minutes, and solubilized with 0.1% Triton X-100 for 5 minutes. Antibodies and reagents used were as follows: anti-β-catenin (dilution 1:200; Transduction Laboratories Clone 14); pAb anti-Ki67 (Novocastra, Newcastle, UK); cleaved caspase-3 (Cell Signaling); Peroxidase-, Cy3-, or Alexa488-conjugated secondary antibodies (Jackson Immuno-research); and TRITC-phalloidin and Hoechst 33258 (Sigma). Cells and tissue sections were viewed using a fluorescence mi-

croscope (Zeiss, Göttingen, Germany) or a confocal microscope (LSM510, Zeiss, Göttingen, Germany). Images were processed using Adobe Photoshop Software (San Jose, CA). For evaluation of β-catenin staining, antigen retrieval treatment was performed (10 minutes in boiling 10 mmol/L Tris/Cl, 1 mmol/L EDTA, pH 8.0), followed by incubation with the specific antibody overnight at 4°C. Localization of peroxidase activity was detected with the SIGMA FAST DAB system (Sigma), after brief hematoxylin counterstaining.

For the comparative evaluation of nuclear β-catenin accumulation between tumors derived from *Apc*<sup>+ /1638N</sup> and *KRAS*<sup>V12G</sup>/*Apc*<sup>+ /1638N</sup> mice, a previously established protocol was used<sup>29</sup> based on 2 independent blinded observers. In brief, tumor cells with nuclear β-catenin were counted from immunohistochemistry (IHC) sections and scored according to staining intensity when compared with the few normal crypt cells within the same section that, as previously reported, also encompass nuclear β-catenin. The ratio between the tumor area, measured in millimeters squared, using the PALM MicroBeam microscope system (P.A.L.M. Microlaser Technologies AG-Bernried, Germany), and the absolute numbers of positive cells were calculated for each tumor sample based on at least 2 serial sections representative of the whole tumor. Statistical analysis was performed using R software (version 1.9.1., Free Software Foundation, Boston, MA).

**Generation of *Apc*/*KRAS* Mutant ES Cell Lines**

ES cell lines containing both *Apc* and *KRAS* mutations were generated by stable cotransfection by electroporation of wild-type and *Apc*<sup>1638N/1638N</sup> ES cell lines (E14; 129 Ola) with a pPGK expression vector containing either the human wild-type

**Table 2.** Onset and Development of Neoplasia in *KRAS*<sup>V12G</sup>/*Apc*<sup>+ /1638N</sup> Mice

Genotype	3–5 Mo			6–12 Mo			>12 Mo		
	Incidence, n	Tumors/ animal	Size S/M/L (%)	Incidence, n	Tumors/ animal	Size S/M/L (%)	Incidence, n	Tumors/ animal	Size S/M/L (%)
<i>KRAS</i> <sup>V12G</sup>	0/4	0	—	6/10 60%	1.4	21/79/0	6/8 75%	3.4	7/93/0
<i>Apc</i> <sup>+ /1638N</sup>	7/8 88%	1.9	54/46/0	6/6 100%	3.8	14/36/50	6/6 100%	6.0	3/28/69
<i>KRAS</i> <sup>V12G</sup> / <i>Apc</i> <sup>+ /1638N</sup>	14/14 100%	15.4	32/51/17	6/6 100%	32.8	19/56/25	—	—	—

NOTE. Size distribution (diameter): small, <1 mm; medium, 1–3 mm; large, >3 mm.

**Table 3.** Histopathologic Staging of Tumors at 3.5 Months of Age

Genotype	Mice (n)	Adenoma	Carcinoma <i>in situ</i>	Carcinoma inf.	Tumors (n)	Adenoma/carcinoma ratio
<i>KRAS</i> <sup>V12G</sup>	4	0	0	0	0	—
<i>Apc</i> <sup>+ /1638N</sup>	4	4	3	1	8	1:1
<i>KRAS</i> <sup>V12G</sup> / <i>Apc</i> <sup>+ /1638N</sup>	4	3	15	16	34	1:10.3 <sup>a</sup>

NOTE. Carcinoma inf. = infiltrative carcinoma, invasion through the *muscularis mucosae* into the *submucosa*.

<sup>a</sup>*P* = .0167, Fisher exact test.

*KRAS* or the human oncogenic *KRAS*<sup>V12G</sup> together with a pPGK-puromycin selection vector. To select for stable clones, the ES cells were cultured in the presence of puromycin (Sigma) at a final concentration of 2 μg/mL for 2 weeks.

### TOPFLASH/FOPFLASH Reporter Assays

Twenty hours before transfection, 10<sup>5</sup> ES cells per well were plated on tissue culture plates coated by primary, mitomycin C inactivated, murine embryonic fibroblasts. ES cells were transfected in each well with 500 ng of pTOPFLASH or pFOPFLASH vector (kindly provided by Dr H. Clevers) and 5 ng luciferase from *Renilla reniformis* using Lipofectamine 2000 (Life Technologies) as recommended by the manufacturer. After 24 hours, luciferase activities were measured in a luminometer (Lumat LB 9507, Berthold, Bad Wildbad, Germany) and normalized for transfection efficiency by the Dual Luciferase Reporter Assay system (Promega, Madison, WI). Luciferase activities were evaluated as ratio of pTOPFLASH vs pFOPFLASH levels for 3 different experiments, each carried out in duplicate.

### Annexin V Staining of ES Cells

ES cells were prepared following the Vibrant Apoptosis Assay kit No. 2 protocol (Molecular Probes). Five thousand events were analyzed per test in list mode using a FACScan flow cytometer (Becton Dickinson, San Jose, CA). To quantify changes associated with cell differentiations, 2 regions were created on the dot-plot graphs using the Forward Scatter/Side Scatter. Bivariate distributions of Annexin-V content (Alexa 488) vs DNA content (PI) were measured. Mean ± SD of 3 experiments is shown.

### Expression Profiling by Oligonucleotide Microarray

Tumor-specific expression profiles were analyzed in 4 *Apc*<sup>+ /1638N</sup> and 4 *KRAS*<sup>V12G</sup>/*Apc*<sup>+ /1638N</sup> tumors collected from a total of 7 mice of 6–8 months of age and same genetic background. All tumors were highly dysplastic and localized in the upper duodenum. Samples were laser-capture microdissected (LCM) from cryosections of Tissue-tek OCT (Sakura) embedded snap-frozen tumors. Ten-micrometer sections were briefly stained with H&E, and consecutive sections were carefully microdissected using a PALM MicroBeam microscope system (P.A.L.M. Microlaser Technologies AG- Bernried, Germany). On average, 2000 cells were isolated from each sample. The RNA was isolated using the Rneasy kit (QIAGEN) with a DNase digestion step. Quality of RNA was checked on 2100 Bioanalyzer (Agilent Technologies, Inc, Waldbronn, Germany) and labeled according to Affymetrix protocols for 2 rounds of amplification (Small Sample Labeling Protocol vII). Labeled cRNA was hybridized to Genechip MOE430A arrays (Affymetrix, Inc., Santa Clara, CA) according to standard protocols. Data were

normalized using vsn software (variance stabilization and calibrations for microarray data) using a package provided by Bioconductor.<sup>30</sup> The hierarchical *t* test<sup>31</sup> was performed in the R (version 1.9.1) environment.<sup>32</sup> Unsupervised clustering was performed using the Rosetta software (Rosetta Inpharmatics LLC, Knowledge Systems Group, Dept. of Computer and Information Science, Norwegian University of Science and Technology, Trondheim, Norway).

## Results

### Intestinal Tumor Multiplicity and Progression Is Significantly Increased in *KRAS*<sup>V12G</sup>/*Apc*<sup>+ /1638N</sup> Mice

To study the interaction between oncogenic *KRAS* and deregulated Wnt pathway, we bred transgenic mice expressing the activated human *KRAS*<sup>V12G</sup> oncogene driven by the intestine-specific villin promoter<sup>22</sup> with *Apc*<sup>+ /1638N</sup> mice carrying a targeted nonsense mutation at the endogenous *Apc* gene.<sup>21</sup> Compound mutant mice showed significant increase in morbidity and mortality when compared with the single transgenic littermates (Figure 1A, see Supplementary Table 1 online at [www.gastrojournal.org](http://www.gastrojournal.org)). In fact, no compound mutant animal survived for more than 33 weeks. We examined and counted the occurrence of tumors in the gastrointestinal tract from compound *KRAS*<sup>V12G</sup>/*Apc*<sup>+ /1638N</sup> mice and compared those with their control littermates at 6–12 months of age or when moribund. Compound *KRAS*<sup>V12G</sup>/*Apc*<sup>+ /1638N</sup> animals (n = 20) developed an average of 29.5 tumors per mouse (Figure 1B; Table 1). This represents a highly significant 15-fold and 7-fold increase over *KRAS*<sup>V12G</sup> and *Apc*<sup>+ /1638N</sup> animals, respectively (*P* < .001, Mann–Whitney rank sum test). The increase in tumor multiplicity was already apparent in young animals (Tables 2 and 3).

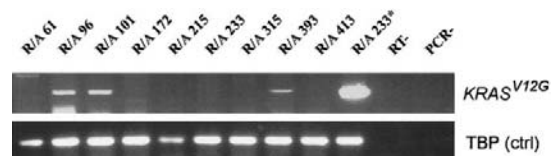


**Figure 2.** Detection of disseminated tumor cells in the livers from *Apc*<sup>1638N/+</sup>/*KRAS*<sup>V12G</sup> animals. Detection of the transgenic *KRAS*<sup>V12G</sup> transcript with a specific primer combination that only recognizes transgenically expressed *KRAS* but not endogenous *KRAS*. The mucosa from a compound mutant animal was used as positive control (R/A 233\*). Six out of 22 livers tested were positive (27%). Positive bands were sequenced in all cases to confirm the identity of the oncogenic *KRAS* transcript. The control transcript *TBP* is expressed ubiquitously; lanes labeled (RT-) and (PCR-) indicate negative controls without reverse transcriptase and without cDNA template, respectively.

A broad spectrum of tumor stages was found, ranging from aberrant crypts and small dysplastic polyps, to large invasive carcinomas (Figure 1C). Pseudoinvasion was ruled out because the invasive front of the tumor was observed on several serial sections, invariably encompassing multiple glands and in association with stromal reaction. All compound mutant mice had lesions in both duodenum and jejunum, and tumors of the large intestine occurred more frequently (41%) than in *Apc*<sup>+/-1638N</sup> littermates (19%). To evaluate tumor progression, 4 animals of each genotype were killed at 3.5 months, and tissue sections covering complete segments of the small intestine were carefully scored. As expected for this age, we did not detect lesions in *KRAS*<sup>V12G</sup> mice.<sup>22</sup> In the *Apc*<sup>+/-1638N</sup> littermates, half of the lesions had progressed to malignancy (adenoma/carcinoma ratio of 1:1) (see Supplementary Figure 1 online at [www.gastrojournal.org](http://www.gastrojournal.org)). In contrast, the compound mutant mice showed an adenoma/carcinoma ratio of 1:10 (*P* = .0167, Fisher

exact test; Table 3). No metastases were observed by histopathologic analysis of mesenteric lymph nodes, livers, and lungs from *KRAS*<sup>V12G</sup>/*Apc*<sup>+/-1638N</sup> mice carrying locally invasive carcinomas. However, we detected disseminated intestinal tumor cells in livers from compound mice by RT-PCR. By using primers that specifically amplify the mRNA from the *KRAS*<sup>V12G</sup> transgene under control of the villin promoter, exclusively expressed in intestinal epithelial cells and in tumor cells derived from these epithelia, transcripts were detected in 6 of 22 livers from compound mutant animals (Figure 2). To control for the specificity of the assay, livers from wild-type animals and from tumor-bearing *KRAS*<sup>V12G</sup> animals (n = 10, mean age: 17.5 months) were analyzed, and none was found positive.

**Somatic Loss of the Wild-Type *Apc* Allele and Expression of Oncogenic *KRAS*<sup>V12G</sup> in *KRAS*<sup>V12G</sup>/*Apc*<sup>+/-1638N</sup> Tumors**

LOH at the *APC* locus characterizes the vast majority of tumors from FAP and sporadic CRC patients and from mouse models carrying heterozygous *Apc* mutations.<sup>5,33</sup> Out of 10 intestinal lesions from *KRAS*<sup>V12G</sup>/*Apc*<sup>+/-1638N</sup> animals analyzed, all showed LOH at the wild-type *Apc* locus regardless of size and histologic stage of the tumors analyzed (Figure 3A). In contrast, we could not detect mutations in the tumor suppressor gene *TP53* in 7 tumors from *KRAS*<sup>V12G</sup>/*Apc*<sup>+/-1638N</sup> animals, using a yeast-based functional assay.<sup>22</sup> Furthermore, only 1 out of 10 tumors from *KRAS*<sup>V12G</sup>/*Apc*<sup>+/-1638N</sup> mice revealed LOH at *TP53* (not shown). In *KRAS*<sup>V12G</sup> tumors, *TP53* LOH and point mutations occur in 40% of the cases.<sup>22</sup>

Expression levels of the *KRAS*<sup>V12G</sup> transgene in both normal intestinal mucosa and tumors were stable but rather low; the amount of transgene was 12% ± 3% of total endogenous Ras (Figure 2B). A GTP-Ras pull-down assay showed clear activity in small intestinal mucosa and tumor extracts from compound

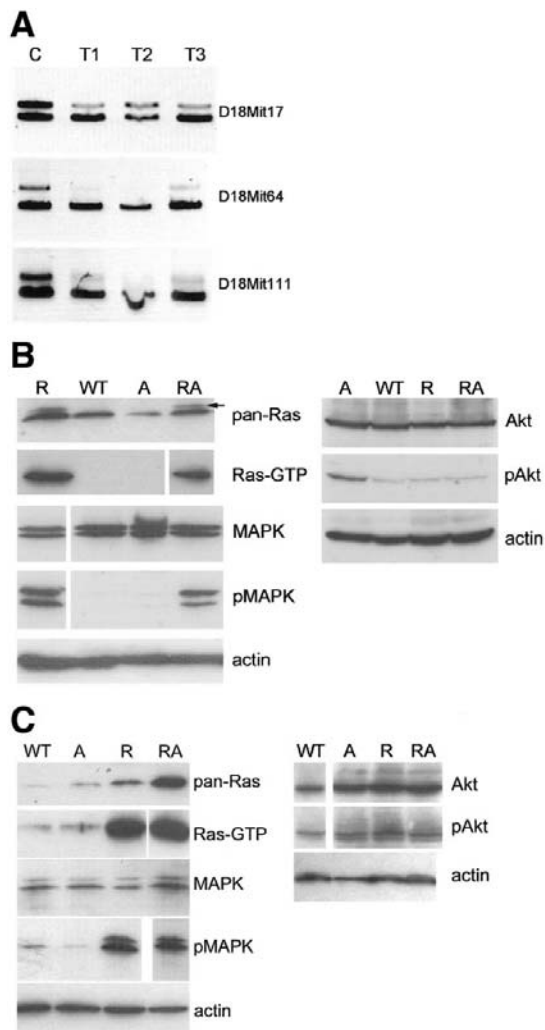
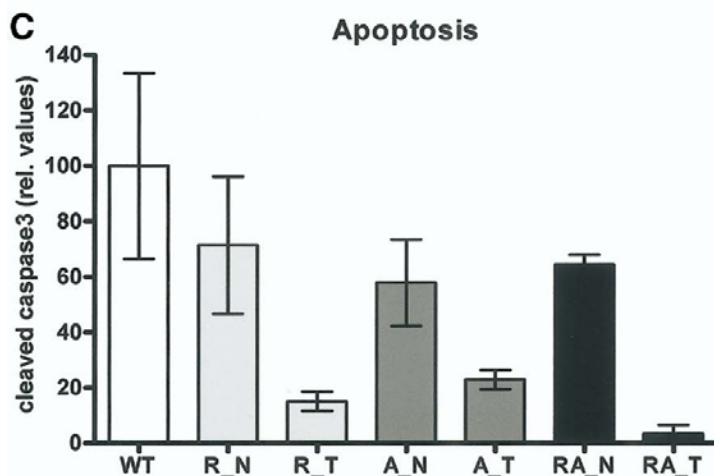
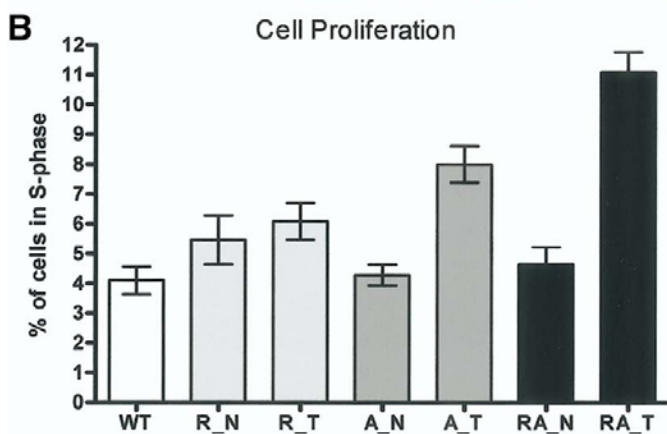
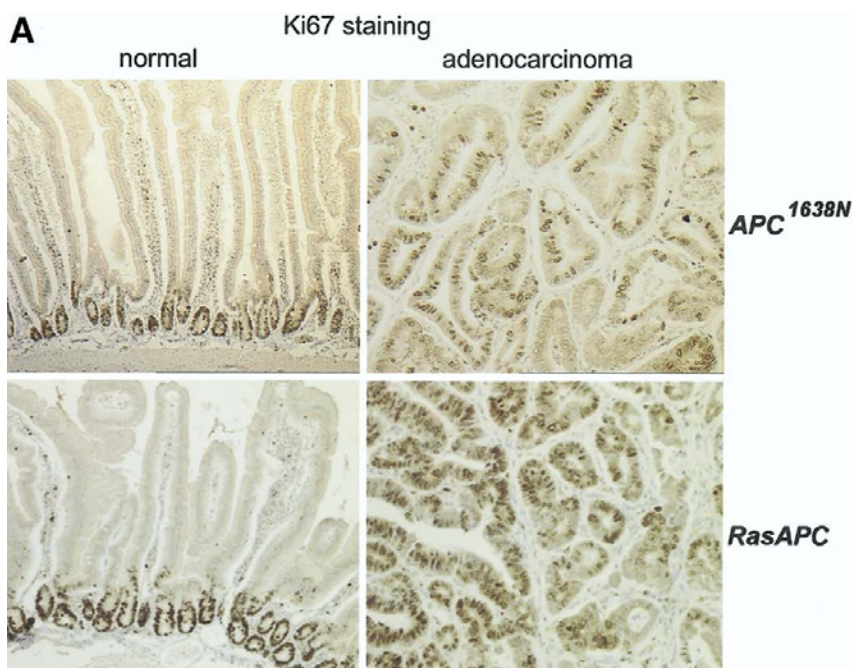


**Figure 3.** (A) Loss of heterozygosity (LOH) at the *Apc* locus in tumors from *KRAS*<sup>V12G</sup>/*Apc*<sup>+/-1638N</sup> animals. (A) Three microsatellite markers were PCR amplified from control tissue (C) and 3 independent tumors (*T1*, *T2*, *T3*) of a *KRAS*<sup>V12G</sup>/*Apc*<sup>+/-1638N</sup> animal. The position of the employed chromosome 18 markers relative to the *Apc* locus (15 centiMorgan [cM]) are *D18Mit64* (2 cM), *D18Mit111* (11 cM), and *D18Mit17* (20 cM). (B) Oncogenic *KRAS*<sup>V12G</sup> activates MAP kinase, but not AKT, in mouse intestinal epithelia. Total Ras, GTP-Ras pull down, MAPK, and AKT activation analysis in intestinal mucosa tissue lysates from wild-type (*WT*), *KRAS*<sup>V12G</sup> (*R*), *Apc*<sup>+/-1638N</sup> (*A*), and *KRAS*<sup>V12G</sup>/*Apc*<sup>+/-1638N</sup> (*RA*) mice. Top to bottom: anti-Ras antibody reveals distinct endogenous Ras and transgenic *KRAS*<sup>V12G</sup> (arrow) proteins. Ras-GTP pull-down assay shows strong activity in *KRAS*<sup>V12G</sup> and compound *KRAS*<sup>V12G</sup>/*Apc*<sup>+/-1638N</sup> mice. MAPK1/2 are clearly activated by *KRAS*<sup>V12G</sup> as revealed by a phosphospecific antibody. Total MAPK as well as total and phosphorylated AKT were essentially unchanged. *Actin*: loading control. (C) Oncogenic *KRAS*<sup>V12G</sup> activates MAPK but not AKT in stable ES cells lines. Representative examples of independent clones for each line shown: wild-type E14 (*WT*), *Apc*<sup>1638N/1638N</sup> (*A*), *Apc*<sup>+/-1638N</sup>/*KRAS*<sup>V12G</sup> (*R*), and *Apc*<sup>1638N/1638N</sup>/*KRAS*<sup>V12G</sup> (*RA*). *Actin*: loading control. Analysis with pan-Ras antibody reveals significant increase in protein levels in cell lysates from *Apc*<sup>+/-1638N</sup>/*KRAS*<sup>V12G</sup> and *Apc*<sup>1638N/1638N</sup>/*KRAS*<sup>V12G</sup> ES cells. Ras-GTP pull-down assay shows activity in compound mutant lines. MAPK1/2 are clearly activated by oncogenic *KRAS*<sup>V12G</sup>. Total MAPK levels as well as total and phosphorylated AKT levels were essentially unchanged.

BASIC-ALIMENTARY TRACT



mutant animals but not in control tissue (Figure 3). The mitogen-activated protein kinases ERK1 and ERK2 were constitutively phosphorylated in intestinal mucosa lysates of  $KRAS^{V12G}$  transgene carrying animals, without changes in total levels of expression (Figure 3B). This stable increase of MAPK activity in response to oncogenic KRAS signaling was comparable with single transgenic mice.<sup>22</sup> It has recently been shown that sustained expression of oncogenic KRAS causes a decrease in MAPK activity in mouse embryonic fibroblasts,<sup>34</sup> possibly reflecting cell type-specific differences between epithelial and mesenchymal cells.<sup>35</sup> The protein kinase Akt/PKB is a common RAS effector. However, the expression or phosphorylation levels of Akt did not differ significantly between transgenic and control animals (Figure 3B).

To recapitulate the mutations characteristic of the  $KRAS^{V12G}/Apc^{+/1638N}$  mice in an in vitro model easily amenable to biochemical analysis, we stably transfected  $Apc^{1638N/1638N}$  mouse embryonic stem (ES) cells<sup>36</sup> with a human  $KRAS^{V12G}$  expression construct driven by the PGK promoter. In cell lysates from stably transfected ES clones, expression of total Ras was quantified, and a pull-down assay with recombinant RalGDS was performed to test for functional, activated GTP-RAS (Figure 3C). In accordance with the observations in mouse tissue, the MAPK cascade was activated upon oncogenic KRAS expression, but no Akt activation was detectable (Figure 3C).

#### **Tumors From Compound $KRAS^{V12G}/Apc^{+/1638N}$ Mice Show Increased Proliferation and Reduced Apoptosis Rates**

To detect changes in cellular proliferation, we have performed Ki67 staining on tissue sections and analysis by flow cytometry after in vivo BrdU incorporation (Figures 4A and B). In tumors from compound mutant animals, we frequently detected a striking increase in cellular proliferation pattern. The S-phase fraction (SPF) fraction was significantly elevated in adenocarcinomas from  $KRAS^{V12G}/Apc^{+/1638N}$  mice (SPF: 11.1%,  $n = 13$  tumors), whereas normal mucosa samples were not significantly different from wild-type. Notably, proliferation rates in lesions from compound mutant mice were significantly higher than in tumors from single transgenic  $KRAS^{V12G}$  littermates ( $P = .001$ ) and from  $Apc^{+/1638N}$  mice ( $P = .013$ ).

Next, we analyzed protein lysates from normal tissue and tumors for the activated, cleaved form of caspase-3 (Figure 4C). Caspase-3 plays a central role in apoptosis because it is responsible for the proteolytic cleavage and activation of other caspases and of additional key apoptotic proteins.<sup>37</sup> Tumors from all groups of animals showed reduced amounts of cleaved caspase-3 when compared with normal control tissue. Notably, tumors from compound mutant mice had significantly lower levels of cleaved

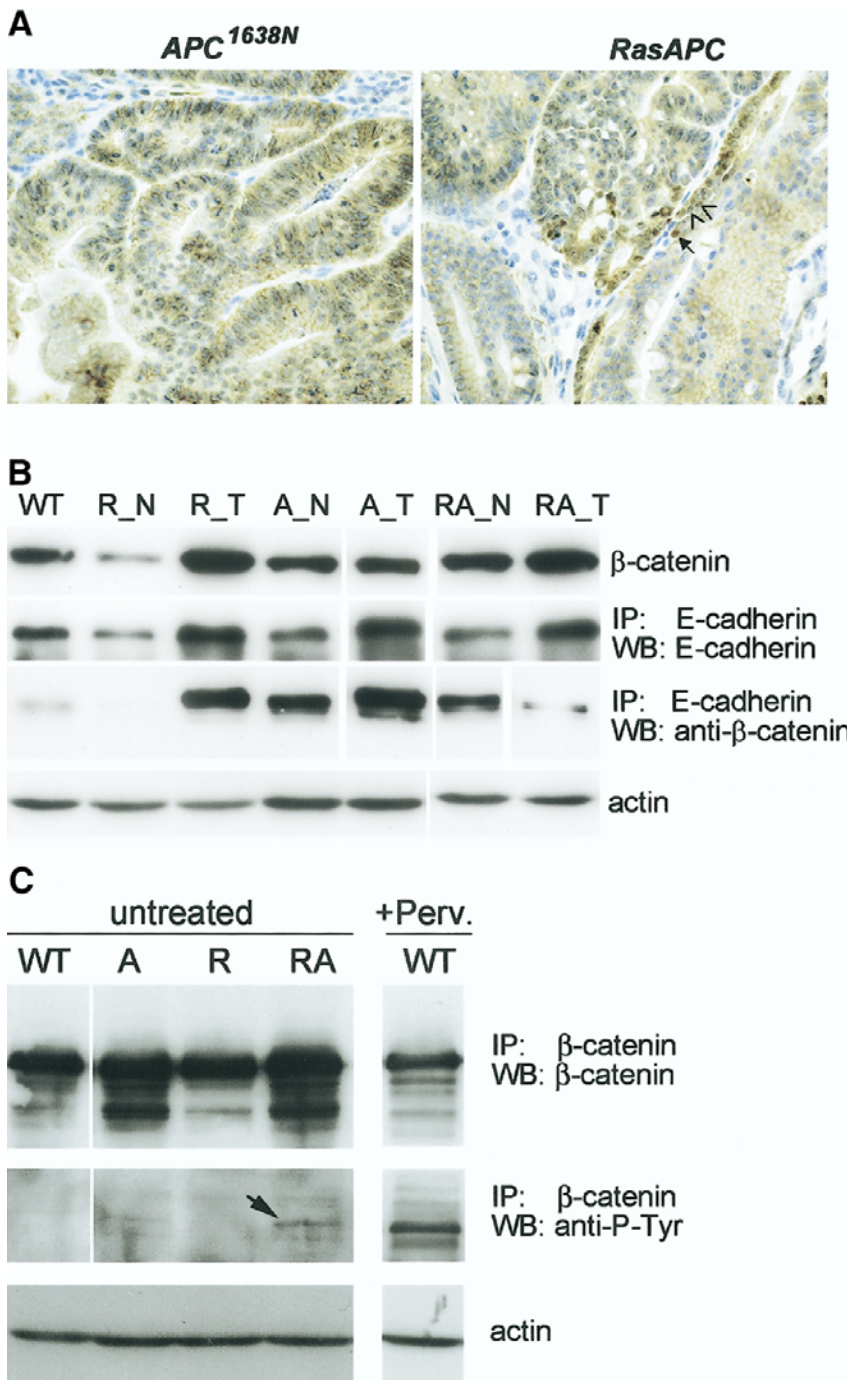
caspase-3 than the single mutant  $Apc^{+/1638N}$  littermates ( $P = .0076$ ), whereas the levels of uncleaved, full-length caspase-3 did not differ significantly between the different groups (Figure 4C). The difference in apoptosis between tumor and normal tissue also significantly differs between single mutant  $Apc^{+/1638N}$  mice and compound mutant animals ( $P = .029$ ). Essentially the same result was observed for poly (ADP-ribose) polymerase 1 (PARP), a main downstream target of caspase-3 (not shown). In accordance, we observed a significant reduction of apoptosis in  $Apc^{1638N/1638N}$  mutant ES cell lines upon stable expression of oncogenic  $KRAS^{V12G}$ , in committed as well as in undifferentiated cells (see Supplementary Figure 2 online at [www.gastrojournal.org](http://www.gastrojournal.org)).

#### **The Canonical Wnt/ $\beta$ -Catenin Signaling Pathway Is Enhanced by Oncogenic $KRAS^{V12G}$**

It has been shown that oncogenic KRAS results in the dissociation of  $\beta$ -catenin from E-cadherin at the adherens junctions of epithelial cells.<sup>38</sup> This leads to an increase of the cytoplasmic  $\beta$ -catenin pool, which, under physiologic ( $Apc^{+/+}$ ) conditions, is efficiently degraded by the proteolytic machinery. Thus, in a mutant  $Apc$  background, oncogenic KRAS may underlie subtle but significant changes in  $\beta$ -catenin subcellular localization and signaling. To analyze putative changes in nuclear accumulation of  $\beta$ -catenin between tumors from  $KRAS^{V12G}/Apc^{+/1638N}$  and  $Apc^{+/1638N}$  littermates, IHC was performed on a total of 61 lesions ( $n = 18$  animals; Figure 5A). The subcellular distribution of  $\beta$ -catenin was heterogeneous throughout each tumor, as previously reported.<sup>39,40</sup> Using a previously established protocol,<sup>29</sup> tumors from  $KRAS^{V12G}/Apc^{+/1638N}$  animals showed a statistically significant increase of cells with nuclear  $\beta$ -catenin (Table 4). Analysis of tumors from  $KRAS^{V12G}$  mice at the same age did not reveal  $\beta$ -catenin nuclear accumulation (data not shown). To corroborate these observations, we performed coimmunoprecipitation (IP) analyses on tissue lysates. IPs were first performed with an antibody against E-cadherin and analyzed by immunoblotting with an anti- $\beta$ -catenin antibody. The fraction of  $\beta$ -catenin bound to E-cadherin was compared with total  $\beta$ -catenin levels. The IP fraction of  $\beta$ -catenin was markedly decreased in tumors from compound mutant mice compared with their control littermates (Figure 5B).

The ES cell lines stably transfected with oncogenic KRAS in  $Apc^{+/+}$  and  $Apc^{1638N/1638N}$  backgrounds represent a convenient mean to validate and strengthen the above observations. First, we tested the subcellular localization of  $\beta$ -catenin by immunofluorescence and confocal microscopy upon LIF withdrawal. Indeed, nuclear accumulation of  $\beta$ -catenin was evident in the  $KRAS^{V12G}/Apc^{1638N/1638N}$  ES lines (Figure 6A and see Supplementary Figure 3 online at [www.gastrojournal.org](http://www.gastrojournal.org)).

**Figure 4.** Proliferation and apoptosis rates in tumors from  $KRAS^{V12G}/Apc^{+/1638N}$  mice. (A) Proliferation is increased in tumors from  $KRAS^{V12G}/Apc^{+/1638N}$  mice (bottom) when compared with  $Apc^{+/1638N}$  littermates (top) as shown by immunohistochemical detection of the proliferation marker Ki67. (B) Analysis of cell proliferation by flow cytometry after BrdU incorporation in normal (N) and tumor (T) tissue samples from wild-type (WT),  $KRAS^{V12G}$  (R),  $Apc^{+/1638N}$  (A), and  $KRAS^{V12G}/Apc^{+/1638N}$  (RA) mice. S-phase fractions are indicated as mean  $\pm$  SEM. Tumors from compound mutant  $KRAS^{V12G}/Apc^{+/1638N}$  mice have significantly higher proliferation rates than tumors from  $KRAS^{V12G}$  littermates ( $P = .0001$ ) or from  $Apc^{+/1638N}$  littermates ( $P = .0026$ ). (C) Apoptosis is suppressed in tumors from  $KRAS^{V12G}/Apc^{+/1638N}$  mice. Levels of full-length and cleaved caspase 3 were quantified from Western blots. Mean  $\pm$  SEM was calculated (2 tumors per animal,  $n = 4$  mice/group). Compound mutant  $KRAS^{V12G}/Apc^{+/1638N}$  mice have significantly lower cleaved caspase-3 levels in tumors than single transgenic littermates ( $P < .005$ ).



BASIC-ALIMENTARY TRACT

*Apc*<sup>1638N/1638N</sup> ES cells showed only occasional  $\beta$ -catenin nuclear accumulation, although not as prominently as in the presence of oncogenic *KRAS*. Essentially the same results were obtained from primary cultures of tumor cells from single and compound transgenic animals (not shown). Immunofluorescence analysis of intracellular distribution of  $\beta$ -catenin clearly indicated a prominent increase of nuclear  $\beta$ -catenin in tumor cells from compound mutant animals, as compared with *Apc*-only mutated tumors. We then measured the levels of transcriptionally active nuclear  $\beta$ -catenin levels in the various mutant ES lines by the TCF/ $\beta$ -catenin responsive reporter assay TOPFLASH.<sup>8,41</sup> Although stable transfection of wild-type ES cells with oncogenic *KRAS* was not sufficient to induce reporter activity, *KRAS*<sup>V12G</sup>/*Apc*<sup>1638N/1638N</sup> ES cell lines showed a 2-fold increase in TOPFLASH activity when compared with the *Apc*<sup>1638N/1638N</sup> parental cell line (Figure 6A, inset). The increase in  $\beta$ -catenin nuclear accumulation in *Apc*<sup>1638N/1638N</sup> cells upon *KRAS*<sup>V12G</sup> expression coincides with the observed increase in Wnt reporter activity, clearly demonstrating a synergistic role of activated *KRAS* in enhancing Wnt signaling.

Oncogenic *KRAS* has been shown to induce tyrosine phosphorylation of  $\beta$ -catenin, leading to a disruption of its binding to E-cadherin.<sup>38</sup> This induces a shift in  $\beta$ -catenin intracellular distribution by increasing the intracellular (Wnt signaling) pool. Moreover, increased tyrosine-phosphorylation of  $\beta$ -catenin has been associated with malignancy.<sup>42</sup> Thus, tyrosine-phosphorylation of  $\beta$ -catenin, induced by *KRAS*<sup>V12G</sup>, might be responsible for the observed nuclear accumulation of  $\beta$ -catenin and increased Wnt signaling.

To test for putative changes on  $\beta$ -catenin tyrosine-phosphorylation, we have carried out biochemical analysis on the *Apc*/*KRAS* mutant ES cell lines. Endogenous  $\beta$ -catenin was immunoprecipitated, and phospho-tyrosine was revealed with a pan anti-phospho-tyrosine-specific antibody (Figure 5C). In *Apc*<sup>1638N/1638N</sup> cells, a faint phospho-tyrosine band was occasionally observed but never in wild-type or *KRAS*<sup>V12G</sup> cells on an *Apc*<sup>+/+</sup> background. A clearly increased phospho-tyrosine band was observed in compound *KRAS*<sup>V12G</sup>/*Apc*<sup>1638N/1638N</sup> mutant cells (Figure 5C). As a positive control for tyrosine-phosphorylation, we treated ES cells with pervanadate prior to the immunoprecipitation. As expected, a strong increase in phosphorylation signal was detectable in all cell lines (shown only for wild-type cells in Figure 5C). Pervanadate, an inhibitor of protein tyrosine phosphatases, induces the intracellular redistribution of  $\beta$ -catenin from the cell membrane to the cytosol.<sup>43</sup> Treatment of *Apc*-mutant ES cell lines with pervanadate indeed

**Table 4.** Nuclear  $\beta$ -Catenin Accumulation Is Increased in *KRAS*<sup>V12G</sup>/*Apc*<sup>+/1638N</sup> Tumors

Genotype	Tumors (n)	Mean nuclear $\beta$ -catenin expression ratio
<i>Apc</i> <sup>+/1638N</sup>	27	0.058
<i>KRAS</i> <sup>V12G</sup> / <i>Apc</i> <sup>+/1638N</sup>	34	0.128 <sup>a</sup>

NOTE. Ratio between the absolute number of positive nuclear cells and the area of the tumor section analyzed (mm<sup>2</sup>).

<sup>a</sup>P = .03874, Welch 2 sample t test.

resulted in  $\beta$ -catenin nuclear accumulation (Figure 6B). Notably, the same treatment did not induce  $\beta$ -catenin nuclear accumulation in *Apc*<sup>+/+</sup> cells. *KRAS*<sup>V12G</sup>/*Apc*<sup>1638N/1638N</sup> ES cells are already characterized by  $\beta$ -catenin nuclear accumulation, and the intracellular distribution did not change upon pervanadate treatment. These results indicate that tyrosine-phosphorylation is per se insufficient to induce nuclear accumulation of  $\beta$ -catenin but can significantly promote a marked intracellular redistribution of  $\beta$ -catenin upon loss of *Apc* function.

### Expression of Target Genes in Tumors From Compound *KRAS*<sup>V12G</sup>/*Apc*<sup>+/1638N</sup> Mice

We have analyzed the expression levels of known Wnt/ $\beta$ -catenin targets by real-time PCR and immunoblot analysis. The *c-Myc* oncogene is a direct target of  $\beta$ -catenin/TCF and a major mediator of tumorigenic effects.<sup>44</sup> Furthermore, *c-Myc* is known to be stabilized at the protein level by the Ras/Raf/MAPK cascade.<sup>45</sup> A significant increase in *c-Myc* transcript levels is evident in tumors from *KRAS*<sup>V12G</sup>/*Apc*<sup>+/1638N</sup> animals as compared with tumors from either *KRAS*<sup>V12G</sup> or *Apc*<sup>+/1638N</sup> mice (Supplementary Figure 4 online at [www.gastrojournal.org](http://www.gastrojournal.org)).

The cell cycle regulator Cyclin D1 represents another Wnt target thought to be relevant for cancer.<sup>46</sup> Cyclin D1 transcript levels were uniformly up-regulated in tumors, with no significant differences among the genotypes. Essentially the same was observed for Cyclin D1 protein levels quantified by Western blot analysis. These results are in agreement with a more recent study that argues the role of Cyclin D1 as a Wnt/ $\beta$ -catenin downstream target.<sup>47</sup>

To analyze further the genome-wide expression differences between tumors from compound *KRAS*<sup>V12G</sup>/*Apc*<sup>+/1638N</sup> animals

**Figure 5.** Increase in nuclear  $\beta$ -catenin accumulation in tumors from *KRAS*<sup>V12G</sup>/*Apc*<sup>+/1638N</sup> mice. (A) Tumor sections from *KRAS*<sup>V12G</sup>/*Apc*<sup>+/1638N</sup> mice (right panel) show increased nuclear  $\beta$ -catenin compared with tumors from *Apc*<sup>+/1638N</sup> animals (left panel). All tumor cells with strong (arrow) and mild (arrowheads) nuclear  $\beta$ -catenin staining were scored (see Results section). (B) Immunoblot analysis and coimmunoprecipitation of total and E-cadherin-associated  $\beta$ -catenin levels in normal (N) and tumor (T) tissue specimens from *KRAS*<sup>V12G</sup> (R), *Apc*<sup>+/1638N</sup> (A), and *KRAS*<sup>V12G</sup>/*Apc*<sup>+/1638N</sup> (RA) mice. Top 3 panels: total  $\beta$ -catenin, immunoprecipitated E-cadherin, and  $\beta$ -catenin bound to E-cadherin. Note the reduction of  $\beta$ -catenin associated to E-cadherin in compound mutant tumors. Bottom panel: actin staining (2 tumors per animal, n = 2 mice/genotype). (C) Increase in tyrosine-phosphorylation on immunoprecipitated  $\beta$ -catenin in *Apc*-mutant ES cells expressing *KRAS*<sup>V12G</sup>, as compared with *Apc*-only mutated cells. Endogenous  $\beta$ -catenin was immunoprecipitated from wild-type E14 mouse ES cells (WT), *Apc*<sup>1638N/1638N</sup> (A), *Apc*<sup>+/+</sup>/*KRAS*<sup>V12G</sup> (R), and *Apc*<sup>1638N/1638N</sup>/*KRAS*<sup>V12G</sup> (RA) ES cells. Top to bottom: Immunoprecipitated  $\beta$ -catenin, phospho-tyrosine revealed with anti-phospho-tyrosine antibody on the  $\beta$ -catenin IP, and actin as loading control. Note the presence of a faint phospho-tyrosine band in *Apc*<sup>1638N/1638N</sup> cells, but not in wild-type or *KRAS*<sup>V12G</sup> cells, and an enhanced signal in the lane from compound mutant cells (RA, marked by arrow). As a positive control for tyrosine-phosphorylation, ES cells were treated with pervanadate prior to immunoprecipitation. As expected, strong phosphorylation signals were detectable in all cell lines (shown here only for WT cells).

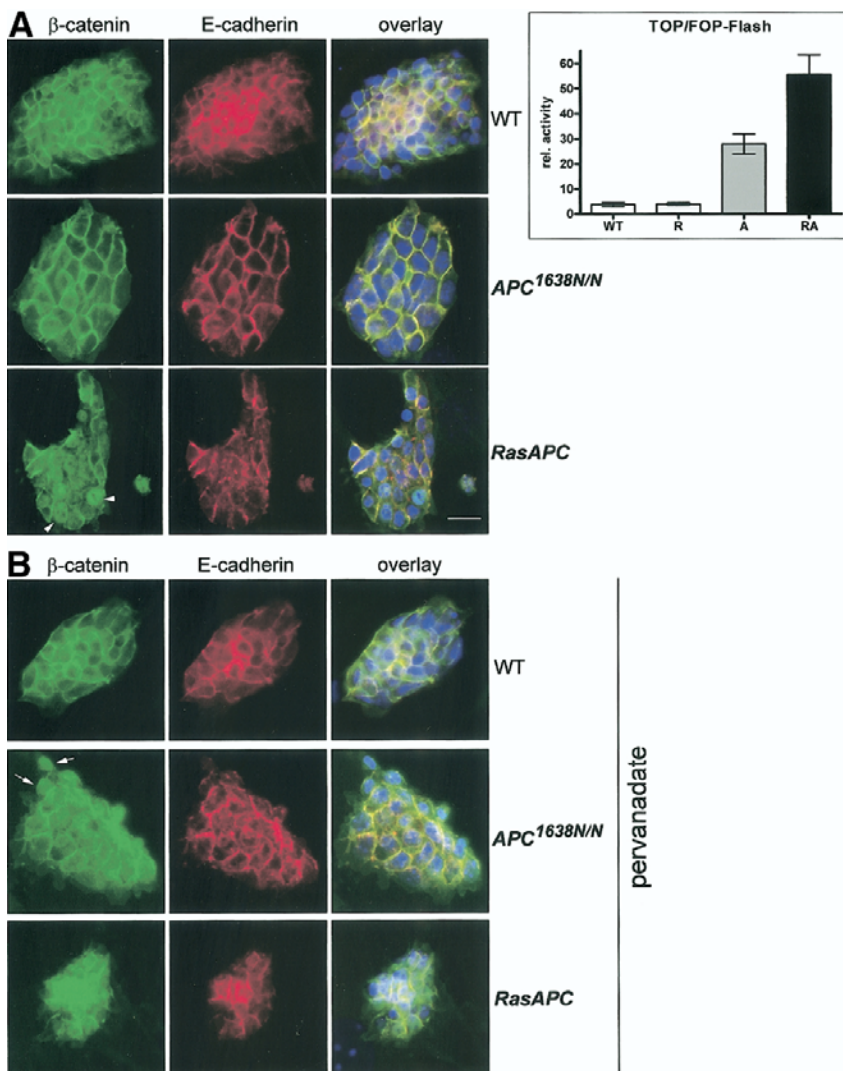


**Figure 6.** Increase in nuclear  $\beta$ -catenin accumulation and Wnt/ $\beta$ -catenin signaling in *Apc*-mutant ES cells expressing *KRAS*<sup>V12G</sup>. (A) Confocal microscopy analysis of  $\beta$ -catenin and E-cadherin intracellular distribution in wild-type E14 (WT), *Apc*<sup>1638N/1638N</sup> (A), *Apc*<sup>+/+/KRAS</sup>V12G (R), and *Apc*<sup>1638N/1638N/KRAS</sup>V12G (RA) ES cells. Note: nuclear accumulation of  $\beta$ -catenin in compound mutant cells (arrowheads), in addition to the normal localization at cell-cell contact sites. Overlay with DAPI (nuclear stain) to indicate the position of the nuclei. Yellow in the overlay indicates colocalization of  $\beta$ -catenin and E-cadherin at the cell-cell junctions, demonstrating the presence of  $\beta$ -catenin in adhesion complexes. Inset: TOP Flash reporter analysis of Wnt-signaling activity in wild-type E14 (WT), *Apc*<sup>1638N/1638N</sup> (A), *Apc*<sup>+/+/KRAS</sup>V12G (R), and *Apc*<sup>1638N/1638N/KRAS</sup>V12G (RA) ES cells. Mean  $\pm$  SEM for 3 independent replicas. (B) Pervanadate treatment induces  $\beta$ -catenin nuclear accumulation in *Apc*-mutant but not in wild-type ES cells. Nuclear  $\beta$ -catenin (green, arrows) is visible in *Apc*<sup>1638N/1638N</sup> (A) and *Apc*<sup>1638N/1638N/KRAS</sup>V12G (RA) ES cells but not in wild-type cells.

and from single transgenic mice, we used Laser Capture Microdissection (LCM) and expression profiling by Affymetrix oligonucleotide microarrays. Total RNA was isolated from microdissected parenchymal cells from histology-matched (high dysplasia) *Apc*<sup>+/1638N</sup> (n = 4) and *KRAS*<sup>V12G/Apc</sup><sup>+/1638N</sup> (n = 4) adenomas. Notably, unsupervised hierarchical clustering of the data revealed that the tumors do not segregate according to

their genotype (see Supplementary Figure 5 online at [www.gastrojournal.org](http://www.gastrojournal.org)). Analysis by hierarchical *t* test<sup>31</sup> also revealed no significant differences between the 2 groups. However, we cannot exclude that further filtering and bioinformatic analysis of these expression profiling data will detect differentially expressed genes, as shown above for *c-Myc* (see Supplementary Figures 4 and 5 online at [www.gastrojournal.org](http://www.gastrojournal.org)).

## Discussion

We have generated a compound mouse model that recapitulates the tumor-specific mutations characteristic of the majority of human CRC patients<sup>20</sup> by combining loss of *Apc* tumor suppressor function with intestine-specific expression of oncogenic *KRAS*. Compound *KRAS*<sup>V12G</sup>/*Apc*<sup>+ /1638N</sup> mice displayed an average of 30 intestinal tumors, a 15-fold and a 7-fold increase over the *pVill-KRAS*<sup>V12G</sup> and *Apc*<sup>+ /1638N</sup> littermates, respectively. Rather than simply adding up the tumor phenotypes of the parental strains, the compound mutant animals showed an increase in progression toward malignancy with severe morbidity and mortality. Tumors from compound mutant animals proliferated at significantly higher rates than their single transgenic littermates. Furthermore, levels of apoptosis were reduced in tumors, as well as in a complementary ES cell model system that recapitulates the genetic mutations of the tumors. As shown here, the synergism between mutant *KRAS* and *APC* in enhancing Wnt/ $\beta$ -catenin signaling is likely to underlie the observed phenotypic differences. Accordingly, TOPFLASH reporter analysis shows that *KRAS*<sup>V12G</sup> expression significantly enhances Wnt/ $\beta$ -catenin signaling in *Apc*-mutant but not in wild-type ES cells. The latter is confirmed by the increased nuclear  $\beta$ -catenin accumulation in both *Apc*-mutant ES cells and intestinal tumors upon oncogenic *KRAS* activation. In tumors from *KRAS*<sup>V12G</sup>/*Apc*<sup>+ /1638N</sup> mice, a significant increase in the number of cells with nuclear  $\beta$ -catenin accumulation was observed when compared with age- and histology-matched tumors from *Apc*<sup>+ /1638N</sup> animals. However, the intratumor  $\beta$ -catenin pattern is extremely heterogeneous, with the majority of parenchymal cells showing membranous and/or cytoplasmic staining (Figure 5A). This may explain why expression profiling did not reveal any significant difference between the 2 groups of tumors. Thus, the synergism between oncogenic *KRAS* and mutated *Apc* is likely to exert its effects through the enhanced activation of a common downstream signaling pathway, namely the Wnt/ $\beta$ -catenin pathway, in a subset of tumor cells. The latter is of relevance in view of the role of Wnt signaling in the regulation of stem cell renewal and differentiation.<sup>10,36,48,49</sup> By synergistically enhancing Wnt signaling, *KRAS* and *APC* mutations are likely to increase the relative number of putative "cancer stem cells" (CSCs) earmarked by nuclear  $\beta$ -catenin accumulation. Previous reports have shown that also in human CRC, the intracellular distribution of  $\beta$ -catenin is very heterogeneous: tumor cells with nuclear  $\beta$ -catenin are predominantly located at the invasion front where they undergo epithelial-mesenchymal transitions when invading stromal compartments. In contrast, the majority of tumor cells retain a membranous staining, comparable with normal colon.<sup>39,50,51</sup> Notably, the intratumor heterogeneity of  $\beta$ -catenin localization and its ability to confer "stemness" to the cancer cell appear to be conserved in other tumor types including leukemia.<sup>52</sup> Loss of *APC* function is necessary but not sufficient for nuclear  $\beta$ -catenin accumulation and full-blown Wnt-signaling constitutive activation. Locally secreted growth factors and/or other morphogens are likely to synergistically coactivate Wnt/ $\beta$ -catenin signaling in few *APC*-mutant tumor cells located in the proximity of stromal compartments.<sup>53</sup> Enhanced Wnt signaling may confer additional plasticity and "stemness" to these putative CSCs that proliferate in asymmetric fashion, thereby increasing tumor mass, and may induce transdifferentiation (epi-

thelial-mesenchymal transition), thus facilitating local invasion and metastasis.

In colon and breast cancer cell lines, growth factors secreted by the tumor microenvironment or by the tumor itself are known to activate various receptor tyrosine kinases, some of which can phosphorylate  $\beta$ -catenin at specific tyrosine residues.<sup>54-56</sup> The synergism between *KRAS* and *Apc* is also likely to be explained at the molecular level by *KRAS*-induced tyrosine phosphorylation of  $\beta$ -catenin. It has been shown that oncogenic RAS triggers tyrosine phosphorylation of  $\beta$ -catenin, leading to the disruption of its binding to E-cadherin within the adherens junction complex<sup>38,56</sup> and to the subsequent increase of its intracellular (signaling) pool. Mutant *HRAS* can also redistribute the intracellular localization of  $\beta$ -catenin from the membrane to the cytoplasm in a PI3K-dependent fashion,<sup>57</sup> and oncogenic *KRAS* can inhibit GSK3 $\beta$ -kinase activity, dependent on PI3K,<sup>58</sup> thus suggesting a connection of the Ras/PI3K and Wnt-signaling pathways.<sup>59,60</sup> Our results are supportive of the role of oncogenic *KRAS* in inducing nuclear accumulation of  $\beta$ -catenin and enhanced Wnt-signaling activation, although exclusively in an *Apc*-mutant cellular background. Co-IP analysis demonstrated a significant reduction of E-cadherin-bound  $\beta$ -catenin in tumors from compound mutant mice as compared with those from *Apc*-only mutated animals. Notwithstanding the lack of Tyr-P  $\beta$ -catenin-specific antibodies, the role of tyrosine-phosphorylation of  $\beta$ -catenin in enhancing Wnt signaling was analyzed by more indirect methods in ES cells. Treatment of ES cells with pervanadate, an inhibitor of protein tyrosine phosphatases, induces a clear shift in the intracellular distribution of  $\beta$ -catenin from the membrane to the nucleus. Notably, the latter was observed exclusively in *Apc*-mutant but not in wild-type ES cells. Accordingly, co-IP analysis revealed enhanced  $\beta$ -catenin tyrosine phosphorylation in compound *KRAS*<sup>V12G</sup>/*Apc*<sup>c1638N/1638N</sup> ES cells when compared with *Apc*<sup>1638N/1638N</sup> cells.

The synergistic activation of specific downstream targets of the *KRAS* and Wnt-signaling pathways can also explain the observed increased multiplicity and aggressive tumor behavior in compound *KRAS*<sup>V12G</sup>/*Apc*<sup>+ /1638N</sup> mice. An example in human CRC is gastrin, which is synergistically activated by oncogenic Ras and  $\beta$ -catenin.<sup>59,60</sup> It is well documented that the oncogene *c-Myc* is activated both by activated RAS, at the protein level, as well as by Wnt/ $\beta$ -catenin signaling at the transcriptional level. Indeed, we have found that *c-Myc* transcripts as well as protein levels are significantly increased in tumors from compound mutant animals as compared with their control littermates. In conclusion, our data show that the coexistence of *Apc* and *KRAS* mutations in CRC synergistically enhances Wnt signaling by translocating  $\beta$ -catenin to the nucleus. Notably, the effect on  $\beta$ -catenin intracellular localization is subtle, although significant, and seems to affect only a minority of tumor cells. However, its consequences on tumor multiplicity and progression toward malignancy of *KRAS*<sup>V12G</sup>/*Apc*<sup>+ /1638N</sup> mice are remarkable. The failure to detect significant differential expression between the transcription profiles of these 2 groups of tumors by standard microarray analysis raises questions on the prognostic value of this common molecular approach.<sup>61</sup> The intratumoral heterogeneity is likely to obscure subtle differences in expression patterns, which may go un-

detected by standard unsupervised analysis of gene expression profiles. Also, recent studies have highlighted the relevance of the tumor microenvironment in contributing specific expression profiles with significant differences in overall survival<sup>62</sup> and tumor promoting effects.<sup>63</sup> Omics analysis of specific subpopulations (eg, cancer stem cells, other differentiated parenchymal cells, surrounding stromal fibroblasts) microdissected from clinical samples may provide more accurate predictions of tumor behavior and response to treatment.

## Appendix

### Supplementary data

Supplementary data associated with this article can be found, in the online version, at doi:10.1053/j.gastro.2006.08.011.

### References

1. Fearon ER, Vogelstein B. A genetic model for colorectal tumorigenesis. *Cell* 1990;61:759–767.
2. Kinzler KW, Vogelstein B. Lessons from hereditary colorectal cancer. *Cell* 1996;87:159–170.
3. Parkin DM, Pisani P, Ferlay J. Estimates of the worldwide incidence of 25 major cancers in 1990. *Int J Cancer* 1999;80:827–841.
4. Pisani P, Parkin DM, Bray F, Ferlay J. Estimates of the worldwide mortality from 25 cancers in 1990. *Int J Cancer* 1999;83:18–29.
5. Fodde R, Smits R, Clevers H. APC, signal transduction and genetic instability in colorectal cancer. *Nat Rev Cancer* 2001;1:55–67.
6. Powell SM, Zilz N, Beazer-Barclay Y, Bryan TM, Hamilton SR, Thibodeau SN, Vogelstein B, Kinzler KW. APC mutations occur early during colorectal tumorigenesis. *Nature* 1992;359:235–237.
7. Polakis P. The adenomatous polyposis coli (APC) tumor suppressor. *Biochim Biophys Acta* 1997;1332:127–147.
8. Korinek V, Barker N, Morin PJ, van Wichen D, de Weger R, Kinzler KW, Vogelstein B, Clevers H. Constitutive transcriptional activation by a  $\beta$ -catenin-Tcf complex in APC<sup>-/-</sup> colon carcinoma. *Science* 1997;275:1784–1787.
9. Morin PJ, Sparks AB, Korinek V, Barker N, Clevers H, Vogelstein B, Kinzler KW. Activation of  $\beta$ -catenin-Tcf signaling in colon cancer by mutations in  $\beta$ -catenin or APC. *Science* 1997;275:1787–1790.
10. Battle E, Henderson JT, Beghtel H, van den Born MM, Sancho E, Huls G, Meeldijk J, Robertson J, van de Wetering M, Pawson T, Clevers H.  $\beta$ -Catenin and TCF mediate cell positioning in the intestinal epithelium by controlling the expression of EphB/ephrinB. *Cell* 2002;111:251–263.
11. Polakis P. The oncogenic activation of  $\beta$ -catenin. *Curr Opin Genet Dev* 1999;9:15–21.
12. Bos JL, Fearon ER, Hamilton SR, Verlaan-de Vries M, van Boom JH, van der Eb AJ, Vogelstein B. Prevalence of ras gene mutations in human colorectal cancers. *Nature* 1987;327:293–297.
13. Campbell SL, Khosravi-Far R, Rossman KL, Clark GJ, Der CJ. Increasing complexity of Ras signaling. *Oncogene* 1998;17:1395–1413.
14. Downward J. Cell cycle: routine role for Ras. *Curr Biol* 1997;7:258–260.
15. Zuber J, Tchernitsa OI, Hinzmann B, Schmitz AC, Grips M, Hellriegel M, Sers C, Rosenthal A, Schafer R. A genome-wide survey of RAS transformation targets. *Nat Genet* 2000;24:144–152.
16. Gille H, Strahl T, Shaw PE. Activation of ternary complex factor Elk-1 by stress-activated protein kinases. *Curr Biol* 1995;5:1191–1200.
17. Marais R, Marshall CJ. Control of the ERK MAP kinase cascade by Ras and Raf. *Cancer Surv* 1996;27:101–125.
18. Smith AJ, Stern HS, Penner M, Hay K, Mitri A, Bapat BV, Gallinger S. Somatic APC and K-ras codon 12 mutations in aberrant crypt foci from human colons. *Cancer Res* 1994;54:5527–5530.
19. Jen J, Powell SM, Papadopoulos N, Smith KJ, Hamilton SR, Vogelstein B, Kinzler KW. Molecular determinants of dysplasia in colorectal lesions. *Cancer Res* 1994;54:5523–5526.
20. Zhang B, Ougolkov A, Yamashita K, Takahashi Y, Mai M, Minamoto T.  $\beta$ -Catenin and ras oncogenes detect most human colorectal cancer. *Clin Cancer Res* 2003;9:3073–3079.
21. Fodde R, Edelmann W, Yang K, van Leeuwen C, Carlson C, Renault B, Breukel C, Alt E, Lipkin M, Khan PM, et al. A targeted chain-termination mutation in the mouse Apc gene results in multiple intestinal tumors. *Proc Natl Acad Sci U S A* 1994;91:8969–8973.
22. Janssen KP, el-Marjou F, Pinto D, Sastre X, Rouillard D, Fouquet C, Soussi T, Louvard D, Robine S. Targeted expression of oncogenic K-ras in intestinal epithelium causes spontaneous tumorigenesis in mice. *Gastroenterology* 2002;123:492–504.
23. Smits R, van der Houven van Oordt W, Luz A, Zurcher C, Jagmohan-Changur S, Breukel C, Khan PM, Fodde R. Apc1638N: a mouse model for familial adenomatous polyposis-associated desmoid tumors and cutaneous cysts. *Gastroenterology* 1998;114:275–283.
24. Smits R, Kartheuser A, Jagmohan-Changur S, Leblanc V, Breukel C, de Vries A, van Kranen H, van Krieken JH, Williamson S, Edelmann W, Kucherlapati R, Khan PM, Fodde R. Loss of Apc and the entire chromosome 18 but absence of mutations at the Ras and Tp53 genes in intestinal tumors from Apc1638N, a mouse model for Apc-driven carcinogenesis. *Carcinogenesis* 1997;18:321–327.
25. Blake JA, Richardson JE, Bult CJ, Kadin JA, Eppig JT. MGD: the Mouse Genome Database. *Nucleic Acids Res* 2003;31:193–195.
26. Flaman JM, Frebourg T, Moreau V, Charbonnier F, Martin C, Chappuis P, Sappino AP, Limacher IM, Bron L, Benhattar J, et al. A simple p53 functional assay for screening cell lines, blood, and tumors. *Proc Natl Acad Sci U S A* 1995;92:3963–3967.
27. Ba Y. Analysis of transcript mutations due to transcriptional slippage in rat p53 tumor suppressor gene with the use of yeast functional assay. *Hokkaido Igaku Zasshi* 1999;74:173–188.
28. Araki Y, Okamura S, Hussain SP, Nagashima M, He P, Shiseki M, Miura K, Harris CC. Regulation of cyclooxygenase-2 expression by the Wnt and ras pathways. *Cancer Res* 2003;63:728–734.
29. Jung A, Schrauder M, Oswald U, Knoll C, Sellberg P, Palmqvist R, Niedobitek G, Brabletz T, Kirchner T. The invasion front of human colorectal adenocarcinomas shows co-localization of nuclear  $\beta$ -catenin, cyclin D1, and p16INK4A and is a region of low proliferation. *Am J Pathol* 2001;159:1613–1617.
30. Gentleman RC, Carey VJ, Bates DM, Bolstad B, Dettling M, Dudoit S, Ellis B, Gautier L, Ge Y, Gentry J, Hornik K, Hothorn T, Huber W, Iacus S, Irizarry R, Leisch F, Li C, Maechler M, Rossini AJ, Sawitzki G, Smith C, Smyth G, Tierney L, Yang JY, Zhang J. Bioconductor: open software development for computational biology and bioinformatics. *Genome Biol* 2004;5:R80.
31. Menezes RX, Boer JM, van Houwelingen HC. Microarray data analysis: a hierarchical T-test to handle heteroscedasticity. *Appl Bioinformatics* 2004;3:229–235.
32. Ihaka R, Gentleman R. R: language for data analysis and graphics. *J Comput Graph Statist* 1996;3:229–235.
33. Fodde R, Smits R. Disease model: familial adenomatous polyposis. *Trends Mol Med* 2001;7:369–373.

34. Tuveson DA, Shaw AT, Willis NA, Silver DP, Jackson EL, Chang S, Mercer KL, Grochow R, Hock H, Crowley D, Hingorani SR, Zaks T, King C, Jacobetz MA, Wang L, Bronson RT, Orkin SH, DePinho RA, Jacks T. Endogenous oncogenic K-ras (G12D) stimulates proliferation and widespread neoplastic and developmental defects. *Cancer Cell* 2004;5:375–387.
35. Yu Q, Geng Y, Sicinski P. Specific protection against breast cancers by cyclin D1 ablation. *Nature* 2001;411:1017–1021.
36. Kielman MF, Rindapaa M, Gaspar C, van Poppel N, Breukel C, van Leeuwen S, Taketo MM, Roberts S, Smits R, Fodde R. Apc modulates embryonic stem-cell differentiation by controlling the dosage of  $\beta$ -catenin signaling. *Nat Genet* 2002;32:594–605.
37. Lazebnik YA, Kaufmann SH, Desnoyers S, Poirier GG, Earnshaw WC. Cleavage of poly(ADP-ribose) polymerase by a proteinase with properties like ICE. *Nature* 1994;371:346–347.
38. Kinch MS, Clark GJ, Der CJ, Burridge K. Tyrosine phosphorylation regulates the adhesions of ras-transformed breast epithelia. *J Cell Biol* 1995;130:461–471.
39. Brabletz T, Jung A, Hermann K, Gunther K, Hohenberger W, Kirchner T. Nuclear overexpression of the oncoprotein  $\beta$ -catenin in colorectal cancer is localized predominantly at the invasion front. *Pathol Res Pract* 1998;194:701–704.
40. Jung A, Schrauder M, Oswald U, Knoll C, Sellberg P, Palmqvist R, Niedobitek G, Brabletz T, Kirchner T. The invasion front of human colorectal adenocarcinomas shows co-localization of nuclear  $\beta$ -catenin, cyclin D1, and p16INK4A and is a region of low proliferation. *Am J Pathol* 2001;159:1613–1617.
41. Smits R, Kielman MF, Breukel C, Zurcher C, Neufeld K, Jagmohan-Changur S, Hofland N, van Dijk J, White R, Edelmann W, Kucherlapati R, Khan PM, Fodde R. Apc1638T: a mouse model delineating critical domains of the adenomatous polyposis coli protein involved in tumorigenesis and development. *Genes Dev* 1999;13:1309–1321.
42. Kim K, Daniels KJ, Hay ED. Tissue-specific expression of  $\beta$ -catenin in normal mesenchyme and uveal melanomas and its effect on invasiveness. *Exp Cell Res* 1998;245:79–90.
43. Kim K, Lee KY. Tyrosine phosphorylation translocates  $\beta$ -catenin from cell-to-cell interface to the cytoplasm, but does not significantly enhance the LEF-1-dependent transactivating function. *Cell Biol Int* 2001;25:421–427.
44. He TC, Sparks AB, Rago C, Hermeking H, Zawel L, da Costa LT, Morin PJ, Vogelstein B, Kinzler KW. Identification of c-MYC as a target of the APC pathway. *Science* 1998;281:1509–1512.
45. Sears R, Leone G, DeGregori J, Nevins JR. Ras enhances Myc protein stability. *Mol Cell* 1999;3:169–179.
46. Tetsu O, McCormick F.  $\beta$ -Catenin regulates expression of cyclin D1 in colon carcinoma cells. *Nature* 1999;398:422–426.
47. Sansom OJ, Reed KR, van de Wetering M, Muncan V, Winton DJ, Clevers H, Clarke AR. Cyclin D1 is not an immediate target of  $\beta$ -catenin following Apc loss in the intestine. *J Biol Chem* 2005;280:28463–28467.
48. Korinek V, Barker N, Moerer P, van Donselaar E, Huls G, Peters PJ, Clevers H. Depletion of epithelial stem-cell compartments in the small intestine of mice lacking Tcf4. *Nat Genet* 1998;19:379–383.
49. van de Wetering M, Sancho E, Verweij C, de Lau W, Oving I, Hurlstone A, van der Horn K, Batlle E, Coudreuse D, Haramis AP, Tjon-Pon-Fong M, Moerer P, van den Born M, Soete G, Pals S, Eilers M, Medema R, Clevers H. The  $\beta$ -catenin/TCF-4 complex imposes a crypt progenitor phenotype on colorectal cancer cells. *Cell* 2002;111:241–250.
50. Brabletz T, Jung A, Reu S, Porzner M, Hlubek F, Kunz-Schughart LA, Knuechel R, Kirchner T. Variable  $\beta$ -catenin expression in colorectal cancers indicates tumor progression driven by the tumor environment. *Proc Natl Acad Sci U S A* 2001;98:10356–10361.
51. Kirchner T, Brabletz T. Patterning and nuclear  $\beta$ -catenin expression in the colonic adenoma-carcinoma sequence. Analogies with embryonic gastrulation. *Am J Pathol* 2000;157:1113–1121.
52. Jamieson CH, Ailles LE, Dylla SJ, Muijtjens M, Jones C, Zehnder JL, Gotlib J, Li K, Manz MG, Keating A, Sawyers CL, Weissman IL. Granulocyte-macrophage progenitors as candidate leukemic stem cells in blast-crisis CML. *N Engl J Med* 2004;351:657–667.
53. Lilien J, Balsamo J, Arregui C, Xu G. Turn-off, drop-out: functional state switching of cadherins. *Dev Dyn* 2002;224:18–29.
54. Hiscox S, Jiang WG. Association of the HGF/SF receptor, c-met, with the cell-surface adhesion molecule, E-cadherin, and catenins in human tumor cells. *Biochem Biophys Res Commun* 1999;261:406–411.
55. Hiscox S, Jiang WG. Hepatocyte growth factor/scatter factor disrupts epithelial tumour cell-cell adhesion: involvement of  $\beta$ -catenin. *Anticancer Res* 1999;19:509–517.
56. Shibamoto S, Hayakawa M, Takeuchi K, Hori T, Oku N, Miyazawa K, Kitamura N, Takeichi M, Ito F. Tyrosine phosphorylation of  $\beta$ -catenin and plakoglobin enhanced by hepatocyte growth factor and epidermal growth factor in human carcinoma cells. *Cell Adhes Commun* 1994;1:295–305.
57. Espada J, Perez-Moreno M, Braga VM, Rodriguez-Viciano P, Cano A. H-Ras activation promotes cytoplasmic accumulation and phosphoinositide 3-OH kinase association of  $\beta$ -catenin in epidermal keratinocytes. *J Cell Biol* 1999;146:967–980.
58. Li J, Mizukami Y, Zhang X, Jo WS, Chung DC. Oncogenic K-ras stimulates Wnt signaling in colon cancer through inhibition of GSK-3 $\beta$ . *Gastroenterology* 2005;128:1907–1918.
59. Chakladar A, Dubeykovskiy A, Wojtukiewicz LJ, Pratap J, Lei S, Wang TC. Synergistic activation of the murine gastrin promoter by oncogenic Ras and  $\beta$ -catenin involves SMAD recruitment. *Biochem Biophys Res Commun* 2005;336:190–196.
60. Espada J, Peinado H, Esteller M, Cano A. Direct metabolic regulation of  $\beta$ -catenin activity by the p85 $\alpha$  regulatory subunit of phosphoinositide 3-OH kinase. *Exp Cell Res* 2005;305:409–417.
61. Bernards R, Weinberg RA. A progression puzzle. *Nature* 2002;418:823.
62. West RB, Nuyten DS, Subramanian S, Nielsen TO, Corless CL, Rubin BP, Montgomery K, Zhu S, Patel R, Hernandez-Boussard T, Goldblum JR, Brown PO, van de Vijver M, van de Rijn M. Determination of stromal signatures in breast carcinoma. *PLoS Biol* 2005;3:e187.
63. Orimo A, Gupta PB, Sgroi DC, Arenzana-Seisdedos F, Delaunay T, Naeem R, Carey VJ, Richardson AL, Weinberg RA. Stromal fibroblasts present in invasive human breast carcinomas promote tumor growth and angiogenesis through elevated SDF-1/CXCL12 secretion. *Cell* 2005;121:335–348.

Received February 17, 2006. Accepted June 21, 2006.

Address requests for reprints to: Sylvie Robine, PhD, CNRS-UMR144/Institut Curie, 26 rue d'Ulm, 75248 Paris Cedex 05, France. e-mail: sylvie.robine@curie.fr; fax: (33) 1-4234-6377 and Riccardo Fodde, PhD, Department of Pathology, Erasmus MC, PO Box 1738, 3000 DR Rotterdam, The Netherlands. e-mail: r.fodde@erasmusmc.nl; fax: (31) 10 4088450.

Supported by grants from the Deutsche Forschungsgemeinschaft and the KKF/MRI (to K-P.J.); from the ARC/Biologie du développement et physiologie intégrative (to S.R.); and from the NWO/Vici, the Dutch Cancer Society (KWF), and the BSIK program of the Dutch Government (to R.F.; BSIK 03038).

K-P.J. and P.A. have contributed equally to this work.

The authors thank Dr Z. Maciorowski for help with cytometry; Dr R. Menezes for help with the expression profiling data; and A. Bittner, C. Geninet, and G. Bousquet for experimental assistance.

---

## Chapter 3.

**Aneuploidy arises at early stages of *Apc*-driven intestinal tumorigenesis and pinpoints conserved chromosomal loci of allelic imbalance between mouse and human.**

***Am J Pathol. 2007;170:377-87.***



## Tumorigenesis and Neoplastic Progression

# Aneuploidy Arises at Early Stages of *Apc*-Driven Intestinal Tumorigenesis and Pinpoints Conserved Chromosomal Loci of Allelic Imbalance between Mouse and Human

Paola Alberici,\* Emma de Pater,\* Joana Cardoso,\* Mieke Bevelander,\* Lia Molenaar,\* Jos Jonkers,<sup>†</sup> and Riccardo Fodde\*

From the Department of Pathology,\* Josephine Nefkens Institute, Erasmus University Medical Center, Rotterdam, and the Division of Molecular Biology,<sup>†</sup> The Netherlands Cancer Institute, Amsterdam, The Netherlands

**Although chromosomal instability characterizes the majority of human colorectal cancers, the contribution of genes such as adenomatous polyposis coli (*APC*), *KRAS*, and *p53* to this form of genetic instability is still under debate. Here, we have assessed chromosomal imbalances in tumors from mouse models of intestinal cancer, namely *Apc*<sup>+1638N</sup>, *Apc*<sup>+1638N</sup>/*KRAS*<sup>V12G</sup>, and *Apc*<sup>+1638N</sup>/*Tp53*<sup>-/-</sup>, by array comparative genomic hybridization. All intestinal adenomas from *Apc*<sup>+1638N</sup> mice displayed chromosomal alterations, thus confirming the presence of a chromosomal instability defect at early stages of the adenoma-carcinoma sequence. Moreover, loss of the *Tp53* tumor suppressor gene, but not *KRAS* oncogenic activation, results in an increase of gains and losses of whole chromosomes in the *Apc*-mutant genetic background. Comparative analysis of the overall genomic alterations found in mouse intestinal tumors allowed us to identify a subset of loci syntenic with human chromosomal regions (eg, 1p34-p36, 12q24, 9q34, and 22q) frequently gained or lost in familial adenomas and sporadic colorectal cancers. The latter indicate that, during intestinal tumor development, the genetic mechanisms and the underlying functional defects are conserved across species. Hence, our array comparative genomic hybridization analysis of *Apc*-mutant intestinal tumors allows the definition of minimal aneuploidy regions conserved between mouse and human and likely to encompass rate-limiting genes for intestinal tumor initiation and**

**progression.** (*Am J Pathol* 2007, 170:377-387; DOI: 10.2353/ajpath.2007.060853)

Colorectal cancer (CRC) is caused by a multistep process that involves the accumulation of several genetic defects. Genetic instability facilitates the acquisition of these multiple gene hits, thus underlying colorectal tumor progression and malignant transformation. Chromosomal instability (CIN), in particular, is thought to cause aneuploidy as frequently observed in both sporadic and familial CRC.<sup>1,2</sup>

Along the adenoma-carcinoma sequence characteristic of colorectal tumorigenesis, specific genetic alterations have been identified. Mutations in the adenomatous polyposis coli (*APC*) gene are considered as a rate-limiting step for adenoma formation both in familial (familial adenomatous polyposis; FAP) and sporadic CRCs. Mutations in the *KRAS* oncogene, found in ~50% of the cases, promote growth of the nascent adenomas. Loss of heterozygosity (LOH) at specific chromosomal regions, including 17p and 18q, characterizes more advanced stages and is thought to be centered around the *TP53* and *SMAD4* genes, respectively.

The progressive increase in genetic instability levels along the adenoma-carcinoma sequence in CRC is likely to be attributable to the acquisition of mutations in caretaker genes, such as *BUB1*, *BUBR1*, and *ATM*, with a broad spectrum of functional activities ranging from surveillance of chromosome segregation, response to DNA damage, cell cycle regulation, and mitotic checkpoint.

---

Supported by the Dutch Cancer Society (grant EMCR 2001-2482), the Dutch Research Council (grant NWO/Vice 016.036.636), and the Besluit Subsidies Investeren Kennisinfrastructuur (BSIK) program of the Dutch Government (grant 03038).

Accepted for publication October 10, 2006.

Address reprint requests to Prof. Dr. Riccardo Fodde, Ph.D., Dept. of Pathology, Josephine Nefkens Institute, Erasmus University Medical Center, P.O. Box 2040, 3000 CA Rotterdam, The Netherlands. E-mail: r.fodde@erasmusmc.nl.

However, only a few of the above genes have been found to be mutated in CRC, and the incidence of these mutations is rather low.<sup>3-6</sup> Notably, loss of *APC* function has been shown to result in structural mitotic defects (ie, microtubule attachment to the kinetochore and centrosomal abnormalities) and in both tetraploidy and aneuploidy, thus triggering CIN at the start of the adenoma-carcinoma sequence.<sup>7-10</sup> Accordingly, low but significant levels of aneuploid changes have been observed at the adenoma stage both in sporadic and hereditary cases.<sup>2,11</sup> Notwithstanding the latter, additional somatic hits seem to be necessary to promote the full-blown CIN phenotype observed in more advanced stages of CRC.<sup>1</sup>

Mouse models carrying targeted *Apc* mutations provide unique tools for the analysis of *Apc*-driven CIN and for identification of those genes that synergize for CIN with the *Apc* tumor suppressor along the adenoma-carcinoma sequence.<sup>12</sup> However, in contrast to what has been observed in human intestinal tumors, very few somatic mutations, if any, have been reported to occur in these mouse intestinal tumors; in fact, no *Kras* or *Tp53* mutations have been found in gastrointestinal (GI) tumors from *Apc*<sup>+1638N</sup> animals,<sup>13</sup> and no other similar studies have been reported in the literature. Thus, to humanize the mouse model, we have bred the *Apc*<sup>+1638N</sup> model<sup>14,15</sup> with mice carrying transgenic and targeted mutations at the *KRAS* and *Tp53* genes to generate *Apc*<sup>+1638N</sup>/*KRAS*<sup>V12G</sup> and *Apc*<sup>+1638N</sup>/*Tp53*<sup>-/-</sup> compound mice. Here, we have used array-based comparative genomic hybridization (array CGH) to evaluate quantitative and qualitative aspects of CIN in intestinal tumors from the above mice when compared with those arising in the *Apc*<sup>+1638N</sup> genetic background. Moreover, we have performed a cross-species comparison of the chromosomal regions more frequently affected by aneuploidy between adenomas from *Apc*-mutant mice and FAP patients carrying germline *APC* mutations.

## Materials and Methods

### Mouse Strains and Tumor Samples

The *Apc*<sup>+1638N</sup> mice used in this study<sup>14</sup> have been backcrossed to C57BL/6J for more than 20 generations and are regarded as fully inbred. *Apc*<sup>+1638N</sup> animals were bred with the transgenic model pVillin-*KRAS*<sup>V12G</sup> expressing the human *KRAS*<sup>V12G</sup> oncogene under the control of the villin promoter.<sup>16</sup> Because the latter model was available in the B6D2 (C57BL/6JxDBA/2) genetic background, the compound *Apc*<sup>+1638N</sup>/*KRAS*<sup>V12G</sup> animals used for the present study were backcrossed to C57BL/6J for five to seven generations to limit confounding effects by undesired genetic modifiers.

For the analysis of the effects of loss of *Tp53* function on *Apc*-driven aneuploidy, *Apc*<sup>+1638N</sup> mice were bred with *Tp53*<sup>+tm1Tyj</sup> (*Tp53*<sup>+/-</sup>) animals carrying a constitutive deletion of the endogenous mouse *Tp53* gene.<sup>17</sup> Compound heterozygous *Apc*<sup>+1638N</sup>/*Tp53*<sup>+/-</sup> mice were

then intercrossed to generate *Apc*<sup>+1638N</sup>/*Tp53*<sup>-/-</sup> experimental animals.

After macroscopic dissection of the GI, tumors of ~2 to 3 mm<sup>3</sup> in size and normal tissues were snap-frozen in Tissue-Tec (Sakura Finetek Europe B.V., Zoeterwoude, The Netherlands) embedding medium in dry ice. Ten- $\mu$ m sections were briefly stained with hematoxylin and eosin (H&E), and consecutive sections were carefully laser-capture microdissected (LCM) using a PALM MicroBeam microscope system (P.A.L.M. Microlaser Technologies AG, Bernried, Germany) to limit contaminations from normal cells and obtain almost pure parenchymal cell samples. Adenomas were scored as either low or high dysplastic according to Boivin and colleagues.<sup>18</sup> On average, 1500 parenchymal cells (900,000  $\mu$ m<sup>2</sup> area) were isolated from each tumor or normal specimen.

### DNA Extraction and $\phi$ 29 Amplification

DNA extractions and  $\phi$ 29 genomic amplifications were performed as previously described.<sup>19</sup> All samples were quality-controlled by a polymerase chain reaction (PCR) to amplify for the mouse *Myh* gene with the following primers: mY5-2, 5'-CCTGGTGCAAAGGCCTGA-3'; and mYe14, 5'-GCAGTAGACACAGCTGCAT-3'.

### CGH Array, Labeling, and Hybridization

The mouse bacterial artificial chromosome (BAC) microarray slides here used for array CGH encompass 2803 unique BAC clones at 1 Mb spacing and were obtained from the Central Microarray Facility of The Netherlands Cancer Institute in Amsterdam.<sup>20</sup> DNA labeling was performed as previously described<sup>19</sup> using a mixture of male genomic DNA extracted from the kidneys of two C57BL/6J mice as reference DNA. The Cy3-labeled sample and Cy5-labeled reference DNAs were precipitated together with 135  $\mu$ g of mouse Cot-1 DNA (Invitrogen, Breda, The Netherlands). DNA pellets were then redissolved in 120  $\mu$ l of hybridization buffer (50% formamide, 10% dextran sulfate, 0.1% Tween 20, 2 $\times$  standard saline citrate, and 10 mmol/L Tris-HCl, pH 7.4) together with 600  $\mu$ g of yeast tRNA (Invitrogen). Probe DNA was denatured for 10 minutes at 70°C and incubated for 1 hour at 37°C before application on the prehybridized BAC microarray slides. Array slides were prehybridized for 1 hour at 37°C with 90  $\mu$ l of denatured hybridization buffer containing 540  $\mu$ g of herring sperm DNA and 90  $\mu$ g of mouse Cot-1 DNA. Hybridizations were performed as previously described.<sup>21</sup> After hybridization, slides were washed serially in solution 1 (0.05% Tween 20 in phosphate-buffered saline) for 10 minutes at room temperature, in solution 2 (50% formamide, 2 $\times$  standard saline citrate) at 42°C for 30 minutes, and twice in solution 1 at room temperature for 10 minutes. Finally, slides were spin-dried for 5 minutes at 1000 rpm. Image scans and their analysis were obtained by ScanArray Express HT (Perkin-Elmer Life Sciences, Boston, MA) and GenePix Pro 5.0 software (Axon Instruments, Union City, CA), respectively.

## Data Analysis

BAC clone position map annotation and chromosomes order were according to Ensembl Build m34 ([http://www.ensembl.org/mus\\_musculus/](http://www.ensembl.org/mus_musculus/)). All of the data were normalized using the Marray Tool and vsn packages into R environment as described elsewhere.<sup>2</sup> To facilitate detection of data trends and discriminate gain or loss events from variation introduced by the whole-genome amplification technique, we performed smoothing of the log<sub>2</sub> ratio of the normalized data with the aCGH-Smooth software.<sup>22</sup> Bioinformatic data analysis was performed using the Ensembl mouse genome server ([http://www.ensembl.org/mus\\_musculus/](http://www.ensembl.org/mus_musculus/)) and the NCBI mouse genome resources (<http://www.ncbi.nlm.nih.gov/genome/guide/mouse/>). The analysis of mouse/human homology regions was performed by using the NCBI Comparative Maps, available at <http://www.ncbi.nlm.nih.gov/Homology/>.

## Array CGH Data Validation by Single Nucleotide Polymorphism (SNP) Analysis

Selection of SNP markers polymorphic between the C57BL/6J and 129/Ola strains to be used as validation tools was performed by consulting the Mouse Genome Informatics (MGI) database (<http://www.informatics.jax.org/>). DNA extractions from LCM paraffin-embedded tumor sections from *Apc*<sup>+/<sup>1638N</sup></sup> F1 129Ola/C57BL/6J mice was performed as previously described.<sup>23</sup> Two sets of primers were used to analyze SNPs rs3707129, rs3707206, and rs3707619 on chromosome 4 (Mb 128.087890-953) and SNPs rs3704911, rs3704966, rs4136991, and rs4136994 on chromosome 5 (Mb 107.544061-122), where two genomic regions were found to be frequently affected by gain/loss events. The primer sequences were as follows: chromosome 4 (forward) 5'-GCCTTCTGCTGTGTCTGAAG-3'; chromosome 4 (reverse) 5'-CCTTCTCTGAGGTTTGCTTGA; chromosome 5 (forward) 5'-GGGTGGCCAGACTGTTTAC-3'; and chromosome 5 (reverse) 5'-TTCCAAAGTCTGAGTTCAA-3'. PCR products were sequenced in both directions using the same primers. Sequencing was performed on an ABI 3700 capillary sequencer (Applied Biosystems, Foster City, CA) according to the manufacturer's instructions.

## Results

### Genomic Profiling of *Apc*<sup>+/<sup>1638N</sup></sup> Mouse Intestinal Tumors by Array CGH

To determine the presence of genomic alterations in mouse intestinal tumors driven by loss of *Apc* function, we performed array CGH analysis of LCM intestinal tumors derived from the *Apc*<sup>+/<sup>1638N</sup></sup> mouse model.<sup>14</sup> This method is highly sensitive and quantitative, and it allows the detection of chromosomal gains and losses in a small number of microdissected tumor cells with a resolution of ~1 Mb.<sup>2,19</sup>

First, we analyzed 10 mouse intestinal tumors derived from *Apc*<sup>+/<sup>1638N</sup></sup> animals encompassing both low ( $n = 7$ ) and high ( $n = 3$ ) dysplastic adenomas but no carcinoma.

Chromosomal aberrations were scored after smoothing the log<sub>2</sub> ratio between normal and tumor DNA by aCGH-Smooth, a tool for automatic breakpoint identification and smoothing of array CGH data.<sup>22</sup> To exclude putative artifacts attributable to the  $\phi$  amplification procedure (see Materials and Methods), we excluded gain/loss events affecting single BACs. The results are depicted in Figure 1 as a heat-map overview of the chromosomal regions affected by aneuploidy throughout the tumor and normal samples analyzed in the study.

The four microdissected normal control samples collected from the intestine of inbred C57BL/6J wild-type animals displayed near-diploid genomic profiles with no aberrations in one case and up to two independent aberrations (an interstitial gain within chromosome 5 in two cases, and a loss within chromosome 11 in one case) in the remaining three cases. The same aneuploid changes were found in three (chromosome 5 gain) and two (chromosome 11 loss) tumors, respectively, and were accordingly excluded from all of the subsequent statistical analyses.

All *Apc*<sup>+/<sup>1638N</sup></sup> tumor samples showed chromosomal number imbalances affecting either whole chromosomes or interstitial segments with a median of 11 events per sample (range, 4 to 21; SD = 6.5) (Table 1). No differences were observed in the number of aberrations between adenomas with high and low dysplasia (median, 12 and 10 events per sample, respectively). Notably, loss events were more frequent than gains among the tumor samples, with a median of two gain events per sample compared with 8.5 losses ( $P < 0.001$ , Wilcoxon signed ranks test). Gain of chromosome 1 (Mbp 94-130.6; 4 of 10 tumors) and losses of chromosome 2 (Mbp 25.1-33.7; 6 of 10 tumors), chromosome 4 (Mbp 117.4-153.1; 6 of 10 tumors), chromosome 5 (Mbp 108.5-148.5; 7 of 10 tumors), chromosome 8 (Mbp 121.7-125.9; 7 of 10 tumors), chromosome 10 (Mbp 80.1-80.6; 8 of 10 tumors), and chromosome 15 (Mbp 74.6-102.3; 9 of 10 tumors) were among the most frequently observed alterations (Figure 1). Whole chromosome loss/gain events were observed in three samples, namely loss of chromosome 8 (sample *Apc*9), loss of chromosomes 11 and 7 (sample *Apc*15), and loss of chromosomes 11 and 7 and gain of chromosome 18 (sample *Apc*18). The less frequent occurrence of gain/loss events at chromosome 18, where the *Apc* gene has been localized, confirms previous reports indicating that homologous somatic recombination is the principal pathway for allelic imbalance (AI) in adenomas in *Apc*<sup>+/-</sup> mice, leading to duplication of the chromosome harboring the *Apc* mutant allele<sup>24</sup> (see Discussion).

### Array CGH Validation by LOH Analysis Using SNPs

To validate the results obtained by array CGH on amplified LCM tumor samples, we performed LOH analysis by SNPs in an independent set of *Apc*<sup>+/<sup>1638N</sup></sup> adenomas. Three sets of primers were designed to amplify the genomic regions on chromosomes 4 and 5 frequently lost in the *Apc*<sup>+/<sup>1638N</sup></sup> mouse intestinal tumors. Each set of primers amplifies a region that contains at least three

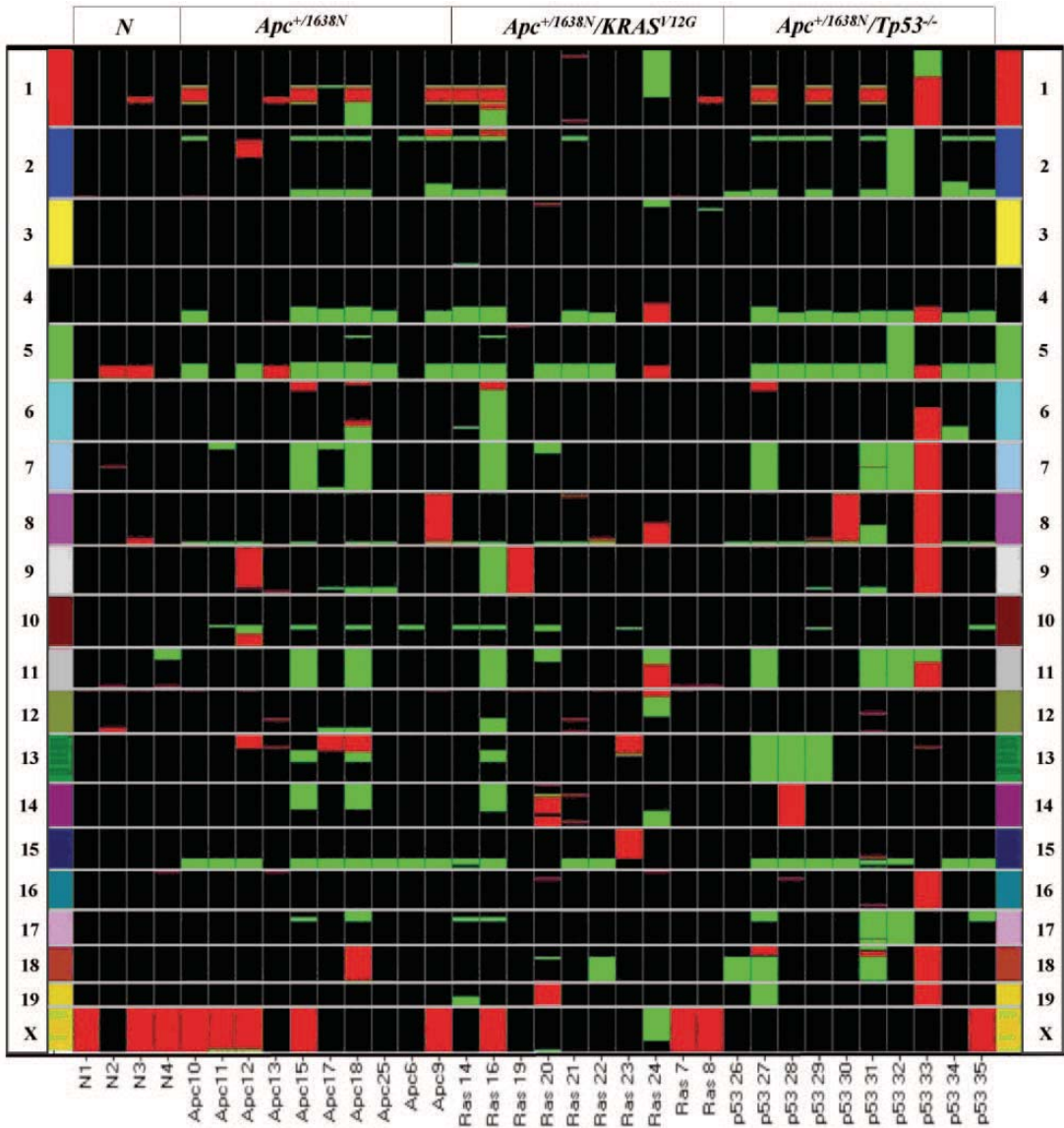


**Figure 1.** Heat map visualization of the CGH results for the three groups of tumors analyzed in the present study. After normalization and two-log smoothing of the array CGH ratios from the 30 tumor samples and four normal intestinal epithelia, the data were loaded onto SpotFire Decision Site 8.1 to obtain the heat map here represented. Data are ordered in the X bar according to the sample genotypes as normal (N), *Apc*<sup>+/1638N</sup> (*Apc*), *Apc*<sup>+/1638N/KRAS</sup><sup>V12G</sup> (*Ras*), and *Apc*<sup>+/1638N/</sup>*Trp53*<sup>-/-</sup> (*p53*), and in the Y bar according to the chromosome and Mb position of the BAC clones (color code at both sides of the heat map). The color code of the samples indicates BAC copy number changes: green, loss; red, gain; and black, no change.

SNPs known to be informative between the mouse strains C57BL/6J and Ola/129. To this aim, we used an independent group of tumors collected from *Apc*<sup>+/1638N</sup> animals obtained by breeding C57BL/6J *Apc*<sup>+/1638N</sup> mice with Ola/129 wild-type mice (*Apc*<sup>+/1638N</sup> F1 C57BL/6J × Ola/129).

The presence of allelic imbalance was evaluated by direct sequence analysis of the PCR-amplified SNPs. LOH at chromosome 5 (Mbp 108.5-148.5) was observed

in four of seven tumors (57%) with concordant loss within the same PCR reaction of the Ola/129 alleles (Figure 2). Similar results were obtained with chromosome 4 (three of six, 50%) SNPs. The data not only confirm and validate the array CGH results relative to loss of distinct loci on chromosomes 4 and 5 but also indicate that allelic imbalance at these loci is a common event during *Apc*-driven intestinal tumorigenesis, acting independently of the genetic background.

**Table 1.** Aneuploid Changes Observed in Upper GI Polyps from  $Apc^{+/1638N}$ ,  $Apc^{+/1638N}/KRAS^{V12G}$ , and  $Apc^{+/1638N}/Tp53^{-/-}$  Mice

Genotype	Number of mice	Mean age (months)	Number of tumors analyzed	Medians of gains and losses/tumor (range)	Medians of gains and losses/tumor according to histology*
$Apc^{+/1638N}$	7	6	10	11.5 (4 to 21) <sup>††</sup>	1 (L); 10 (H)
$Apc^{+/1638N}/KRAS^{V12G}$	7	5	10	8.5 (2 to 25) <sup>†§</sup>	9.5 (L); 8.5 (H)
$Apc^{+/1638N}/Tp53^{-/-}$	4	3	10	9.5 (3 to 19) <sup>‡§</sup>	15 (L); 9 (H)

\*Average number of chromosome alterations according to: H, high dysplastic adenomas; L, low dysplastic adenomas.

<sup>†</sup> $P = 0.513$ ; <sup>‡</sup> $P = 0.593$ ; <sup>§</sup> $P = 0.313$ ; Wilcoxon signed ranks test (two-tailed).

*Genomic Profiles of Intestinal Tumors from  $Apc^{+/1638N}/KRAS^{V12G}$  and  $Apc^{+/1638N}/Tp53^{-/-}$  Animals*

The above results indicate that aneuploidy occurs at very early stages of *Apc*-driven intestinal tumorigenesis, in agreement with our own array CGH analysis of human polyps from patients with germline *APC* mutations<sup>2</sup> but also with the previously reported *APC*'s function in mitosis and chromosomal stability.<sup>7,8,16</sup> However, it is plausible that other genes frequently mutated along the adenoma-carcinoma sequence contribute, together with *APC*, to the full-blown CIN phenotype observed in late-stage CRC in human. To explore this hypothesis, we performed array CGH analysis of intestinal tumors from  $Apc^{+/1638N}$  animals bred with either a transgenic model carrying the activated human *KRAS* oncogene under the control of the villin promoter ( $KRAS^{V12G}$ )<sup>16</sup> or with a *Tp53* knockout model carrying a targeted *null* mutation at the endogenous p53 tumor suppressor gene ( $Tp53^{-/-}$ ).<sup>17</sup> Tumors from these compound animals recapitulate the genetic

status of the vast majority of human colorectal tumors during adenoma progression ( $Apc^{1638N}/KRAS^{V12G}$ ) and at later carcinoma stages ( $Apc^{1638N}/Tp53^{-/-}$ ), and are therefore useful to test the above hypothesis. The phenotypic and molecular characterization of these compound models has been described elsewhere.<sup>15,25</sup>

We performed array CGH analysis on 10 tumors from each of the compound  $Apc^{+/1638N}/KRAS^{V12G}$  and  $Apc^{+/1638N}/Tp53^{-/-}$  genotypes, encompassing both low and high dysplastic adenomas (two low and eight high in the former, and three low and seven high in the latter). The results of these analyses are reported in Figure 1 and Table 1. Intestinal adenomas from  $Apc^{+/1638N}/KRAS^{V12G}$  animals showed a median of chromosomal alterations of 8.5 events per sample (range, 2 to 25; SD = 6.8). The latter does not significantly differ from the average number of chromosomal alterations found in  $Apc^{+/1638N}$  tumors (median, 11 events per sample; range, 4 to 21; SD = 6.5). Moreover, no statistically significant differences were observed between low and high dysplastic lesions, although the sample size is admittedly limited (Table 1). Tumors from  $Apc^{+/1638N}/Tp53^{-/-}$  mice presented a median of 9.5 gain/loss events per sample (range, 3 to 19; SD = 5.08) with low dysplastic adenoma characterized by a slight though not significant increase in the number of genomic imbalances when compared with the high dysplastic group (median, 15 versus 9). Moreover, no significant differences were found between the three groups when loss and gain events were analyzed separately. However, when gains and losses affecting whole chromosomes were considered, tumors from  $Apc^{+/1638N}/Tp53^{-/-}$  mice revealed a significant increase when compared with intestinal lesions from  $Apc^{+/1638N}$  (median of one event per sample compared with 0;  $P = 0.008$ ; Wilcoxon signed ranks test) or  $Apc^{+/1638N}/KRAS^{V12G}$  (median of one event per sample compared with 0;  $P = 0.005$ ; Wilcoxon signed ranks test). In addition, when the total number of gains versus losses for all three tumor genotypes is taken into consideration, loss events seem to occur at higher frequency regardless of genotype (median of eight versus two;  $P < 0.001$ ; Wilcoxon signed ranks test).

Overall, the array CGH analysis performed on intestinal tumors from  $Apc^{+/1638N}$ ,  $Apc^{+/1638N}/KRAS^{V12G}$ , and  $Apc^{+/1638N}/Tp53^{-/-}$  mice led to the identification of several chromosomal abnormalities, with evidence of intertumor heterogeneity even among tumors from within the same genotype (Figure 1). However, we also observed the presence of recurrent genomic aberrations likely to result from selection of specific chromosomal regions encompassing

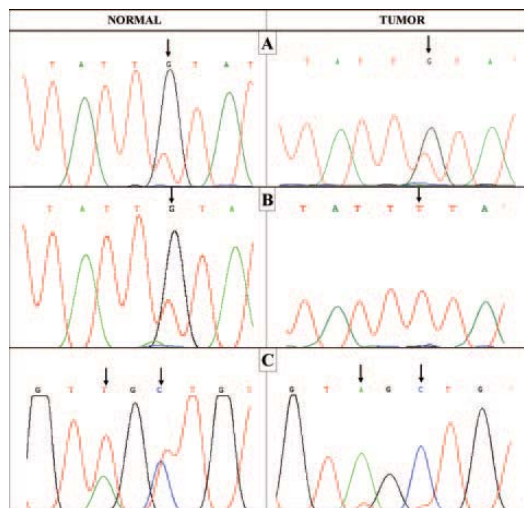


**Figure 2.** LOH analysis performed on  $Apc^{+/1638N}$  F1 C57BL/6J  $\times$  Ola/129 mouse tumors by direct nucleotide sequencing of single nucleotide polymorphisms (SNPs) validates the array CGH results. The examples are relative to three SNPs on chromosome 5: rs3704966, rs4136991, and rs4136994. **A:** Nucleotide sequence analysis of SNP rs3704966 showing retention of both alleles in the tumor sample. **B** and **C:** Nucleotide sequence analysis of SNPs rs3704966 or rs4136991 and rs4136994, respectively, each showing hetero- and hemizygosity in the normal and tumor DNA samples, respectively. The **arrows** indicate the polymorphic nucleotide position for each SNP sequence.

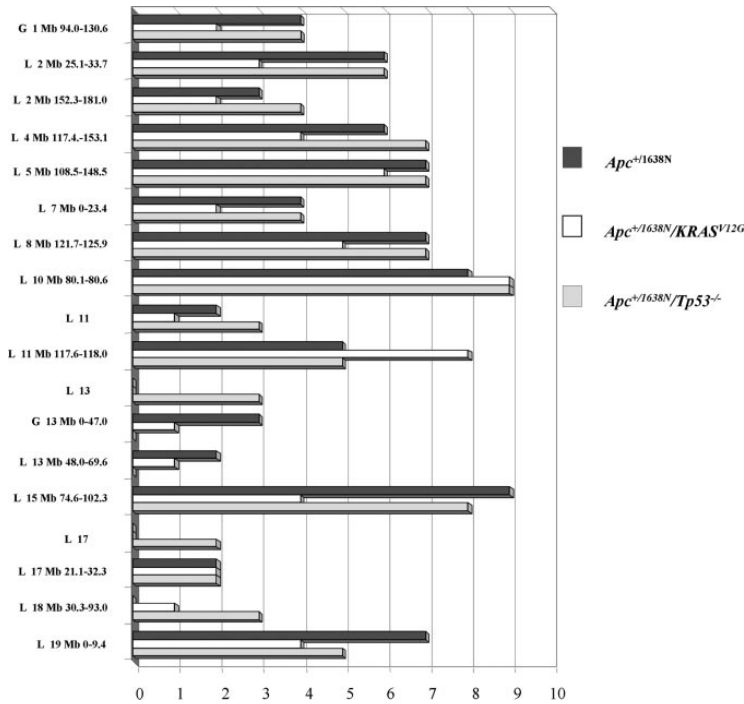


**Figure 3.** Overview of the chromosome copy number changes throughout the 30 mouse intestinal tumors analyzed in this study. Total numbers of all significant gains or loss regions found to be affected by copy number alterations in more than or equal to two tumor samples from at least two independent groups have been plotted separately according to the tumor genotype. Complete or partial chromosome gains and losses are shown separately. Regions are ordered according to their mapped positions along the chromosomes. G, gain; L, loss of the corresponding regions.

highly relevant genes for intestinal tumor progression. All of the chromosomal segments found to be affected by copy number alterations in at least two independent tumor samples from two independent groups have been plotted and are depicted in Figure 3. Specific chromosomal regions of recurrent aneuploidy are present throughout all three adenoma groups; in particular, chromosomes 2, 4, 5, 8, 10, and 15 show copy number alterations in more than 60% of the samples in at least two distinct genotypes. Notably, a total of six (20%) allelic imbalance events (gains and losses) were found at chromosome 18, where the *Apc* and *Smad4* tumor suppressors are localized.

### Comparative Genomic Analysis of Mouse and Human Intestinal Adenomas Reveals Highly Conserved Regions of Aneuploidy

To identify chromosomal loci conserved between human and mouse that recurrently undergo gain/loss events during intestinal tumor progression, we performed a comparative analysis of the mouse array CGH profiles with those derived from our previous array CGH analysis of early adenomas from FAP patients carrying established *APC* mutations.<sup>2</sup> To this aim, we used the human-mouse comparative maps available through the National Center of Biotechnology Information, National Institutes of Health (<http://www.ncbi.nlm.nih.gov/Homology/>). Based on the analysis of the homologous segments, the vast majority of the numerical chromosomal changes found in the mouse correspond to chromosomal regions of frequent allelic imbalance among

FAP adenomas (Table 2). Notably, chromosomal regions with the highest deletion frequencies among mouse intestinal tumors are syntenic to human chromosomal regions with the highest LOH incidence in FAP polyps. Mouse chromosomes 4 and 15 for instance, harbor several regions that are orthologous to human chromosome 1p34-p36 and 22q12-q13, respectively, both known to be lost in human FAP adenomas with a percentage that varies between 67 to 75%. In some cases, the analysis of the homology region between mouse and human chromosomal regions of allelic imbalance allows the definition of a minimal common region, thus providing a powerful gene-discovery tool (see Discussion).

### Discussion

Extensive genome-wide chromosomal alterations, indicative of CIN, characterize the vast majority of human CRCs.<sup>26,27</sup> However, the molecular basis of CIN in CRC is still poorly understood, and although a number of genes have been characterized that may underlie aneuploidy (eg, *BUB1*, *BUBR1*, and *CDC4*),<sup>5,28,29</sup> the frequency at which mutations have been found in their coding regions is too low to justify the high CIN incidence found in human CRC.<sup>29</sup> Notably, loss of *APC* function results in microtubule plus-end attachment defects during mitosis and consequent chromosome misalignment and CIN.<sup>7-9</sup> These observations, made in cultured mammalian cells, indicate a potential role for the *APC* tumor suppressor gene in triggering CIN right from the start of

the adenoma-carcinoma sequence. Accordingly, our array CGH analysis of early-stage adenomas from FAP patients carrying germline *APC* mutations<sup>2</sup> and from *Apc*-mutant mouse models (this study) confirm that aneuploidy is indeed found in nascent benign tumors.

It is generally accepted that the main tumor-suppressing activity of the *APC* gene resides in its capacity to regulate intracellular  $\beta$ -catenin levels as part of the canonical Wnt signal transduction pathway.<sup>1</sup> Hence, the observation that aneuploidy occurs at very early stages of the adenoma-carcinoma sequence is in agreement with a model in which the initial loss of *APC* function triggers intestinal tumor formation by constitutive activation of Wnt/ $\beta$ -catenin signaling and simultaneously results in a low but significant level of CIN. At later stages of tumor progression, somatic mutations in genes involved in mitotic and cell cycle checkpoints, telomere shortening and telomerase expression, centrosome number regulation, and double-strand break repair may work synergistically with the kinetochore and chromosome segregation defects caused by *APC* mutation in eliciting full-blown CIN.<sup>1,10</sup>

Overall, our array CGH analysis has revealed chromosomal aberrations in each of the 30 mouse GI polyps analyzed. Even in the case of small low dysplastic *Apc*<sup>+1638N</sup> adenomas (2 mm<sup>3</sup>), an average of 12 events (gains and losses) per tumor sample is found. Notably, both in *Apc*<sup>+1638N</sup> as well as in FAP adenomas, loss events were more frequently observed than gains.<sup>2</sup> This relatively high incidence of aneuploid changes at very early stages of the adenoma-carcinoma sequence appears to be in contrast with previous reports in which intestinal adenomas from *Apc*<sup>+Min</sup> mice<sup>30</sup> and from FAP patients with known *APC* mutations<sup>31</sup> were shown to have stable karyotypes. This apparent discrepancy is likely to result from the different methods used in these studies. Conventional karyotype analysis and fluorescence-activated cell sorting are less sensitive than array CGH in detecting more subtle subchromosomal changes leading to allelic imbalance. Accordingly, by using a more sensitive PCR-based method, Shih and colleagues<sup>11</sup> also reported widespread allelic imbalance in human sporadic adenomas. As shown in the present and previous study,<sup>2</sup> the quantitative analysis of genomic changes by coupled LCM and whole genome BAC arrays, allows the detection of gain/loss events in small intestinal lesions (1 to 2 mm<sup>2</sup>) with relatively high sensitivity and without the noise introduced by contaminating normal lymphocytes and stromal cells.

Although our results do not allow us to speculate on the mechanisms underlying this early genomic instability, we have established that aneuploid changes are observed at early stages of *APC/Apc*-driven intestinal tumorigenesis in both human<sup>2</sup> and mouse (this study). The question remains whether this genomic instability precedes the rate-limiting second hit at the *Apc* gene or it arises as a consequence of it. In the mouse genome, the *Apc* gene maps to chromosome 18. In agreement with the Knudson's two hit model, the vast majority of intestinal tumors from *Apc*-mutant mice show LOH at the chromosome 18 region encompassing the wild-type *Apc* allele.<sup>13,32,33</sup> As elegantly shown by Haigis and Dove,<sup>24</sup> somatic mitotic recombination (and not aneu-

ploidy) is the principal mechanism underlying loss of the wild-type *Apc* allele in the *Apc*<sup>+Min</sup> mouse model. Because mitotic recombination does not affect copy number, it cannot be detected by array CGH analysis. Accordingly, our array CGH analysis revealed aneuploidy at chromosome 18 only in a minority of adenomas from *Apc*<sup>+1638N</sup> (10%) and from *Apc*<sup>+1638N</sup>/*KRAS*<sup>V12G</sup> and *Apc*<sup>+1638N</sup>/*Tp53*<sup>-/-</sup> (25%) animals. Hence, our results indirectly confirm that, in the majority of the cases, the rate-limiting LOH event at the *Apc* locus does not occur by interstitial deletion or nondisjunction, and is likely to result from mitotic recombination as shown for *Apc*<sup>+Min</sup>. However, aneuploid changes at the *Apc* locus on chromosome 18 still take place in a fraction of the intestinal adenomas initiated by the *Apc*<sup>1638N</sup> targeted mutation, possibly as the result of low but significant CIN levels. That *APC* mutations may act in a dominant-negative manner in eliciting mitotic defects<sup>9,34</sup> may underlie the chromosome 18 aneuploid changes observed by array CGH in adenomas from *Apc*<sup>+1638N</sup>. In these cases, genomic instability may even precede the rate-limiting second hit at the wild-type *Apc* allele. Nevertheless, in the majority of the cases, more significant CIN levels will occur only on complete loss of *Apc* function, ie, after the somatic hit.

During the adenoma-carcinoma progression in CRC, genetic instability progressively increases with the accumulation of somatic mutations at specific tumor suppressor genes and oncogenes.<sup>35</sup> The occurrence of *KRAS* mutations already at early adenoma stages<sup>36-38</sup> suggests the possibility that this oncogene may partly contribute to CIN. In fact, few studies have reported positive correlations between *KRAS* mutations and aneuploidization.<sup>39,40</sup> It has been postulated that constitutive *KRAS* activation may induce genomic instability via the mitogen-activated protein kinase (MAPK) pathway, which affects G<sub>1</sub> and G<sub>2</sub>/M cell-cycle transit times and apoptosis.<sup>41</sup> Moreover, *KRAS* can also have a role in cytoskeletal and microtubule organization of the mitotic spindle, through the regulation of Rho-like GTPases.<sup>42</sup> Notwithstanding these data, our results do not demonstrate any increase in the incidence and type of allelic imbalance in tumors from compound *Apc*<sup>+1638N</sup>/*KRAS*<sup>V12G</sup> mice when compared with *Apc*<sup>+1638N</sup> animals. These results are also corroborated by other studies on human CRC: no association was found between the mutational status of the *KRAS* gene and the number of chromosomal aberrations<sup>43</sup> or genomic instability.<sup>44</sup>

The case for loss of p53 function and CIN is a more solid one. First, the p53 tumor suppressor protein has a well-characterized role as DNA damage checkpoint.<sup>45</sup> Moreover, several cancers characterized by aneuploidy harbor p53 mutations both in human<sup>46-48</sup> and in mouse models.<sup>49</sup> Loss of p53 function is also known to result in an increase in tetraploid and polyploid cells.<sup>50,51</sup> Although the CGH array technique used here does not allow to detect tetraploidy, our results indicate a significant increase in whole chromosome gains and losses among *Apc*<sup>+1638N</sup>/*Tp53*<sup>-/-</sup> adenomas when compared with tumors from *Apc*<sup>+1638N</sup> and *Apc*<sup>+1638N</sup>/*KRAS*<sup>V12G</sup> mice. It has been shown that p53-deficient cells fail to arrest in G<sub>1</sub> leading to tetraploidization and, on further progression through the cell cycle, to abnormal mitoses

**Table 2.** Analysis of the Mouse-Human Chromosome Synteny and Incidence of Genomic Aberrations in Intestinal FAP Adenoma and Sporadic CRC

Mouse chromosome segment (Mbp)	Incidence in mouse adenomas	Human syntenic region (cytogenetic band)	Incidence in human FAP <sup>2</sup>		Incidence in human CRC <sup>68-73*</sup>	
			As gain	As loss	As gain	As loss
<b>Gains</b>						
1 (94 to 130)	33%	5q21 18q21q22-q23 2q12-q13-q14 2cen-q13 2q21-q22		5q21 (13%) 18q (4%)		5q (16%) 18q (42%) 2q (6%)
4 (117 to 153)	6%	1p34-p36		1p36 (57%) 1p (75%)		1p (17%)
8 (whole chr.)	6%	13q33-q34-q14 8p21-p22-p23-p11 4q31-q32-q33- q34-q35-21-q28 19p13-p12 22q13 16q11-q12-q13 16q21-q22-q23- q24 1q42 10p11	1q42 (8%) 10p (2%)	13q (4%) 8p (2%) 19p (73%) 22q13 (63%) 16q (8%) 1q42 (4%)	22q13 (5%) 16q (7%)	8p21p22 (28%) 4q31-q34 (21%)
11 (whole chr.)	6%	22q12 17q25 7p12-q13	7p (8%)	22q (67%) 17q25 (33%)		22q (6%)
13 (0 to 40)	12%	10p14-p15 1q41-q42-q43 7p14-p15 6p21-p22-p24-p14	7p (19%)	10p (2%) 1q (4%)	7p (35%) 6p21 (7%)	
18 (13 to 23)	12%	18q11-q13		18q (4%)		18q (42%)
18 (whole chr.)	6%	10p11 18q11-q12 2q13-q13-q21 5q21-q22-q23- q31-q32-q33 18p11-q21-q22- q23	18q (2%)	10p (2%) 18q (4%) 5q (12%) 18q21 (4%)		18q (42%) 5q (16%) 18p (26%) 18q21 (60%)
<b>Losses</b>						
2 (25 to 33)	50%	9q34		9q (36.5%)	9q (8%)	
2 (152 to 181)	30%	20q11-q13		20q (36.5%)	20q13 (50%)	
4 (117 to 153)	56%	1p34-p36		1p36 (57%) 1p (75%)		1p (17%)
5 (114 to 148)	66%	12q24 13q12 7p11-p22-q11-q22	7p (19%) 7q (19%)	12q (50%) 13q (7.7%) 19q13 (68%)	13q (12%)	
7 (0 to 23)	16%	19q13		19q13 (68%)		
7 (whole chr.)	16%	19q13 11p15-p14 15q11 2p13 15q26 11q13-q14-p15 16p11-p12-p13 1-q26		19q13 (68%) 15q (4%) 16p (2%) 16q (8%)	11q (43%) 16p13 (5%)	
8 (121 to 125)	63%	16q24 1q42	1q (8%)	16q (8%) 1q (4%)		
10 (80.1 to 80.6)	86%	19p13.3		19p (73%)		
11 (whole chr.)	20%	22q12 17q25 7p12-q13	7p (8%)	22q (67%) 17q25 (33%)	7p (25%)	22q (6%)
11 (117 to 118)	60%	17q25		17q (42%)		17q25 (14%)
13 (whole chr.)	10%	10p15 1q41-q42-q43 7p14-p15 6p21-p22-p23-p24-p25 9q21-q22 5q34-q35-q31 9q21-q22 8q22 5p15 5q11-q12-q13- q14-q15	7p (19%) 8q (2%)	10p (2%) 1q (4%) 5q (14%) 5q (11%) 8q (15%)	7p (35%) 6p21 (7%) 9q21 (6%) 8q (63%) 5p (4%)	5q (16%)
13 (48 to 69)	10%	5q34-q35-q31 9q21-q22 8q22 5p15		5q (14%) 8q (15%)	9q21 (6%) 8q (63%) 5p (4%)	5q (16%)
15 (74 to 102)	70%	22q12-q13 12q12-q13		22q (67%) 12q (50%)	12q (5%)	12q (15%)
17 (whole chr.)	6%	6q25-q27 5q15 19q13 6p21 21q22 10p13 7p21-p22 3p24 19p13 5q21 18p11 2p21-p22- p23-p16 18p11	7p (20%)	19p (73%) 5q (12%) 19q13 (58%) 21q (10%)	5q (16%) 7p (25%)	5q (16%) 7p (25%)
17 (21 to 32)	20%	19p13		19p (73%)		

(table continues)

**Table 2.** Continued

Mouse chromosome segment (Mbp)	Incidence in mouse adenomas	Human syntenic region (cytogenetic band)	Incidence in human FAP <sup>2</sup>		Incidence in human CRC <sup>68-73*</sup>	
			As gain	As loss	As gain	As loss
18 (whole chr.)	6%	10p11 18q11-q12 2q13-q13-q21 5q21-q22-q23- q31-q32-q33 18p11-q21-q22- q23		10p (2%) 18q (4%) 5q (12%) 18q21 (4%)		18q (42%) 5q (16%) 18p (26%) 18q21 (60%)
18 (30 to 93)	13%	18q11-q12 2q13- q13-q21 5q21- q22-q23-q31-q32- q33 18p11-q21- q22-q23		18q (4%) 5q (12%) 18q21 4%		18q (42%) 5q (16%) 18p (26%) 18q21 (60%)
19 (0 to 9.4)	53%	11q11-q12-q13				11q (19%) 11q13 (43%)

\*Results are described in References 68 to 72 and are summarized in Reference 73.

and aneuploidy.<sup>52</sup> This mechanism seems to be corroborated by the increased incidence of whole chromosome loss and gain in p53-deficient intestinal tumors.

The array CGH analysis of mouse intestinal adenomas revealed a number of chromosomal loci where allelic imbalances recurrently occur in independent tumors and throughout the three genotypes. It is therefore likely that mutations in genes encompassed within these chromosomal regions are selected at early developmental stages of intestinal tumor onset and progression. However, the chromosomal intervals affected by these recurrent aneuploidy events are usually very large, which makes the identification of individual genes underlying tumor onset and progression a formidable task. Throughout the mouse intestinal adenomas analyzed here, loss of chromosome 10 (Mb 80.1 to 80.6) and of the distal region of chromosome 15 (Mb 74.6 to 102.3) were the most frequent alterations with frequencies of 86 and 70%, respectively. The limited size (~500 kb) delineated by the loss events within chromosome 10 somewhat facilitates the search for putative candidate cancer-related mapping within the Mb 80.1 to 80.6 interval. *In silico* analysis of the mouse genome sequence (<http://www.informatics.jax.org/>) revealed 40 annotated expressed sequences, 26 of which are known genes. The localization of the *Stk11* gene within this region is of particular interest in view of the causative role of this serine/threonine kinase in Peutz-Jeghers syndrome, an inherited susceptibility to intestinal cancer characterized by multiple hamartomatous polyps throughout the upper GI tract and a high risk of developing cancer in the intestine and other organs.<sup>53</sup>

To further restrict the size of the chromosomal intervals affected by gain/loss events and pinpoint specific conserved genes that play rate-limiting roles in intestinal adenoma formation in the mouse and human, we compared array CGH profiles from early FAP adenomas (obtained from carriers of known *APC* germline mutations) and from histology-matched intestinal tumors from *Apc*<sup>+1638N</sup> mice. The results of this comparative analysis (Table 2) have indicated the presence of a surprisingly high number of chromosomal aberrations shared between mouse upper GI and human colorectal

adenomas, notwithstanding the different anatomical location of these two groups of GI tumors. The above-mentioned mouse chromosome 10 region (Mb 80.1 to 80.6), where aneuploid changes have been observed in 86% of the mouse adenomas here analyzed, is orthologous to human chromosome 19p13.3, where LOH has been reported in 73% of FAP adenomas. Besides *STK11*, also the *APC2* gene,<sup>54,55</sup> previously proposed as potential tumor suppressor gene in ovarian and lung cancer,<sup>56,57</sup> map to the 19p13.3 chromosomal interval.

Another example is provided by the interval on mouse chromosome 15 (Mb 74 to 102), the second most frequent (70%) site of allelic imbalance in tumors from *Apc*<sup>+1638N</sup> mice. This region is syntenic to human chromosomes 22q12-q13 and 12q12-q13, both previously reported to undergo LOH in FAP adenomas at high frequencies (67 and 50%, respectively).<sup>2</sup> Notably, at least three genes with known tumor suppressor functions in the GI tract map in human to chromosome 22q13. *ST13* (suppression of tumorigenicity 13) maps to chromosome 22q13.2 and was reported to be down-regulated in CRC tissue when compared with its expression in adjacent normal tissue.<sup>58</sup> Bi-allelic mutations of p300, a transcriptional co-activator binding E1A also localized to chromosome 22q13.2, have been shown in several human cancers. In particular, this gene seems to function as a tumor suppressor gene in the intestinal epithelium,<sup>59</sup> and mutations in its coding region are found at high frequency among CRC cell lines.<sup>60</sup> *NBK/BIK* is another putative tumor suppressor gene localized within a 0.5-cM region of chromosome 22q13 known as the target of frequent allelic loss in human CRC.<sup>61</sup> The proapoptotic function of this *BCL-2* family member indeed suggests a role in tumor suppression for this protein.<sup>62</sup>

The frequently lost interval on mouse chromosome 4 (Mb 117 to 153) is orthologous to human chromosome 1p34-p36. Among FAP adenomas, chromosome 1p36 shows loss in ~60% of the cases,<sup>2</sup> thus restricting the candidate tumor suppressor genes in this 24-Mb region, to a total of 392 transcripts. Among these, the meningioma suppressor gene *ALPL*,<sup>63</sup> the prostate cancer susceptibility gene *HSPG2*,<sup>64</sup> and *CASP9*, a proapoptotic

component of the caspase cascade,<sup>65</sup> represent interesting and worth investigating candidates.

In addition, the mouse chromosome 2 region (Mb 25 to 33) lost in 50% of the *Apc*<sup>1638N</sup> adenomas, is syntenic with human chromosome 9q34. Again, chromosome 9q is frequently lost among FAP polyps.<sup>2</sup> The additional information obtained from the analysis of mouse intestinal tumors allows restriction of the search for candidate tumor suppressor genes to the chromosome 9q34 interval where cancer-related genes such as *TSC1* (tuberous sclerosis 1)<sup>66</sup> and *DAPK1* (death-associated protein kinase 1),<sup>67</sup> are known to be localized. The use of additional comparative tools, such as expression profiling analysis, is likely to further pinpoint critical genes among the still large number of transcripts ( $n = 227$ ) mapping to this subchromosomal region.

In conclusion, we have shown that allelic imbalance and aneuploid changes occur at early stages of *Apc*-driven intestinal tumorigenesis in mouse. Whereas introduction of an oncogenic *KRAS* mutation does not alter the overall frequency and type of aneuploid changes, loss of *Tp53* function increases the incidence of whole chromosome loss and gain events. Notably, the chromosomal intervals frequently affected by aneuploid changes in *Apc*-mutant tumors are syntenic to genomic regions known to be frequently lost or gained in adenomatous polyps from FAP carriers of germline *APC* mutations. This comparative genomic profiling approach, when combined with gene expression signatures from human and mouse tumors and coupled with functional tumor suppression assays, will allow the identification of novel genes involved in intestinal tumor onset and progression.

### Acknowledgment

We thank Dr. Claudia Gaspar for technical assistance and stimulating discussions.

### References

1. Fodde R, Smits R, Clevers H: APC, signal transduction and genetic instability in colorectal cancer. *Nat Rev Cancer* 2001, 1:55–67
2. Cardoso J, Molenaar L, de Menezes RX, van Leerdam M, Rosenberg C, Moslein G, Sampson J, Morreau H, Boer JM, Fodde R: Chromosomal instability in MYH- and APC-mutant adenomatous polyps. *Cancer Res* 2006, 66:2514–2519
3. Cahill DP, Lengauer C, Yu J, Riggins GJ, Willson JK, Markowitz SD, Kinzler KW, Vogelstein B: Mutations of mitotic checkpoint genes in human cancers. *Nature* 1998, 392:300–303
4. Shichiri M, Yoshinaga K, Hisatomi H, Sugihara K, Hirata Y: Genetic and epigenetic inactivation of mitotic checkpoint genes hBUB1 and hBUBR1 and their relationship to survival. *Cancer Res* 2002, 62:13–17
5. Rajagopalan H, Jallepalli PV, Rago C, Velculescu VE, Kinzler KW, Vogelstein B, Lengauer C: Inactivation of hCDC4 can cause chromosomal instability. *Nature* 2004, 428:77–81
6. Michel L, Benezra R, Diaz-Rodriguez E: MAD2 dependent mitotic checkpoint defects in tumorigenesis and tumor cell death: a double edged sword. *Cell Cycle* 2004, 3:990–992
7. Kaplan KB, Burds AA, Swedlow JR, Bekir SS, Sorger PK, Nathke IS: A role for the adenomatous polyposis coli protein in chromosome segregation. *Nat Cell Biol* 2001, 3:429–432
8. Fodde R, Kuipers J, Rosenberg C, Smits R, Kielman M, Gaspar C, van Es JH, Breukel C, Wiegant J, Giles RH, Clevers H: Mutations in the APC tumour suppressor gene cause chromosomal instability. *Nat Cell Biol* 2001, 3:433–438
9. Green RA, Kaplan KB: Chromosome instability in colorectal tumor cells is associated with defects in microtubule plus-end attachments caused by a dominant mutation in APC. *J Cell Biol* 2003, 163:949–961
10. Alberici P, Fodde R: The Role of APC Tumor Suppressor in Chromosomal Instability. Würzburg, Karger, 2006, pp 149–170
11. Shih IM, Zhou W, Goodman SN, Lengauer C, Kinzler KW, Vogelstein B: Evidence that genetic instability occurs at an early stage of colorectal tumorigenesis. *Cancer Res* 2001, 61:818–822
12. Fodde R, Smits R: Disease model: familial adenomatous polyposis. *Trends Mol Med* 2001, 7:369–373
13. Smits R, Kartheuser A, Jagmohan-Changur S, Leblanc V, Breukel C, de Vries A, van Kranen H, van Krieken JH, Williamson S, Edelmann W, Kucherlapati R, Khan P, Fodde R: Loss of Apc and the entire chromosome 18 but absence of mutations at the Ras and Tp53 genes in intestinal tumors from Apc1638N, a mouse model for Apc-driven carcinogenesis. *Carcinogenesis* 1997, 18:321–327
14. Fodde R, Edelmann W, Yang K, van Leeuwen C, Carlson C, Renault B, Breukel C, Alt E, Lipkin M, Khan PM, Kucherlapati R: A targeted chain-termination mutation in the mouse Apc gene results in multiple intestinal tumors. *Proc Natl Acad Sci USA* 1994, 91:8969–8973
15. Smits R, van der Hoven van Oordt W, Luz A, Zurcher C, Jagmohan-Changur S, Breukel C, Khan PM, Fodde R: Apc1638N: a mouse model for familial adenomatous polyposis-associated desmoid tumors and cutaneous cysts. *Gastroenterology* 1998, 114:275–283
16. Janssen KP, el-Marjou F, Pinto D, Sastre X, Rouillard D, Fouquet C, Soussi T, Louvard D, Robine S: Targeted expression of oncogenic K-ras in intestinal epithelium causes spontaneous tumorigenesis in mice. *Gastroenterology* 2002, 123:492–504
17. Jacks T, Remington L, Williams BO, Schmitt EM, Halachmi S, Bronson RT, Weinberg RA: Tumor spectrum analysis in p53-mutant mice. *Curr Biol* 1994, 4:1–7
18. Boivin GP, Washington K, Yang K, Ward JM, Pretlow TP, Russell R, Besselsen DG, Godfrey VL, Doetschman T, Dove WF, Pitot HC, Halberg RB, Itzkowitz SH, Groden J, Coffey RJ: Pathology of mouse models of intestinal cancer: consensus report and recommendations. *Gastroenterology* 2003, 124:762–777
19. Cardoso J, Molenaar L, de Menezes RX, Rosenberg C, Morreau H, Moslein G, Fodde R, Boer JM: Genomic profiling by DNA amplification of laser capture microdissected tissues and array CGH. *Nucleic Acids Res* 2004, 32:e146
20. Chung YJ, Jonkers J, Kitson H, Fiegler H, Humphray S, Scott C, Hunt S, Yu Y, Nishijima I, Velds A, Holstege H, Carter N, Bradley A: A whole-genome mouse BAC microarray with 1-Mb resolution for analysis of DNA copy number changes by array comparative genomic hybridization. *Genome Res* 2004, 14:188–196
21. Fiegler H, Carr P, Douglas EJ, Burford DC, Hunt S, Scott CE, Smith J, Vetrie D, Gorman P, Tomlinson IP, Carter NP: DNA microarrays for comparative genomic hybridization based on DOP-PCR amplification of BAC and PAC clones. *Genes Chromosom Cancer* 2003, 36:361–374
22. Jong K, Marchiori E, van der Vaart A, Ylstra B, Weiss M, Meijer G: Chromosomal Breakpoint Detection in Human Cancer. Heidelberg, Springer, 2003, pp 54–65
23. Alberici P, Jagmohan-Changur S, De Pater E, Van Der Valk M, Smits R, Hohenstein P, Fodde R: Smad4 haploinsufficiency in mouse models for intestinal cancer. *Oncogene* 2006, 25:1841–1851
24. Haigis KM, Dove WF: A Robertsonian translocation suppresses a somatic recombination pathway to loss of heterozygosity. *Nat Genet* 2003, 33:33–39
25. Janssen KP, Alberici P, Fsihi H, Gaspar C, Breukel C, Franken P, Rosty C, Abal M, El Marjou F, Smits R, Louvard D, Fodde R, Robine S: APC and oncogenic KRAS are synergistic in enhancing Wnt signaling in intestinal tumor formation and progression. *Gastroenterology* 2006, 131:1096–1109
26. Lengauer C, Kinzler KW, Vogelstein B: Genetic instability in colorectal cancers. *Nature* 1997, 386:623–627
27. Thiagalasingam S, Laken S, Willson JK, Markowitz SD, Kinzler KW, Vogelstein B, Lengauer C: Mechanisms underlying losses of heterozygosity in human colorectal cancers. *Proc Natl Acad Sci USA* 2001, 98:2698–2702
28. Grady WM: Genomic instability and colon cancer. *Cancer Metastasis Rev* 2004, 23:11–27
29. Rajagopalan H, Lengauer C: hCDC4 and genetic instability in cancer. *Cell Cycle* 2004, 3:693–694
30. Haigis KM, Caya JG, Reichelderfer M, Dove WF: Intestinal adenomas

- can develop with a stable karyotype and stable microsatellites. *Proc Natl Acad Sci USA* 2002, 99:8927–8931
31. Sieber OM, Heinemann K, Gorman P, Lammler H, Crabtree M, Simpson CA, Davies D, Neale K, Hodgson SV, Roylance RR, Phillips RK, Bodmer WF, Tomlinson IP: Analysis of chromosomal instability in human colorectal adenomas with two mutational hits at APC. *Proc Natl Acad Sci USA* 2002, 99:16910–16915
  32. Luongo C, Moser AR, Gledhill S, Dove WF: Loss of Apc<sup>+</sup> in intestinal adenomas from Min mice. *Cancer Res* 1994, 54:5947–5952
  33. Oshima M, Oshima H, Kitagawa K, Kobayashi M, Itakura C, Taketo M: Loss of Apc heterozygosity and abnormal tissue building in nascent intestinal polyps in mice carrying a truncated Apc gene. *Proc Natl Acad Sci USA* 1995, 92:4482–4486
  34. Tighe A, Johnson VL, Taylor SS: Truncating APC mutations have dominant effects on proliferation, spindle checkpoint control, survival and chromosome stability. *J Cell Sci* 2004, 117:6339–6353
  35. Fearon ER, Vogelstein B: A genetic model for colorectal tumorigenesis. *Cell* 1990, 61:759–767
  36. Smith AJ, Stern HS, Penner M, Hay K, Mitri A, Bapat BV, Gallinger S: Somatic APC and K-ras codon 12 mutations in aberrant crypt foci from human colons. *Cancer Res* 1994, 54:5527–5530
  37. Forrester K, Almoguera C, Han K, Grizzle WE, Perucho M: Detection of high incidence of K-ras oncogenes during human colon tumorigenesis. *Nature* 1987, 327:298–303
  38. Pretlow TP, Brasitus TA, Fulton NC, Cheyer C, Kaplan EL: K-ras mutations in putative preneoplastic lesions in human colon. *J Natl Cancer Inst* 1993, 85:2004–2007
  39. Giaretti W, Pujic N, Rapallo A, Nigro S, Di Vinci A, Geido E, Risio M: K-ras-2 G-C and G-T transversions correlate with DNA aneuploidy in colorectal adenomas. *Gastroenterology* 1995, 108:1040–1047
  40. Nigro S, Geido E, Infusini E, Orecchia R, Giaretti W: Transfection of human mutated K-ras in mouse NIH-3T3 cells is associated with increased cloning efficiency and DNA aneuploidization. *Int J Cancer* 1996, 67:871–875
  41. Saavedra HI, Knauf JA, Shirokawa JM, Wang J, Ouyang B, Elisei R, Stambrook PJ, Fagin JA: The RAS oncogene induces genomic instability in thyroid PCCL3 cells via the MAPK pathway. *Oncogene* 2000, 19:3948–3954
  42. Segal M, Clarke DJ: The Ras pathway and spindle assembly collide? *Bioessays* 2001, 23:307–310
  43. Leslie A, Pratt NR, Gillespie K, Sales M, Kernohan NM, Smith G, Wolf CR, Carey FA, Steele RJ: Mutations of APC, K-ras, and p53 are associated with specific chromosomal aberrations in colorectal adenocarcinomas. *Cancer Res* 2003, 63:4656–4661
  44. Bartos JD, Stoler DL, Matsui S, Swede H, Willmott LJ, Sait SN, Petrelli NJ, Anderson GR: Genomic heterogeneity and instability in colorectal cancer: spectral karyotyping, glutathione transferase-M1 and ras. *Mutat Res* 2004, 568:283–292
  45. Bartek J, Lukas J: Mammalian G1- and S-phase checkpoints in response to DNA damage. *Curr Opin Cell Biol* 2001, 13:738–747
  46. Blount PL, Galipeau PC, Sanchez CA, Neshat K, Levine DS, Yin J, Suzuki H, Abraham JM, Meltzer SJ, Reid BJ: 17p allelic losses in diploid cells of patients with Barrett's esophagus who develop aneuploidy. *Cancer Res* 1994, 54:2292–2295
  47. Sugai T, Takahashi H, Habano W, Nakamura S, Sato K, Orii S, Suzuki K: Analysis of genetic alterations, classified according to their DNA ploidy pattern, in the progression of colorectal adenomas and early colorectal carcinomas. *J Pathol* 2003, 200:168–176
  48. Shackney SE, Shankey TV: Common patterns of genetic evolution in human solid tumors. *Cytometry* 1997, 29:1–27
  49. Hingorani SR, Wang L, Multani AS, Combs C, Deramaudt TB, Hruban RH, Rustgi AK, Chang S, Tuveson DA: Trp53R172H and KrasG12D cooperate to promote chromosomal instability and widely metastatic pancreatic ductal adenocarcinoma in mice. *Cancer Cell* 2005, 7:469–483
  50. Margolis RL: Tetraploidy and tumor development. *Cancer Cell* 2005, 8:353–354
  51. Venkatchalam S, Shi YP, Jones SN, Vogel H, Bradley A, Pinkel D, Donehower LA: Retention of wild-type p53 in tumors from p53 heterozygous mice: reduction of p53 dosage can promote cancer formation. *EMBO J* 1998, 17:4657–4667
  52. Andreassen PR, Lohez OD, Lacroix FB, Margolis RL: Tetraploid state induces p53-dependent arrest of nontransformed mammalian cells in G1. *Mol Biol Cell* 2001, 12:1315–1328
  53. Jenner DC, Levitt S: Rectal cancer following colectomy and ileorectal anastomosis for familial adenomatous polyposis. *Aust N Z J Surg* 1998, 68:136–138
  54. Nakagawa H, Murata Y, Koyama K, Fujiyama A, Miyoshi Y, Monden M, Akiyama T, Nakamura Y: Identification of a brain-specific APC homologue, APCL, and its interaction with beta-catenin. *Cancer Res* 1998, 58:5176–5181
  55. van Es JH, Kirkpatrick C, van de Wetering M, Molenaar M, Miles A, Kuipers J, Destree O, Peifer M, Clevers H: Identification of APC2, a homologue of the adenomatous polyposis coli tumour suppressor. *Curr Biol* 1999, 9:105–108
  56. Jarrett CR, Blanco J, Cao T, Bressette DS, Cepeda M, Young PE, King CR, Byers SW: Human APC2 localization and allelic imbalance. *Cancer Res* 2001, 61:7978–7984
  57. Bonner AE, Lemon WJ, Devereux TR, Lubet RA, You M: Molecular profiling of mouse lung tumors: association with tumor progression, lung development, and human lung adenocarcinomas. *Oncogene* 2004, 23:1166–1176
  58. Wang LB, Zheng S, Zhang SZ, Peng JP, Ye F, Fang SC, Wu JM: Expression of ST13 in colorectal cancer and adjacent normal tissues. *World J Gastroenterol* 2005, 11:336–339
  59. Koshiishi N, Chong JM, Fukasawa T, Ikeno R, Hayashi Y, Funata N, Nagai H, Miyaki M, Matsumoto Y, Fukayama M: p300 gene alterations in intestinal and diffuse types of gastric carcinoma. *Gastric Cancer* 2004, 7:85–90
  60. Bryan EJ, Jukubaitis VJ, Chamberlain NL, Baxter SW, Dawson E, Choong DY, Campbell IG: Mutation analysis of EP300 in colon, breast and ovarian carcinomas. *Int J Cancer* 2002, 102:137–141
  61. Castells A, Ino Y, Louis DN, Ramesh V, Gusella JF, Rustgi AK: Mapping of a target region of allelic loss to a 0.5-cM interval on chromosome 22q13 in human colorectal cancer. *Gastroenterology* 1999, 117:831–837
  62. Zou Y, Peng H, Zhou B, Wen Y, Wang SC, Tsai EM, Hung MC: Systemic tumor suppression by the proapoptotic gene bik. *Cancer Res* 2002, 62:8–12
  63. Müller P, Henn W, Niedermayer I, Ketter R, Feiden W, Steudel WI, Zang KD, Steilen-Gimbal H: Deletion of chromosome 1p and loss of expression of alkaline phosphatase indicate progression of meningiomas. *Clin Cancer Res* 1999, 5:3569–3577
  64. Datta MW, Hernandez AM, Schlicht MJ, Kahler AJ, DeGueme AM, Dhir R, Shah RB, Farach-Carson C, Barrett A, Datta S: Perlecan, a candidate gene for the CAPB locus, regulates prostate cancer cell growth via the Sonic Hedgehog pathway. *Mol Cancer* 2006, 5:9
  65. Cho SG, Choi EJ: Apoptotic signaling pathways: caspases and stress-activated protein kinases. *J Biochem Mol Biol* 2002, 35:24–27
  66. Mak BC, Yeung RS: The tuberous sclerosis complex genes in tumor development. *Cancer Invest* 2004, 22:588–603
  67. Cheng YW, Shawber C, Nottelman D, Paty P, Barany F: Multiplexed profiling of candidate genes for CpG island methylation status using a flexible PCR/LDR/universal array assay. *Genome Res* 2006, 16:282–289
  68. Diep CB, Kleivi K, Ribeiro FR, Teixeira MR, Lindgjaerde OC, Lothe RA: The order of genetic events associated with colorectal cancer progression inferred from meta-analysis of copy number changes. *Genes Chromosom Cancer* 2006, 45:31–41
  69. Davison EJ, Tarpey PS, Fiegler H, Tomlinson IP, Carter NP: Deletion at chromosome band 20p12.1 in colorectal cancer revealed by high resolution array comparative genomic hybridization. *Genes Chromosom Cancer* 2005, 44:384–391
  70. Hanks S, Coleman K, Reid S, Plaja A, Firth H, Fitzpatrick D, Kidd A, Mehes K, Nash R, Robin N, Shannon N, Tolmie J, Swansbury J, Irlruth A, Douglas J, Rahman N: Constitutional aneuploidy and cancer predisposition caused by biallelic mutations in BUB1B. *Nat Genet* 2004, 36:1159–1161
  71. Jones AM, Douglas EJ, Halford SE, Fiegler H, Gorman PA, Roylance RR, Carter NP, Tomlinson IP: Array-CGH analysis of microsatellite-stable, near-diploid bowel cancers and comparison with other types of colorectal carcinoma. *Oncogene* 2005, 24:118–129
  72. Nakao K, Mehta KR, Fridlyand J, Moore DH, Jain AN, Lafuente A, Wiencke JW, Terdiman JP, Waldman FM: High-resolution analysis of DNA copy number alterations in colorectal cancer by array-based comparative genomic hybridization. *Carcinogenesis* 2004, 25:1345–1357
  73. Cardoso J, Boer JM, Morreau H, Fodde R: Expression and genomic profiling of colorectal cancer. *Biochim Biophys Acta* (in press)



---

## Chapter 4.

***Smad4* haploinsufficiency in mouse models for  
intestinal cancer.**

***Oncogene. 2006;25:1841-51.***



ORIGINAL ARTICLE

## *Smad4* haploinsufficiency in mouse models for intestinal cancer

P Alberici<sup>1</sup>, S Jagmohan-Changur<sup>2</sup>, E De Pater<sup>1</sup>, M Van Der Valk<sup>3</sup>, R Smits<sup>1</sup>, P Hohenstein<sup>4</sup> and R Fodde<sup>1</sup>

<sup>1</sup>Department of Pathology, Josephine Nefkens Institute, ErasmusMC, Rotterdam, The Netherlands; <sup>2</sup>Center for Human and Clinical Genetics, Leiden University Medical Center, Leiden, The Netherlands; <sup>3</sup>Department of Experimental Animal Pathology, Netherlands Cancer Institute, Amsterdam, The Netherlands and <sup>4</sup>MRC Human Genetics Unit, Edinburgh, UK

The *Smad4*<sup>+/<sup>E6sad</sup> mouse carries a null mutation in the endogenous *Smad4* gene resulting in serrated adenomas and mixed polyposis of the upper gastrointestinal (GI) tract with 100% penetrance. Here, we show by loss of heterozygosity (LOH) analysis and immunohistochemistry (IHC) that, although the majority of the tumors appear at 9 months of age, somatic loss of the wild-type *Smad4* allele occurs only at later stages of tumor progression. Hence, haploinsufficiency underlies *Smad4*-driven tumor initiation in the GI tract. As both the *Apc* and *Smad4* tumor suppressor genes map to mouse chromosome 18, we have bred *Smad4*<sup>+/<sup>E6sad</sup> with the *Apc*<sup>+/<sup>1638N</sup> model to generate two distinct compound heterozygous lines carrying both mutations either *in cis* (CAS) or *in trans* (TAS). Strikingly, both models show increased tumor multiplicities when compared with the single mutant littermates, although CAS mice are more severely affected and became moribund at only 5–6 weeks of age. Phenotypic and molecular analyses indicate that *Smad4* haploinsufficiency is sufficient to significantly affect tumor initiation and progression both prior to and upon loss of *Apc* function. Moreover, complete loss of *Smad4* strongly enhances *Apc*-driven tumor formation. *Oncogene* (2006) 25, 1841–1851. doi:10.1038/sj.onc.1209226; published online 14 November 2005</sup></sup></sup>

**Keywords:** *Smad4*; *Apc*; haploinsufficiency; TGF- $\beta$  signaling; LOH; Wnt signaling; gastrointestinal cancer

### Introduction

Loss of heterozygosity (LOH) and point mutations at the *SMAD4/DPC4* tumor suppressor gene, a key signal transducer in the TGF- $\beta$  and BMP signaling pathways, are usually found at late stages of sporadic colorectal cancer (CRC) (Takagi *et al.*, 1996; Thiagalingam *et al.*, 1996; Koyama *et al.*, 1999). In the classical adenoma-

carcinoma progression sequence originally proposed for CRC by Fearon and Vogelstein, loss of *APC* function triggers tumor initiation, followed by constitutional activation of the *KRAS* oncogene during adenoma progression, and by loss and mutation of the *SMAD2/4* and *TP53* tumor suppressors at chromosome 18p and 17q, respectively, at more advanced stages of adenoma growth and malignant transformation (Fearon and Vogelstein, 1990). On the other hand, germline mutations of the *SMAD4* gene are responsible for a subset of familial Juvenile Polyposis (JP), an autosomal dominant predisposition to the development of multiple hamartomatous polyps and GI cancer (Howe *et al.*, 1998).

In order to elucidate the role played by *SMAD4* in intestinal tumor initiation and progression, several mouse models have been generated that carry targeted inactivating mutations in the endogenous mouse *Smad4* gene (Sirard *et al.*, 1998; Takaku *et al.*, 1999; Xu *et al.*, 2000). In all cases, homozygosity for the *Smad4* mutation results in embryonic lethality prior to E9.5 due to defects in gastrulation and mesodermal development. Heterozygous *Smad4*<sup>+/-</sup> mice develop gastric and duodenal tumors with features reminiscent of human juvenile polyps. Notably, Xu and co-workers detected LOH at the *Smad4* locus only at late stages of tumor progression, namely in large dysplastic polypous tumors.

More recently, our laboratory has reported the *Sad* (*Smad4*<sup>E6sad</sup>) mouse model, characterized by a null mutation of the mouse *Smad4* gene, namely a single-nucleotide deletion in the exon 6 splice acceptor site resulting in an unstable mRNA and undetectable levels of the *Smad4* protein (Hohenstein *et al.*, 2003). Older F1 (129Ola  $\times$  C57BL/6) *Smad4*<sup>+/<sup>E6sad</sup> animals are predisposed to late-onset (18 months) serrated adenomas and mixed adenomatous and hyperplastic polyps, mainly localized immediately distal to the pyloric/duodenal transitional area. In our original report, LOH of the wild-type *Smad4* gene could only be assessed in mice older than 18 months and it was found in the majority of tumors collected from *Smad4*<sup>+/<sup>E6sad</sup> mice. To address the issue of haploinsufficiency in *Smad4*-driven intestinal tumorigenesis, we now have closely monitored inbred C57BL/6J (F5-F8 backcross generation) *Smad4*<sup>+/<sup>E6sad</sup> mice at different ages, from 6 to 18 months, to evaluate the onset of the tumor formation and of *Smad4* LOH during tumor initiation and progression.</sup></sup></sup>

Correspondence: Professor R Fodde, Department of Pathology, ErasmusMC, PO Box 1738, 3000 DR Rotterdam, The Netherlands. E-mail: r.fodde@erasmusmc.nl  
Received 6 June 2005; revised 11 August 2005; accepted 29 September 2005; published online 14 November 2005

Furthermore, to examine the role of *Smad4* status in *Apc*-driven intestinal tumorigenesis, we bred the *Smad4*<sup>E6sad</sup> mutation with the *Apc*<sup>+ /1638N</sup> model, previously developed and characterized in our laboratory (Fodde *et al.*, 1994). As both *Apc* and *Smad4* map to mouse chromosome 18, two different *Apc*<sup>+ /1638N</sup>/*Smad4*<sup>+ /E6sad</sup> compound heterozygous models were generated, in *trans* (mutations on different chromosomes) and, by meiotic recombination, in *cis* (mutations on the same chromosome).

Phenotypic and tumor analysis of the compound *Apc*<sup>+ /1638N</sup>/*Smad4*<sup>+ /E6sad</sup> mice indicates a differential role for *Smad4* in combination with the mutated *Apc* in intestinal tumor initiation and progression.

**Results**

*GI tumor incidence, distribution, and histopathology in Smad4<sup>+ /E6sad</sup> mice*

We previously described the identification and initial characterization of the *Smad4*<sup>+ /E6sad</sup> mouse model (Hohenstein *et al.*, 2003), characterized by hyperplastic and serrated adenomas resulting from a germline null mutation at the endogenous *Smad4* gene. To provide a more detailed characterization of their phenotype and pattern of GI tumor initiation and progression in a genetic background comparable to the other described models (Sirard *et al.*, 1998; Takaku *et al.*, 1999; Xu *et al.*, 2000), *Smad4*<sup>+ /E6sad</sup> mice were backcrossed for 5–8 generations to C57BL/6Jico and analysed at the age of 6, 9, 12, 15 and 18 months. For each time point, at least nine mice of both genders were analysed. Microscopic examination of the GI-tract in 6-month-old mice did not reveal any neoplastic lesions, thus confirming the late-onset nature of the tumor phenotype in this model (not shown). However, already at 9 months, 100% of the *Smad4*<sup>+ /E6sad</sup> mice analysed revealed the presence of polyps in the stomach (fundus) (Table 1). At the same age, tumors were also found in the peri-ampullary region in approximately 50% of *Smad4*<sup>+ /E6sad</sup> mice. At age 12 months and older, the latter proportion increases up to 80–100% of the animals, while a subset (3/11, 27% at 12 months; 3/10, 30% at 15 months; 6/9, 66% at 18

months) showed carpeting (here defined as an area where an extremely high polyp density did not allow counting) of the whole pyloric/duodenal transition area with polyps.

Additional tumors were found throughout the rest of the small intestinal tract (duodenum, jejunum, and ileum) starting from age 9 months, whereas colorectal polyps were only found in few animals at later stages (1/10, 10% at 15 months; 2/9, 22% at 18 months). The average number of gastric polyps per mouse did not increase over time though a slight increase in gastric tumor size was observed (from 3 mm ± 1 at 9 months up to 8 mm ± 2 at 18 months). The number of polyps present throughout the entire intestinal tract clearly increased over time, from an average of 3 at 9 months to 9 at 18 months of age. Analysis of these tumors by histopathology confirmed previously observed features: polyps were hyperplastic with branching villi (Figure 1a) and occasionally with serrated aspects. In the more advanced cases, dilated cysts and foci of frank dysplasia with increased nuclear cytoplasmic ratio and nuclear stratification of the cells were present (Figure 1b). Macroscopic examination of > 1-year-old *Smad4*<sup>+ /E6sad</sup> animals did not reveal the presence of tumors in other tissues/organs including the pancreas.

*Haploinsufficiency at the Smad4 gene in GI tumors from Smad4<sup>+ /E6sad</sup> mice*

To investigate the role of LOH as a tumor-initiating event in the *Smad4*<sup>+ /E6sad</sup> mouse model, a total of 50 tumors and normal controls were analysed both by DNA- and protein-based methods. To enrich in tumor DNA, DNA samples were isolated from tumor cells obtained by laser capture microdissection (LCM) of histological sections. For each age group, from 9 to 18 months of age, at least 10 tumors and two normal intestinal tissue controls, were microdissected by LCM for DNA isolation. LOH of the wild-type *Smad4* allele was established using two CA repeat markers, *d18Mit81* and *d18Mit80*, located, respectively, 7 cM proximal and 2 cM distal to the *Smad4* gene on chromosome 18, as previously described (Hohenstein *et al.*, 2003).

LOH of the *Smad4* allele was not detected in polyps from *Smad4*<sup>+ /E6sad</sup> mice up to 15 months (Table 2). At

**Table 1** Incidence and distribution of intestinal neoplasia in *Smad4*<sup>E6sad</sup> mice at different time points

No. of mice	Age (months)	Incidence (%)	Tumor multiplicity/ animal	Tumor range	Histology	Tumor localization
9	6	0	—	—	—	—
10	9	100	3	2–5	Hyperplastic polyps	S: 100%; P: 50%; D: 10%; J: 30%; I: 0%; C: 0%
10	12	100	5	2–7	Hyperplastic polyps	S: 100%; P: 80%; D: 10%; J: 0%; I: 10%; C: 0%
10	15	100	7	4–12	Low dysplastic polyps	S: 100%; P: 100%; D: 20%; J: 20%; I: 40%; C: 10%
9	18	100	9	3–13	Low dysplastic polyps	S: 100%; P: 100%; D: 10%; J: 10%; I: 11%; C: 22%

Tumor localization: incidence of one or more lesions in the corresponding part of the intestinal tract: S = stomach, P = periampullar region, D = duodenum, J = jejunum, I = ileum, C = colon.

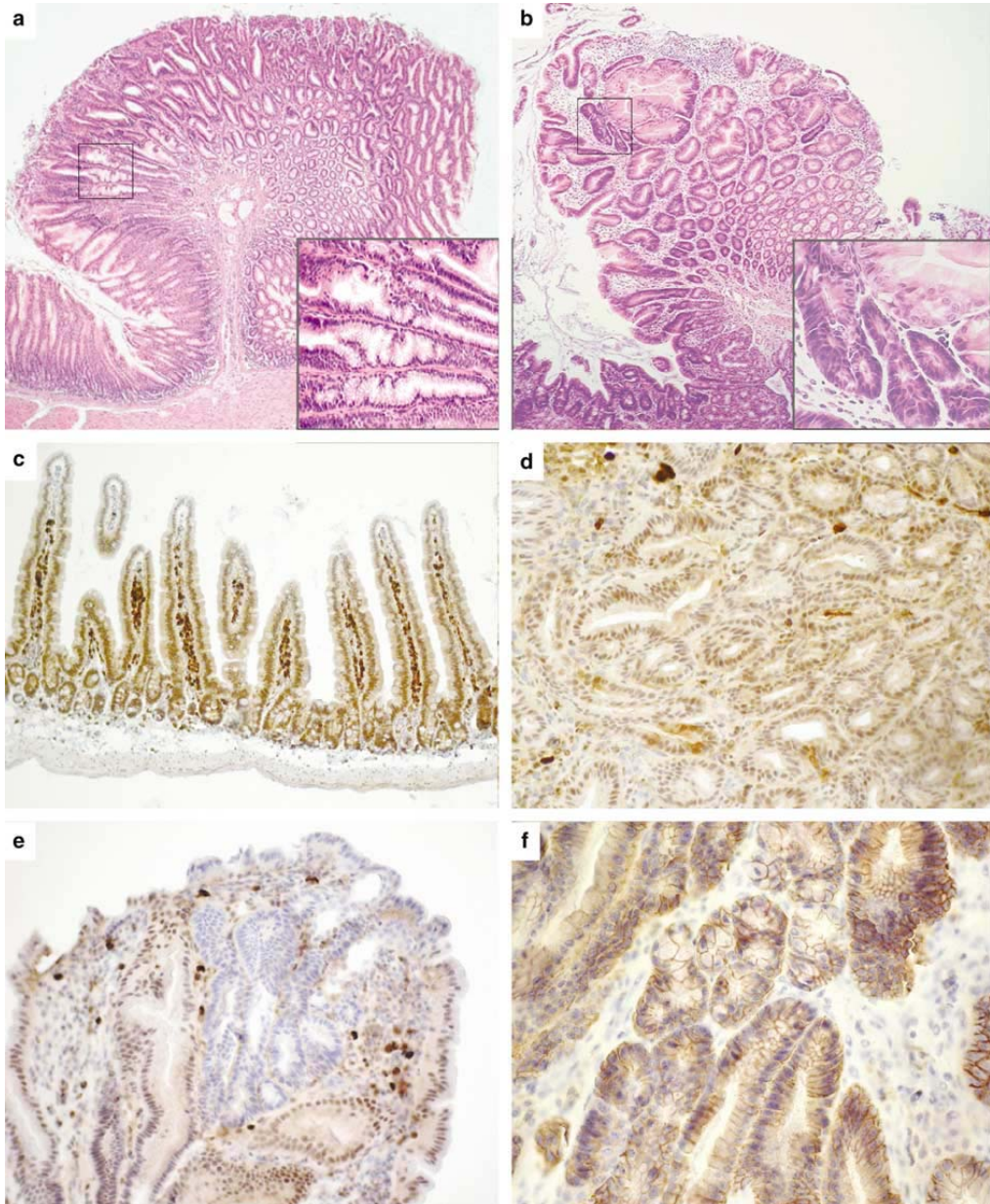


**Figure 1** Histopathology and immunohistochemical analysis of *Smad4*<sup>E65ad</sup> small intestinal polyps at different ages and progression stages. (a) Polyp originated in the gastric epithelium from a 12-month-old *Smad4*<sup>+/E65ad</sup> animal. Inset: higher magnification of a hyperplastic region. Note the gastric epithelium (HE). (b) Advanced polyp from a 15-month-old *Smad4*<sup>+/E65ad</sup> mouse showing areas of frank dysplasia. Inset: higher magnification of a dysplastic region (HE). (c) Smad4 IHC analysis of normal small intestinal epithelium from an *Smad4*<sup>+/E65ad</sup> animal shows nuclear and cytoplasmic staining with a crypt-villus decreasing gradient of expression. The aspecific staining in the lamina propria is due to mouse IgG cross-reaction from the secondary antibody. (d) Smad4 IHC analysis of a tumor from a 12-month-old *Smad4*<sup>+/E65ad</sup> mouse shows positive staining of tumor cells. Staining of stromal cells is due to mouse IgG cross-reaction from the secondary antibody. (e) Smad4 IHC analysis of a tumor from a 15-month-old *Smad4*<sup>+/E65ad</sup> mouse shows an area of negatively stained parenchymal cells within an otherwise positive tumor. (f)  $\beta$ -Catenin IHC analysis of a tumor from a 15-month-old *Smad4*<sup>+/E65ad</sup> animal. The more dysplastic area of the lesion mainly shows membranous staining.

**Table 2** LOH and IHC analysis of *Smad4*<sup>E6sad</sup> intestinal tumors

Age (months)	No. of tumors	LOH incidence	IHC staining
6	NA	NA	NA
9	10	0/10 (0%)	+
12	10	0/10 (0%)	+
15	10	4/10 (40%)	- (patchy)
18	14	9/14 (64%)	- (patchy)

NA, not applicable.

this age, four out of 10 (40%) tumors showed LOH. In older mice (18 months), the fraction of tumors presenting LOH at the *Smad4* locus increases (9/14: 64%) in accordance with our own previously published results obtained with mice older than 18 months (Hohenstein *et al.*, 2003).

In the majority of the cases ( $n = 10/10$  LOH negative and  $n = 7/10$  LOH positive), the above data could be confirmed by direct sequence analysis of the *Smad4* gene amplified by PCR from tumor DNA samples. The frameshift visible in the chromatogram of an *Smad4*<sup>+ /E6sad</sup> normal mucosa control sample and due to a single-nucleotide (A) deletion in the exon 6 splice acceptor site of the mutated allele, is lost or clearly reduced in the tumor samples previously shown by CA repeat markers to carry LOH at the *Smad4* locus (Figures 2b and c).

To further confirm the observed haploinsufficiency and late-onset LOH in *Smad4*<sup>E6sad</sup> GI tumors, we performed immunohistochemistry (IHC) on tumor sections with a Smad4-specific antibody (B-8; see Material and methods) (Wilentz *et al.*, 2000; Salovaara *et al.*, 2002). Normal gastric and small intestinal mucosa displayed positive staining for Smad4 in all cases, although the intensity of expression was reduced in gastric mucosa when compared to the intestinal epithelium. In the latter, a gradient of expression was observed along the crypt-villus axis, with strong positive nuclei in the crypt, and cytoplasmic staining in the apical part of the villus, similar to the pattern reported by Salovaara *et al.* (2002) in normal human colonic mucosa (Figure 1c).

Tumors derived from *Smad4*<sup>+ /E6sad</sup> mice up to 12 months of age showed in all cases ( $n = 4$ ) positive staining for the protein (Figure 1d). Only in few tumors collected at 14 and 15 months of age (1/6 and 2/5, respectively), loss of Smad4 protein expression was detected in a 'patchy', heterogeneous pattern: Smad4-negative foci were scattered among otherwise positive tumor cells (Figure 1e) (Table 2).

Overall, the results of our LOH and IHC analyses of GI tumors from *Smad4*<sup>+ /E6sad</sup> mice at different

ages are consistent with the idea that complete loss of Smad4 function is a late event in tumor progression.

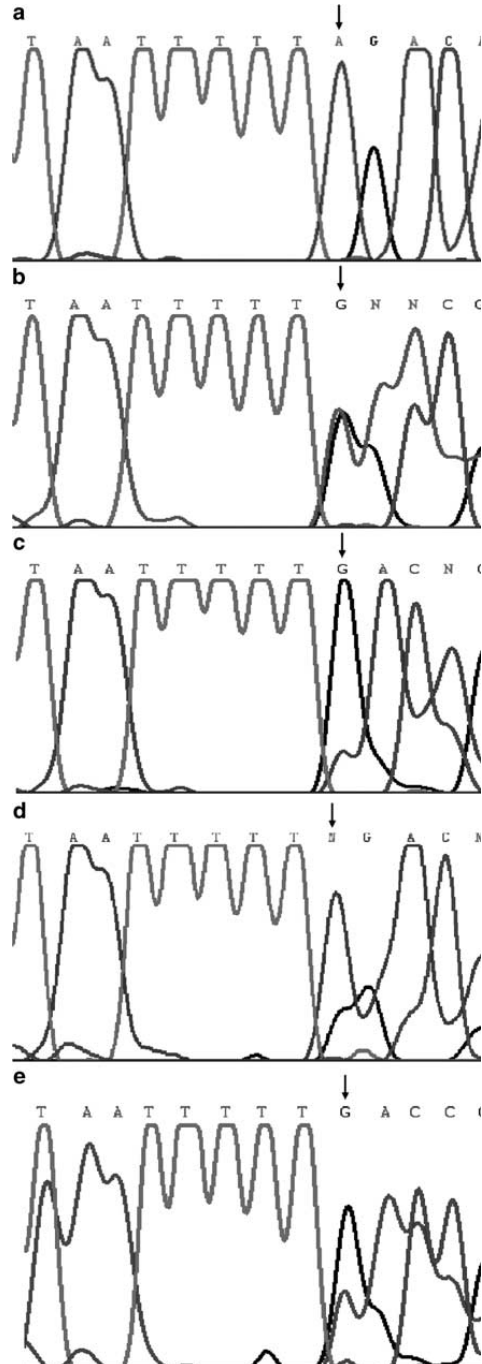


**Figure 2** LOH analysis by direct sequencing of the *Smad4* intron 5-exon 6 boundary from tumor and normal DNA samples. The arrow indicates the nucleotide position (A) deleted in the *Smad4*<sup>E6sad</sup> allele. (a) Wild-type sequence from normal intestinal epithelium. (b) Heterozygous sequence from a normal mucosa of a *Smad4*<sup>+ /E6sad</sup> mouse. (c) Loss of the wild-type *Smad4* allele in intestinal tumor from an 18-month-old *Smad4*<sup>+ /E6sad</sup> mouse. (d) Loss of the *Smad4*<sup>E6sad</sup> allele in a TAS tumor. (e) Loss of the wild-type *Smad4* allele in a CAS tumor.

**Table 3** Incidence and distribution of intestinal tumors in *Apc*<sup>+1638N</sup>/*Smad4*<sup>E6sad</sup> compound TAS and CAS mice and their single transgenic littermates

Genotype	No. of mice	Median age (range)	Incidence (%)	Tumor multiplicity/animal	Tumor range	Histology	Tumor localization
<i>Smad4</i> <sup>E6sad</sup>	6	8 months (6–12)	67	5	2–6	Hyperplastic polyps	S: 100%; P: 100%; D: 32%; J: 55%; I: 23%; C: 12%
<i>Apc</i> <sup>+1638N</sup>	7	8 months (6–18)	100	4	1–10 <sup>a</sup>	Low to high dysplastic polyps	S: 25%; P: 88%; D: 100%; J: 38%; I: 0%; C: 19%
TAS	8	7 months (3–8)	100	20	12–28 <sup>a</sup>	Low to high dysplastic polyps; carcinomas	S: 100%; P: 100%; D: 100%; J: 87%; I: 37%; C: 0%
CAS	7	5 weeks (3–6)	100	60	22–88 <sup>a</sup>	Low to high dysplastic polyps; microadenomas; carcinoma in situ	S: 25%; P: 100%; D: 100%; J: 100%; I: 42%; C: 0%

*P* < 0.001, Mann–Whitney rank sum test. Tumor localization: incidence of one or more lesions in the corresponding part of the intestinal tract: S = stomach, P = periampullar region, D = duodenum, J = jejunum, I = ileum, C = colon.

It is well established that constitutive activation of the Wnt/ $\beta$ -catenin signal transduction pathway, caused by either *Apc* or *Ctmb1* ( $\beta$ -catenin) mutations, represents a rate-limiting event in intestinal tumor formation.  $\beta$ -Catenin nuclear accumulation is the hallmark of Wnt signaling activation and was analysed by IHC on tumor sections from *Smad4*<sup>+E6sad</sup> mice. No  $\beta$ -catenin nuclear accumulation was observed in *Smad4*<sup>+E6sad</sup> tumors, even at later stages of tumor development, thus indicating that Wnt signaling does not play a major role in *Smad4*-driven intestinal tumorigenesis (Figure 1f).

#### Tumor incidence and distribution in Trans (TAS) and Cis (CAS) *Apc*<sup>+1638N</sup>/*Smad4*<sup>+E6sad</sup> compound mutant mice

To further investigate the role of the *Smad4* gene in GI tumor initiation and progression, we have bred *Smad4*<sup>+E6sad</sup> mice with the *Apc*<sup>+1638N</sup> mouse model, previously developed in our laboratory (Fodde et al., 1994). In the mouse genome, both the *Apc* and *Smad4* tumor suppressor genes are located on chromosome 18. Therefore, two different types of compound heterozygous mice were generated: *in Trans* *Apc*<sup>+1638N</sup>/*Smad4*<sup>+E6sad</sup> (TAS), where the two mutations are present on two different chromosome 18 alleles, and *in Cis* *Apc*<sup>+1638N</sup>/*Smad4*<sup>+E6sad</sup> (CAS), obtained by backcrossing TAS animals with C57BL/6 mice. In agreement with the genetic distance between the two tumor suppressor loci (33 cM), the two mutations were found on the same chromosome 18 allele in approximately 15% of the offspring.

The TAS and CAS mouse models showed distinctive phenotypes when compared to the single mutation littermates (Table 3) (Figure 4). For the present study, we analysed eight TAS (four female and four male subjects) and seven CAS (two female and five male subjects) mice.

The TAS lineage is characterized by a normal development, growth, and adult size. At age 6–7 months, mice present with an average of 20 tumors along the GI tract (range: 12–28), mainly in the duodenum. No neoplastic lesions were observed in the

colon. The tumor multiplicity in TAS animals is significantly higher when compared to the *Apc*<sup>+1638N</sup> and *Smad4*<sup>+E6sad</sup> littermates (*P* < 0.001, Mann–Whitney rank sum test) (Table 3). Histological analysis showed that the tumors were mainly villous or tubulovillous adenomas with foci of severe dysplasia and malignancy, similar to what has been observed in late stage *Apc*<sup>+1638N</sup> tumors (Figure 3a). In two animals (age 6 and 7 months), adenocarcinomas with frank invasion of the muscularis mucosa and submucosa were also observed (Figure 3b). All TAS mice also displayed desmoid tumors and cutaneous follicular cysts with similar incidence and distribution as previously observed in the *Apc*<sup>+1638N</sup> mouse model (Smits et al., 1998). Owing to the high GI tumor multiplicity, TAS mice usually became moribund at around 7–8 months of age (Figure 4).

The CAS mouse model showed a more severe phenotype when compared with TAS. CAS mice became moribund at age 6 weeks; two out of nine CAS animals were found dead at 5 weeks and were not included in the analysis (Figure 4). Moribund mice were characterized by frank anemia and spleen enlargement. Macroscopic analysis of the intestinal tract revealed a very thin dystrophic intestinal wall and the presence of an average of 60 tumors per animal (range 22–88). Upon microscopic analysis, we observed numerous smaller lesions along the entire upper GI tract, previously referred to as GIN (gastrointestinal intraepithelial neoplasia) or microadenomas (Figure 3d) (Boivin et al., 2003). The polyps were either sessile or villous, and characterized by mild to severe dysplasia, in some cases with evident foci of malignant transformation, although no clear submucosal invasion was detected among 57 CAS tumors analysed here (Figure 3c).

#### LOH analysis of GI tumors from compound CAS and TAS *Apc*<sup>+1638N</sup>/*Smad4*<sup>+E6sad</sup> mice

The LOH status at the *Apc* and *Smad4* loci was determined in 22 TAS and 16 CAS intestinal tumors. LOH analysis at the *Smad4* locus was carried out as

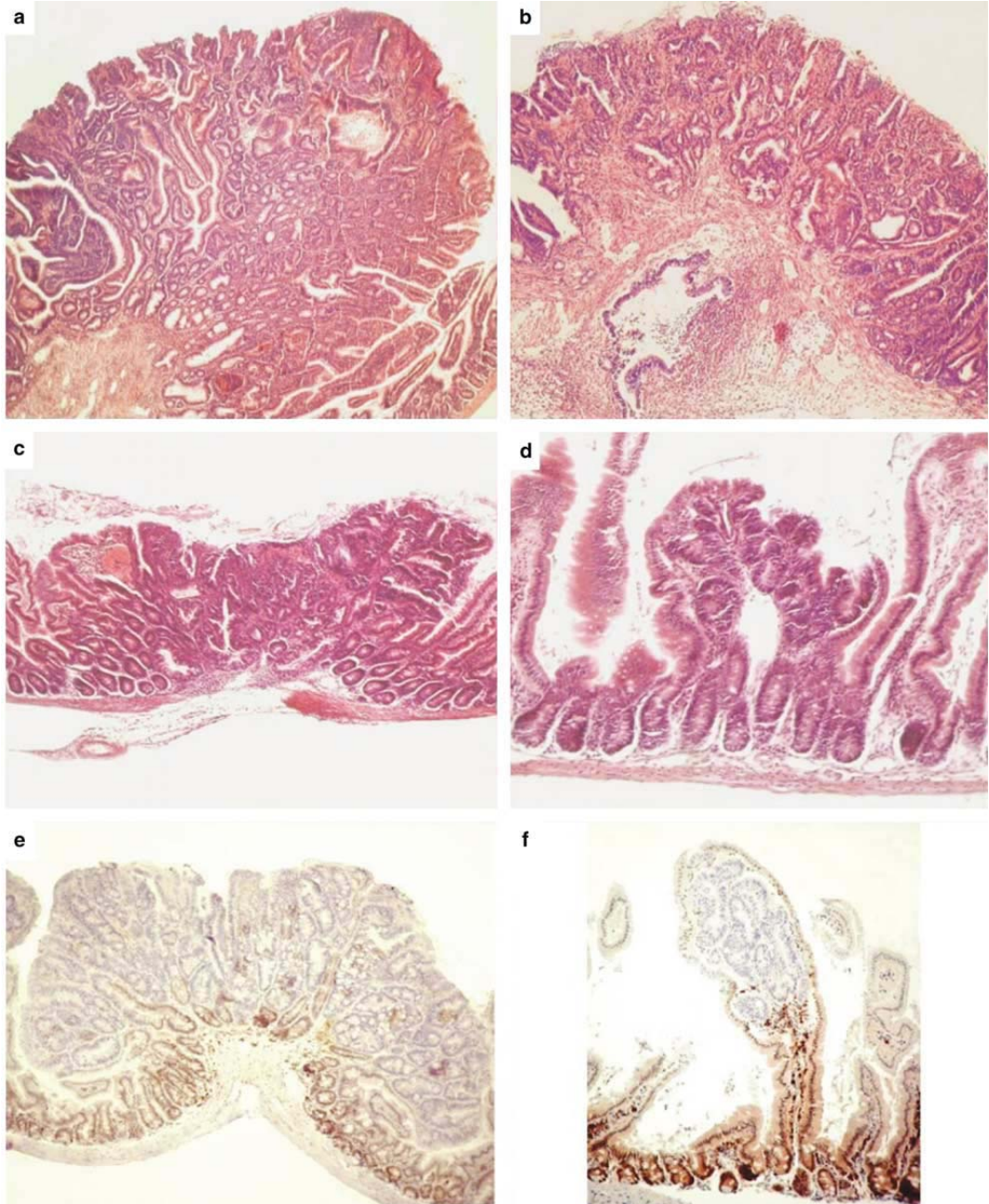


**Figure 3** Histopathology and IHC analysis of intestinal tumors from compound *Apc*<sup>+/<sup>1638N</sup>/*Smad4*<sup>+/<sup>E65d</sup>. (a) A typical dysplastic adenoma observed in TAS animals (HE staining). (b) An example of adenocarcinoma with extensive submucosal invasion from a TAS mouse (HE). (c) Sessile villous adenoma from a CAS mouse with areas of severe dysplasia and cystic formation (HE). (d) A nascent lesion or microadenoma observed in the duodenum of a CAS animal (HE). (e) Smad4 IHC analysis of a CAS tumor shows negative staining, thus indicating LOH of the wild-type allele. (f) Smad4 IHC analysis of a small microadenoma from the same CAS mouse also reveals LOH of the wild-type allele. Note the positively stained cells of the normal epithelial lining surrounding the dysplastic area.</sup></sup>

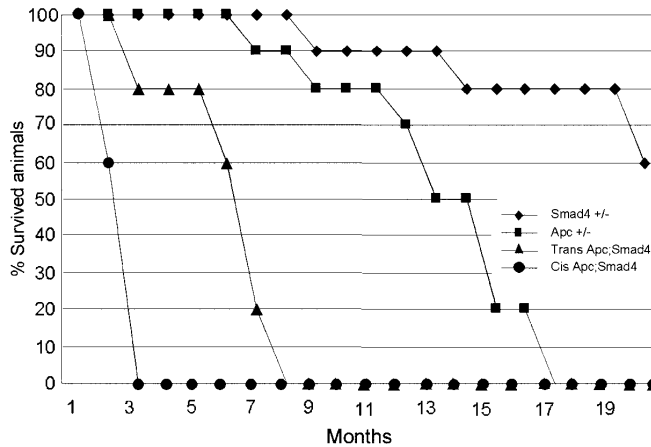


Figure 4 Survival plot of the different mouse models analysed in the present study.

Table 4 *Smad4* LOH and IHC analysis of tumors from compound *Apc*<sup>1638N</sup>/*Smad4*<sup>E65ad</sup> (TAS and CAS) mice

Genotype	No. of tumors	LOH wild-type <i>Apc</i>	LOH <i>Smad4</i>	Concomitant LOH	IHC <i>SMAD4</i>
TAS	22	16/22 (73%)	10/22 <sup>a</sup> (45%)	10/22 (45%)	+
CAS	16	11/16 (69%)	11/16 <sup>b</sup> (69%)	7/16 (44%)	-

<sup>a</sup>Loss of *Smad4*<sup>E65ad</sup> mutant allele. <sup>b</sup>Loss of *Smad4* wild-type allele.

described above. For the *Apc* gene, tumor DNA was amplified with PCR primers specific for the wild-type and targeted *Apc*<sup>1638N</sup> alleles (Smits *et al.*, 1997).

Sixteen (73%) out of 22 TAS tumors showed LOH of the wild-type *Apc* allele, 10 of which (45%) with concomitant loss of the *Smad4*<sup>E65ad</sup> allele, as detected by the 2cM distal flanking marker d18Mit80 (Table 4). Notably, none of the TAS tumors showed LOH at the wild-type *Smad4* allele. The LOH results were validated by direct sequencing of tumor DNA around the *Smad4*<sup>E65ad</sup> mutation site (exon 6 splice acceptor site). Sequence analysis confirmed in all cases (10/10) the results of the LOH analysis: where the loss of the *Smad4*<sup>E65ad</sup> allele was assessed by radioactive PCR, the frameshift, diagnostic for the presence of the mutation in the DNA from normal intestinal mucosa, was absent or strongly reduced in tumor samples (Figure 2d). In the remaining six tumors (27%), no LOH was detected at either loci, by either radioactive PCR and direct sequencing.

Among the CAS tumors, 11 (69%) out of 16 were characterized by LOH at the wild-type *Smad4* locus and the same percentage showed LOH at the wild-type *Apc* allele. In seven cases (44%), loss of both the *Apc* and *Smad4* loci, and presumably of the entire chromosome 18, was observed. In only one CAS tumor, no LOH at either locus was detected (Table 4).

To confirm the above LOH results, *Smad4* IHC analysis was performed on tumors from compound heterozygous *Apc*<sup>+1638N</sup>/*Smad4*<sup>+E65ad</sup> mice. All TAS

tumors analysed by IHC ( $n=6$ ) showed positive staining for the *Smad4* protein, thus confirming that LOH of the wild-type allele does not play a major role in tumor onset of this genetic combination. Unlike the TAS tumors, all CAS tumors analysed by IHC ( $n=15$ ) were characterized by the complete absence of *Smad4* staining, even at early stages of tumor formation, for example, the microadenomas (Figure 3e and f). The IHC data are in agreement with the LOH results obtained by DNA-based analysis where the majority of the tumors showed loss of wild-type *Smad4* and *Apc*, and presumably of the entire chromosome 18.

These results indicate that, although loss of *Apc* function seems to represent the rate-limiting event in tumor initiation in both types of compound *Apc*<sup>+1638N</sup>/*Smad4*<sup>+E65ad</sup> mice, the presence of LOH or haploinsufficiency at the *Smad4* gene differentially affects tumor initiation in the CAS and TAS genetic combinations.

## Discussion

The *SMAD4* tumor suppressor gene has been shown to be inactivated in human colorectal cancer during late stages of the adenoma-carcinoma sequence (Takagi *et al.*, 1996; Thiagalingam *et al.*, 1996; Koyama *et al.*, 1999; Miyaki *et al.*, 1999). Owing to its relevance in GI tumor initiation and progression, and its central role in BMP/TGF- $\beta$  signaling (Shioda *et al.*, 1998; Itoh *et al.*,

2000; Fink *et al.*, 2003), several investigators have generated *Smad4*-mutant mouse models to elucidate the mechanisms and the cellular consequences of its loss of function in intestinal cancer (Sirard *et al.*, 1998; Takaku *et al.*, 1999; Xu *et al.*, 2000). In general, heterozygous *Smad4*<sup>+/-</sup> mouse models are predisposed to the development of multiple polyps of the upper GI tract, with variations in polyp numbers, histology, and onset, possibly due to differences in mutation type, for example, causing distinct defects in BMP/TGF- $\beta$  signaling, and/or in genetic background. Among these, the *Smad4*<sup>+/<sup>E6sad</sup></sup> mouse model has been previously reported and described by us as a model for serrated and hyperplastic adenoma due to a *null* mutation in the *Smad4* gene. In man, a consistent percentage of invasive colorectal carcinomas seems to originate from serrated and hyperplastic polyps (Jass, 2001; Makinen *et al.*, 2001; Hawkins *et al.*, 2002). From this perspective, the *Smad4*<sup>+/<sup>E6sad</sup></sup> mouse is an interesting model to study alternative routes of intestinal carcinogenesis, other than the classic adenoma-carcinoma sequence.

In the present study, we first further characterized the phenotypic features of *Smad4*<sup>+/<sup>E6sad</sup></sup> mice on an inbred C57BL6 genetic background, and investigated the mechanisms of somatic *Smad4* inactivation during GI tumor development and progression.

Onset of gastric and periampullary polyp formation occurs in *Smad4*<sup>+/<sup>E6sad</sup></sup> mice between 6 and 9 months of age with 100% penetrance. Notably, penetrance of upper GI polyps was reported to be incomplete at around this age in other *Smad4* models (Takaku *et al.*, 1999; Xu *et al.*, 2000). *Smad4*<sup>+/<sup>E6sad</sup></sup> mice were also affected by tumors in more distal locations along the intestine, namely in the duodenum, ileum, and in fewer cases in the colon. Also, unlike the *Smad4* model described by Xu *et al.* (2000), *Smad4*<sup>+/<sup>E6sad</sup></sup> mice did not develop any carcinomas up to 18 months of age. Differences in the genetic background of the analysed mice may partly explain these discrepancies, as shown by the exclusive presence of gastric and periampullary tumors in the original F1 (129  $\times$  C57BL/6) *Smad4*<sup>+/<sup>E6sad</sup></sup> animals (Hohenstein *et al.*, 2003), whereas on the B6 background we also observed several tumors throughout the intestinal tract. However, differences in the molecular consequences of the targeted mutations may also underlie the phenotypic features of the individual models. In the case of the *Smad4*<sup>E6sad</sup> mutation, the splice acceptor mutation in exon 6 was shown by both RT-PCR and Western analysis to significantly affect mRNA stability and thus represent a *bona fide null* allele (Hohenstein *et al.*, 2003). Unfortunately, similar molecular analyses were not reported for the other models which does not allow us to exclude that the above phenotypic differences are partly due to specific genotype-phenotype correlations at the *Smad4* locus (Takaku *et al.*, 1999; Xu *et al.*, 2000).

The histopathologic analysis of *Smad4* mutant tumors at different ages showed a slow but continuous progression from initial hyperplastic lesions to more advanced stages with clear dysplasia, similar to what has been observed in human CRC. In GI tumors from

*Smad4*<sup>+/<sup>E6sad</sup></sup> animals, LOH of the wild-type *Smad4* allele was only detected in advanced cases of tumor progression, with the majority of the tumors retaining heterozygosity in mice up to 12 months of age. IHC analysis with an antibody directed against the Smad4 protein confirmed that complete loss of Smad4 function is a late event in tumor progression, at first limited to more dysplastic areas of the neoplasms. These observations confirm the previous report by Xu *et al.* (2000), where tumors up to 0.4 cm in size were shown to retain the wild-type *Smad4* allele. Accordingly, somatic mutation analysis in cases of Familial Juvenile Polyposis (FJP) caused by *SMAD4* germline mutations showed LOH in only 9% (1/11) (Howe *et al.*, 1998) and 23% (4/17) (Woodford-Richens *et al.*, 2000) of the polyps, thus suggesting that a tumor suppressor gene dosage reduction, rather than its complete functional inactivation, characterizes the initial steps of *SMAD4*-driven GI tumor initiation and progression in mouse and man. We have previously shown that dosage variations in Wnt/ $\beta$ -catenin signaling differentially affect stem cell differentiation and multiorgan tumor predisposition in *Apc*-mutant mice (Gaspar and Fodde, 2004). Similarly, dosage fluctuations in BMP/TGF- $\beta$  signaling in haploinsufficient *Smad4* intestinal cells may occasionally trigger epithelial hyperplasia either in combination with somatic mutations at genes other than *Smad4*, or due to gene dosage fluctuations under a putative BMP/TGF- $\beta$  signaling threshold. In fact, impairment of BMP signaling may very well underlie tumor onset in *Smad4*<sup>+/<sup>E6sad</sup></sup> mice, as inhibition of this pathway has been reported to result in the formation of numerous ectopic crypt units and frequent occurrence of intraepithelial neoplasia in mouse (Haramis *et al.*, 2004). During tumor progression, complete loss of *Smad4* function blocks BMP and TGF- $\beta$  signals from being transduced to the nucleus and is likely to underlie progression towards malignancy.

To further expand on the role of *Smad4* haploinsufficiency in intestinal tumor initiation and progression, and to study putative interaction between Wnt activation and BMP/TGF- $\beta$  signaling impairment, we have bred *Smad4*<sup>+/<sup>E6sad</sup></sup> animals with *Apc*<sup>+/<sup>1638N</sup></sup>, a mouse model previously developed in our laboratory, mainly characterized by tumors of the GI tract, desmoids, and epidermal tumors (Fodde *et al.*, 1994; Smits *et al.*, 1998). As both the *Apc* and *Smad4* genes are located on mouse chromosome 18, compound heterozygous *Apc*<sup>+/<sup>1638N</sup></sup>/*Smad4*<sup>+/<sup>E6sad</sup></sup> mice were generated and studied in both the *in trans* (TAS) and *in cis* (CAS) genetic combinations. Both compound animals are characterized by an increase in tumor multiplicity, progression, morbidity, and mortality when compared to the single littermates. In CAS animals in particular, the presence of the two mutations on the same chromosome resulted in an extremely severe phenotype.

Notably, the compound heterozygotes generated in our study substantially differ from the *Dpc4*<sup>+/-</sup>; *Apc*<sup>A716+/-</sup> *in trans* and *cis* models previously reported by Takaku *et al.* (1998). In this study, the *in trans* compound mice do not show phenotypic differences

when compared with the single *Apc*<sup>+/A716</sup> littermates. Also, the *in cis* compound mice are characterized by a decrease in polyp number and an increase in polyp size, with accelerated tumor progression and malignant transformation, still without affecting the survival.

The explanations for these phenotypic discrepancies may both reside in the difference in genetic background (B6 vs mixed 129/B6), and in the different molecular nature of the *Smad4*- and *Apc*-targeted mutations employed in the two studies. Indeed, the relatively mild intestinal tumor phenotype characteristic of *Apc*<sup>+/1638N</sup> mice is in sharp contrast with the severe morbidity of *Apc*<sup>+/A716</sup> animals with more than 500 GI tumors at 3 months of age. Also, the demonstrated hypomorphic nature of the *Apc*<sup>1638N</sup> mutation encoding for residual  $\beta$ -catenin regulating activity (Smits *et al.*, 1999; Kielman *et al.*, 2002) is likely to differ from *Apc*<sup>A716</sup> resulting in a truncated Apc protein deprived of any  $\beta$ -catenin down-regulating activity with putative dominant-negative effects (Takaku *et al.*, 1998). In the presence of such a highly penetrant *Apc* mutation, the *Smad4* mutation does not affect the tumor initiation event, whereas its effects are noticeable in the *Apc*<sup>+/1638N</sup> genetic background.

Loss of BMP signaling in CAS tumors upon loss of the *Smad4* wild-type allele can also contribute to the extremely severe phenotype observed in these mice. Notably, BMP signaling has been described to suppress Wnt signaling, ensuring a balance in the control of stem cell self-renewal (He *et al.*, 2004). Loss of BMP-driven  $\beta$ -catenin regulation in CAS tumors may result in further enhancement of Wnt/ $\beta$ -catenin signaling to the nucleus and increased tumor formation.

An additional difference, although precise phenotypic comparisons between mouse strains in different animal facilities are not straightforward, consists in the apparently more severe intestinal tumor phenotype of *Smad4*<sup>+/E6sad</sup> mice in comparison with the targeted *Smad4* allele described by Takaku *et al.* (1998, 1999) (Hohenstein *et al.*, 2003).

Here, we show that in both the TAS and CAS animals, approximately half (44%) of the tumors have concomitant LOH of the *Apc* and *Smad4* loci in the same chromosome, possibly as the result of homologous somatic recombination between homologs (Haigis and Dove, 2003). Notably, in TAS polyps, tumor formation is driven by the loss of wild-type *Apc* (73% of the tumors) rather than by the loss of the wild-type *Smad4* allele (none observed). Hence, LOH at the *Apc* locus is the rate-limiting event for tumor formation in TAS mice. However, *Smad4* haploinsufficiency clearly affects *Apc*-driven tumor initiation as indicated by the increased tumor multiplicity in TAS animals when compared with *Apc*<sup>+/1638N</sup>. *Smad4* haploinsufficiency effects on *Apc*-driven tumor formation and progression can explain this result. First, as reported here and elsewhere, the observed *Smad4* haploinsufficiency in mouse and human polyps indicates that BMP/TGF- $\beta$  signaling dosage fluctuations may contribute 'fertile soil' for polyp formation in the intestine. This may positively affect *Apc*-driven tumor formation both before and after

the second hit at the wild-type *Apc* allele, possibly due to cumulative and/or synergistic effects of the concomitant signaling dosage defects. Accordingly, it has been shown that induction of TGF- $\beta$  signaling in a nontransformed epithelial cell line reduces APC protein levels at the post-transcriptional level, and increases  $\beta$ -catenin mRNA and protein levels, causing its nuclear accumulation and transcriptional activation of Wnt downstream targets (Satterwhite and Neufeld, 2004). Wnt and TGF- $\beta$  signaling may also cooperatively regulate a subset of downstream targets. Expression of the growth factor gastrin, a well-known Wnt target gene and GI-cancer promoter in mouse (Koh *et al.*, 2000), is finely regulated by synergistic complexes of TGF- $\beta$ /Smads and Wnt/ $\beta$ -catenin transcription factors (Lei *et al.*, 2004).

In conclusion, our results confirm that *Smad4* haploinsufficiency is sufficient for intestinal tumor initiation and that loss of the wild-type allele underlies more advanced stages of tumor progression and dysplastic changes. More importantly, the analysis of the compound TAS and CAS mice has revealed a role for BMP/TGF- $\beta$  signaling in *Apc*-driven tumor formation and possibly during progression towards malignancy. Reporter assay analysis of Wnt and BMP/TGF- $\beta$  signaling activity in different genetic combinations and identification of the specific downstream targets will open the way for tailor-made therapeutic intervention.

## Materials and methods

### Mouse strains and tumor samples

All *Apc*<sup>+/1638N</sup> mice employed in this study were on an inbred C57BL/6Jico (B6) background. The employed *Smad4*<sup>+/E6sad</sup> mice were derived from F5-F8 backcross generations to C57BL/6 of the original F1 129Ola/C57BL/6Jico *Smad4*<sup>+/E6sad</sup> founder (Hohenstein *et al.*, 2003). The *in Trans Apc*<sup>+/1638N</sup>/*Smad4*<sup>+/E6sad</sup> (TAS) compound animals were generated by breeding *Smad4*<sup>+/E6sad</sup> with *Apc*<sup>+/1638N</sup> mice. The presence of both mutations in individual littermates is indicative of the TAS genotype.

The *in Cis Apc*<sup>+/1638N</sup>/*Smad4*<sup>+/E6sad</sup> (CAS) model was obtained by backcrossing TAS animals with wild-type C57BL/6J mice. As both genes localize to the same chromosome 18, the presence of both mutations in individual littermates from TAS  $\times$  C57BL/6J matings is indicative of a recombination event that has brought the mutant *Apc*- and *Smad4* alleles on the same chromosome 18. In agreement with the genetic distance between the two tumor suppressor loci (33 cM), the two mutations were found on the same chromosome 18 allele in approximately 15% of the offspring.

Tumors were obtained by macroscopic dissection of the GI tract and overnight fixation in Notox<sup>®</sup> (Earth Safe Industries, Inc., Bellemead, NJ, USA), as previous described (Smits *et al.*, 1997), or after 4 h in 4% paraformaldehyde (PFA). Tumor sections were stained with hematoxylin and eosin (HE) and the histopathological analysis was performed using standard classification criteria (Boivin *et al.*, 2003). The term polyp in this context was used to describe a macroscopic lesion that protrudes in the GI lumen. By histopathological analysis, the polyps were then defined as hyperplastic or

dysplastic-adenomatous polyps if they showed, respectively, gross thickening or proliferative dysplasia of the mucosa.

#### Laser capture microdissection and DNA extraction of intestinal tumors and normal mucosa

We employed laser capture microdissection (LCM) to obtain pure tumor cell populations from selected areas of paraffin-embedded tissue sections. In total, 10  $\mu$ m Notox-fixed sections were deparaffinized, rehydrated, and briefly stained by HE. Consecutive sections were carefully microdissected using a PALM<sup>®</sup> MicroBeam microscope system (PALM MicroLaser Technologies AG-Bernried, Germany). On average, 3000 cells were isolated from each designated area. For DNA isolation, LCM material was resuspended in 100  $\mu$ l of extraction buffer (100 mM NaCl, 10 mM TrisHCl pH=8.0, 25 mM EDTA pH=8.0, 0.5% SDS) with 0.6 mg/ml Proteinase K, and incubated overnight at 60°C. After phenol/chloroform and chloroform extraction, DNA was precipitated for 30 min at -20°C with 200  $\mu$ l of 100% ethanol, 50  $\mu$ l 7.5 M NH<sub>4</sub>Ac, and 10  $\mu$ g GenEluteTM linear polyacrylamide (Sigma), and suspended in 15  $\mu$ l TE<sup>-4</sup> buffer (10 mM Tris-HCl pH 8.0, 0.1 mM EDTA).

#### LOH analysis at the *Apc* and *Smad4* genes

LOH analysis of the *Apc* gene was performed using three primers that amplify in a single PCR reaction both the wild-type and the targeted *Apc*<sup>1638N</sup> allele, as previously described (Smits *et al.*, 1997). LOH analysis of the *Smad4* gene was carried out by genotyping the microsatellite repeat markers d18Mit81 and d18Mit80, informative in the employed *Smad4*<sup>+/E65ad</sup> mice, located 7 and 2 cM, respectively, proximal and distal to the *Smad4* gene on chromosome 18. PCR products were resolved on 6% polyacrylamide gels and quantified using a Typhoon<sup>™</sup> 9410 and ImageQuant<sup>™</sup> TL (Molecular Dynamics). LOH was scored when the allelic ratio of the two bands, normalized for the average ratio of normal controls, was  $\geq 1.5$  (Smits *et al.*, 1997).

#### References

Boivin GP, Washington K, Yang K, Ward JM, Pretlow TP, Russell R *et al.* (2003). *Gastroenterology* **124**: 762–777.

Fearon ER, Vogelstein B. (1990). *Cell* **61**: 759–767.

Fink SP, Mikkola D, Willson JK, Markowitz S. (2003). *Oncogene* **22**: 1317–1323.

Fodde R, Edelmann W, Yang K, van Leeuwen C, Carlson C, Renault B *et al.* (1994). *Proc Natl Acad Sci USA* **91**: 8969–8973.

Gaspar C, Fodde R. (2004). *Int J Dev Biol* **48**: 377–386.

Haignis KM, Dove WF. (2003). *Nat Genet* **33**: 33–39.

Haramis AP, Begthel H, van den Born M, van Es J, Jonkheer S, Offerhaus GJ *et al.* (2004). *Science* **303**: 1684–1686.

Hawkins NJ, Bariol C, Ward RL. (2002). *Pathology* **34**: 548–555.

He XC, Zhang J, Tong WG, Tawfik O, Ross J, Scoville DH *et al.* (2004). *Nat Genet* **36**: 1117–1121.

Hohenstein P, Molenaar L, Elsinga J, Morreau H, van der Klift H, Struijk A *et al.* (2003). *Genes Chromosomes Cancer* **36**: 273–282.

Howe JR, Roth S, Ringold JC, Summers RW, Jarvinen HJ, Sistonen P *et al.* (1998). *Science* **280**: 1086–1088.

Itoh S, Itoh F, Goumans MJ, Ten Dijke P. (2000). *Eur J Biochem* **267**: 6954–6967.

Jass JR. (2001). *J Pathol* **193**: 283–285.

Kielman MF, Rindapaa M, Gaspar C, van Poppel N, Breukel C, van Leeuwen S *et al.* (2002). *Nat Genet* **32**: 594–605.

#### LOH analysis by sequence analysis

The following primer pair was employed to PCR amplify the *Smad4*<sup>E65ad</sup> mutation site within the intron5/exon6 boundary: *Smad4* F1-GGACAGCAGCAGAATGGATT and *Smad4* R1-ATGGCCGTTTTGGTGGTGAG.

PCR products were sequenced in both directions using the same primers. Sequencing was performed on an ABI 3700 capillary sequencer (Applied Biosystem, Foster City, CA, USA) according to the manufacturer's instructions.

#### Immunohistochemical analysis of *Smad4* and $\beta$ -catenin

Notox and PFA-fixed paraffin-embedded tumor sections (4  $\mu$ m) were immunostained with mouse monoclonal antibodies direct against *Smad4* (clone B-8, sc-7966, Santa Cruz Biotechnology, Santa Cruz, CA, USA; dilution 1:100) and  $\beta$ -catenin (Transduction Laboratories, clone 14; dilution 1:200). The specificity of the B-8 antibody has been previously tested and validated (Wilentz *et al.*, 2000; Salovaara *et al.*, 2002). After antigen retrieval treatment (10 min boiling in Tris-EDTA pH 8.0), endogenous peroxidases were inactivated by 1% H<sub>2</sub>O<sub>2</sub>/PBS. A preincubation step of 30 min in 5% nonfat dry milk in PBS was followed by incubation with the specific antibody overnight at 4°C in preincubation buffer. Sections were then incubated and stained with the Envision HRP-ChemMate kit (DAKO) for the *Smad4* antibody, and with a goat antibody against mouse IgG/IgM conjugated with peroxidase (Jackson ImmunoResearch Laboratories) for  $\beta$ -catenin. The evaluation of *Smad4* IHC staining was performed after brief hematoxylin counterstaining of the slides.

#### Acknowledgements

This work has been made possible by funds from the Dutch Cancer Society, the Dutch Research Council (NWO VICI), and BSIK (ICES/KIS-3). PH is supported by a grant from the Association for International cancer Research (AICR).

Koh TJ, Bulitta CJ, Fleming JV, Dockray GJ, Varro A, Wang TC. (2000). *J Clin Invest* **106**: 533–539.

Koyama M, Ito M, Nagai H, Emi M, Moriyama Y. (1999). *Mutat Res* **406**: 71–77.

Lei S, Dubeykovskiy A, Chakladar A, Wojtukiewicz L, Wang TC. (2004). *J Biol Chem* **279**: 42492–42502.

Makinen MJ, George SM, Jernvall P, Makela J, Vihko P, Karttunen TJ. (2001). *J Pathol* **193**: 286–294.

Miyaki M, Iijima T, Konishi M, Sakai K, Ishii A, Yasuno M *et al.* (1999). *Oncogene* **18**: 3098–3103.

Salovaara R, Roth S, Loukola A, Launonen V, Sistonen P, Avizienyte E *et al.* (2002). *Gut* **51**: 56–59.

Satterwhite DJ, Neufeld KL. (2004). *Cell Cycle* **3**: 1069–1073.

Shioda T, Lechleider RJ, Dunwoodie SL, Li H, Yahata T, de Caestecker MP *et al.* (1998). *Proc Natl Acad Sci USA* **95**: 9785–9790.

Sirard C, de la Pompa JL, Elia A, Itie A, Mirtsos C, Cheung A *et al.* (1998). *Genes Dev* **12**: 107–119.

Smits R, Kartheuser A, Jagmohan-Changur S, Leblanc V, Breukel C, de Vries A *et al.* (1997). *Carcinogenesis* **18**: 321–327.

Smits R, Kielman MF, Breukel C, Zurcher C, Neufeld K, Jagmohan-Changur S *et al.* (1999). *Genes Dev* **13**: 1309–1321.

- Smits R, van der Houven van Oordt W, Luz A, Zurcher C, Jagmohan-Changur S, Breukel C *et al.* (1998). *Gastroenterology* **114**: 275–283.
- Takagi Y, Kohmura H, Futamura M, Kida H, Tanemura H, Shimokawa K *et al.* (1996). *Gastroenterology* **111**: 1369–1372.
- Takaku K, Miyoshi H, Matsunaga A, Oshima M, Sasaki N, Taketo MM. (1999). *Cancer Res* **59**: 6113–6117.
- Takaku K, Oshima M, Miyoshi H, Matsui M, Seldin MF, Taketo MM. (1998). *Cell* **92**: 645–656.
- Thiagalingam S, Lengauer C, Leach FS, Schutte M, Hahn SA, Overhauser J *et al.* (1996). *Nat Genet* **13**: 343–346.
- Wilentz RE, Su GH, Dai JL, Sparks AB, Argani P, Sohn TA *et al.* (2000). *Am J Pathol* **156**: 37–43.
- Woodford-Richens K, Williamson J, Bevan S, Young J, Leggett B, Frayling I *et al.* (2000). *Cancer Res* **60**: 2477–2482.
- Xu X, Brodie SG, Yang X, Im YH, Parks WT, Chen L *et al.* (2000). *Oncogene* **19**: 1868–1874.



---

## Chapter 5.

***Smad4* haploinsufficiency results in partial inhibition of TGF $\beta$ /BMP signal transduction and in differential regulation of a subset of dosage-dependent downstream targets**

***Submitted***



***Smad4* haploinsufficiency results in partial inhibition of TGF- $\beta$ /BMP  
signal transduction and in differential regulation of a subset of dosage-  
dependent downstream targets**

Paola Alberici<sup>1,5</sup>, Claudia Gaspar<sup>1</sup>, Marcin M.Górski<sup>2</sup>, Patrick Franken<sup>1</sup>, Lauri A.  
Aaltonen<sup>3</sup>, Rodney Scott<sup>4</sup> and Riccardo Fodde<sup>1\*</sup>.

<sup>1</sup>Department of Pathology, Josephine Nefkens Institute, ErasmusMC, Rotterdam, The Netherlands

<sup>2</sup>Department of Biochemistry, ErasmusMC, Rotterdam, The Netherlands

<sup>3</sup>Department of Medical Genetics, Molecular and Cancer Biology Research Program, University of Helsinki, 00014 Helsinki, Finland

<sup>4</sup>Newcastle Bowel Cancer Research Collaborative, Hunter Medical Research Institute, John Hunter Hospital and The University of Newcastle, NSW 2308, Australia

<sup>5</sup>Present address: Department of Molecular Cell Biology, Leiden University Medical Center, Leiden, The Netherlands

\*Corresponding author: Prof. Riccardo Fodde, PhD  
Dept. of Pathology, Josephine Nefkens Institute  
Erasmus University Medical Center,  
P.O. Box 2040, 3000 CA Rotterdam, The Netherlands;  
Phone: +31 10 408 84 90 Fax: +31 10 408 84 50  
Email: [r.fodde@erasmusmc.nl](mailto:r.fodde@erasmusmc.nl)

### Abstract

The *SMAD4* gene is a tumor suppressor involved in pancreatic and colorectal tumorigenesis. In *Smad4*-mutant mouse models, haploinsufficiency characterizes the development of gastro-intestinal polyps with initial retention of the wild type allele and protein expression in tumor tissues. Here, we show that, in mouse embryonic and intestinal cells heterozygous for a targeted *Smad4 null* mutation, Smad4 protein levels correlate with gene copy number with reduced expression. Also, retention of protein expression was confirmed in human polyps from *SMAD4* germline mutation carriers. Reporter assay analysis confirmed that mouse *Smad4*<sup>+/-</sup> cells exert intermediate inhibitory effects on both TGF- $\beta$  and BMP signalling. Expression profiling of homo- and heterozygous ES cells identified a subset of Smad4 dosage-dependent transcriptional target genes encompassing, among others, members of the TGF- $\beta$  and Wnt signalling pathways. Our results show that *Smad4* haploinsufficiency results in the alteration of TGF- $\beta$  /BMP signal transduction and in the differential expression of a subset of target genes likely to underlie intestinal polyp formation.

### Introduction

Haploinsufficiency is defined as the condition where mutation or loss of a single allele is sufficient to alter the phenotype of a diploid cell (Payne & Kemp, 2005). Haploinsufficiency at a tumor suppressor locus may overcome the need for the somatic loss or mutation of its wild type allele, predicted as the rate-limiting event for tumor development by the Knudson's two-hit model (Knudson, 1971) (Fodde & Smits, 2002). To date, experimental evidence for haploinsufficiency in cancer predisposition comes from the analysis of tumors obtained from mouse models or from hereditary cancer patients carrying heterozygous *null* mutations at known tumor suppressor genes. The absence of the second hit in a subset of these tumors has been attributed to inactivation of the remaining allele by alternative mechanisms such as epigenetic silencing, mutations in non-coding sequences, or to limited sensitivity of the employed mutation detection protocol. However, *bona fide* haploinsufficiency has been demonstrated for a subset of tumor suppressor loci including *ATM* (Lu et al., 2006), *PTEN* (Kwabi-Addo et al., 2001), *BRCA2* (Arnold et al., 2006), *LKB1* (Miyoshi et al., 2002), *BLM* (Goss et al., 2002), *Nkx3.1* (Magee et al., 2003), and *Tp53* (French et al., 2001).

SMAD4 is an intracellular mediator of the TGF- $\beta$  and BMP signal transduction pathways. Binding of the TGFBR2 receptor to the TGF- $\beta$  ligand triggers its heterodimerization with the TGFBR1 receptor and to the phosphorylation of members of the SMAD family of intracellular mediators, namely SMAD2 and SMAD3. These receptor-activated SMADs bind to SMAD4 and translocate the complex to the nucleus where it modulates the transcription of a broad spectrum of target genes involved in cell growth inhibition, apoptosis, differentiation, and matrix production (Duff & Clarke, 1998; Heldin et al., 1997). Somatic *SMAD4* gene mutations are found in 30-40% of sporadic CRC (Salovaara et al., 2002), whereas germline *SMAD4* mutations are responsible for a subset of patients affected by Familial Juvenile Polyposis (FJP) (Roth et al., 1999; Woodford-Richens et al., 2000), an autosomal dominant intestinal cancer syndrome. Previously, we and others (Alberici et al., 2006; Xu et al., 2000) showed that *Smad4*-mutant mouse models develop gastro-intestinal polyps with initial retention of the wild type *Smad4* allele and with complete functional loss only at later stages of tumor progression.

In the present study, we explored the possibility that TGF- $\beta$  downstream target genes may be affected in a dosage-dependent fashion by *SMAD4* haploinsufficiency. To this aim, *Smad4* haploinsufficient mouse cells were analyzed for their TGF- $\beta$  and BMP signaling levels and genome-wide transcription and compared with their *Smad4* proficient and deficient counterparts. Moreover, we analyzed intestinal tumors from FJP patients with established germline *SMAD4* mutation to validate the haploinsufficiency model in human tumorigenesis.

## **Results**

### ***Smad4* protein haploinsufficiency in *Smad4*<sup>+/-</sup> cells**

Haploinsufficiency of the *Smad4* gene has been previously shown to underlie gastrointestinal tumor development in two different mouse models (Xu et al., 2000; Alberici et al., 2006). In order to shed light on the molecular and cellular mechanisms underlying this defect, we set to evaluate *Smad4* protein expression in wild type (*Smad4*<sup>+/+</sup>), hetero- (*Smad4*<sup>+/*E6sad*</sup>), and homozygous (*Smad4*<sup>*E6sad/E6sad*</sup>) embryonic stem (ES) cells derived from pre-implantation blastocysts obtained by breeding of C57Bl6/J *Smad4*<sup>+/*E6sad*</sup> mice (Hohenstein et al., 2003; Alberici et al., 2006).

Two independent heterozygous and homozygous ES clones were analyzed by western blot with the B-8 antibody (Wilentz et al., 2000a; Wilentz et al., 2000b), as shown in Figure 1A. Homozygous *Smad4*<sup>E6sad/E6sad</sup> ES lysates do not reveal any protein expression, whereas both heterozygous clones show a consistent reduction in protein expression when compared with

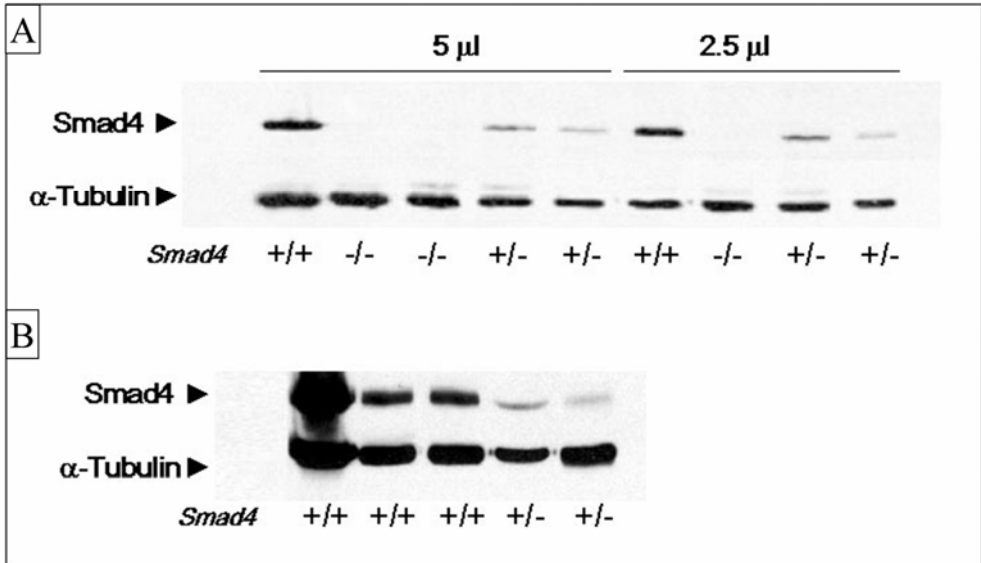


**Figure 1.**

SMAD4 western blot analysis demonstrates haploinsufficiency at the protein level in ES and adult intestinal cells from *Smad4*<sup>+/-E6sad</sup> mice. A. ES cell lysates loaded at two different amounts of protein; B. Normal intestinal tissue lysates from *wild type* and *Smad4*<sup>+/-E6sad</sup> mice.

wild type ES cells, thus confirming haploinsufficiency at the protein level in *Smad4*<sup>+/-E6sad</sup> cells. Moreover, western blot analysis performed on intestinal cells from *Smad4*<sup>+/-E6sad</sup> mice indicated that protein haploinsufficiency is not limited to ES cells but is also confirmed in adult tissues (Figure 1B).

#### **Smad4 haploinsufficiency affects both TGF-β and BMP signaling**

The Smad4 protein acts, together with the receptor-activated Smads, as the main signal transducer for the TGF-β family of signalling pathways, namely TGF-β and BMP. To determine whether the observed reduction of Smad4 expression in *Smad4*<sup>+/-E6sad</sup> cells impairs these signalling routes, we first measured the levels of the Smad2/Smad3/Smad4

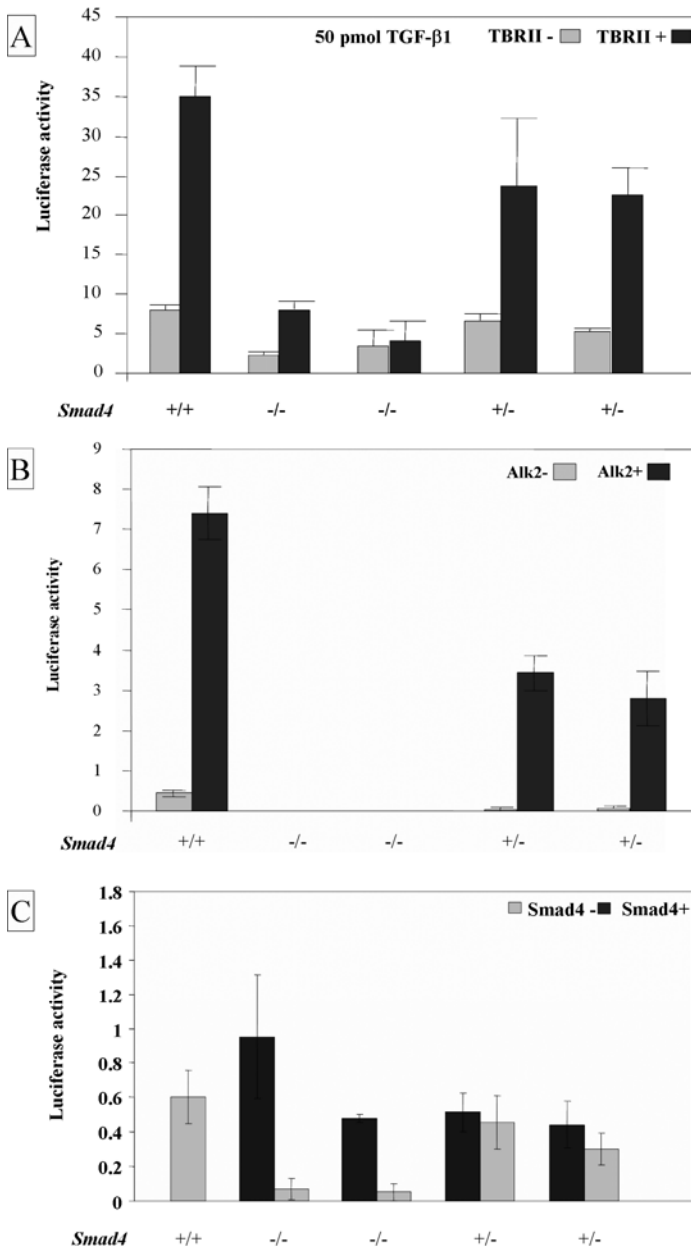


**Figure 2.**

Reporter assay analysis of *Smad4*-mutant and wild type ES cell lines. A. TGF-β reporter (CAGA-luc) and B. BMP reporter assay were carried out in wild type (+/+), *Smad4*<sup>+/*E6*sad</sup> (+/-), and *Smad4*<sup>*E6*sad/*E6*sad</sup> (-/-) ES cell lines. Normalized CAGA-luc and BRE-luc levels are indicated for each cell line. In C. TGF-β reporter assays analysis was carried out after transfection with a *Smad4*-expressing vector. Each bar represents the average of three independent experiments.

As the type II TGF- $\beta$  receptor (TGFBR2) is expressed in ES cells at insufficient levels to provide significant activation of TGF- $\beta$  signaling (data not shown), we co-transfected the ES cells with an expression vector (pCMV5 TBR2) encoding for the type II TGF- $\beta$  receptor (Wrana et al., 1992) together with the reporter assay constructs.

As shown in Figure 2A, *Smad4*<sup>E6sad/E6sad</sup> ES cells show a dramatic decrease in TGF- $\beta$  signaling activity when compared with the wild type control. Moreover, the decrease in activity is already present in the two independent *Smad4*<sup>+/-E6sad</sup> ES clones, both showing a level of luciferase activity intermediate between wild type and homozygous cells.

The *Smad4*-mutant ES lines were furthermore analysed for their BMP signalling activity. To this aim, we transfected the ES cells with the BRE- luc reporter assay, previously shown to be specifically responsive to BMP signalling levels (Korchynski & ten Dijke, 2002) together with a constitutively active ActR-I receptor (Korchynski & ten Dijke, 2002). As shown in Figure 2B, the results clearly demonstrate that, as for TGF- $\beta$  signaling, *Smad4* protein haploinsufficiency results in a decrease of BMP signal transduction activation, at an intermediate level between that of wild type and homozygous cells. Also, rescue of *Smad4* expression in homozygous *Smad4*<sup>E6sad/E6sad</sup> ES cells by transfection with a *Smad4* expression vector (Nakao et al., 1997) was able to restore TGF- $\beta$  signaling levels thus indicating that the observed inhibitory and dosage-dependent effects are *Smad4*-specific (Figure 2C).

### **SMAD4 IHC analysis of Juvenile Polyps confirms haploinsufficiency in human tumors**

*SMAD4* germline mutations characterize a fraction of patients affected by the Juvenile Polyposis Syndrome (JPS). This autosomal dominant condition is characterized by the presence of hamartomatous polyps in the GI tract with early onset and increased cancer risk. In order to determine whether haploinsufficiency at the human *SMAD4* gene features the initial step of juvenile polyp formation, i.e. without somatic mutation or loss of heterozygosity (LOH) of the wild type *SMAD4* allele as previously reported in *Smad4*-mutant mouse models for intestinal polyposis (Xu et al., 2000; Alberici et al., 2006), we performed SMAD4 immuno-histochemical (IHC) analysis of polyps from JPS patients known to carry established germline mutations in the *SMAD4* gene. Out of a total of five unrelated cases, two showed clear retention of SMAD4 expression in large areas of the polyps (Figure 3A and B). In the remaining cases, SMAD4 IHC was instead on average

negative, with only few scattered groups of cells characterized by weak nuclear staining (Figure 3C). Notably, the polyps characterized by retention of SMAD4 staining are the smallest in our series, measuring 0.4 x 0.6 cm. and 0.4 x 0.5 cm. respectively. Juvenile polyps with loss of SMAD4 staining measured instead between 2x2 and 3x3 cm, thus suggesting that complete loss of SMAD4 function only occurs at a later stage of juvenile

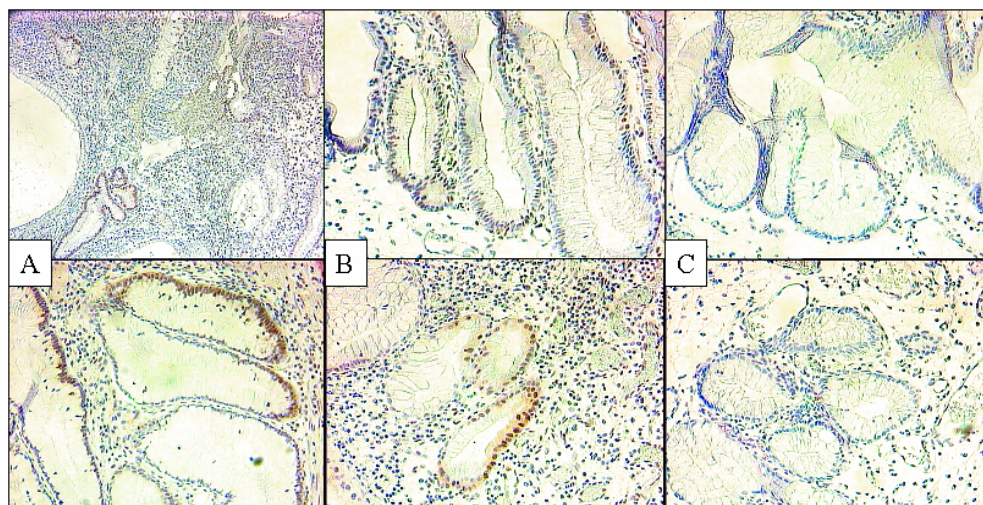


**Figure 3.**

Immunohistochemical analysis of SMAD4 protein expression performed on polyps from three unrelated Familial Juvenile Polyposis patients with established *SMAD4* germline mutation. A. Polyp with SMAD4 nuclear staining. B. Polyp with heterogeneous SMAD4 expression pattern with patches of positively and negatively staining tumor cells. C. SMAD4 negative juvenile polyp.

polyp progression, whereas the initial step of polyp formation occurs in haploinsufficient cells, i.e. without loss of the *SMAD4* wild type allele. These observations are in agreement with our own previous study on intestinal polyps from the *Smad4*<sup>+/*E6sad*</sup> mouse model where complete loss of Smad4 protein expression occurs at late progression stages in tumors characterized by increased dysplasia (Alberici et al 2006).

Overall, these results indicate that, in partial disagreement with Knudson's two-hit model for tumor formation, somatic loss of the wild type allele is not a rate-limiting event in *SMAD4*-driven intestinal polyp formation both in man and mouse. Tumor formation occurs in a haploinsufficient genetic background with reduced SMAD4 protein expression levels

as shown above (Figure 1) and with intermediate inhibitory effects on the TGF- $\beta$  and BMP signaling pathways (Figure 2).

### **Expression profiling analysis reveals a subset of Smad4 dosage-dependent transcripts.**

As described above, *Smad4* haploinsufficiency negatively affects both TGF- $\beta$  and BMP signal transduction. Next, we wanted to characterize the effects on gene transcription caused by the different TGF- $\beta$  and BMP signalling levels observed in *Smad4*<sup>+/*E6sad*</sup> and *Smad4*<sup>*E6sad*/*E6sad*</sup> cells, in an attempt to elucidate the downstream pathways and putative cellular alterations which underlie tumor formation and progression. To this aim, genome-wide expression profiling analysis of total RNA samples from wild type, *Smad4*<sup>+/*E6sad*</sup> and *Smad4*<sup>*E6sad*/*E6sad*</sup> ES cells was performed with the Affymetrix MOE430 2.0 array encompassing over 39,000 transcripts. Two independent clones for each genotype were used for the expression profiling analysis.

A set of differentially expressed genes was identified in both heterozygous and homozygous cells when compared with *Smad4*<sup>+/*+*</sup> cells, thus showing that *Smad4* haploinsufficiency is sufficient to affect transcription of a subset of downstream target genes. These dosage-dependent *Smad4* target gene signatures provide a unique opportunity to study the differential effects of haploinsufficiency and complete loss of *Smad4* function at the molecular and cellular level. In order to focus on genes with *Smad4* dosage-dependent expression patterns, we crossed the lists of genes differentially expressed (compared with wild type cells) with a threshold of  $p < 0.01$  for the homo- and  $p < 0.05$  for the heterozygous cells. This approach led to the identification of 79 individual gene transcripts differentially expressed in both *Smad4*-mutant genotypes when compared with *Smad4*<sup>+/*+*</sup> ES cells including 31 up- and 48 down-regulated genes, respectively. Among the 79 gene signature, 24 and 40 transcripts represent functionally annotated genes in the up- and down-regulated group, respectively (Table 1). The presence of the *Smad4* gene itself within the list of downstream target corroborates the validity of our approach. Among the functionally annotated and differentially expressed entries, several functional categories are represented: members of known signal transduction pathways (e.g. *Mdm2*, *Axin2*, *Smad7*, *Zak*), growth factors (*Fgf5*, *Fgf8*, *Igfbp3*, *Lefty2*), immunity related genes (*Irgm*, *Il23a*, *Cxcl14*), and transcription factors (*Nrip1*, *Eomes*, *Stat3*, *Cnot6*, *T* brachyury homolog) among others. Notably, when the fold changes levels relative to these 79 genes are plotted to follow their behaviour according to the *Smad4* genotypes, a gradient of transcriptional

response becomes apparent, thus indicating a Smad4 dosage-dependent control of downstream target gene expression (Figure 4).

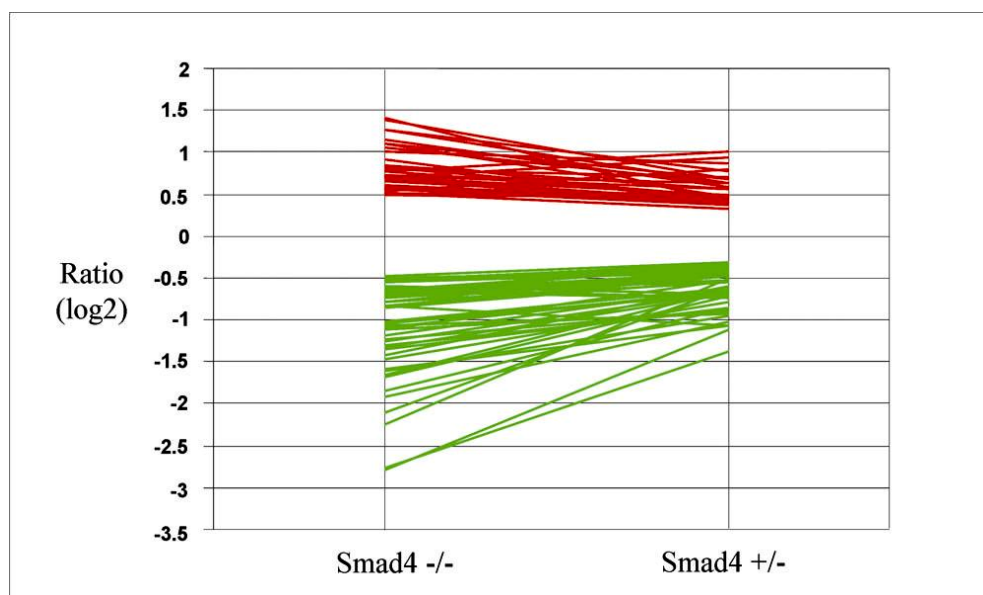


**Figure 4.** Expression profiling analysis of the subset of 79 genes (corresponding to 88 Affymetrix probes) found to be differentially expressed in both *Smad4*<sup>+/*E6sad*</sup> and *Smad4*<sup>*E6sad/E6sad*</sup> ES cells. The fold changes are represented as (log<sub>2</sub>) ratio values.

#### **Quantitative real-time RT-PCR validates Smad4-dosage dependent target genes in intestinal tissues from *Smad4*<sup>+/*E6sad*</sup> mice**

To determine whether the Smad4 dosage-dependent genes identified by expression profiling of *Smad4*–mutant ES cells are similarly affected by differential expression also in the intestine of adult *Smad4*<sup>+/*E6sad*</sup> mice, we analyzed the mRNA levels of a selection (n=6) of the 79 genes by quantitative real-time RT-PCR on laser-capture microdissected (LCM) normal intestinal cells obtained from 2 wild type and 3 heterozygous animals. This methodology allows highly quantitative measurements of target gene expression and can be performed on the limited amounts of mRNA extracted from microdissected epithelial cells. The selected genes are all known to be expressed in the gastrointestinal tract and are characterized by at least one fold change level in the ES cells expression profiling data (log<sub>2</sub>>1). As a control, we also performed qPCR analysis of *Smad4* gene expression, expected to be reduced in the normal intestine of *Smad4*<sup>+/*E6sad*</sup> mice when compared with

wild type animals. As internal reference standard, we employed the crystallin zeta quinone reductase-like 1 (*Cryz11*) gene, previously shown to retain constant expression levels between wild type and *Smad4*-mutant ES and adult intestinal cells by expression profiling (data not shown). The primers used for the qPCR analysis are listed in Supplementary Table 1. As shown in Figure 5, both up- (*Prkar1b* and *Tgb1*) and down-regulated (*Smad7*, *Irgm*, *Arts-1* and *Igfbp1*) genes showed consistent changes in gene expression levels in *Smad4*<sup>+/*E6sad*</sup> normal intestine when compared with the wild type tissues, concordant with the ES cells expression profiling results.

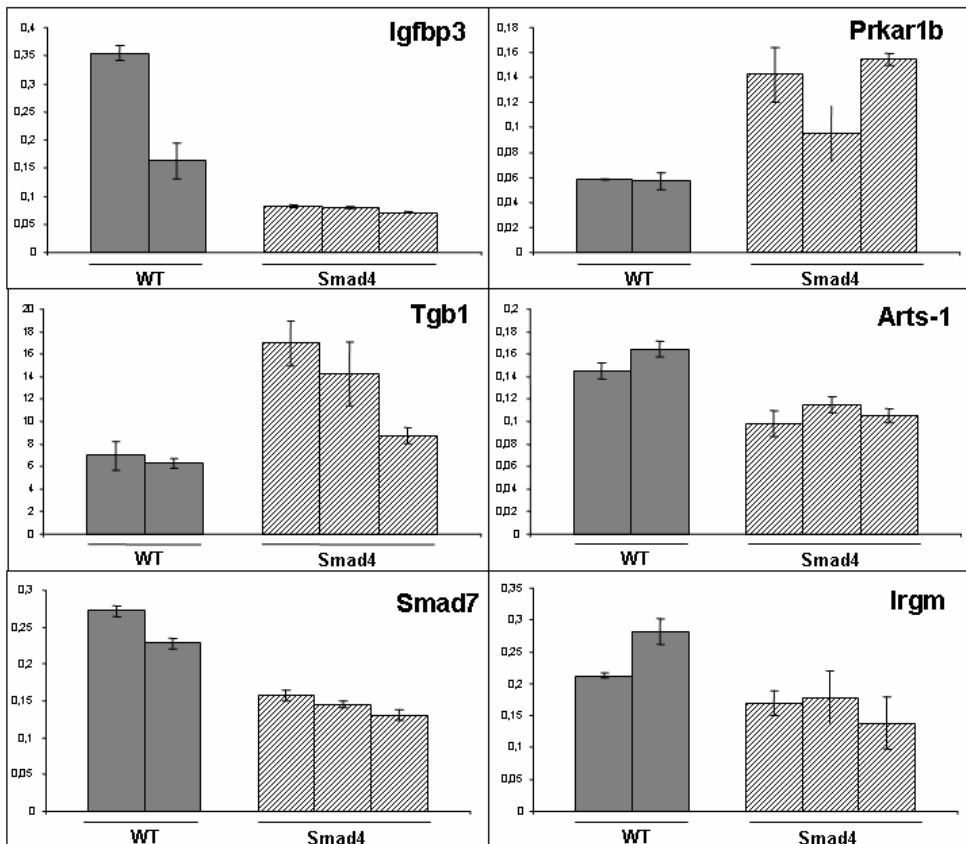


**Figure 5.**

Quantitative PCR analysis of a selection of six genes differentially regulated in *Smad4*<sup>+/*E6sad*</sup> cells. Gene expression was quantified in normal intestinal tissues from two wild type (*WT*) and three *Smad4*<sup>+/*E6sad*</sup> (*Smad4*) animals and is plotted as ratio over the reference gene, as explained in the Material and Methods. Each bar represents the average of three independent experiments.

**Table 1.** List of 64 functionally annotated genes differentially expressed in *Smad4<sup>+/ESrad</sup>* and *Smad4<sup>ESrad/ESrad</sup>* ES cell lines compared with wild type. Expression profiling values are expressed as the (log<sub>2</sub>) fold change ratio when compared to *Smad4<sup>+/+</sup>* ES cells.

Gene Symbol and Name	UniGene	Fold Change	Fold Change
		<i>Smad4<sup>ESrad/ESrad</sup></i>	<i>Smad4<sup>+/ESrad</sup></i>
<b>Immunity Response</b>			
ARTS-1 (type I tumor necrosis factor receptor shedding aminopeptidase regulator)	Mm.83526	-1.479528635	-0.77719934
CXCL14 (chemokine (C-X-C motif) ligand 14)	Mm.30211	0.739985038	-0.895453086
GBP6 (guanylate binding protein family, member 6)	Mm.45740	-1.222910059	-0.885663139
IL23A (interleukin 23, alpha subunit p19)	Mm.125482	0.566113119	0.364305658
IRGM (immunity-related GTPase family, M)	Mm.29938	-1.919739116	-1.023252754
TAPBP (TAP binding protein, tapasin)	Mm.392082	-0.725129901	-0.483967456
<b>Molecular Transport</b>			
ATP11A (ATPase, Class VI, type 11A)	Mm.426811	0.838793115	0.556606929
LMAN1 (lectin, mannose-binding, 1)	Mm.290857	-1.294382173	-0.88791057
SERPINH1 (serpin peptidase inhibitor, clade H (heat shock protein 47), member 1)	Mm.22708	0.812682409	0.472372138
STEAP1 (six transmembrane epithelial antigen of the prostate 1)	Mm.85429	0.797881173	0.692198993
CYP26A1 (cytochrome P450, family 26, subfamily A, polypeptide 1)	Mm.42230	-0.626983032	-1.01244189
<b>Signal Transduction</b>			
AXIN2 (axin 2, conductin, axil)	Mm.71710	-0.631968418	-0.746104287
COMMMD3 (COMM domain containing 3)	Mm.249586	1.108450328	0.680946917
FGF5 (fibroblast growth factor 5)	Mm.5055	-2.766113339	-1.377425378
FGF8 (fibroblast growth factor 8, androgen-induced)	Mm.4012	-1.31858955	-0.689242111
GPRI124 (G protein-coupled receptor 124)	Mm.87046	1.004876393	0.861919148

IGFBP3 (insulin-like growth factor binding protein 3)	Mm.29254	-1.609613286	-0.945544949
MDM2 (Mdm2, transformed 3T3 cell double minute 2, p53 binding protein)	Mm.22670	0.583604813	0.387567158
PARD6G (par-6 partitioning defective 6 homolog gamma)	Mm.24678	0.779787267	0.470633264
PRKAR1B (protein kinase, cAMP-dependent, regulatory, type I, beta)	Mm.306163	1.391725721	0.67106604
PTDSR (phosphatidylserine receptor)	Mm.383423	-0.663796169	-0.354594974
PTPRN2 (protein tyrosine phosphatase, receptor type, N polypeptide 2)	Mm.206054	-0.659733126	-0.423255005
RHOF (ras homolog gene family, member F (in filopodia))	Mm.253876	-0.63244674	-0.367897137
SH3BP5 (SH3-domain binding protein 5 (BTK-associated))	Mm.383198	0.733454507	0.557584138
SMAD4 (SMAD, mothers against DPP homolog 4 (Drosophila))	Mm.100399	-1.411644669	-0.596542113
SMAD7 (SMAD, mothers against DPP homolog 7 (Drosophila))	Mm.34407	-1.841318063	-0.847729451
STAT3 (signal transducer and activator of transcription 3)	Mm.249934	-0.726889321	-0.482104469
TULP4 (tubby like protein 4)	Mm.28251	0.725714735	0.63040039
<b>Development</b>			
T (T, brachyury homolog, in mouse)	Mm.913	-2.801639816	-1.116757616
ODZ4 (odz, odd Oz/ten-m homolog 4 in Drosophila)	Mm.254610	0.495834321	0.457162659
ZIC5 (Zic family member 5 (odd-paired homolog, Drosophila))	Mm.390761	-1.015016618	-0.695652534
<b>Transcription and Translation Regulation</b>			
CNOT6 (CCR4-NOT transcription complex, subunit 6)	Mm.247113	-0.640715822	-0.447892731
EIF4E2 (eukaryotic translation initiation factor 4E member 2)	Mm.227183	-0.535582452	-0.338370666
EOMES (eomesodermin homolog, in Xenopus laevis)	Mm.200692	-1.066716547	-0.921524759
NR1P1 (nuclear receptor interacting protein 1)	Mm.390915	0.567563851	0.485717219
RARA (retinoic acid receptor, alpha)	Mm.103336	-0.536083782	-0.350183603
ZFP28 (zinc finger protein 28 homolog, in mouse)	Mm.127014	0.589656513	-0.36245756
ZNF524 (zinc finger protein 524)	Mm.19974	-0.492103362	-0.396424066

ZNRF3 (zinc and ring finger 3)

Mm.216313

-0.66798835

-0.742694685

### **Metabolism**

PSMB8 (proteasome (prosome, macropain) subunit, beta type, 8)

Mm.180191

-1.648772706

-0.648394947

RPL17 (ribosomal protein L17)

Mm.276337

-2.240592232

-0.508254776

TRIM12 (tripartite motif protein 12)

Mm.327033

-1.098317241

-0.642611843

CYP2A1 (cytochrome P450, family 26, subfamily A, polypeptide 1)

Mm.42230

-1.01244189

-0.626983032

GALNT10 (UDP-N-acetyl-alpha-D-galactosamine:polypeptide N-acetyl-galactosaminyltransferase 10)

Mm.271670

-0.784055422

-0.544632838

SEPP1 (selenoprotein P, plasma, 1)

Mm.392203

-0.579623409

0.415780255

ENPP3 (ectonucleotide pyrophosphatase/phosphodiesterase 3)

Mm.338425

-0.589418878

0.403041963

HERC5 (hect domain and RLD)

Mm.9002

-1.591365941

-1.074199143

### **Blood coagulation**

ANXA8 (annexin A8)

Mm.3267

0.532178099

0.787223561

### **Cell Proliferation**

DERL2 (Der1-like domain family, member 2)

Mm.28131

-0.483695221

-0.319079191

LEFTY2 (left-right determination factor 2)

Mm.87078

-2.107217098

-0.612221721

PEG10 (paternally expressed 10)

Mm.320575

0.501183232

0.431440805

### **Cell Adhesion**

CYR61 (cysteine-rich, angiogenic inducer, 61)

Mm.1231

-0.820871332

-1.057790626

TGFBI (transforming growth factor, beta-induced, 68kDa)

Mm.14455

1.1111755916

0.456266768

### **Cell Cycle**

PMP22 (peripheral myelin protein 22)

Mm.1237

1.405947145

0.400953986

ZAK (sterile alpha motif and leucine zipper containing kinase AZK)

Hs.444451

0.707312841

0.492873167

**Cytoskeleton**

ENC1 (ectodermal-neural cortex (with BTB-like domain))

Mm.241073 -0.521179495 -0.376208853

**Unknown**

DDIT4L (DNA-damage-inducible transcript 4-like)

Mm.250841 1.279528967 0.638642471

DENND1C (DENN/MADD domain containing 1C)

Mm.284447 -0.598544244 -0.686240144

GBP4 (guanylate binding protein 4)

Mm.275893 -1.110818959 -0.526149912

KIAA0738 (KIAA0738 gene product)

Mm.24652 0.646405004 0.432359635

KLHL26 (kelch-like 26, in Drosophila)

Mm.187090 0.833941271 0.413239094

NOPE (likely ortholog of mouse neighbor of Punc E11)

Mm.209041 0.779871083 1.010120212

PHF19 (PHD finger protein 19)

Mm.65691 -1.053502332 -0.657427767

PLEKHG2 (pleckstrin homology domain containing, family G member 2)

Mm.235700 -0.718000665 -0.525350818

PSORS1C2 (psoriasis susceptibility 1 candidate 2)

Mm.34201 -1.176463979 -0.628014275

## Supplementary Table 1.

Sequences of the primers employed for the qPCR analysis.

Gene	Forward Primer	Reverse Primer
<i>Cryz11</i>	5'-AGCTGCTGGGCGTCATCCG-3'	5'-CTGTGGTGGGCTAACTGAATGG-3'
<i>Smad4</i>	5'-GTGACTGTGGATGGCTATGTGG-3'	5'-GCAACCTCGCTCTCTCAATCC-3'
<i>Arts-1</i>	5'-GCAGACTTGGACAGATGAAGG-3'	5'-TGACTTCCACTCTCTGAAATAGC-3'
<i>Smad7</i>	5'-TGCCCTCGGACAGCTCAATTCC-3'	5'-CCCACACGCCATPCCACTTCC-3'
<i>Pkrar1b</i>	5'-GCCCGAATCCCTGTCCCTTG-3'	5'-TGGCTGGCTCATATACACACTCC-3'
<i>Irgm</i>	5'-ACAGGCTCCAGCAGGTTACC-3'	5'-TTGCCACAGTCTCTCTTGATTCC-3'
<i>Tgfb1</i>	5'-CAAACAGGCGTCAAGCATTCC-3'	5'-GGCTCTCCTCTCCGCTTTCC-3'
<i>Igfbp1</i>	5'-CCCAGAGGCGTCCACATCC-3'	5'-GTCCACACAGCAGCAGAAAGC-3'

## Discussion

The precise molecular events that occur during the very first steps of tumor formation are still poorly understood. In the case of tumour suppressor genes (TSGs), the two-hit model predicts that the somatic loss or mutation of the wild type allele is an absolute requirement to trigger tumour formation. However, over the last few years it has become clear that in a subset of TSGs this rate-limiting event does not accompany the initial steps of tumor formation (Santarosa & Ashworth, 2004). In these cases it is plausible to assume that haploinsufficiency, i.e. the functional loss of a single TSG allele, can already affect normal cell function and homeostasis, possibly in a synergistic fashion with other genetic or epigenetic somatic hits at unrelated cancer genes.

Mouse models carrying targeted loss of function mutations at the *Smad4* tumor suppressor gene (Alberici et al., 2006; Xu et al., 2000) represent illustrative examples of haploinsufficiency, as GI-tract tumors initially develop in these animals by retaining the wild type *Smad4* allele and its reduced protein expression. Here, we show that *Smad4* haploinsufficiency results in dosage-dependent inhibition of TGF- $\beta$  and BMP signalling, two well-known pathways controlling epithelial cell proliferation and differentiation and likely to underlie tumorigenesis in these mice. Expression profiling of the *Smad4* haploinsufficient cells confirmed the existence of a subset of target genes whose expression is specifically regulated by different *Smad4* protein (and presumably TGF- $\beta$  and BMP signalling) dosages.

In the haploinsufficiency model, the steady-state levels of a tumor suppressor gene product fluctuate around a mean threshold value that, in case of haploid gene expression, is approx. 50% of the diploid state (Cook et al., 1998). However, transient fluctuations below critical threshold levels may affect proper protein function and cellular homeostasis. Tissue-specific differences in the expression of tumor suppressor proteins and their spatial distribution within specific tissues, as illustrated by the gradient of SMAD4 protein expression observed along the crypt-villus axis in the GI tract, are likely to play relevant roles in modulating the phenotypic outcome of haploinsufficiency. Also, specific organs may be differentially exposed to environmental mutagens thus increasing the chance of synergistic somatic hits. In JPS patients carrying heterozygous *SMAD4* germline mutations and in *Smad4*<sup>+/-</sup> mice, haploinsufficiency features all somatic cells but exerts a tumor phenotype predominantly in the GI tract, possibly due to additional exposure to oxidative and chemical stress in the intestine. Alternatively, the rapid epithelial turnover

characteristic of the mammalian intestinal tract may represent a microenvironment particularly susceptible to the observed effects of SMAD4 haploinsufficiency on and TGF- $\beta$  and BMP signalling and on specific downstream transcriptional targets.

Polyyps from JPS patients with *SMAD4* germline mutations were previously shown to carry second hit mutations at the wild type allele only in 9% (1/11) (Howe et al., 1998) and 23% (4/17) (Woodford-Richens et al., 2000) of the cases. In the present study, we validated these observations by IHC analysis. Small hamartomatous polyps from JPS patients with established germline *SMAD4* mutations retain protein staining, whereas bigger and more advanced polyps are either negative or 'patchy', with small areas of weak protein staining.

Haploinsufficiency of the *SMAD4* gene has also been shown to be relevant in the context of sporadic colorectal carcinoma development. Several studies based on coupled LOH and mutation analysis of sporadic colorectal cancers have failed to identify two independent mutation hits in the *SMAD4* gene in the majority of the cases (Mamot et al., 2003; Hadzija et al., 2004). These negative results are generally attributed to lack of sensitivity of the employed mutation-detection protocol, or to sampling bias (e.g. early tumor stages). Recently however, Tatsuya and co-workers (Ando et al., 2005) demonstrated that only 1 out of 25 CRC cases with allelic imbalance at the *SMAD4* gene locus harbor additional mutations in the remaining allele, confirming the possibility that *SMAD4* gene dosage reduction may indeed play a role in sporadic colorectal cancer. Moreover, it has been shown that complete loss of SMAD4 expression in CRC associates with poor prognosis (Alhopuro et al., 2005). Reduced tumor SMAD4 protein levels were also associated with a significant decrease in disease-free and overall survival after potentially curative surgery in Dukes C colorectal cancer patients (Alhopuro et al., 2005). In the same study, *SMAD4* mRNA levels predicted treatment response in Dukes C patients. Accordingly, SMAD4 mRNA and protein levels were found to further decrease in lymph node metastases when compared to primary tumors. Overall, the combined genetic and protein expression data from both JPS patients and mouse models support a model for *SMAD4*-driven tumorigenesis where the initial mutation leads to haploinsufficiency and increased susceptibility to intestinal tumor formation due to specific effects on TGF- $\beta$  and BMP signalling and on the transcription of a subset of downstream targets. Bi-allelic inactivation of *SMAD4* leading to its complete functional loss and even more severe transcriptional and signaling defects, predominantly occurs at later stages of malignant progression.

The genes shown to be differentially up- or down-regulated in a Smad4 dosage-dependent fashion include well-known members of signal transduction pathways (Table 1). The MDM2 protein, for example, acts as a major regulator of the tumor suppressor p53 by targeting it for proteosomal degradation (Momand et al., 1992), and plays a role as negative regulator of RB (Xiao et al., 1995). Mdm2 up-regulation, as observed in *Smad4*<sup>+/*E6sad*</sup> cells, may favor tumor transformation by inhibiting p53-mediated transactivation (Sdek et al., 2005) and by destabilizing RB.

The scaffold protein *Axin2* (conductin) has been previously implicated in canonical Wnt signaling pathway and CRC pathogenesis (Liu et al., 2000). Loss of *Axin2* function leads to defects in cell cycle regulation and apoptosis through the transcriptional activation of Wnt downstream targets such as c-Myc and Cyclin D1, among others. The observed *Axin2* downregulation in *Smad4*<sup>+/*E6sad*</sup> cells may indicate a cross-talk between TGF- $\beta$  and Wnt signal transduction already in haploinsufficiency. However, TOP-Flash reporter assays of *Smad4*<sup>+/*E6sad*</sup> and *Smad4*<sup>*E6sad*/*E6sad*</sup> ES cells did not show significant increase in Wnt/ $\beta$ -catenin signaling when compared with wild type cells (unpublished).

The expression of two known downstream targets of the TGF- $\beta$  pathway, namely *Smad7* and *Tgfb1*, is also affected by Smad4 haploinsufficiency. *Smad7* is both a well-characterized inhibitor of TGF- $\beta$  signaling and itself a TGF- $\beta$  downstream target, possibly as the result of a negative regulatory loop. *Smad7* down-regulation, as observed in the *Smad4*<sup>+/*E6sa*</sup> ES cells, likely reflects the observed inhibition of TGF- $\beta$  signaling. *Tgfb1* is an extracellular protein with only poorly characterized functions. The up-regulation of the *Tgfb1* gene in *Smad4*<sup>+/*E6sa*</sup> ES cells possibly reflects its highly significantly over-expression in sporadic CRC (Buckhaults et al., 2001).

Down-regulation of the insulin growth factor binding protein *Igfbp3* in *Smad4*<sup>+/*E6sa*</sup> ES and intestinal cells may also represent a relevant initial alteration in tumor formation. *Igfbp3* has been described as tumor suppressor gene (Xi et al., 2006), due to its role in the regulation of cell proliferation and apoptosis. In addition, methylation of its promoter and expression silencing has been observed in 50% of the CRC cases analyzed (Tomii et al., 2007).

TGF- $\beta$  signaling defects play important roles not only in tumor cells but also in their direct microenvironment (Bierie & Moses, 2006). Communication between tumor and stromal cells through different cytokines and growth factors actively regulates and promotes tumor

progression. TGF- $\beta$ -mediated regulation of the tumour microenvironment can occur at different levels including cell-autonomous signaling, stromal–epithelial interactions, inflammation, immune evasion and angiogenesis. Recently, Kim et al showed that transgenic animals engineered to induce loss of *Smad4* exclusively in the T-cell compartment develop intestinal lesions characterized by expansion of the stromal compartment reminiscent of JPS polyps (Kim et al., 2006). Moreover, further support of the role of *Smad4* dosage effects in tumor initiation came from the observation in the same study according to which loss of a single *Smad4* allele resulted in polyp formation and hyperplasia in the GI tract, similar to what previously observed in our *Smad4*<sup>+/*E6sa*</sup> model (Alberici et al., 2006). Although in our model the specific contribution of the stromal component to the neoplastic process cannot be dissected from that of the parenchymal tumor cells due to the constitutive nature of *Smad4* haploinsufficiency in these animals, the observation that more advanced lesions show complete loss of *Smad4* expression might indicate a progression model where total loss of TGF- $\beta$  and BMP signaling in the epithelial compartment is necessary for full-blow carcinogenesis.

In conclusion, it is likely to assume that *Smad4* haploinsufficiency results in intestinal polyp formation not only by the direct inhibition of TGF- $\beta$  and BMP signaling and their downstream effectors in both the parenchymal cell and its direct microenvironment, but also through a number of more indirect and/or independent downstream targets thus affecting a broad spectrum of cellular functions including apoptosis, cell cycle regulation, cell adhesion, immune response, and others.

## **Material and methods**

### *Animal models and tissue samples*

The *Smad4*<sup>+/*E6sad*</sup> mouse model (Alberici et al., 2006; Hohenstein et al., 2003) is available on the inbred C57Bl/6J background. Mice were maintained under a 12 hour light-dark cycle and fed with standard diet and water *ad libitum*. All experiments on mice were performed in accordance with institutional and national guidelines and regulations. Frozen laser capture microdissected (LCM) intestinal tissues (approx. 6000 cells) were collected using a PALM MicroBeam microscope system as previously described (Alberici et al., 2007).

### *Generation of Smad4-mutant ES cell lines*

## Chapter 5

---

*Smad4*<sup>+/*E6sad*</sup> mice were inter-bred and the resulting blastocytes were harvested after fertilization at 3.5 dpc. Flushed pre-implantation blastocytes were then individually cultured on 96-well dishes coated with mouse embryonic fibroblasts (MEFs) as previously described (Matise M.P., 2000). Two independent ES cell lines were generated for each genotype.

### *Smad4 western analysis*

Equal amounts (40 µg) of protein lysates were separated on 12% SDS polyacrylamide gels, and further subjected to immunoblotting according to standard procedures. Several studies have validated the specificity and sensitivity of the B-8; sc-7966 monoclonal antibody against SMAD4 (Santa Cruz Biotechnology) to detect alterations of protein expression in both mouse and human specimens (Wilentz et al., 2000a; Wilentz et al., 2000b). The B-8; sc-7966 primary antibody was for western analysis at a 1:100 dilution. Peroxidase-conjugated secondary antibodies (Jackson ImmunoResearch) were visualized with an enhanced chemiluminescence (ECL) system (10 ml Sodium Luminol from Sigma in 0.1 M Tris-HCl, pH 8,6 + 100 µL Enhancer (para-hydroxyl-Coumaric acid from Sigma, in DMSO) + 3 µL H<sub>2</sub>O<sub>2</sub>).

### *Reporter assay analysis*

ES cells grown on tissue culture dishes coated by mitotically inactivated primary MEFs were transfected by Lipofectamine 2000 (Life Technologies) with 250 ng of the reporter plasmid [(CAGA)12-MLP-luciferase for the TGF-β signaling or BRE-luciferase for the BMP signaling], 100 ng of receptor-expressing vector [TGFBRII or, for BMP signaling, a constitutively active form of ALK2] (Wrana et al., 1992; Korchynskiy & ten Dijke, 2002) (all kindly provided by Prof. P. ten Dijke), and 5 ng of a *Renilla reniformis* luciferase-expressing vector. For the rescue experiments, 100 ng of the *Smad4*-pCMV5 expression vector (Nakao et al., 1997) were transfected together with (CAGA) 12-MLP-luciferase and TGFBRII. After 24 hours, ES cells transfected with the (CAGA)12-MLP-luciferase were stimulated with recombinant human TGF-β (50pmol) for 1 hour before to measure the luciferase activities with the luminometer Fluoroskan Ascent CF (Labsystems) using the Dual Luciferase Reporter Assay system (Promega). Luciferase activities were evaluated as ratio of (CAGA)12-MLP-luciferase vs Renilla luciferase levels for 3 different experiments, each carried out in triplicate.

### *Immuno-histochemical analysis*

Formalin-fixed, paraffin embedded intestinal polyps were prepared as 4  $\mu\text{m}$  sections and immunostained with the mouse Smad4 B-8; sc-7966 monoclonal antibody directed against Smad4 (Santa Cruz Biotechnology Inc., dilution 1:100). After antigen retrieval treatment (10 min boiling in Tris-EDTA pH 8.0), endogenous peroxidases were inactivated by 1% H<sub>2</sub>O<sub>2</sub>/PBS. A 30 min. pre-incubation step in 5% non-fat dry milk in PBS, was followed by incubation with the Smad4 antibody overnight at 4°C in pre-incubation buffer. Sections were then incubated and stained with the Envision HRP-ChemMate kit (DAKO). Smad4 IHC staining was evaluated after brief hematoxylin counterstaining of the slides.

#### *Expression profiling analysis*

Total RNA was isolated using the RNeasy Midi Kit (QIAGEN) by lysing the ES cells directly in culture dishes; an extra DNase step on the column was performed according to manufacturer's instructions. RNA was labelled using the GeneChip One-Cycle Target Labeling and Control Reagents kit, and hybridized to the MOE430 2.0 Affymetrix oligonucleotide arrays, a comprehensive whole mouse genome expression platform encompassing more than 39,000 transcripts, according to manufacturer's instructions. Raw signal intensities were extracted and summarized from cel-files, followed by normalization using RMA (Robust Multi-Array Average expression measure) implemented in the Bioconductor package affyLmGUI (Wettenhall & Smyth, 2004). No filtering was applied to the data. A Bayesian linear regression model was used to detect differentially expressed genes implemented in the Bioconductor package LIMMA (Smyth, 2004; Smyth, 2005). All Bioconductor packages were used with R statistical Computing Software v2.2.1 (Team, 2005).

#### *Quantitative real-time RT-PCR analysis*

Total RNA was extracted from laser-capture microdissected tissues by using the RNeasy Micro Kit (Qiagen). cDNA was synthesized by SuperScript™ II Reverse Transcriptase (Invitrogen) with the Oligo(dT)<sub>20</sub> primer (Invitrogen). Each PCR was carried out in triplicates in 25  $\mu\text{l}$  volumes using 1  $\mu\text{l}$  of cDNA and SYBR® Green Dye (Applied Biosystems) on the MyiQ Single-Color Real-Time PCR Detection System (Bio-Rad). Primers sequences are listed in Supplementary Table 1. Standard curves for the target genes and the reference *CryzII* gene were generated and the normalization and ratio were calculated as described (Pfaffl, 2001).

## Acknowledgements

We thank Prof. Dr. Peter ten Dijke for providing us the plasmids used in the experiments and Dr. Hang Le for her assistance with the western analysis. These studies were supported by grants from the Maag lever Daarm Stichting (MLDS), the Dutch Research Council (NWO/Vici 016.036.636), and the BSIK program of the Dutch Government grant 03038.

## References

- Alberici, P., de Pater, E., Cardoso, J., Bevelander, M., Molenaar, L., Jonkers, J. & Fodde, R. (2007). *Am J Pathol*, **170**, 377-87.
- Alberici, P., Jagmohan-Changur, S., De Pater, E., Van Der Valk, M., Smits, R., Hohenstein, P. & Fodde, R. (2006). *Oncogene*, **25**, 1841-51.
- Alhopuro, P., Alazzouzi, H., Sammalkorpi, H., Davalos, V., Salovaara, R., Hemminki, A., Jarvinen, H., Mecklin, J.P., Schwartz, S., Jr., Aaltonen, L.A. & Arango, D. (2005). *Clin Cancer Res*, **11**, 6311-6.
- Ando, T., Sugai, T., Habano, W., Jiao, Y.F. & Suzuki, K. (2005). *J Gastroenterol*, **40**, 708-15.
- Arnold, K., Kim, M.K., Frerk, K., Edler, L., Savelyeva, L., Schmezer, P. & Wiedemeyer, R. (2006). *Cancer Lett*, **243**, 90-100.
- Bierie, B. & Moses, H.L. (2006). *Nat Rev Cancer*, **6**, 506-20.
- Buckhaults, P., Rago, C., St Croix, B., Romans, K.E., Saha, S., Zhang, L., Vogelstein, B. & Kinzler, K.W. (2001). *Cancer Res*, **61**, 6996-7001.
- Cook, D.L., Gerber, A.N. & Tapscott, S.J. (1998). *Proc Natl Acad Sci U S A*, **95**, 15641-6.
- Dennler, S., Itoh, S., Vivien, D., ten Dijke, P., Huet, S. & Gauthier, J.M. (1998). *Embo J*, **17**, 3091-100.
- Duff, E.K. & Clarke, A.R. (1998). *Br J Cancer*, **78**, 1615-9.
- Fodde, R. & Smits, R. (2002). *Science*, **298**, 761-3.
- French, J.E., Lacks, G.D., Trempus, C., Dunnick, J.K., Foley, J., Mahler, J., Tice, R.R. & Tennant, R.W. (2001). *Carcinogenesis*, **22**, 99-106.
- Goss, K.H., Risinger, M.A., Kordich, J.J., Sanz, M.M., Straughen, J.E., Slovek, L.E., Capobianco, A.J., German, J., Boivin, G.P. & Groden, J. (2002). *Science*, **297**, 2051-3.
- Hadzija, M.P., Radošević, S., Kovacević, D., Lukac, J., Hadzija, M., Spaventi, R., Pavelić, K. & Kapitanović, S. (2004). *Mutat Res*, **548**, 61-73.
- Heldin, C.H., Miyazono, K. & ten Dijke, P. (1997). *Nature*, **390**, 465-71.
- Hohenstein, P., Molenaar, L., Elsinga, J., Morreau, H., van der Klift, H., Struijk, A., Jagmohan-Changur, S., Smits, R., van Kranen, H., van Ommen, G.J., Cornelisse, C., Devilee, P. & Fodde, R. (2003). *Genes Chromosomes Cancer*, **36**, 273-82.
- Howe, J.R., Roth, S., Ringold, J.C., Summers, R.W., Jarvinen, H.J., Sistonen, P., Tomlinson, I.P., Houlston, R.S., Bevan, S., Mitros, F.A., Stone, E.M. & Aaltonen, L.A. (1998). *Science*, **280**, 1086-8.
- Kim, B.G., Li, C., Qiao, W., Mamura, M., Kasprzak, B., Anver, M., Wolfrim, L., Hong, S., Mushinski, E., Potter, M., Kim, S.J., Fu, X.Y., Deng, C. & Letterio, J.J. (2006). *Nature*, **441**, 1015-9.
- Knudson, A.G., Jr. (1971). *Proc Natl Acad Sci U S A*, **68**, 820-3.
- Korchynskyi, O. & ten Dijke, P. (2002). *J Biol Chem*, **277**, 4883-91.

- Kwabi-Addo, B., Giri, D., Schmidt, K., Podsypanina, K., Parsons, R., Greenberg, N. & Ittmann, M. (2001). *Proc Natl Acad Sci U S A*, **98**, 11563-8.
- Liu, W., Dong, X., Mai, M., Seelan, R.S., Taniguchi, K., Krishnadath, K.K., Halling, K.C., Cunningham, J.M., Qian, C., Christensen, E., Roche, P.C., Smith, D.I. & Thibodeau, S.N. (2000). *Nat Genet*, **26**, 146-7.
- Lu, S., Shen, K., Wang, Y., Santner, S.J., Chen, J., Brooks, S.C. & Wang, Y.A. (2006). *Carcinogenesis*, **27**, 848-55.
- Magee, J.A., Abdulkadir, S.A. & Milbrandt, J. (2003). *Cancer Cell*, **3**, 273-83.
- Mamot, C., Mild, G., Reuter, J., Laffer, U., Metzger, U., Terracciano, L., Boulay, J.L., Herrmann, R. & Rochlitz, C. (2003). *Br J Cancer*, **88**, 420-3.
- Matisse M.P., A.W., and Joyner A.L. (2000). *Gene Targeting, A Practical Approach*. A.L.Joyner (ed.). Oxford University Press: Oxford, pp 129-131.
- Millar, S.E. (2006). *Dev Cell*, **11**, 274-6.
- Miyoshi, H., Nakau, M., Ishikawa, T.O., Seldin, M.F., Oshima, M. & Taketo, M.M. (2002). *Cancer Res*, **62**, 2261-6.
- Momand, J., Zambetti, G.P., Olson, D.C., George, D. & Levine, A.J. (1992). *Cell*, **69**, 1237-45.
- Nakao, A., Imamura, T., Souchelnytskyi, S., Kawabata, M., Ishisaki, A., Oeda, E., Tamaki, K., Hanai, J., Heldin, C.H., Miyazono, K. & ten Dijke, P. (1997). *Embo J*, **16**, 5353-62.
- Payne, S.R. & Kemp, C.J. (2005). *Carcinogenesis*, **26**, 2031-45.
- Pfaffl, M.W. (2001). *Nucleic Acids Res*, **29**, e45.
- Roth, S., Sistonen, P., Salovaara, R., Hemminki, A., Loukola, A., Johansson, M., Avizienyte, E., Cleary, K.A., Lynch, P., Amos, C.I., Kristo, P., Mecklin, J.P., Kellokumpu, I., Jarvinen, H. & Aaltonen, L.A. (1999). *Genes Chromosomes Cancer*, **26**, 54-61.
- Salovaara, R., Roth, S., Loukola, A., Launonen, V., Sistonen, P., Avizienyte, E., Kristo, P., Jarvinen, H., Souchelnytskyi, S., Sarlomo-Rikala, M. & Aaltonen, L.A. (2002). *Gut*, **51**, 56-9.
- Santarosa, M. & Ashworth, A. (2004). *Biochim Biophys Acta*, **1654**, 105-22.
- Sdek, P., Ying, H., Chang, D.L., Qiu, W., Zheng, H., Toutou, R., Allday, M.J. & Xiao, Z.X. (2005). *Mol Cell*, **20**, 699-708.
- Smyth, G.K. (2004). *Stat Appl Genet Mol Biol*, **3**, Article3.
- Smyth, G.K. (2005). *Bioinformatics and Computational Biology Solutions using R and Bioconductor*. R. Gentleman, V. C., S. Dudoit, R. Irizarry, W. Huber (ed.). Springer: New York, pp 397-420.
- Team, R.D.C. *R: A language and environment for statistical computing*. R Foundation for Statistical Computing: Vienna.
- Tomii, K., Tsukuda, K., Toyooka, S., Dote, H., Hanafusa, T., Asano, H., Naitou, M., Doihara, H., Kisimoto, T., Katayama, H., Pass, H.I., Date, H. & Shimizu, N. (2007). *Int J Cancer*, **120**, 566-73.
- Wettenhall, J.M. & Smyth, G.K. (2004). *Bioinformatics*, **20**, 3705-6.
- Wilentz, R.E., Iacobuzio-Donahue, C.A., Argani, P., McCarthy, D.M., Parsons, J.L., Yeo, C.J., Kern, S.E. & Hruban, R.H. (2000a). *Cancer Res*, **60**, 2002-6.
- Wilentz, R.E., Su, G.H., Dai, J.L., Sparks, A.B., Argani, P., Sohn, T.A., Yeo, C.J., Kern, S.E. & Hruban, R.H. (2000b). *Am J Pathol*, **156**, 37-43.
- Woodford-Richens, K., Williamson, J., Bevan, S., Young, J., Leggett, B., Frayling, I., Thway, Y., Hodgson, S., Kim, J.C., Iwama, T., Novelli, M., Sheer, D., Poulson, R., Wright, N., Houlston, R. & Tomlinson, I. (2000). *Cancer Res*, **60**, 2477-82.

- Wrana, J.L., Attisano, L., Carcamo, J., Zentella, A., Doody, J., Laiho, M., Wang, X.F. & Massague, J. (1992). *Cell*, **71**, 1003-14.
- Xi, Y., Nakajima, G., Hamil, T., Fodstad, O., Riker, A. & Ju, J. (2006). *Mol Cancer Ther*, **5**, 3078-84.
- Xiao, Z.X., Chen, J., Levine, A.J., Modjtahedi, N., Xing, J., Sellers, W.R. & Livingston, D.M. (1995). *Nature*, **375**, 694-8.
- Xu, X., Brodie, S.G., Yang, X., Im, Y.H., Parks, W.T., Chen, L., Zhou, Y.X., Weinstein, M., Kim, S.J. & Deng, C.X. (2000). *Oncogene*, **19**, 1868-74.

---

## **Chapter 6.**

### **Discussion**



### **6.1. CIN in the adenoma-carcinoma sequence**

The debate around the role of chromosomal instability (CIN) in cancer onset and/or progression has been going on for decades. In the most simplistic scenario, mutations leading to CIN are selected for in tumor cells because aneuploidy enhances the rate of LOH at tumor suppressor genes and upregulates oncogenes by allelic gains. However, excessive DNA damage resulting from increased genomic instability does not represent a direct growth advantage as it is deleterious for the individual cell and it is rather likely to decrease its fitness compared with cells with intact genome surveillance through activation of programmed cell death (apoptosis). Only 'just-right' levels of chromosomal instability will allow the tumor cells to acquire the gene mutations necessary to overcome the natural selection barriers (see Fig.1).

The origin of CIN and its role in tumor initiation or progression are still controversial issues in cancer research (Rajagopalan & Lengauer, 2004). However, two more recent lines of evidences clearly indicate that CIN is likely to represent a very early event along the adenoma-carcinoma sequence in colorectal cancer: 1. the notion that loss of APC function results in mitotic defects and in chromosomal instability (Fodde et al., 2001; Kaplan et al., 2001); and 2. the observation according to which aneuploidy occurs at very early stages in colorectal cancer development in man (Giaretti, 1994; Bardi et al., 1997; Shih et al., 2001; Cardoso et al., 2006). In Chapter 3 of this thesis, we established that in *Apc*-mutant mouse models for intestinal tumorigenesis aneuploidy is also observed at very early adenoma stages (Alberici et al., 2007). The assessment of chromosomal instability by a quantitative assay such as BAC array-CGH demonstrated not only that even initial intestinal lesions, namely small low dysplastic adenomas, already present characteristic features of CIN with frequent chromosomal gains and losses, but also that all of the early adenoma from *Apc*<sup>+1638N</sup> animals were invariably aneuploid. These data, obtained from *Apc*-mutant mouse models and from FAP patients carrying germline *APC* mutations clearly point to a central role of the *APC* tumor suppressor not only in regulating Wnt/ $\beta$ -catenin signaling, but also in chromosomal segregation at mitosis. In fact, it is now known that APC localizes at and takes part in several

structural complexes and pathways involved in mitosis (i.e. kinetochore, microtubules, centrosomes and spindle checkpoints) that are also implicated in the origin of both numerical and structural chromosomal defects (Introduction, paragraph 1.4).

To date, considerable experimental evidence proving the causative role of APC in mitotic defects and chromosomal instability have been published (Fodde et al., 2001; Kaplan et al., 2001; Green & Kaplan, 2003; Dikovskaya et al., 2004). More recently, by means of RNA interference, Draviam and colleagues (Draviam et al., 2006) demonstrated that *APC* knockdown results in defects in movement and orientation of sister chromatids at the metaphase plate. Moreover, these defects lead to a low though significant level of chromosome missegregation accompanied by chromosome loss during anaphase.

Chromosomal instability in CRC tumors is likely to confer the neoplastic cell with random somatic mutations from which those providing growth advantages will be selected. In yeast, more than 100 genes involved in mitotic spindle assembly and dynamics, chromosome metabolism, cell-cycle regulation, and checkpoint control has been proved to cause chromosomal instability (Spencer et al., 1990). In the majority of the cases, the human homologues of these genes has been characterized, though only a few mutations have been found in tumors so far (Cahill et al., 1998; Shichiri et al., 2000; Imai et al., 1999; Rajagopalan et al., 2004). One could argue that mutations in these 'genome integrity' genes would result in excessive genetic instability and apoptosis. *APC* mutations instead, possibly together with other mutations that drive "mild" mitosis defects (see Introduction), could confer the "just-right" type of CIN able to escape the checkpoint surveillance machinery, as it has been recently demonstrated (Draviam et al., 2006).

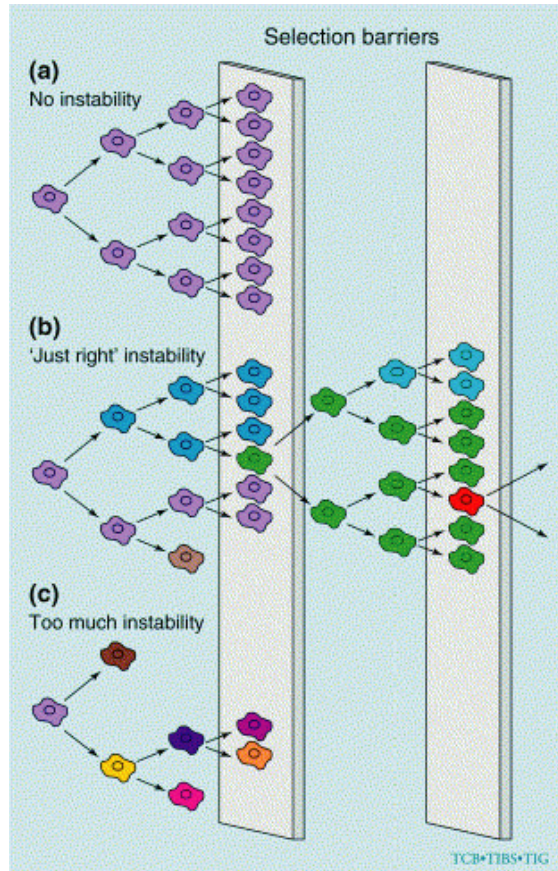


**Figure 1.** Overcoming selection barriers during tumor formation and progression. In normal cells (a), the intrinsic rate of instability is low. As none of the cells contains the genetic alteration required to overcome the selection barriers, tumour formation is prevented. Tumour cell precursors (b), are characterized by an increased level of genetic instability. In this case, the broad cellular heterogeneity virtually guarantees that at least one of the cells contains the requisite genetic alteration to overcome the selection barrier and proceed in tumour progression. If the level of genetic instability is too high (c), the damage accumulated from cell division rapidly rises above the threshold for viability – apoptotic pathways are activated and cell death ensues. At the level of the cellular population, this leads to extinction. Not enough cells reach the first selection barrier to select a malignant clone effectively.

Reprinted from "Genetic instability and darwinian selection" Trends in Cell Biology Vol 9 (Dec 12) 1999 Cahill DP, Kinzler KW, Vogelstein with permission from Elsevier.

## **6.2. Accommodating haploinsufficiency of tumor suppressor genes in the adenoma-carcinoma sequence**

The classical mechanism that explains how loss of a tumor suppressor gene leads to tumor formation is represented by Knudson's "two hits hypothesis" (Knudson, 1971). Using a mathematical model of cancer incidence in hereditary and sporadic retinoblastoma, Alfred Knudson postulated that in somatic cells two mutations at a putative recessive cancer predisposition locus are necessary to trigger tumorigenesis. This model was proven in 1996 when, after the cloning of the *RB* tumor suppressor gene, loss of heterozygosity (LOH) and mutation analysis revealed biallelic inactivation of this gene in retinoblastoma (Friend et al., 1986). Hence, tumor suppressor genes are recessive at cellular level and require complete (i.e. biallelic) loss of function in order to manifest the neoplastic phenotype.

In general, gene expression levels in diploid organism reflect the combined transcription of both alleles even though for many genes a single functional allele is sufficient to maintain normal protein synthesis and activity. Recently however, experiments performed in our and other laboratories contributed to clarify that specific tumor suppressor genes encodes for proteins whose function is dependent on dosage levels and where monoallelic inactivation may already exert phenotypic consequences. To date, several studies have shown that mutation or loss of a single allele is sufficient to reduce protein dosage and subsequently alter the cellular phenotype (Payne & Kemp, 2005) (see also Chapters 4 and 5). This gene dosage effect is often referred to as haploinsufficiency. Haploinsufficiency at a tumor suppressor locus may overcome the need for a somatic hit at the wild type allele as a rate-limiting event for tumor development.

Despite the concept of haploinsufficiency has been known already for several decades from classic *Drosophila* genetic studies, only with the recent availability of mouse models carrying targeted gene defects and technologies able to measure subtle but consistent variation in gene/protein expression levels, it was possible to deliver experimental evidences for the effects of mono-allelic mutations on tissue homeostasis. The first experimental evidence supporting a role for haploinsufficiency in tumorigenesis came from the analysis of the *p27* gene in

human neoplasia and knockout mice (Pietenpol et al., 1995; Nakayama et al., 1996; Kiyokawa et al., 1996). Tissues from p27<sup>+/-</sup> mice express approx. 50% of this cyclin-dependent kinase inhibitor involved in the regulation of cell cycle. Heterozygous mice show an intermediate tumor phenotype between wild type and p27<sup>-/-</sup> animals when challenged with 1,2-dimethylhydrazine, an agent that induces adenomas and adenocarcinomas in the colon (Philipp-Staheli et al., 2002). More importantly, heterozygous animals retain the expression of the wild-type allele in the corresponding colorectal tumors, thus in apparent contradiction with the "two hits" model. This evidence, in combination with the fact that the reduction of p27Kip1 expression is frequently observed in human colorectal cancer often in correlation with poor prognosis (reviewed in Hershko & Shapira, 2006), suggests that haploinsufficiency of specific tumor suppressor genes may exert a modifying effect on gastrointestinal (GI) tumors onset and progression. Since this observation, several studies have shown haploinsufficiency at genes known to be involved in gastrointestinal tumorigenesis, as summarized in Table 1. In fact, the availability of specific heterozygous mouse models in inbred genetic background to examine the different stages of intestinal carcinogenesis, allows to test the contribution of different dosage of tumor suppressor genes to tumor development and progression.

In Chapter 4 and 5, we have examined the mechanisms and consequences of *Smad4* haploinsufficiency in intestinal tumorigenesis. Previous evidence for a role of *SMAD4* haploinsufficiency in altering intestinal homeostasis was provided by the observation that gastrointestinal hamartomas from patients affected by juvenile polyposis syndrome (JPS) and carrying germline *SMAD4* mutations, almost invariably retain the wild type allele (Howe et al., 1998). Our *SMAD4* IHC analysis of JPS polyps from *SMAD4* mutation carriers and of GI tumors from *Smad4*<sup>+/-</sup> mutant mice has provided further evidence for *SMAD4* haploinsufficiency during the initial stages of tumor formation (Alberici et al., 2006; Alberici et al. 2007, *submitted*).

The possibility that loss of expression of a single *SMAD4* allele characterizes a distinct subset of CRC patients might have important clinical consequences.

Gene	Function	Human cancer association	Haploinsufficient phenotype
<i>RAD51B</i>	Homologous recombination, double-strand breaks (DSB) repair	Risk modifier in BRCA2 carriers	Chromosome fragmentation and increase aneuploidy in HCT116 CRC cell line (Date et al., 2006)
<i>APC</i>	Wnt signal transduction; mitotic spindle	Familial Adenomatous Polyposis; sporadic colorectal cancer	Responsible for a fraction of FAP patients without truncating <i>APC</i> (Sieber et al., 2002) (Yan et al., 2002) (Venuesio et al., 2003)
<i>FEN1</i>	Endonuclease involved in DNA replication and repair	To date, rarely mutated in sporadic cancer	Increase number of adenoma and carcinoma in <i>Apc<sup>+/+</sup>/Fen<sup>-/-</sup></i> mice compared with <i>Apc<sup>+/+</sup>/Fen<sup>+/-</sup></i> animals (Kucherlapati et al., 2002)
<i>MSH2</i>	DNA mismatch repair	Mutated both in hereditary and sporadic CRC with microsatellite instability (Fishel et al., 1993)	Increase of frameshift mutations in mouse colon (Zhang et al., 2002) Reduced induction of sister-chromatid exchanges (SCEs) by methyl nitrosourea (MNU) in mouse (Bouffler et al., 2000)
<i>BLM</i>	RecQ DNA elicase, DNA repair	Bloom Syndrome	Enhanced tumor formation in <i>Bml<sup>-/-</sup></i> mice (Goss et al., 2002)
<i>CDH1</i>	Cell-cell adhesion	Mutation in many carcinoma (Hajra & Fearon, 2002) and in CRC (Kanazawa et al., 2002)	Increased tumor formation in <i>Apc<sup>+/+</sup>/Ecad<sup>-/-</sup></i> mice compared with <i>Apc<sup>+/+</sup>/Ecad<sup>+/-</sup></i> animals (Smits et al., 2000)
<i>PTEN</i>	Phosphatase involved in signal transduction	Harmatomatous syndromes (e.s. Cowden syndrome), multiple sporadic cancer types (Simpson & Parsons, 2001), colon cancer (Liu et al., 2004)	<i>PTEN<sup>-/-</sup></i> induces increase of prostate adenocarcinoma and PIN in a transgenic adenocarcinoma of mouse prostate (TRAMP) mice (Kwabi-Addo et al., 2001)
<i>LKB1</i>	Protein Kinase	Peutz-Jeghers syndrome, mutated in lung, pancreatic and biliary cancer. Allelic loss at the LKB1 locus relatively frequently in sporadic colon cancers (Forster et al., 2000)	Spontaneous gastric and intestinal adenomas in <i>LKB1<sup>+/-</sup></i> mouse (Miyoshi et al., 2002)
<i>APAF-1</i>	Mitochondrial apoptotic pathway	B-CLL (Sturm et al., 2006), glioblastoma, melanoma, and CRC (Yamamoto et al., 2000)	Allelic imbalance of APAF-1 locus at 12q23 is associated with progression of colorectal carcinoma (Umetani et al., 2004)

**Table1.** List of haploinsufficient genes implicate in gastrointestinal tumor formation

It has been previously shown that loss of SMAD4 expression in CRC associates with poor prognosis (Alhopuro et al., 2005). Reduced tumor SMAD4 protein levels were associated with significant decrease in disease-free and overall survival after potentially curative surgery in Dukes C colorectal cancer patients. Also, SMAD4 mRNA levels predict treatment response in Dukes C patients. Accordingly, SMAD4 mRNA and protein levels were found to further decrease in lymph node metastases when compared to primary tumors.

Mathematical modeling of the effects of gene dosage reduction from diploidy to haploidy indicates that haploinsufficiency phenotypes might result from stochastic fluctuations in gene and protein expression below a critical functional threshold (Cook et al., 1998), as illustrated in Fig.2. In this model, the steady-state gene product levels fluctuate around a mean. In case of haploid gene expression, this mean is 50% of the diploid state. However, transient fluctuations below the 50% level could reach a critical threshold and eventually result in null-like phenotypes for the gene in question and the pathway it regulates.

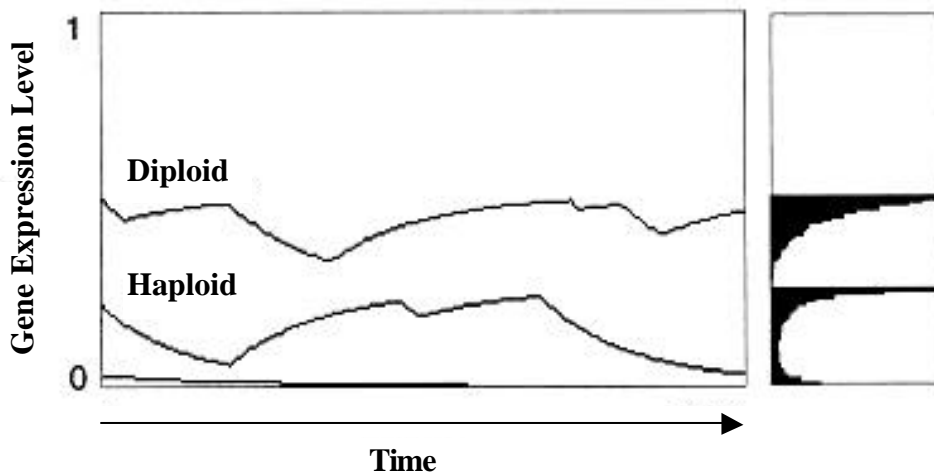


**Figure 2.** Model of the variance in gene expression between a diploid and a haploid cell for a specific allele. In this stochastic model there is more variance in the haploid than in the diploid system, thus in the haploid system the level of gene expression gene may approach 10% of the wild-type. Adapted from (Cook et al., 1998). Copyright (1998) National Academy of Sciences, U.S.A; reprint with permission.

Activity, concentration and spatial role distribution of a protein within a specific tissue context are also likely to play key roles in determining the haploinsufficient phenotype. Indeed, signaling proteins like SMAD4 and  $\beta$ -catenin are known to be expressed as a gradient along the crypt-villus axis in the intestinal epithelium (Salovaara et al., 2002 ; Batlle et al., 2002).

In Chapter 5, the identification by expression profiling of genes whose expression in ES cells and in gastrointestinal tissue is altered in response to *SMAD4* haploinsufficiency, indicates how gene dosage imbalances may alter cellular homeostasis and predispose to GI neoplasia.

As indicated by the experimental results presented in Chapter 5, it is plausible to postulate that *Smad4* haploinsufficiency triggers intestinal polyp formation by inhibition of TGF- $\beta$  /BMP signaling and their downstream effectors, thus affecting cell proliferation rates and apoptosis, but also through a number of more indirect and/or independent downstream targets (Table 1, Chapter 5). Hence, a broad spectrum of cellular functions may be affected which include apoptosis (through decrease of p53 activity by *Mdm2* upregulation), cell cycle and adhesion (possibly through Wnt signaling activation by *Smad7* and *Axin2* downregulation), immune response (upregulation of TNF activity), and possibly many others, as illustrated in Figure 3.

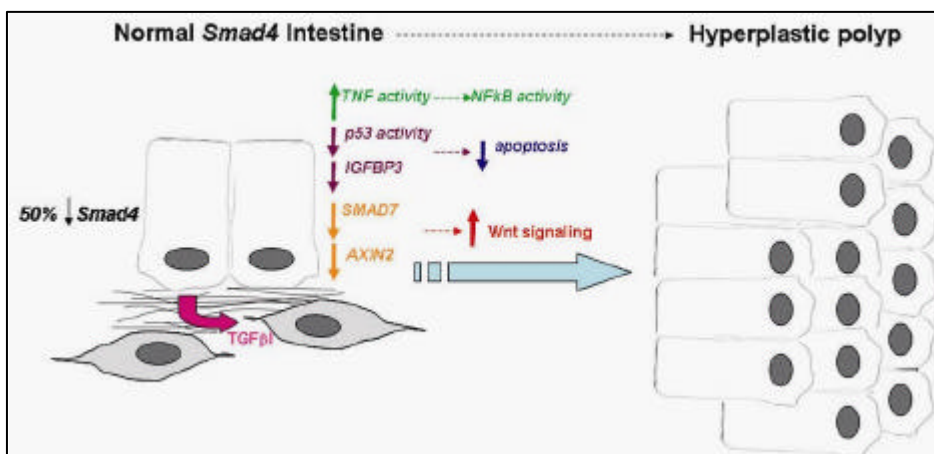


**Figure 3.** Hypothetical model for the molecular and cellular consequences of *Smad4* haploinsufficiency on intestinal homeostasis and cancer onset.

It is interesting to note that in some cases gene dosage defects manifests exclusively in a context where other genetic alterations are already present. This “compound haploinsufficiency” effect has been proven by breeding mouse models carrying targeted mutations in genes such as *Blm* and *E-Cadherin* with *Apc*-mutant animals already known for their predisposition to GI tumorigenesis (Goss et al., 2002; Smits et al., 2000). Whereas in the latter model tumor onset is invariably accompanied by LOH at the wild type *Apc* allele, its characteristic tumor multiplicity and progression rates are affected by the *Blm*<sup>+/-</sup> and *E-Cadherin*<sup>+/-</sup> genetic background without additional somatic hits. These results suggest that compound haploinsufficiency at specific gene loci, either germline or somatic, may modify the individual’s predisposition to tumor formation by more subtle effects on the expression of downstream targets involved in signaling networks and genome stability.

To date, given the present knowledge and experimental evidence, we cannot rule out a role for haploinsufficiency at the *APC* gene. In fact, Yan and co-authors (Yan et al., 2002), by employing a highly quantitative method, challenged the concept that a modest decrease of *APC* tumor suppressor gene expression, even below the 50% reduction that results from heterozygosity for a null allele, may result in the development of attenuated forms of polyposis. Similar conclusions were reported in an independent study where low *APC* mRNA expression levels were observed in patients with mild FAP phenotype (Venesio et al., 2003).

In a study performed by D’Abaco and colleagues (D’Abaco et al., 1996), normal colonic epithelial cell lines established from the Immorto-*Apc*<sup>+/*Min*</sup> model and transfected *in vitro* with the *H-Ras* oncogene show the typical spindle-shaped appearance of transformed cells and develop tumors in immune-deficient recipient mice when compared to the parental line. Notably, these cells retain the wild type *Apc* allele. These experiments not only confirm a synergism between *Apc* and *Ras* in tumorigenesis (see also Chapter 2 and the next paragraph) but also demonstrate how tumorigenesis might proceed without loss or mutation of the wild-type *Apc* allele.

Heterozygosity for mutations and/or polymorphisms at disease-causing or susceptibility genes are detected in many CRC tumors, as shown for instance by many LOH studies. As discussed above, these defects are likely to contribute to the progression of colorectal cancer simply by reducing expression levels of the corresponding proteins.

### **6.3. Signal transductions cross talk**

In Chapter 2 and 4 of this thesis experiments are described where different mouse models characterized by defects in key elements of pathways involved in the homeostasis of normal intestinal epithelia are interbred. The purpose of these studies was to measure the effects that these interactions, which mimic the genetic alterations most frequently observed along the adenoma-carcinoma sequence, may exert at the phenotypic and molecular level in the gastrointestinal tract. Four possible outcomes might be expected when comparing the compound animals with their single mutant counterparts: no effect, antagonism, a cumulative effect, or synergisms. In the specific case of the combinations of *Apc* mutations with defects in the *KRAS* and *Smad4* genes, the analysis revealed that compound animals were affected by dramatic enhancement of the tumor phenotype when compared with the *Apc*-only mutant mice.

The main challenge is then represented by the elucidation of the cumulative or synergistic nature of these interactions at the molecular level. The latter is often a daunting task as different signal transduction pathways known to regulate homeostasis in normal intestinal epithelial cells may interact and cross talk at different levels. In order to dissect and elucidate the nature of these biochemical and genetic interactions we made use of embryonic stem (ES) cells that recapitulate the genetic defects in the compound transgenic mice. These isogenic cell lines allowed us to perform accurate signalling measurements by reporter assays. Next, transcriptome and immunohistochemistry (IHC) analysis of intestinal tumors and ES cells were performed to validate the putative involvement of specific members of the Wnt, Ras and TGF- $\beta$  signalling cascades and their cross talk.

Cross talk between RAS/RTKs and Wnt signaling

Ras proteins play a direct causal role in human cancer as shown by the occurrence of *H*-, *N*-, and *KRAS* mutations at varying frequencies in different tumor types (Bos, 1988). In colorectal cancer, nuclear accumulation of  $\beta$ -catenin, the hallmark of Wnt signaling activation, and oncogene *KRAS* activation characterize the majority of the cases. Moreover, the concomitant activation of these two pathways identify a subset of patients with poor prognosis (Zhang et al., 2003). By generating the compound *Apc/KRAS* mouse model as described in Chapter 2, we succeeded in recapitulating the molecular events underlying malignant transformation characteristic in this subset of CRC patients. These mice are characterized by increased intestinal tumor multiplicity and progression, with early morbidity and mortality (Janssen et al., 2006). Recently, Andrew Clark and colleagues obtained similar results by employing different *Apc* and *Kras* mutant alleles (Sansom et al., 2006). Also, it has been previously demonstrated that primary intestinal cells with compound heterozygous *Apc*<sup>Min</sup>/*Ras* mutations grow *in vitro* under both permissive and non-permissive conditions, and are able to form tumors when transplanted in immune-deficient recipient mice (D'Abaco et al., 1996). These data elegantly demonstrate that a single defective *Apc* allele and an activated *Ras* gene are sufficient to elicit malignant transformation of normal colonic epithelial cells.

Hence, there is ample *in vitro* and *in vivo* experimental evidence that the combination of gain and loss of function mutations at the *KRAS* oncogene and *APC* tumor suppressor gene respectively, underlie tumor onset and progression towards malignancy in the GI tract. However, the question still remains whether these marked cellular and phenotypic effects are the results of a cumulative (i.e. additive) or synergistic (i.e. cross-talk) interaction between the Wnt and RAS signalling pathway. Beside its known signalling role through the RAF-MAPK pathway in inhibiting apoptosis and promoting cell cycle and growth (Kerkhoff & Rapp, 1998), RAS exerts other effects possibly related to the acquisition of the transformed phenotype. Cell-cell adhesion and cytoskeleton interactions are modified upon *RAS* oncogenic transformation *in vitro* and this effect has been proved to be caused by a decreased interaction between  $\beta$ -catenin and E-cadherin at the adhesion junction (Kinch et al., 1995). Moreover, loss of  $\beta$ -catenin/E-

cadherin colocalization at the cell membrane has been associated with the development of metastatic cancers (Daniel & Reynolds, 1997). Accordingly, we evaluated the interaction between  $\beta$ -catenin and E-cadherin by *in vitro* and *in vivo* assays and observed a decrease in E-cadherin-bound  $\beta$ -catenin levels in compound *KRAS/Apc* tumor cells when compared to single mutant controls (Janssen et al., 2006). Upon RAS activation, intracellular tyrosine kinase activity is increased leading to Tyr-phosphorylation of many target proteins among which  $\beta$ -catenin (Kinch et al., 1995). In particular,  $\beta$ -catenin tyrosine phosphorylation at residue 654 has been shown to cause the dislocation of  $\beta$ -catenin from E-cadherin (Roura et al., 1999), while the inhibition of tyrosine kinase activity abolish this effect with restoration of  $\beta$ -catenin/E-cadherin colocalization at the cell membrane (Kinch et al., 1995). Upstream of RAS, activation of receptor tyrosine kinases (RTKs) such as EGFR (epidermal growth factor receptor) and HGF/SF (hepatocyte growth factor; scatter factor) receptor, has been shown to induce scattering of human cancer cells via tyrosine phosphorylation of  $\beta$ -catenin (Shibamoto et al., 1994). It has been proposed that Src might represent the main tyrosine kinase directly responsible for  $\beta$ -catenin phosphorylation (Roura et al., 1999). However, it is plausible that additional RAS-activated protein kinases contribute to the sub-cellular compartmentalization of  $\beta$ -catenin through its phosphorylation at specific Tyr residues.

Activation of RAS and RTKs may regulate  $\beta$ -catenin function and activity by two distinct mechanisms. First, Ras/RTK-mediated  $\beta$ -catenin Tyr-phosphorylation results in loss of cell-cell adhesion by disturbing the functionality of the adherens junction functionality through E-cadherin destabilization and loss of contact with the actin cytoskeleton (Daniel & Reynolds, 1997). These effects on cell-cell adhesion underlie epithelial to mesenchymal transitions (EMT) and are known to contribute to local invasion and distant cancer metastasis. A second outcome of Ras/RTK-dependent  $\beta$ -catenin phosphorylation is represented by the increase of  $\beta$ -catenin signaling pool in the cytoplasm. The release of Tyr-P  $\beta$ -catenin from E-cadherin at the adherens junctions is likely to result in its intracellular accumulation and increased Wnt signal transduction activity to the nucleus where  $\beta$ -catenin binds

TCF/LEF1 transcription factors thus modulating the expression of Wnt target genes.

Notably, the Ras/RTK-mediated effects on  $\beta$ -catenin signaling and cell adhesion function appear necessary for malignant transformation in the context of loss of APC function. However, they are insufficient to efficiently initiate tumorigenesis in the intestine in the presence of functional APC. Single *villin-KRas* transgenic mice occasionally develop few intestinal tumors at over 1 year of age, thus only after a long latency that allows the acquisition of somatic synergistic p53 mutations. Moreover, the exclusive presence of *KRAS* mutations in human ACF does not confer dysplastic characteristics and the lesions appear to be quiescent when compared to those encompassing both *APC* and *KRAS* defects (Jen et al., 1994). Therefore, it appears that loss of *APC* function is the rate-limiting event for tumor initiation through the constitutive activation of Wnt/ $\beta$ -catenin signaling. However, this is necessary but insufficient for full-blown  $\beta$ -catenin nuclear translocation and further enhancement of Wnt signaling activity is necessary for tumor progression towards malignant transformation. The latter is achieved upon *KRAS*/RTK-driven tyrosine phosphorylation of  $\beta$ -catenin and the consequent increase of its signaling pool. The effects of this increase of the transcriptional activity of  $\beta$ -catenin only become noticeable in the context of loss of *APC* function, i.e. upon loss of proper  $\beta$ -catenin regulation by the destruction complex.

The cross-talk between the RAS-RAF-MAPK and Wnt signalling cascades is likely to occur at different levels. For example, both pathways modulate expression levels, protein activity and stability of cyclin D1 and cMyc, together with other important factors implicated in the regulation of cell cycle progression (He et al., 1998; Tetsu & McCormick, 1999; Sears et al., 1999). The Wnt/RAS cooperation also operates on the activity of another member of the destruction complex, namely the Ser-Thr protein kinase GSK-3 $\beta$ . Oncogene RAS activation can inhibit GSK-3 $\beta$  kinase activity thus further contributing to the deregulation of intracellular  $\beta$ -catenin levels (Li et al., 2005).

Angiogenesis has also been shown to be stimulated in a synergistic fashion by Wnt and RAS signaling. Proficient vascularization is a key factor for tumor growth and Vascular Endothelial Growth Factor (VEGF) represents the main agent to positively

regulate neo-vascularization. Zhang and co-authors (Zhang et al., 2001) showed that not only VEGF represent a downstream target of Wnt signaling, but also that the concomitant presence of oncogenic *KRAS* mutations further increase the transcription of this very growth factor.

In conclusion, the coordinated pattern of synergistic gene regulation between Wnt and Ras signal transduction is likely to affect a broad spectrum of genes with distinct roles the pathogenesis of colon cancer.

#### *Cross talk between TGF- $\beta$ and WNT signaling*

Recently, emerging data have suggested the presence of multiple levels of interaction between Wnt and two related signal transduction pathways, namely TGF- $\beta$  and BMP (see Appendix 2). Members of the TGF- $\beta$  family of signalling factors are involved in a broad spectrum of cellular activities related to growth and development in a variety of tissues, including the gastrointestinal tract (Massague, 1998). Once ligand-activated by phosphorylation of the activated receptors, SMAD proteins migrate to the nucleus, where they recruit others transcriptional factors thus stimulating the expression of target genes implicated in the regulation of relevant biological functions. A specific aspect of this signaling pathway is that, depending on the cellular type and context, the net effect of the cellular response to TGF- $\beta$  might be either growth arrest (thus explaining the classical tumor suppressing function of TGF- $\beta$ ), or the transition from benign to malignant carcinoma, with structural changes of the extracellular matrix, stimulation of angiogenesis and depression of the immune response. Whether TGF- $\beta$  signaling is transduced as a growth inhibiting or promoting stimulus is likely to depend on tissue-specific differences in the distribution of nuclear cofactors that bind to specific subsets of target genes thus modulating their transcriptional activation.

Several transcriptional elements of the Wnt pathways have been shown to participate into Smad complexes in the nucleus. The first evidence of a physical interaction between TGF- $\beta$  and Wnt signaling components was demonstrated in *Xenopus* (Nishita et al., 2000; Letamendia et al., 2001). These two independent sets of experiments showed that in the nucleus Smad4 interacts with Wnt DNA binding transcription factors TCF/LEF1 to activate transcription of the *Xtwn* gene.

The possibility of Smad regulation of LEF1 target elements was shown to result not only from the physical interaction of these proteins, but also from the presence of a DNA Smad Binding Element (SBE) adjacent to the LEF1 binding site.

Subsequent to these observations, a synergistic action of Wnt/TGF- $\beta$  was identified for additional target genes in mammalian tumor cell lines.

Gastrin is a gastrointestinal hormone and growth factor shown to represent a downstream target of the Wnt signaling pathway (Koh et al., 2000). Incompletely processed gastrins (progastrin and glycine-extended gastrin) are capable of inducing colonic proliferation both *in vitro* and *in vivo* (Koh et al., 1999; Stepan et al., 1999; Aly et al., 2001; Singh et al., 1996; Baldwin, 1994). The combination of TGF- $\beta$  and Wnt signaling in gastric adenocarcinoma cells results in a strong synergistic promotion of Gastrin gene expression, as shown by the presence of a complex composed of Smad proteins, TCF4, and  $\beta$ -catenin in malignant cells (Lei et al., 2004), that possibly accelerates the neoplastic process in the GI tract.

Wnt/ $\beta$ -catenin and Smad4-dependent signaling pathways can also cooperatively drive the transcription of the homeobox-containing gene *MSX2* (Hussein et al., 2003). Activation of the *MSX2* promoter by Wnt and Smads is dependent on p300/CBP, as also shown for the murine gastrin promoter (model proposed in Figure 4). These results show how Wnt and TGF- $\beta$  can interact and act cooperatively in tumorigenesis. However, antagonist effects between these signaling pathways have also been demonstrated in the regulation of the *c-Myc* oncogene, a key regulator of cell-cycle progression (Sasaki et al., 2003). In the presence of Wnt ligand but in the absence of TGF- $\beta$  signals, TCF-4/ $\beta$ -catenin binds to its responsive element within the *c-Myc* promoter, thus activating its transcription (Figure 5). Upon combined Wnt and TGF- $\beta$  signaling, Smad3 nuclear translocation dislocates  $\beta$ -catenin from the *c-Myc* promoter and represses its transcriptional activity.

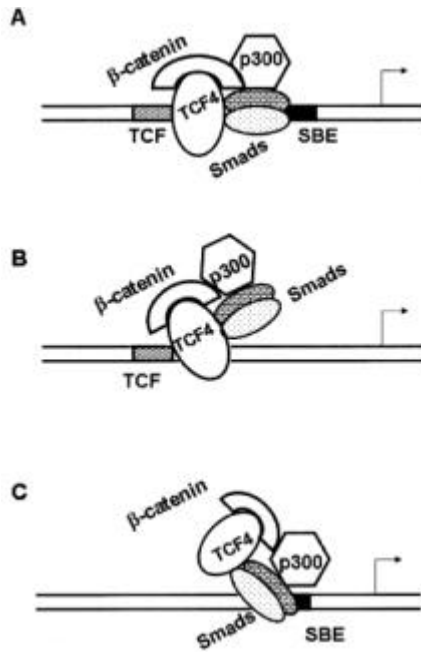


**Figure 4.** Model for intersection of TGF- $\beta$ /Smad and Wnt pathways. The interaction between the Smad3/4 and  $\beta$ -catenin/TCF complexes is mediated by TCF4, but this interaction could occur at adjacent TCF and SBE sites (shown in A), at isolated TCF sites (shown in B), or at isolated SBE sites (shown in C). In B, the Smad3/4 complex functions as a co-activator, whereas in C, the  $\beta$ -catenin/TCF4 complex acts as a co-activator. The additional recruitment of the cofactor p300/CBP, known to interact with both Smad3/4 and  $\beta$ -catenin, is also shown. From "The Murine Gastrin Promoter Is Synergistically Activated by Transforming Growth Factor- $\beta$ /Smad and Wnt Signaling Pathways" THE JOURNAL OF BIOLOGICAL CHEMISTRY 2004 Shi Lei, Alexander Dubeykovskiy, Abhijit Chakladar, Lindsay Wojtukiewicz, and Timothy C. Wang Reprint with permission from Editor

However, TGF- $\beta$  signalling does not affect Wnt-driven transcriptional activation of the c-Myc gene when the LEF-1/ $\beta$ -catenin complex binds to the c-Myc promoter instead of TCF-4/ $\beta$ -catenin (Figure 5). Hence, enhanced *LEF-1* expression, frequently observed in colon cancer, may underlie the malignant behavior characteristic of a subset of advanced CRCs that fail to undergo growth arrest upon TGF- $\beta$  signaling.

The above mentioned synergistic and antagonistic outcomes of Wnt/TGF- $\beta$  cross-talk occur at the transcriptional level. However, additional levels of regulatory interaction can also be envisaged.

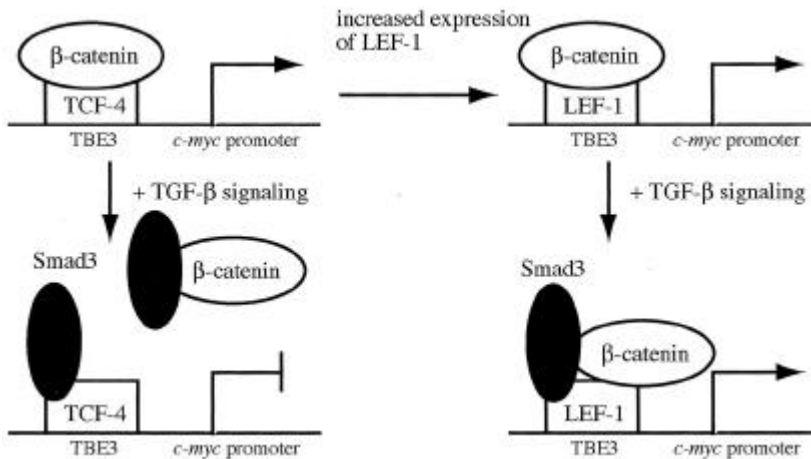


**Figure 5.** Model showing how the increased expression of LEF-1 may release the repression of *c-myc* expression induced by TGF- $\beta$ . Reprinted from "Lymphoid enhancer factor 1 makes cells resistant to transforming growth factor beta-induced repression of *c-myc*" Sasaki, T., Suzuki, H., Yagi, K., Furuhashi, M., Yao, R., Susa, S., Noda, T., Arai, Y., Miyazono, K. & Kato, M. (2003). *Cancer Res*, **63**, 801-6. With permission from the Editor.

It has been reported that oncogenic  $\beta$ -catenin or loss of *APC* function in human colon cancer cells lead to the expression and secretion of the TGF- $\beta$  family member BMP4 (bone morphogenetic protein 4) (Kim et al., 2002) possibly representing an alternative mechanism, though yet to be entirely elucidated, of Wnt/TGF- $\beta$  cross-talk in the deregulation of differentiation of colorectal cancer cells. The BMP signaling pathway has been implicated in the early steps of gut development and plays a central role in intestinal epithelial homeostasis. BMPs molecules moreover, are expressed in the stromal compartment of the villus. Accordingly, phosphorylated SMAD1, 5, and 8, indicative of active BMP signalling, show a gradient of nuclear expression in epithelial cells from the crypt (no expression) to the villus (highest levels of expression).

In Chapter 5, we showed that a *Smad4* loss of function mutation affects in a dosage-dependent fashion the expression of several target genes. In particular, both in heterozygous (*Smad4*<sup>+/-</sup>) and more pronouncedly in homozygous (*Smad4*<sup>-/-</sup>) ES cells, the transcription of Conductin (also known as Axin2) is down-regulated. Conductin, together with APC, GSK-3 $\beta$  and Axin1, participates in the destruction complex that regulates the activity of  $\beta$ -catenin along the Wnt signaling cascade (Appendix 1). Mutations in Conductin have been frequently reported in CRCs with DNA mismatch repair defects (microsatellite instable tumors, MSI) (Liu et al., 2000) and also in the germline of few familial cases (Lammi et al., 2004). Taken together, it appears that defective TGF- $\beta$  signaling, resulting from *Smad4* mutations, may directly affect and increase Wnt signaling. Loss of BMP signaling, by targeted inactivation of its main receptor (BMPR1a), causes an expansion of the mouse intestinal stem cell population leading to the formation of intestinal polyps with concomitant Wnt signaling activation (He et al., 2004).

Also, loss of *PTEN* function causes activation of Akt, thus positively contributing to nuclear  $\beta$ -catenin accumulation in intestinal stem cells (Persad et al., 2001). Since BMP is able to increase PTEN protein levels by inhibiting its degradation by the proteasome (Waite & Eng, 2003), the net effect of BMP activation is the inhibition of Wnt signaling in the intestinal crypt, thus regulating the proliferation of the stem and transient amplifying compartments (Figure 6). The *Smad4*-mutant mouse model described in this thesis (Chapter 2) might also be affected, to a certain extent, by the same mechanism with net increase of Wnt signaling. However,  $\beta$ -catenin IHC analysis of gastrointestinal polyps from these animals did not show evidence of nuclear accumulation.

Additional Wnt/TGF- $\beta$  interactions take place outside the nucleus. In adult mesenchymal stem cells (MSCs), TGF- $\beta$ 1 induces rapid nuclear translocation of  $\beta$ -catenin in a Smad3-dependent manner, independently of changes in  $\beta$ -catenin stability and phosphorylation status (Jian et al., 2006). This synergistic cooperation between TGF- $\beta$  and Wnt signaling in the specific MSC cellular context controls self-renewal and differentiation.

Reporter assay analysis of TGF- $\beta$  signaling in the *Apc*<sup>1638N/1638N</sup> ES cells revealed an increase of signaling activation (Alberici et al. manuscript in preparation), as

also confirmed in wild type ES transiently transfected by *Apc*-specific siRNAs. Notably, the same effect was not observed in Wnt-stimulated ES cells, thus indicating a possible direct effect of *APC* down-regulation on TGF- $\beta$  signaling.

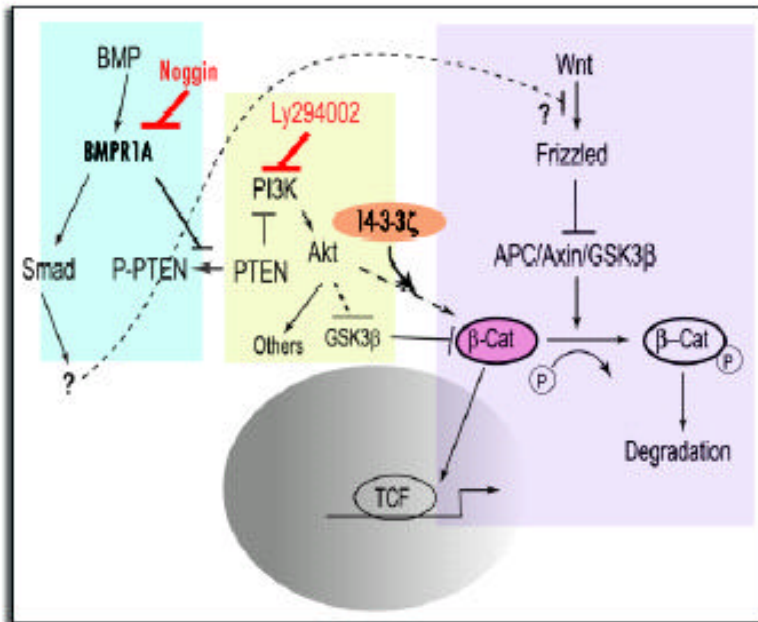


**Figure 6.** Illustration of the regulatory cross-talk network between BMP and Wnt signalings mediated by PTEN-PI3K pathway that controls the stem cell behaviour and the transition between quiescent and activated states. This network allows a balanced control of stem cell-renewal through a convergent downstream component.

From Bridging the BMP and Wnt pathways by PI3 kinase/Akt and 14-3-3 $\zeta$ . By Qian T. et al Cell Cycle. 2005 Feb;4(2):215-6. Reproduced with permission.

An additional Wnt/TGF- $\beta$  connection has been shown between Axin1 and Smad3 that can explain our reporter assay data: Axin1 binds to Smad3 and promotes his phosphorylation by the membrane-bound type I receptor TGFBR1, with the total effect of increasing TGF- $\beta$  signaling (Furuhashi et al., 2001). The same net increase in TGF- $\beta$  signaling is further substantiated by the observation that Axin1 also contributes to the downregulation of the inhibitor Smad7 through sequestration

and polyubiquitination-mediated degradation as represented in Figure 6 (Liu et al., 2006)

In conclusion, as illustrated in this PhD thesis, the elucidation of the complex network of interactions among different signalling pathways in colorectal cancer have contributed to the improved understanding of how adult intestinal cells

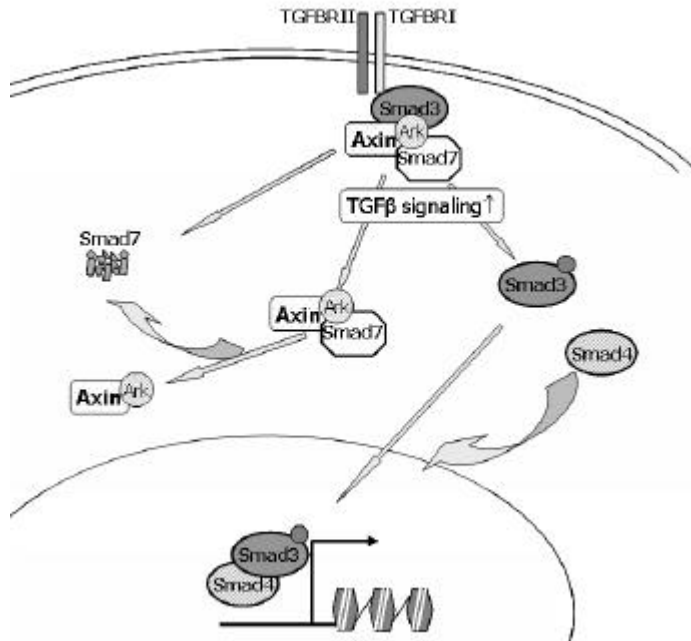


**Figure 7.** Model for a scaffolding roles of Axin in TGF- $\beta$  signalling (Liu et al., 2006). Following ligand stimulation, Axin promotes Smad3 phosphorylation causing the dissociation of Smad3 from the receptor complex. Axin acts as well onto Arkadia (Ark) to facilitate Smad7 polyubiquitination, independently of TGF- $\beta$  signalling, thus leading to Smad7 degradation.

regulate stemness, commitment to specific cell-fates, and proliferation. Understanding the cellular context in which these pathways converge and operate in specific cellular phenotypes will be crucial to elucidate the mechanisms that contribute to the overall preservation of intestinal homeostasis and thus identify the specific alterations in mechanisms that are responsible to the neoplastic process.

## References

- Alberici, P., de Pater, E., Cardoso, J., Bevelander, M., Molenaar, L., Jonkers, J. & Fodde, R. (2007). *Am J Pathol*, **170**, 377-87.
- Alberici, P., Jagmohan-Changur, S., De Pater, E., Van Der Valk, M., Smits, R., Hohenstein, P. & Fodde, R. (2006). *Oncogene*, **25**, 1841-51.
- Alberici, P. & Fodde, R. The Role of APC Tumor Suppressor in Chromosomal Instability. *Genome and Disease, Genome Dynamics*; Karger: Würzburg.
- Albuquerque, C., Breukel, C., van der Luijt, R., Fidalgo, P., Lage, P., Slors, F.J., Leitao, C.N., Fodde, R. & Smits, R. (2002). *Hum Mol Genet*, **11**, 1549-60.
- Alhopuro, P., Alazzouzi, H., Sammalkorpi, H., Davalos, V., Salovaara, R., Hemminki, A., Jarvinen, H., Mecklin, J.P., Schwartz, S., Jr., Aaltonen, L.A. & Arango, D. (2005). *Clin Cancer Res*, **11**, 6311-6.
- Aly, A., Shulkes, A. & Baldwin, G.S. (2001). *Int J Cancer*, **94**, 307-13.
- Baldwin, G.S. (1994). *Proc Natl Acad Sci U S A*, **91**, 7593-7.
- Baker, S.J., Fearon, E.R., Nigro, J.M., Hamilton, S.R., Preisinger, A.C., Jessup, J.M., vanTuinen, P., Ledbetter, D.H., Barker, D.F., Nakamura, Y. & et al. (1989). *Science*, **244**, 217-21.
- Baker, S.J., Preisinger, A.C., Jessup, J.M., Paraskeva, C., Markowitz, S., Willson, J.K., Hamilton, S. & Vogelstein, B. (1990). *Cancer Res*, **50**, 7717-22.
- Bardi, G., Parada, L.A., Bomme, L., Pandis, N., Willen, R., Johansson, B., Jeppsson, B., Beroukas, K., Heim, S. & Mitelman, F. (1997). *Br J Cancer*, **76**, 765-9.
- Batlle, E., Henderson, J.T., Beghtel, H., van den Born, M.M., Sancho, E., Huls, G., Meeldijk, J., Robertson, J., van de Wetering, M., Pawson, T. & Clevers, H. (2002). *Cell*, **111**, 251-63.
- Beach, R., Chan, A.O., Wu, T.T., White, J.A., Morris, J.S., Lunagomez, S., Broaddus, R.R., Issa, J.P., Hamilton, S.R. & Rashid, A. (2005). *Am J Pathol*, **166**, 1069-75.
- Boland, C.R., Sato, J., Appelman, H.D., Bresalier, R.S. & Feinberg, A.P. (1995). *Nat Med*, **1**, 902-9.
- Bos, J.L. (1988). *Mutat Res*, **195**, 255-71.
- Bouffler, S.D., Hofland, N., Cox, R. & Fodde, R. (2000). *Br J Cancer*, **83**, 1291-4.
- Burns, T.F. & El-Deiry, W.S. (1999). *J Cell Physiol*, **181**, 231-9.
- Cahill, D.P., Lengauer, C., Yu, J., Riggins, G.J., Willson, J.K., Markowitz, S.D., Kinzler, K.W. & Vogelstein, B. (1998). *Nature*, **392**, 300-3.
- Cardoso, J., Molenaar, L., de Menezes, R.X., van Leerdam, M., Rosenberg, C., Moslein, G., Sampson, J., Morreau, H., Boer, J.M. & Fodde, R. (2006). *Cancer Res*, **66**, 2514-9.
- Cho, K.R., Oliner, J.D., Simons, J.W., Hedrick, L., Fearon, E.R., Preisinger, A.C., Hedge, P., Silverman, G.A. & Vogelstein, B. (1994). *Genomics*, **19**, 525-31.
- Clevers, H. (2000). *Nat Genet*, **24**, 206-8.
- Cook, D.L., Gerber, A.N. & Tapscott, S.J. (1998). *Proc Natl Acad Sci U S A*, **95**, 15641-6.
- D'Abaco, G.M., Whitehead, R.H. & Burgess, A.W. (1996). *Mol Cell Biol*, **16**, 884-91.
- Daniel, J.M. & Reynolds, A.B. (1997). *Bioessays*, **19**, 883-91.

- Date, O., Katsura, M., Ishida, M., Yoshihara, T., Kinomura, A., Sueda, T. & Miyagawa, K. (2006). *Cancer Res*, **66**, 6018-24.
- Dikovskaya, D., Newton, I.P. & Nathke, I.S. (2004). *Mol Biol Cell*, **15**, 2978-91.
- Draviam, V.M., Shapiro, I., Aldridge, B. & Sorger, P.K. (2006). *Embo J*, **25**, 2814-27.
- Duff, E.K. & Clarke, A.R. (1998). *Br J Cancer*, **78**, 1615-9.
- Fishel, R., Lescoe, M.K., Rao, M.R., Copeland, N.G., Jenkins, N.A., Garber, J., Kane, M. & Kolodner, R. (1993). *Cell*, **75**, 1027-38.
- Fodde, R., Kuipers, J., Rosenberg, C., Smits, R., Kielman, M., Gaspar, C., van Es, J.H., Breukel, C., Wiegant, J., Giles, R.H. & Clevers, H. (2001). *Nat Cell Biol*, **3**, 433-438.
- Forrester, K., Almoguera, C., Han, K., Grizzle, W.E. & Perucho, M. (1987). *Nature*, **327**, 298-303.
- Forster, L.F., Defres, S., Goudie, D.R., Baty, D.U. & Carey, F.A. (2000). *J Clin Pathol*, **53**, 791-3.
- Friend, S.H., Bernards, R., Rogelji, S., Weinberg, R.A., Rapaport, J.M., Albert, D.M. & Dryja, T.P. (1986). *Nature*, **323**, 643-6.
- Furuhashi, M., Yagi, K., Yamamoto, H., Furukawa, Y., Shimada, S., Nakamura, Y., Kikuchi, A., Miyazono, K. & Kato, M. (2001). *Mol Cell Biol*, **21**, 5132-41.
- Giaretti, W. (1994). *Lab Invest*, **71**, 904-10.
- Goss, K.H., Risinger, M.A., Kordich, J.J., Sanz, M.M., Straughen, J.E., Slovek, L.E., Capobianco, A.J., German, J., Boivin, G.P. & Groden, J. (2002). *Science*, **297**, 2051-3.
- Grady, W.M., Myeroff, L.L., Swinler, S.E., Rajput, A., Thiagalingam, S., Lutterbaugh, J.D., Neumann, A., Brattain, M.G., Chang, J., Kim, S.J., Kinzler, K.W., Vogelstein, B., Willson, J.K. & Markowitz, S. (1999). *Cancer Res*, **59**, 320-4.
- Green, R.A. & Kaplan, K.B. (2003). *J Cell Biol*, **163**, 949-61.
- Hajra, K.M. & Fearon, E.R. (2002). *Genes Chromosomes Cancer*, **34**, 255-68.
- He, T.C., Sparks, A.B., Rago, C., Hermeking, H., Zawel, L., da Costa, L.T., Morin, P.J., Vogelstein, B. & Kinzler, K.W. (1998). *Science*, **281**, 1509-12.
- He, X.C., Zhang, J., Tong, W.G., Tawfik, O., Ross, J., Scoville, D.H., Tian, Q., Zeng, X., He, X., Wiedemann, L.M., Mishina, Y. & Li, L. (2004). *Nat Genet*.
- Heldin, C.H., Miyazono, K. & ten Dijke, P. (1997). *Nature*, **390**, 465-71.
- Hershko, D.D. & Shapira, M. (2006). *Cancer*, **107**, 668-75.
- Howe, J.R., Ringold, J.C., Summers, R.W., Mitros, F.A., Nishimura, D.Y. & Stone, E.M. (1998). *Am J Hum Genet*, **62**, 1129-36.
- Hurlstone, D.P. & Cross, S.S. (2005). *J Gastroenterol Hepatol*, **20**, 173-81.
- Hussein, S.M., Duff, E.K. & Sirard, C. (2003). *J Biol Chem*, **278**, 48805-14.
- Imai, Y., Shiratori, Y., Kato, N., Inoue, T. & Omata, M. (1999). *Jpn J Cancer Res*, **90**, 837-40.
- Janssen, K.P., Alberici, P., Fsihi, H., Gaspar, C., Breukel, C., Franken, P., Rosty, C., Abal, M., El Marjou, F., Smits, R., Louvard, D., Fodde, R. & Robine, S. (2006). *Gastroenterology*, **131**:1096-109.
- Jen, J., Kim, H., Piantadosi, S., Liu, Z.F., Levitt, R.C., Sistonen, P., Kinzler, K.W., Vogelstein, B. & Hamilton, S.R. (1994a). *N Engl J Med*, **331**, 213-21.
- Jen, J., Powell, S.M., Papadopoulos, N., Smith, K.J., Hamilton, S.R., Vogelstein, B. & Kinzler, K.W. (1994). *Cancer Res*, **54**, 5523-6.

- Jian, H., Shen, X., Liu, I., Semenov, M., He, X. & Wang, X.F. (2006). *Genes Dev*, **20**, 666-74.
- Kaklamanis, L., Gatter, K.C., Mortensen, N., Baigrie, R.J., Heryet, A., Lane, D.P. & Harris, A.L. (1993). *Am J Pathol*, **142**, 87-93.
- Kanazawa, T., Watanabe, T., Kazama, S., Tada, T., Koketsu, S. & Nagawa, H. (2002). *Int J Cancer*, **102**, 225-9.
- Kaplan, K.B., Burds, A.A., Swedlow, J.R., Bekir, S.S., Sorger, P.K. & Nathke, I.S. (2001). *Nat Cell Biol*, **3**, 429-432.
- Kaserer, K., Schmaus, J., Bethge, U., Migschitz, B., Fasching, S., Walch, A., Herbst, F., Teleky, B. & Wrba, F. (2000). *J Pathol*, **190**, 450-6.
- Keino-Masu, K., Masu, M., Hinck, L., Leonardo, E.D., Chan, S.S., Culotti, J.G. & Tessier-Lavigne, M. (1996). *Cell*, **87**, 175-85.
- Kerkhoff, E. & Rapp, U.R. (1998). *Oncogene*, **17**, 1457-62.
- Kim, E.C. & Lance, P. (1997). *Gastroenterol Clin North Am*, **26**, 1-17.
- Kim, J.S., Crooks, H., Dracheva, T., Nishanian, T.G., Singh, B., Jen, J. & Waldman, T. (2002). *Cancer Res*, **62**, 2744-8.
- Kinch, M.S., Clark, G.J., Der, C.J. & Burridge, K. (1995). *J Cell Biol*, **130**, 461-71.
- Kinzler, K.W. & Vogelstein, B. (1996). *Cell*, **87**, 159-70.
- Kiyokawa, H., Kineman, R.D., Manova-Todorova, K.O., Soares, V.C., Hoffman, E.S., Ono, M., Khanam, D., Hayday, A.C., Frohman, L.A. & Koff, A. (1996). *Cell*, **85**, 721-32.
- Knudson, A.G., Jr. (1971). *Proc Natl Acad Sci U S A*, **68**, 820-3.
- Koh, T.J., Bulitta, C.J., Fleming, J.V., Dockray, G.J., Varro, A. & Wang, T.C. (2000). *J Clin Invest*, **106**, 533-9.
- Koh, T.J., Dockray, G.J., Varro, A., Cahill, R.J., Dangler, C.A., Fox, J.G. & Wang, T.C. (1999). *J Clin Invest*, **103**, 1119-26.
- Korinek, V., Barker, N., Morin, P.J., van Wichen, D., de Weger, R., Kinzler, K.W., Vogelstein, B. & Clevers, H. (1997). *Science*, **275**, 1784-7.
- Kucherlapati, M., Yang, K., Kuraguchi, M., Zhao, J., Lia, M., Heyer, J., Kane, M.F., Fan, K., Russell, R., Brown, A.M., Kneitz, B., Edelman, W., Kolodner, R.D., Lipkin, M. & Kucherlapati, R. (2002). *Proc Natl Acad Sci U S A*, **99**, 9924-9.
- Kwabi-Addo, B., Giri, D., Schmidt, K., Podsypanina, K., Parsons, R., Greenberg, N. & Ittmann, M. (2001). *Proc Natl Acad Sci U S A*, **98**, 11563-8.
- Lamlum, H., Ilyas, M., Rowan, A., Clark, S., Johnson, V., Bell, J., Frayling, I., Efsthathiou, J., Pack, K., Payne, S., Roylance, R., Gorman, P., Sheer, D., Neale, K., Phillips, R., Talbot, I., Bodmer, W. & Tomlinson, I. (1999). *Nat Med*, **5**, 1071-5.
- Lammi, L., Arte, S., Somer, M., Jarvinen, H., Lahermo, P., Thesleff, I., Pirinen, S. & Nieminen, P. (2004). *Am J Hum Genet*, **74**, 1043-50.
- Lane, D.P. (1992). *Nature*, **358**, 15-6.
- Lei, S., Dubeykovskiy, A., Chakladar, A., Wojtukiewicz, L. & Wang, T.C. (2004). *J Biol Chem*, **279**, 42492-502.
- Letamendia, A., Labbe, E. & Attisano, L. (2001). *J Bone Joint Surg Am*, **83-A Suppl 1**, S31-9.
- Li, J., Mizukami, Y., Zhang, X., Jo, W.S. & Chung, D.C. (2005). *Gastroenterology*, **128**, 1907-18.

- Liu, W., Dong, X., Mai, M., Seelan, R.S., Taniguchi, K., Krishnadath, K.K., Halling, K.C., Cunningham, J.M., Qian, C., Christensen, E., Roche, P.C., Smith, D.I. & Thibodeau, S.N. (2000). *Nat Genet*, **26**, 146-7.
- Liu, W., Rui, H., Wang, J., Lin, S., He, Y., Chen, M., Li, Q., Ye, Z., Zhang, S., Chan, S.C., Chen, Y.G., Han, J. & Lin, S.C. (2006). *Embo J*, **25**, 1646-58.
- Liu, W.H., Kaur, M., Wang, G., Zhu, P., Zhang, Y. & Makrigiorgos, G.M. (2004). *Cancer Res*, **64**, 2544-51.
- Massague, J. (1998). *Annu Rev Biochem*, **67**, 753-91.
- McLellan, E.A. & Bird, R.P. (1988). *Cancer Res*, **48**, 6183-6.
- Miyoshi, Y., Nagase, H., Ando, H., Horii, A., Ichii, S., Nakatsuru, S., Aoki, T., Miki, Y., Mori, T. & Nakamura, Y. (1992). *Hum Mol Genet*, **1**, 229-33.
- Miyoshi, H., Nakau, M., Ishikawa, T.O., Seldin, M.F., Oshima, M. & Taketo, M.M. (2002). *Cancer Res*, **62**, 2261-6.
- Morin, P.J., Sparks, A.B., Korinek, V., Barker, N., Clevers, H., Vogelstein, B. & Kinzler, K.W. (1997). *Science*, **275**, 1787-90.
- Nakayama, K., Ishida, N., Shirane, M., Inomata, A., Inoue, T., Shishido, N., Horii, I. & Loh, D.Y. (1996). *Cell*, **85**, 707-20.
- Nishita, M., Hashimoto, M.K., Ogata, S., Laurent, M.N., Ueno, N., Shibuya, H. & Cho, K.W. (2000). *Nature*, **403**, 781-5.
- Ohue, M., Tomita, N., Monden, T., Fujita, M., Fukunaga, M., Takami, K., Yana, I., Ohnishi, T., Enomoto, T., Inoue, M. & et al. (1994). *Cancer Res*, **54**, 4798-804.
- Payne, S.R. & Kemp, C.J. (2005). *Carcinogenesis*, **26**, 2031-45.
- Persad, S., Troussard, A.A., McPhee, T.R., Mulholland, D.J. & Dedhar, S. (2001). *J Cell Biol*, **153**, 1161-74.
- Philipp-Staheli, J., Kim, K.H., Payne, S.R., Gurley, K.E., Liggitt, D., Longton, G. & Kemp, C.J. (2002). *Cancer Cell*, **1**, 355-68.
- Pietenpol, J.A., Bohlander, S.K., Sato, Y., Papadopoulos, N., Liu, B., Friedman, C., Trask, B.J., Roberts, J.M., Kinzler, K.W., Rowley, J.D. & et al. (1995). *Cancer Res*, **55**, 1206-10.
- Powell, S.M., Zilz, N., Beazer-Barclay, Y., Bryan, T.M., Hamilton, S.R., Thibodeau, S.N., Vogelstein, B. & Kinzler, K.W. (1992). *Nature*, **359**, 235-7.
- Rajagopalan, H., Jallepalli, P.V., Rago, C., Velculescu, V.E., Kinzler, K.W., Vogelstein, B. & Lengauer, C. (2004). *Nature*, **428**, 77-81.
- Rajagopalan, H. & Lengauer, C. (2004). *Cancer Chemother Pharmacol*, **54 Suppl 1**, S65-8.
- Roura, S., Miravet, S., Piedra, J., Garcia de Herreros, A. & Dunach, M. (1999). *J Biol Chem*, **274**, 36734-40.
- Salovaara, R., Roth, S., Loukola, A., Launonen, V., Sistonen, P., Avizienyte, E., Kristo, P., Jarvinen, H., Souchelnytskyi, S., Sarlomo-Rikala, M. & Aaltonen, L.A. (2002). *Gut*, **51**, 56-9.
- Sansom, O.J., Meniel, V., Wilkins, J.A., Cole, A.M., Oien, K.A., Marsh, V., Jamieson, T.J., Guerra, C., Ashton, G.H., Barbacid, M. & Clarke, A.R. (2006). *Proc Natl Acad Sci U S A*, **103**, 14122-7.
- Sasaki, T., Suzuki, H., Yagi, K., Furuhashi, M., Yao, R., Susa, S., Noda, T., Arai, Y., Miyazono, K. & Kato, M. (2003). *Cancer Res*, **63**, 801-6.
- Satoh, S., Daigo, Y., Furukawa, Y., Kato, T., Miwa, N., Nishiwaki, T., Kawasoe, T., Ishiguro, H., Fujita, M., Tokino, T., Sasaki, Y., Imaoka, S., Murata, M., Shimano, T., Yamaoka, Y. & Nakamura, Y. (2000). *Nat Genet*, **24**, 245-50.

- Sears, R., Leone, G., DeGregori, J. & Nevins, J.R. (1999). *Mol Cell*, **3**, 169-79.
- Shibamoto, S., Hayakawa, M., Takeuchi, K., Hori, T., Oku, N., Miyazawa, K., Kitamura, N., Takeichi, M. & Ito, F. (1994). *Cell Adhes Commun*, **1**, 295-305.
- Shichiri, M., Yoshinaga, K., Hisatomi, H., Sugihara, K. & Hirata, Y. (2002). *Cancer Res*, **62**, 13-7.
- Shih, I.M., Zhou, W., Goodman, S.N., Lengauer, C., Kinzler, K.W. & Vogelstein, B. (2001). *Cancer Res*, **61**, 818-22.
- Sieber, O.M., Lamlum, H., Crabtree, M.D., Rowan, A.J., Barclay, E., Lipton, L., Hodgson, S., Thomas, H.J., Neale, K., Phillips, R.K., Farrington, S.M., Dunlop, M.G., Mueller, H.J., Bisgaard, M.L., Bulow, S., Fidalgo, P., Albuquerque, C., Scarano, M.I., Bodmer, W., Tomlinson, I.P. & Heinemann, K. (2002). *Proc Natl Acad Sci U S A*, **99**, 2954-8.
- Simpson, L. & Parsons, R. (2001). *Exp Cell Res*, **264**, 29-41.
- Singh, P., Owlia, A., Varro, A., Dai, B., Rajaraman, S. & Wood, T. (1996). *Cancer Res*, **56**, 4111-5.
- Smith, A.J., Stern, H.S., Penner, M., Hay, K., Mitri, A., Bapat, B.V. & Gallinger, S. (1994). *Cancer Res*, **54**, 5527-30.
- Smith, K.J., Johnson, K.A., Bryan, T.M., Hill, D.E., Markowitz, S., Willson, J.K., Paraskeva, C., Petersen, G.M., Hamilton, S.R., Vogelstein, B. & Kinzler, K.W. (1993). *Proc Natl Acad Sci U S A*, **90**, 2846-50.
- Smits, R., Kielman, M.F., Breukel, C., Zurcher, C., Neufeld, K., Jagmohan-Changur, S., Hofland, N., van Dijk, J., White, R., Edelmann, W., Kucherlapati, R., Khan, P.M. & Fodde, R. (1999). *Genes Dev*, **13**, 1309-21.
- Smits, R., Ruiz, P., Diaz-Cano, S., Luz, A., Jagmohan-Changur, S., Breukel, C., Birchmeier, C., Birchmeier, W. & Fodde, R. (2000). *Gastroenterology*, **119**, 1045-53.
- Sparks, A.B., Morin, P.J., Vogelstein, B. & Kinzler, K.W. (1998). *Cancer Res*, **58**, 1130-4.
- Spencer, F., Gerring, S.L., Connelly, C. & Hieter, P. (1990). *Genetics*, **124**, 237-49.
- Stepan, V.M., Sawada, M., Todisco, A. & Dickinson, C.J. (1999). *Mol Med*, **5**, 147-59.
- Sturm, I., Bosanquet, A.G., Radetzki, S., Hummel, M., Dorken, B. & Daniel, P.T. (2006). *Int J Cancer*, **118**, 2329-36.
- Takata, M., Yao, T., Nishiyama, K.I., Nawata, H. & Tsuneyoshi, M. (2003). *Histopathology*, **43**, 332-9.
- Tetsu, O. & McCormick, F. (1999). *Nature*, **398**, 422-6.
- Umetani, N., Fujimoto, A., Takeuchi, H., Shinozaki, M., Bilchik, A.J. & Hoon, D.S. (2004). *Oncogene*, **23**, 8292-300.
- Venesio, T., Balsamo, A., Rondo-Spaudo, M., Varesco, L., Risio, M. & Ranzani, G.N. (2003). *Lab Invest*, **83**, 1859-66.
- Vinay Kumar, A.K.A., Nelson Fausto. *Robbins & Cotran Pathologic Basis of Disease*, 7th edn. Saunders.
- Vogelstein, B., Fearon, E.R., Hamilton, S.R., Kern, S.E., Preisinger, A.C., Leppert, M., Nakamura, Y., White, R., Smits, A.M. & Bos, J.L. (1988). *N Engl J Med*, **319**, 525-32.
- Vogelstein, B., Fearon, E.R., Kern, S.E., Hamilton, S.R., Preisinger, A.C., Nakamura, Y. & White, R. (1989). *Science*, **244**, 207-11.
- Waite, K.A. & Eng, C. (2003). *Hum Mol Genet*, **12**, 679-84.

## References

---

- Waldman, T., Kinzler, K.W. & Vogelstein, B. (1995). *Cancer Res*, **55**, 5187-90.
- Yamaguchi, A., Makimoto, K., Goi, T., Takeuchi, K., Maehara, M., Isobe, Y. & Nakagawara, G. (1994). *Oncology*, **51**, 224-7.
- Yamamoto, H., Gil, J., Schwartz, S., Jr. & Perucho, M. (2000). *Cell Death Differ*, **7**, 238-9.
- Yan, H., Dobbie, Z., Gruber, S.B., Markowitz, S., Romans, K., Giardiello, F.M., Kinzler, K.W. & Vogelstein, B. (2002). *Nat Genet*, **30**, 25-6.
- Zhang, B., Ougolkov, A., Yamashita, K., Takahashi, Y., Mai, M. & Minamoto, T. (2003). *Clin Cancer Res*, **9**, 3073-9.
- Zhang, S., Lloyd, R., Bowden, G., Glickman, B.W. & de Boer, J.G. (2002). *Environ Mol Mutagen*, **40**, 243-50.
- Zhang, X., Gaspard, J.P. & Chung, D.C. (2001). *Cancer Res*, **61**, 6050-4.





## SUMMARY

Colorectal cancer represents not only the second leading cause of cancer-related death in Western world but also an ideal model to investigate and elucidate the genetic alterations that underlie tumor onset and progression, the so-called adenoma-carcinoma sequence. This sequence of events towards malignancy and metastasis is characterized by the progressive increase in signal transduction activity and chromosomal instability levels resulting from the accumulation of somatic mutations in specific tumor suppressor genes and oncogenes.

Loss of function mutations at the *APC* tumor suppressor gene leading to aberrant Wnt signaling and the synchronous oncogenic *KRAS* activation are early and frequent events in colorectal cancer, often associated with poor prognosis. In **CHAPTER 2** we report the generation and analysis of compound *KRAS*<sup>V12G</sup>/*Apc*<sup>+1638N</sup> mutant mice. These animals are characterized by increased tumor initiation and progression with enhanced morbidity and mortality. We demonstrated by *in vitro* and *in vivo* analysis that activated *KRAS*, via tyrosine phosphorylation of  $\beta$ -catenin, leads to its release from E-cadherin at the adherens junctions, and to its consequent nuclear translocation and increased transcription of Wnt downstream target genes.

Although chromosomal instability (CIN) characterizes the majority of human colorectal cancers, the contribution of genes such as *APC*, *KRAS* and *p53* to this form of genetic instability is still a matter of debate. In **CHAPTER 3** we have assessed chromosomal imbalances in tumors derived from mouse models of intestinal cancer, namely *Apc*<sup>+1638N</sup>, *Apc*<sup>+1638N</sup>/*KRAS*<sup>V12G</sup>, and *Apc*<sup>+1638N</sup>/*Tp53*<sup>-/-</sup>, by array-CGH (comparative genomic hybridization). All intestinal adenomas displayed chromosomal alterations, thus confirming the presence of a chromosomal instability defect at very early stages of the adenoma-carcinoma sequence. Moreover, loss of the *Tp53* tumor suppressor gene, but not *KRAS* oncogenic activation, results in an increase of gains and losses of whole chromosomes in the *Apc*-mutant genetic background. Through the comparative analysis of the overall genomic alterations found in human and mouse intestinal adenomas, we identified

a subset of syntenic regions likely to encompass rate-limiting genes for intestinal tumor initiation and progression.

The *SMAD4* tumor suppressor gene, a key element for the transduction of TGF- $\beta$  signals, is involved in the pathogenesis of pancreatic and colorectal cancers. In **CHAPTER 4**, the detailed analysis of intestinal tumors from *Smad4*<sup>+/*E6sad*</sup> mouse showed that loss of heterozygosity (LOH) of the wild type *Smad4* allele is not an essential requirement for tumor formation and that complete loss of protein expression occurs only at later stages of tumour progression. Hence, haploinsufficiency underlies *Smad4*-driven tumor initiation in the GI tract. We have then bred *Smad4*<sup>+/*E6sad*</sup> with the *Apc*<sup>+/*1638N*</sup> model to generate two distinct compound heterozygous lines carrying both mutations either *in cis* (CAS) or *in trans* (TAS) on chromosome 18. Notably, both models show increased tumor multiplicities when compared with the single mutant littermates, though CAS mice are more severely affected. Phenotypic and molecular analyses indicate that *Smad4* haploinsufficiency is sufficient to significantly affect tumor initiation and progression both prior to and upon loss of *Apc* function. Moreover, complete loss of *Smad4* strongly enhances *Apc*-driven tumor formation.

In **CHAPTER 5** we defined the molecular defect resulting from *SMAD4* haploinsufficiency. In *Smad4*<sup>+/-</sup> and *Smad4*<sup>-/-</sup> ES cells derived from *Smad4*<sup>*E6sad*</sup> animals, the *Smad4* protein expression level perfectly correlates with the gene copy number (~50% reduction in heterozygous cells and no protein expression in homozygous cells). Reporter assay analysis showed the presence of TGF- $\beta$  and BMP signaling defects already in heterozygous cells in transduction pathways.

Expression profiling of these ES cell lines allowed the identification of a shortlist of *Smad4* dosage-related target genes involved in signaling, metabolism and regulation of the transcription. We validate a subset of these differentially expressed genes by real-time PCR on normal intestinal tissue from *Smad4*<sup>+/-</sup> mice, confirming the presence of a primary defect. IHC analysis of polyps from Familial Juvenile Polyposis patients carrying *Smad4* germline mutations also retained *Smad4* expression in the earliest stage of polyp formation, hence in agreement with the haploinsufficiency model.

These observations indicate that relatively small fluctuations in Smad4 levels in intestinal epithelial cells may contribute to alterations of cellular pathways and networks responsible for polyps formation without complete loss of Smad4 function.

In conclusion, this thesis aims to describe and illustrate the multiple interactions and mutual influences of defective signal transduction pathways in CRC and the mechanisms that are responsible for 'just-right' level of genetic instability. Both these elements contribute to the establishment of the multiple cellular defects necessary to promote tumor progression and malignancy.



---

## SAMENVATTING

Dikkedarmkanker is niet alleen de tweede oorzaak van kanker gerelateerd overlijden in de Westerse wereld, maar ook een ideaal model om de onderliggende genetische oorzaak van het ontstaan van tumoren en tumorprogressie, de zogenaamde adenoma-carcinoma reeks, te onderzoeken en op te helderen. De reeks van gebeurtenissen voorafgaand aan kwaadaardigheid en metastasering wordt gekarakteriseerd door een continue toename van signaaltransductie activiteit en mate van chromosomale instabiliteit als gevolg van de opeenhoping van somatische mutaties in specifieke tumor suppressor genen en oncogenen.

Functieverlies gevende mutaties in het *APC* tumor suppressor gen die leiden tot een verhoogde Wnt signalering en een simultane oncogene *KRAS* mutatie zijn vroege en veel voorkomende gebeurtenissen in dikkedarmkanker en vaak geassocieerd met een slechte prognose. In **Hoofdstuk 2** vermelden we de generatie en analyse van samengestelde *KRAS*<sup>V12G</sup>/*Apc*<sup>+1638N</sup> mutante muizen. Deze dieren hebben een verhoogde tumor initiatie en progressie met een verhoogde morbiditeit en mortaliteit. We hebben door *in vitro* en *in vivo* analyse laten zien dat geactiveerd *KRAS*, via tyrosine fosforylering,  $\beta$ -catenine los maakt van E-cadherine in de *adherent junctions*, en dat deze als gevolg hiervan naar de kern gaat en de transcriptie van Wnt gereguleerde genen verhoogt.

Hoewel chromosomale instabiliteit (CIN) karakteristiek is voor een meerderheid van humane dikkedarmkankers, is de bijdrage van genen als *APC*, *KRAS* en *p53* in deze vorm van genetische instabiliteit nog steeds onderwerp van discussie. In **Hoofdstuk 3** hebben we de chromosomale onbalans in tumoren afkomstig van muismodellen voor darmkanker, namelijk *Apc*<sup>+1638N</sup>, *Apc*<sup>+1638N</sup>/*KRAS*<sup>V12G</sup> en *Apc*<sup>+1638N</sup>/*Tp53*<sup>-/-</sup>, vastgesteld door middel van array-CGH (Comparatieve Genomische Hybridisatie). Alle darm-adenomen vertoonden chromosomale afwijkingen, daarmee de aanwezigheid van een chromosoominstabiliteitsdefect in erg vroege stadia van de adenoma-carcinoma reeks bevestigend.

Bovendien resulteerde het verlies van het *Tp53* tumor suppressor gen wél, maar oncogene *KRAS* activatie niet in een toename van winst en verlies van hele chromosomen in de *Apc*-mutant achtergrond. Door de vergelijkende analyse van

de algemene genomische veranderingen, gevonden in humane en muizen darm adenoma's, identificeerden we een subgroep van syntenische regio's die waarschijnlijk de snelheidsbepalende genen voor darmkanker initiatie en progressie bevatten.

Het *SMAD4* tumor suppressor gen, een sleutelfactor voor de doorgifte van TGF- $\beta$  signalen, is betrokken bij de pathogenese van pancreas- en dikkedarm-kanker. In **Hoofdstuk 4** liet de gedetailleerde analyse van darmtumoren van *Smad4*<sup>+/*E6sad*</sup> muizen zien dat verlies van heterozygotie (LOH) van het wild type *Smad4* allel niet absoluut vereist is voor tumorvorming en dat een volledig verlies van eiwitexpressie pas voorkomt in latere stadia van tumorprogressie. Daarom is haplo-insufficiëntie de oorzaak van *Smad4* gedreven tumorinitiatie in het maagdarmkanaal. We hebben toen het *Smad4*<sup>+/*E6sad*</sup> met het *Apc*<sup>+/*1638N*</sup> model gekruist om twee verschillende, samengestelde heterozygote lijnen te maken die beide mutaties dragen *in cis* (CAS) of *in trans* (TAS) op chromosoom 18. Opvallend is dat beide modellen een verhoogd tumor aantal hebben vergeleken met de enkelvoudige mutante nestgenoten, hoewel de CAS muizen zwaarder zijn aangedaan. Fenotypische en moleculaire analyse laten zien dat *Smad4* haplo-insufficiëntie voldoende is om de tumor initiatie en progressie significant te beïnvloeden, zowel voor als na verlies van *Apc* functie. Bovendien versterkt een compleet verlies van *Smad4* de *Apc* aangedreven tumor vorming zeer.

In **Hoofdstuk 5** hebben we het moleculaire defect achterhaald dat het gevolg is van *SMAD4* haploinsufficiëntie. In *Smad4*<sup>+/-</sup> en *Smad4*<sup>-/-</sup> ES cellen afkomstig van *Smad4*<sup>*E6sad*</sup> dieren, correleert de mate van *Smad4* eiwit expressie perfect met het aantal gen copieën (~50% reductie in heterozygote cellen en geen expressie in homozygote cellen). *Reporter assay* analyse liet zien dat TGF- $\beta$  en BMP signaaltransductiedefecten reeds aanwezig zijn in heterozygote cellen.

Expressie profilering van deze ES cellijnen maakte het mogelijk een *shortlist* op te stellen van *Smad4* dosis-gerelateerde doel genen die betrokken zijn bij signalering, metabolisme en transcriptieregulatie. We valideerden een sub-set van deze differentieel ge-expresserde genen door middel van *real time PCR* op normaal darm weefsel van *Smad4*<sup>+/-</sup> muizen, en bevestigden daarmee het bestaan van een primair effect. IHC analyse liet zien dat poliepen van *Familial Juvenile Polyposis*

patiënten die *Smad4* kiembaan mutaties dragen ook de *Smad4* expressie behielden in de eerste stadia van poliep vorming, dit in overeenstemming met het haploinsufficiëntie model.

Deze observaties geven aan dat relatief kleine fluctuaties in *Smad4* hoeveelheden in darmepitheel-cellen kunnen bijdragen tot veranderingen in cellulaire paden en netwerken en daardoor verantwoordelijk zijn voor poliepvorming zonder volledig verlies van *Smad4* functionaliteit.

Concluderend, dit proefschrift heeft als doel de veelvoudige interacties en wederkerige invloeden van defecte signaaltransductiepaden in dikkedarmkanker en de mechanismen die verantwoordelijk zijn voor een 'precies-goed' mate van genetische instabiliteit te beschrijven en te illustreren. Deze beide elementen dragen bij aan het ontstaan van de meerdere cellulaire defecten die nodig zijn voor het bevorderen van tumor progressie en maligniteit.



## **Curriculum Vitae**

Paola Alberici was born in Milan, Italy, on April 7, 1972. After finished high school at the Conservatorio G.Verdi of Milan in 1991, she studied Medicine and Surgery at "Università degli Studi" of Milan. She graduated as Medical Doctor in October 1997 with an experimental thesis on the molecular genetics of breast cancer which work was performed at the Telethon Institute of Genetics and Medicine (TIGEM) of Milan. For this work in 1998 she won the Prize for Experimental thesis in cancer genetics conferred by the Istituto Lombardo Accademia di Scienze e Lettere of Milan.

In 1998-2001 she worked as fellow of the Specialization School in Medical Genetics at experimental oncology division of the Istituto Nazionale dei Tumori, Milan under the supervision of Dr.Marco Pierotti and Dr.Paolo Radice. During this period she also dedicated a year as genetic counsellor in Cancer Genetic at the Predictive and Preventive Medicine Department, Istituto Nazionale per lo Studio e la Cura dei Tumori, Milan, under the supervision of Dr.Barbara Pasini. Paola specialized as Medical Genetist at the "Università degli Studi of Milano" in November 2001 with the experimental thesis "MLH1 promoter methylation levels analysis in sporadic and familial colorectal cancers". In 2001 she won the AIRC/FIRC "Leonino Fontana e Maria Lionello" Fellowship.

Beginning 2002 she moved to The Netherlands where she started her PhD at the Department of Human and Clinical Genetics, Leiden University Medical Center, in Leiden under the supervision of Prof.Dr.Riccardo Fodde. In September 2003 at the 4<sup>th</sup> Joint Meeting of the Leeds Castle Polyposis Group and International Collaborative Group for Hereditary Non-Polyposis Colorectal Cancer in Cleveland, US, she won the Young researcher Award in Familial Adenomatous Polyposis.

In January 2004 with Prof. Fodde research group, she moved to the Erasmus University Medical Center, at the Department of Pathology, Josephine Nefkens Institute, where she continued to work on her PhD research project which results are presented in this thesis.

From Janury 2007 she is PostDoctoral fellow at the Department of Molecular and Cell Biology, Leiden University Medical Center, in Leiden with Prof.Dr.Peter ten Dijke.



## List of publications

Nigro CL, Venesio T, Reymond A, Meroni G, Alberici P, Cainarca S, Enrico F, Stack M, Ledbetter DH, Liscia DS, Ballabio A, Carrozzo R.

The human ROX gene: genomic structure and mutation analysis in human breast tumors.

Genomics. 1998;49:275-82.

Frattini M, Balestra D, Suardi S, Oggionni M, Alberici P, Radice P, Costa A, Daidone MG, Leo E, Pilotti S, Bertario L, Pierotti MA.

Different genetic features associated with colon and rectal carcinogenesis.

Clin Cancer Res. 2004;10:4015-21.

Alberici P, Jagmohan-Changur S, De Pater E, Van Der Valk M, Smits R, Hohenstein P, Fodde R.

Smad4 haploinsufficiency in mouse models for intestinal cancer.

Oncogene. 2006;25:1841-51.

Alberici P. & Fodde, R.

The Role of APC Tumor Suppressor in Chromosomal Instability.

Genome and Disease, Genome Dynamics. 2006; 1:149-170

Janssen KP, Alberici P, Fsihi H, Gaspar C, Breukel C, Franken P, Rosty C, Abal M, El Marjou F, Smits R, Louvard D, Fodde R, Robine S.

APC and oncogenic KRAS are synergistic in enhancing Wnt signaling in intestinal tumor formation and progression.

Gastroenterology. 2006;131:1096-109.

Alberici P, de Pater E, Cardoso J, Bevelander M, Molenaar L, Jonkers J, Fodde R.

Aneuploidy arises at early stages of Apc-driven intestinal tumorigenesis and pinpoints conserved chromosomal loci of allelic imbalance between mouse and human.

Am J Pathol. 2007;170:377-87.



## **Acknowledgments**

The work described in this thesis wouldn't be possible without the contribution and help of several people: wonderful colleagues and precious collaborators that help me to carry on my PhD research and to grow as scientist.

My Dutch life started in the loved Leiden, biking against a strong wind and fighting against the winter storms...

In the department of Human and Clinical Genetics at LUMC I was introduced in the world of molecular biology by Cor and I learned how to be a "mouse doctor" from Shantie. Thank you both for teaching me your techniques and for your patience. Thanks to Vladimir with whom in the beginning I spent quite some time exploring the Cobra-FISH technique, pity we couldn't go on with those experiments. I would also like to thank the other members of the group there: Ada, Juul, Helen, and Els for creating a familiar and collaborative environment in the lab. I like to remember all the coffee breaks spent on discussing the different Dutch-Italian-Portuguese habits... I could write a next dissertation about it!

Then I moved on with my PhD... and end up in Rotterdam! With Lia, Claudia, Patrick, Joana and later on "the american" Ron (the "hard stack" of the Fodde's lab) we've got a new hospital, a new department, the one of Pathology at the JNl, a fresh brand new lab and some new colleagues to work with...In the beginning not everything was so smooth (fighting the mouse database, or multiple options for scan a simply CGH arrays...) but we quickly adapted.

With Petra, Ingrid, Jos, Mehrnaz, Law, Hang, Mieke and later on Celia and Joana M. we've created a good lab team I've always liked to work with. Ingrid has been my support, together with Patrick, for Dutch translation, Rotterdam-life gigs and we all shared some good sport-related events. Petra: we've work hard together on the PepChip project and I wish soon you would end up with some good results. I like to thank a lot our precious PA Marieke that solved for me hundreds of bureaucratic problems and questions.

All of you guys have been my "adoptive family" and I'm not sure I could make it thorough all these years without your help and supports.

## *Acknowledgments*

---

Joana, how many late hours in the lab we've cheer up together, talking about our families and nieces left in our country? Thank you for teaching me the good side of the statistical analysis and to be there as friend where I needed one. Claudia, with you I will always have an "open bill": so many times we have been working together trying to make some sense out of expression profiling data, desperately fighting the PALM or looking at each other mice experiments that I believe my PhD wouldn't be the same without you. Not only I need to thank you Claudia for the support of my scientific life, but also my personal one when, together with Joana, hosted me at your places on many occasions and helping me to shake off any "homesickness's" I might have had. As a good friend you are always there to help. That's why you end up being my paranimf (sorry!).

I like to thank my first student Emma for the experience we shared together, not always so easy but with your enthusiasm and stubbornness I think will end up having some good lab results, and I hope has been a good time for you too.

A special thanks to Mieke, you were a great help in this last year of my PhD, sorry for all the hours I've put you on the PALM...

Finally Riccardo Fodde, Professor, boss and friend: it's impossible for me to express all my gratitude to you in just two lines. You thought me how to be a good scientist and a good person. I don't know if I have met all the expectation you put on me from the beginning, but on my side, I can say that I've got much more than just what is described in this book. And I hope more will come even though I'm not in the lab anymore.

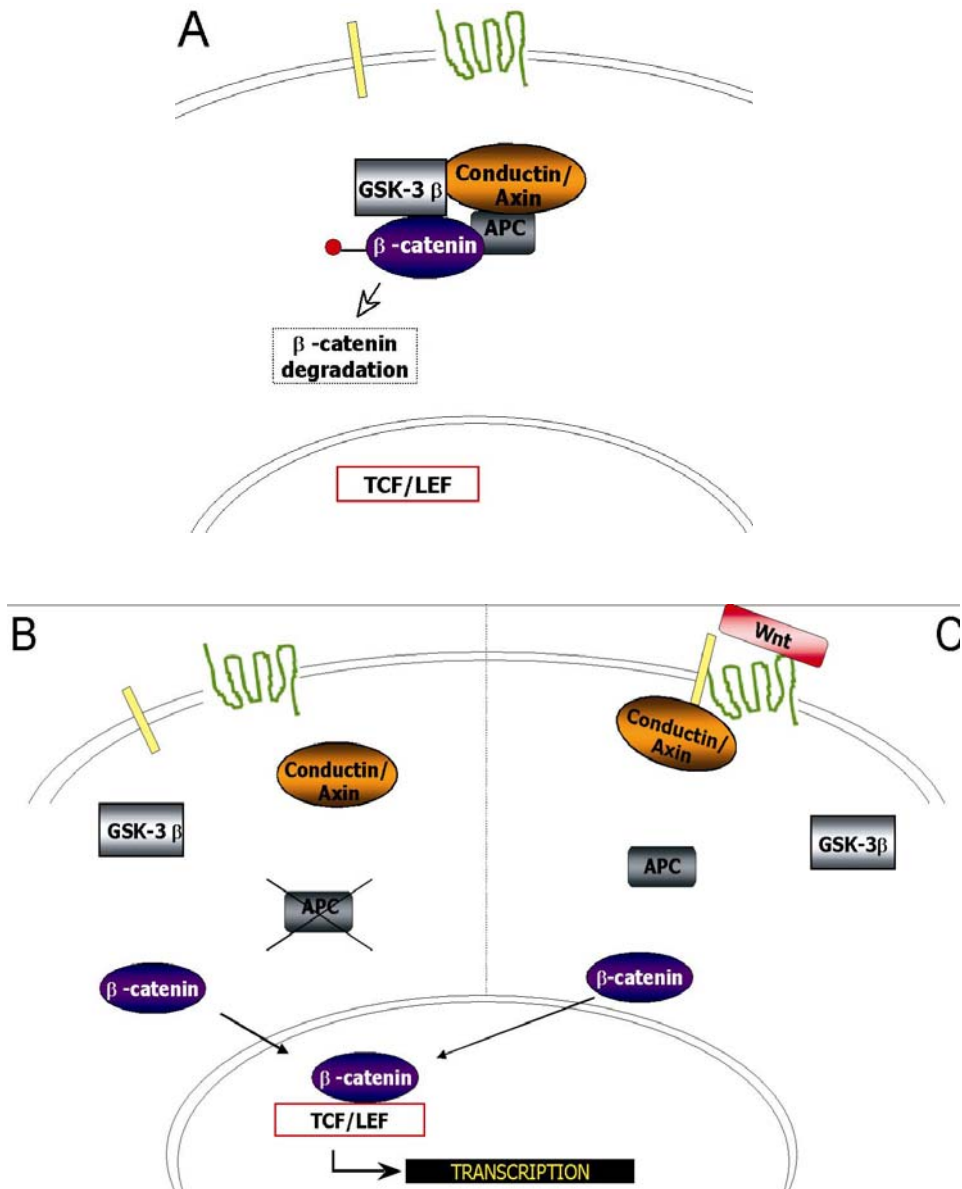
Nothing of this could be done without the infinitive support I have from my family. Grazie mamma Marisa e papà Antonio, con Gianluigi, Luisa, Mati e Pietro, perché nonostante la lontananza non sia stata facile, con il vostro amore e attenzione non mi avete mai fatto sentire sola in questa avventura. Questo titolo di Dottorato è anche merito vostro.

Marcin, my love, husband and paranimf, what could I do without you? You are the best part of my life and the family we are building up together it's a fantastic reality.

Grazie a tutti! Dank je wel, Many thanks, Obrigado, Dziekuie bardzo.

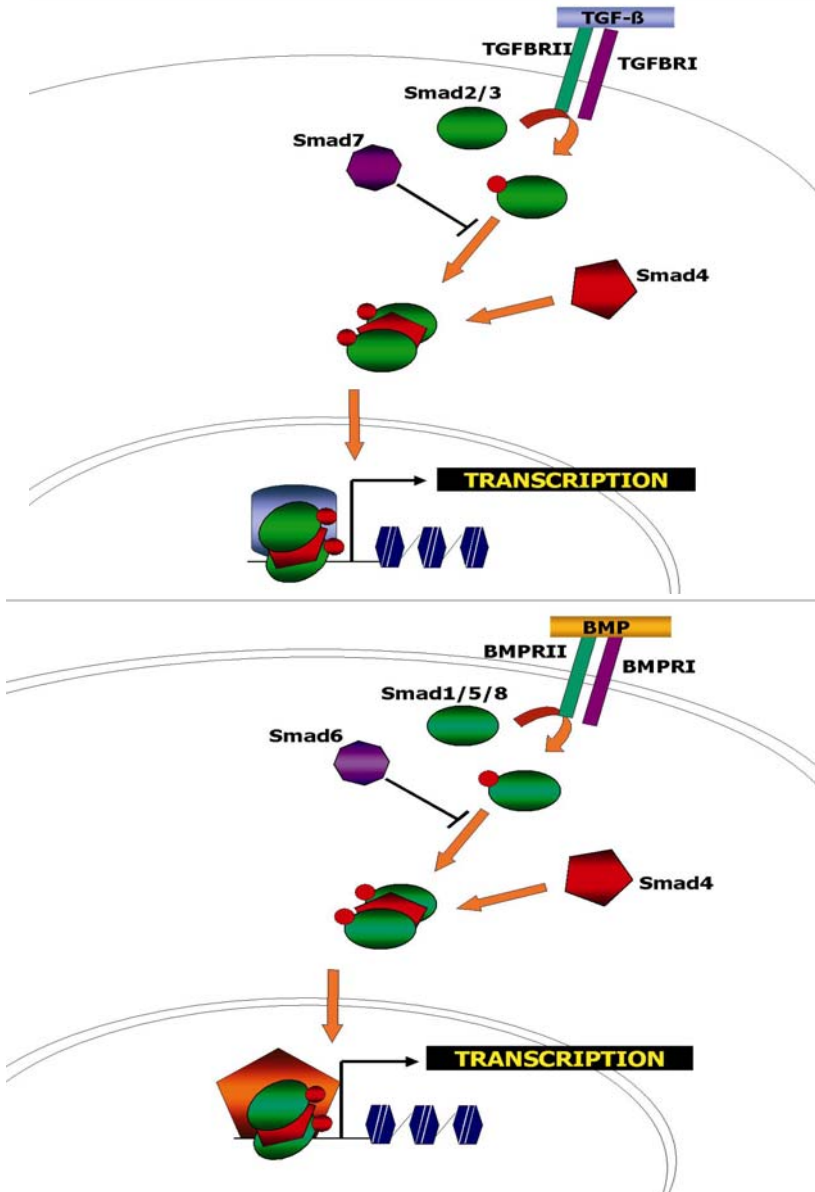
## **Appendix and Colour Figures**



Appendix 1. The WNT/ $\beta$  catenin signal transduction pathway

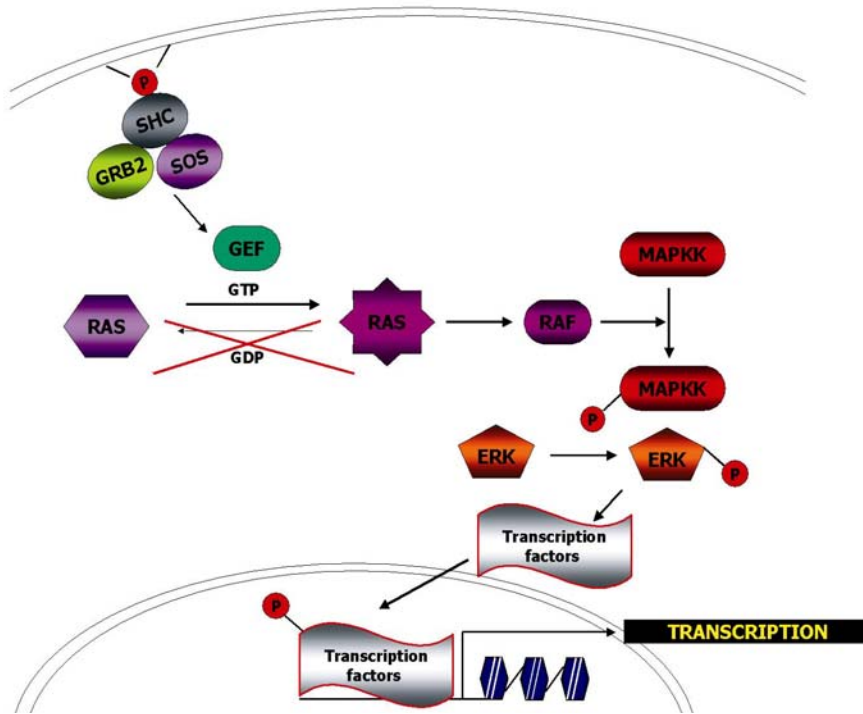
A schematic representation of the canonical Wnt/ $\beta$ -catenin signaling pathway. (A) In the absence of Wnt ligand,  $\beta$ -catenin is earmarked for proteolytic degradation by the destruction complex. (B) Upon loss of APC function, or (C) in the presence of Wnt ligand,  $\beta$ -catenin accumulates in the cytoplasm and eventually translocates in the nucleus to act as transcriptional co-activator with T-cell factor/lymphoid enhancer (TCF/LEF) family.

## Appendix 2. The TGF- $\beta$ /BMP signal transduction pathways



A schematic representation of the TGF- $\beta$  (upper panel) and BMP (lower panel) signaling pathways. The specific ligand (TGF- $\beta$  or BMP) binds to the receptor type 2 (TGFBR2) which complexes with the receptor type 1 (TGFBR1) thus triggering its phosphorylation. The activated receptor is responsible for the phosphorylation of the specific R-Smads, which then bind the co-Smad (Smad4). The heterodimer translocates to the nucleus where it induces transcription of specific downstream target genes.

### Appendix 3. The RAS/RTK signal transduction pathway



A schematic representation of the RAS/RTK signaling pathway. Activation of growth factor receptors in the cell membrane activates RAS through GDP-GTP exchange. With the following cascade of phosphorylation of the downstream members of the pathway MAPK and ERK, the RAS signaling results in the activation of factors that regulate the transcription of target genes.

From Chapter 1 Introduction:

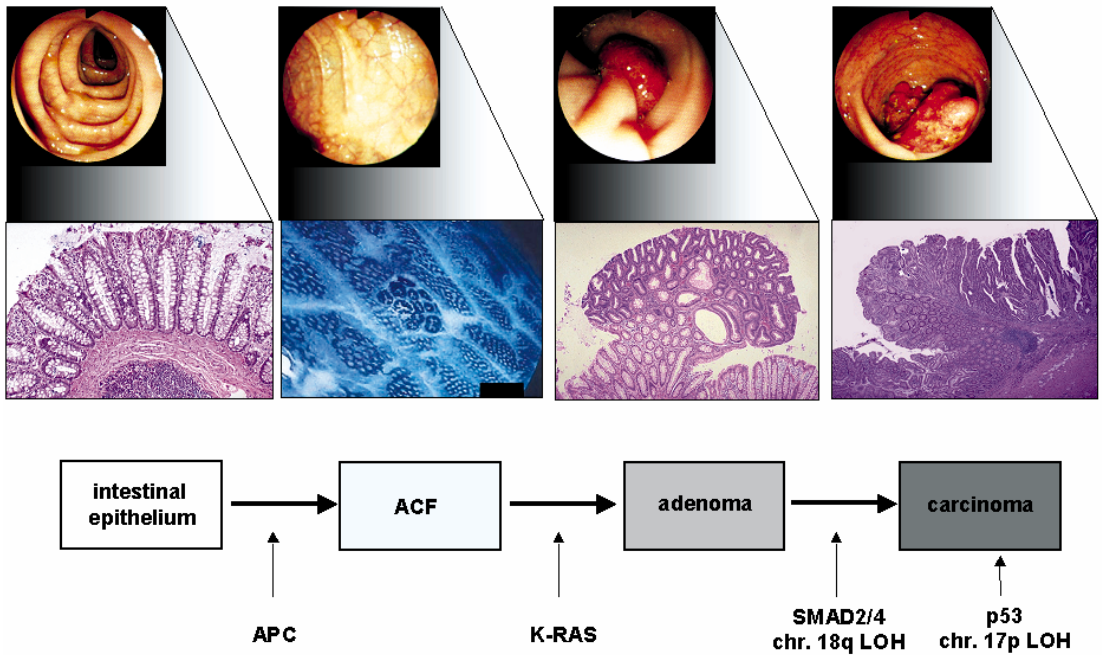


**Figure 1.** The adenoma-carcinoma sequence: a stepwise progression from normal epithelium to carcinoma due to a series of genetic changes. Macro- and microscopical representations of the progression changes are depicted. See text for details.

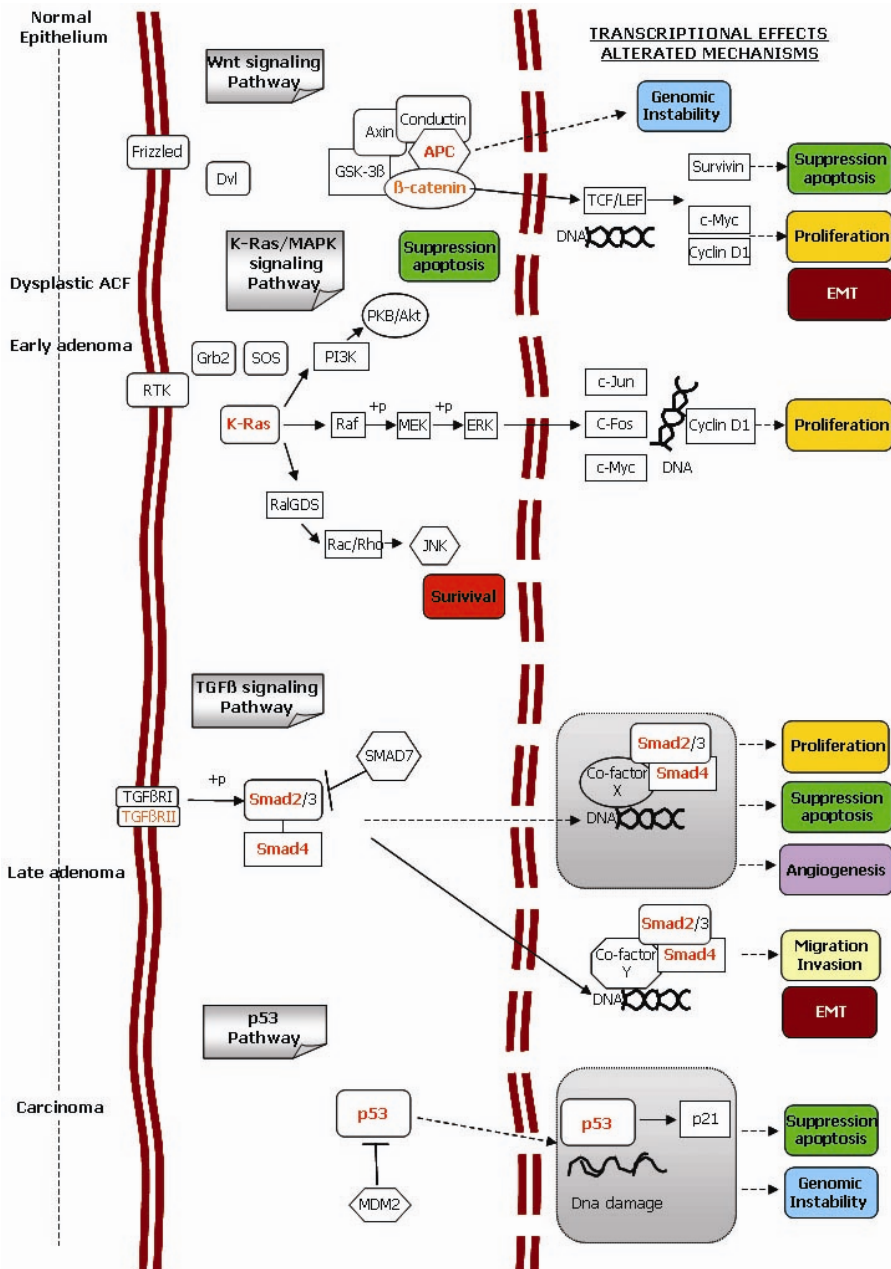


**Figure 2.** Schematic representation of the accumulation of alterations in different pathways along the adenoma-carcinoma sequence. In red are shown the genes frequently mutated in CRC. The different cellular alterations resulting from the accumulations of these signaling defects are listed in the right column.

**From Chapter 1.4:**

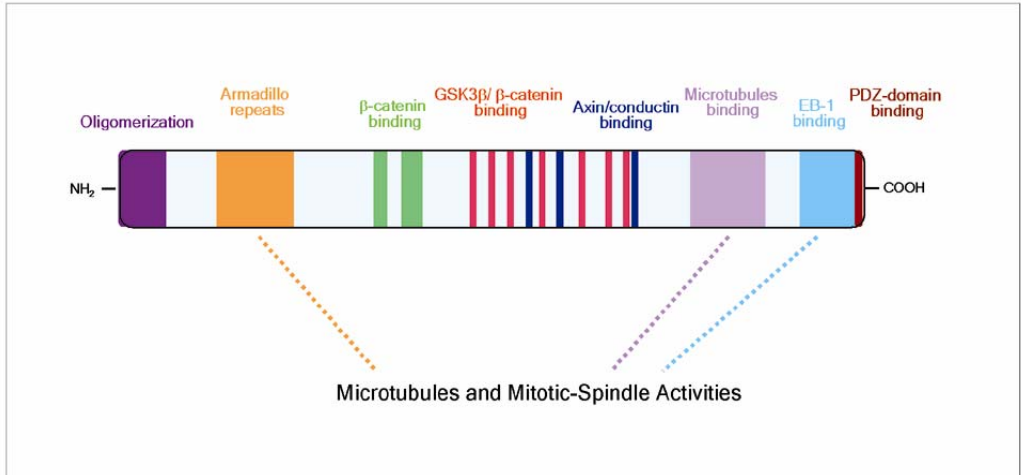


**Figure 1.** Schematic representation of the APC protein with its functional motifs.

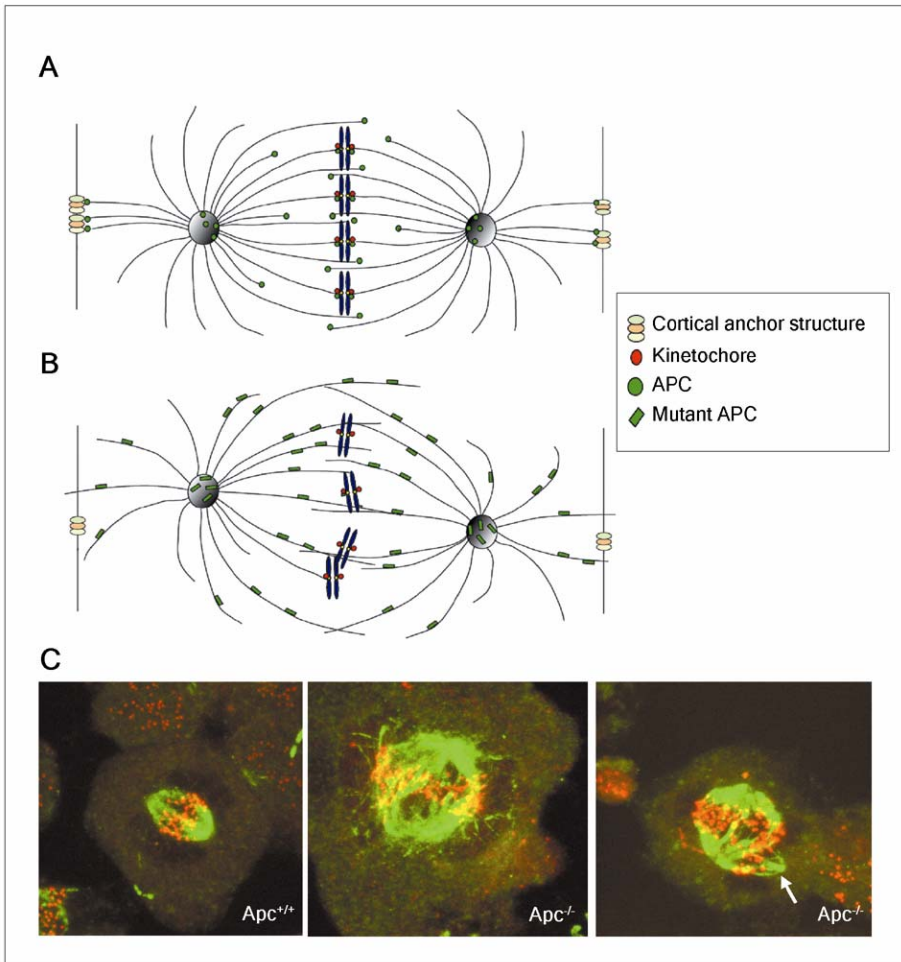


**Figure 2.** Mitotic spindle defects in *Apc* mutant cells. In (a) a representation of a normal mitotic figure with localization of APC at the kinetochores and at the plus-ends of the microtubules is shown. The hypothetical binding of APC on astral microtubules to the cortical anchor structure allows keeping the mitotic spindle parallel to the epithelial plane. In (b) there is represented a mitosis in an APC mutant cell with defects in the spindle organization and the failure of the APC binding to the kinetochores and to the cortical anchor structure. In (c) examples of spindles formed in *Apc* wild type and mutant ES cell lines are shown. In green the  $\gamma$ -tubulin staining marks the spindle, whereas in red the CREST/kinetochores structure is stained. Note in the *Apc* mutants the spindle abnormalities with most of the microtubules projecting in a chaotic manner in the cytoplasm. In the right *Apc*<sup>-/-</sup> picture, the white arrow designates an extra centrosome.

From Chapter 2:

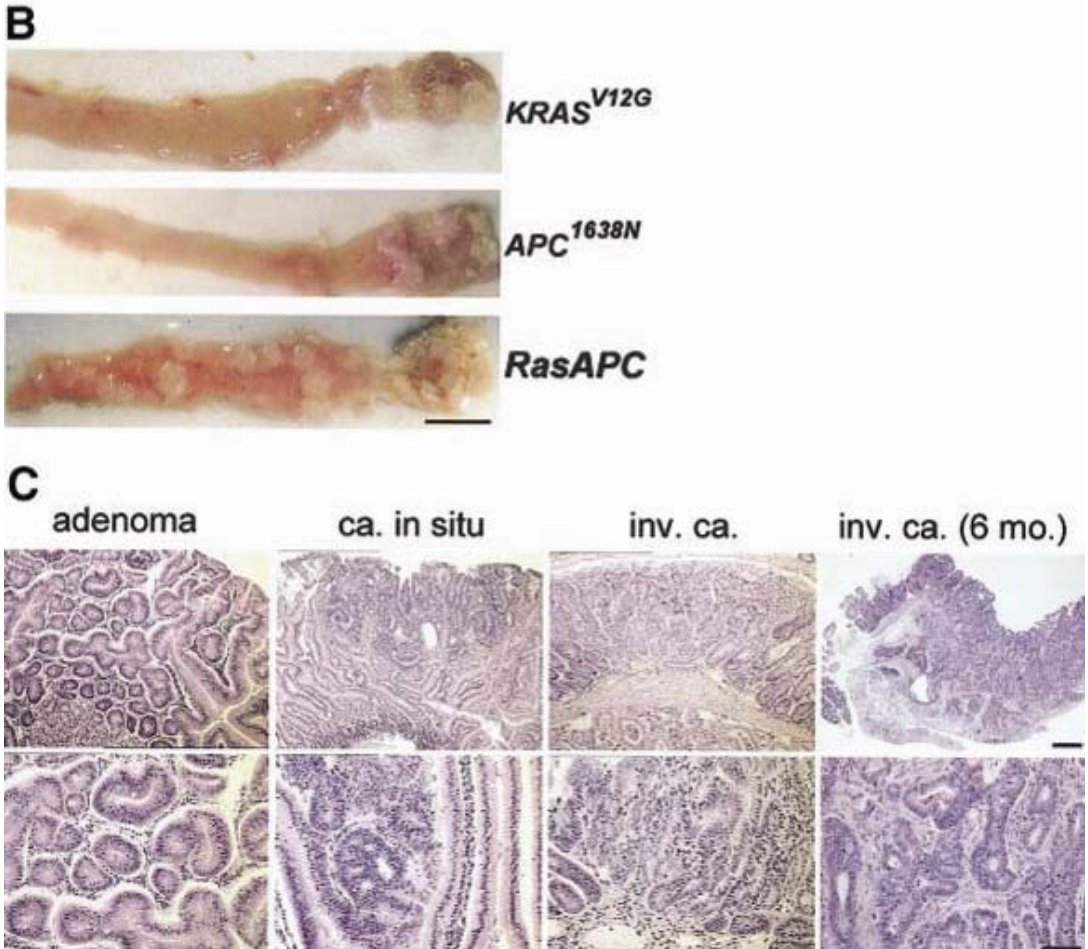


**Figure 1, Panel B and C.**

Increased tumor multiplicity and progression in  $KRAS^{V12G}/Apc^{+/1638N}$  mice (B) Macroscopic view of longitudinally dissected small intestinal tissue specimens representative for 6 months of age. No tumors can be observed in  $KRAS^{V12G}$  mice at this age, and few (2–4) lesions in  $Apc^{+/1638N}$  mice.  $KRAS^{V12G}/Apc^{+/1638N}$  ( $RasAPC$ ) mice show abundant, multiple lesions throughout the upper GI tract. Scale bar = 1 cm. (C) H&E stained sections from  $KRAS^{V12G}/Apc^{+/1638N}$  animals. Left to right: benign adenoma at 3.5 months; in situ carcinoma at 3.5 months; invasive adenocarcinoma at 3.5 months; invasive carcinoma at 6 months. Scale bars = 200  $\mu$ m (upper row) and 50  $\mu$ m (lower row).

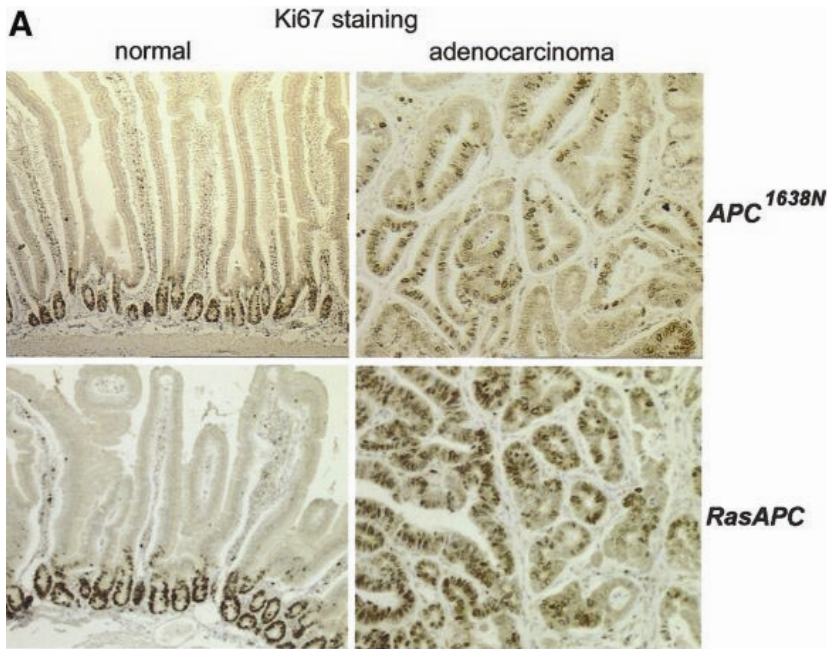


**Figure 4, Panel A.** Proliferation and apoptosis rates in tumors from  $KRAS^{V12G}/Apc^{+/1638N}$  mice. (A) Proliferation is increased in tumors from  $KRAS^{V12G}/Apc^{+/1638N}$  mice (bottom) when compared with  $Apc^{+/1638N}$  littermates (top) as shown by immunohistochemical detection of the proliferation marker Ki67.

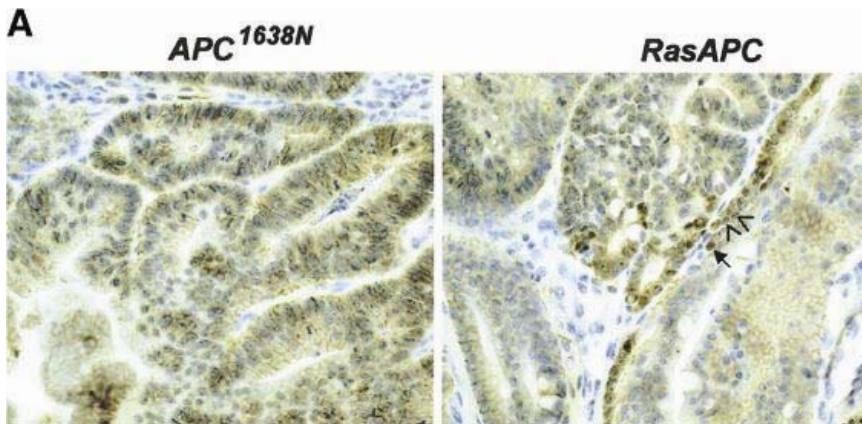


**Figure 5, Panel A.** Increase in nuclear  $\beta$ -catenin accumulation in tumors from  $KRAS^{V12G}/Apc^{+/1638N}$  mice. (A) Tumor sections from  $KRAS^{V12G}/Apc^{+/1638N}$  mice (right panel) show increased nuclear  $\beta$ -catenin compared with tumors from  $Apc^{+/1638N}$  animals (left panel). All tumor cells with strong (arrow) and mild (arrowheads) nuclear  $\beta$ -catenin staining were scored (see Results section).

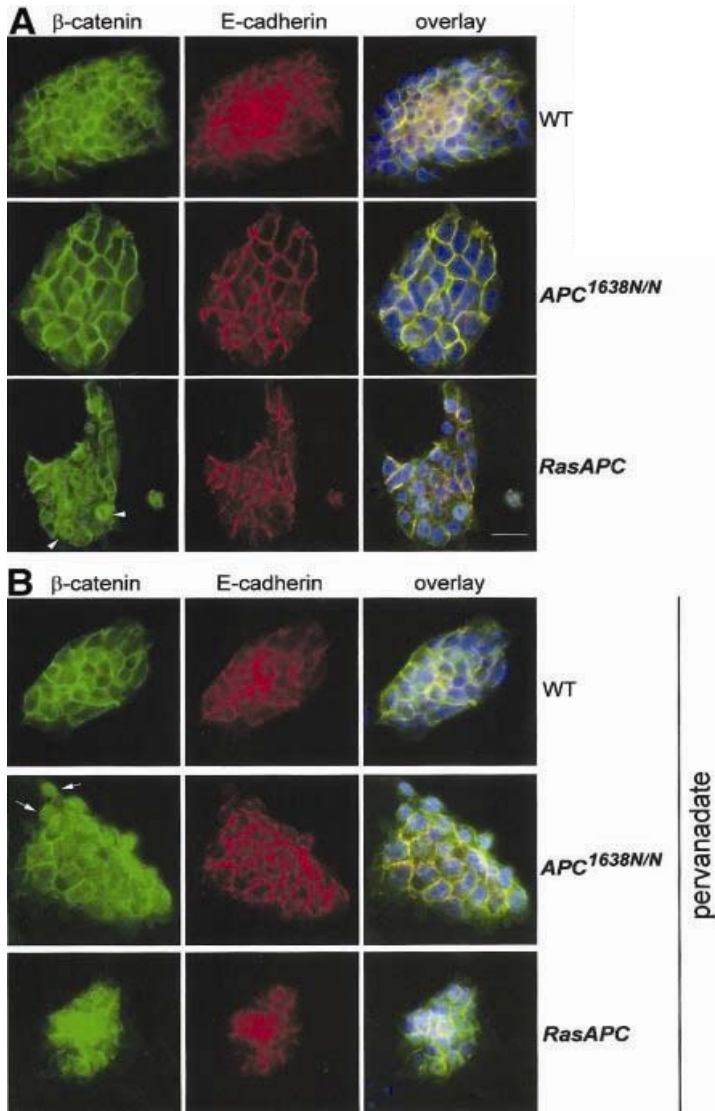


**Figure 6.** Increase in nuclear  $\beta$ -catenin accumulation and Wnt/ $\beta$ -catenin signaling in *Apc*-mutant ES cells expressing  $KRAS^{V12G}$ . (A) Confocal microscopy analysis of  $\beta$ -catenin and E-cadherin intracellular distribution in wild-type E14 (WT),  $Apc^{1638N/1638N}$  (A),  $Apc^{+/+}/KRAS^{V12G}$  (R), and  $Apc^{1638N/1638N}/KRAS^{V12G}$  (RA) ES cells. Note: nuclear accumulation of  $\beta$ -catenin in compound mutant cells (arrowheads), in addition to the normal localization at cell-cell contact sites. Overlay with DAPI (nuclear stain) to indicate the position of the nuclei. Yellow in the overlay indicates colocalization of  $\beta$ -catenin and E-cadherin at the cell-cell junctions, demonstrating the presence of  $\beta$ -catenin in adhesion complexes. (B) Pervanadate treatment induces  $\beta$ -catenin nuclear accumulation in *Apc*-mutant but not in wild-type ES cells. Nuclear  $\beta$ -catenin (green, arrows) is visible in  $Apc^{1638N/1638N}$  (A) and  $Apc^{1638N/1638N}/KRAS^{V12G}$  (RA) ES cells but not in wild-type cells.

## From Chapter 3:

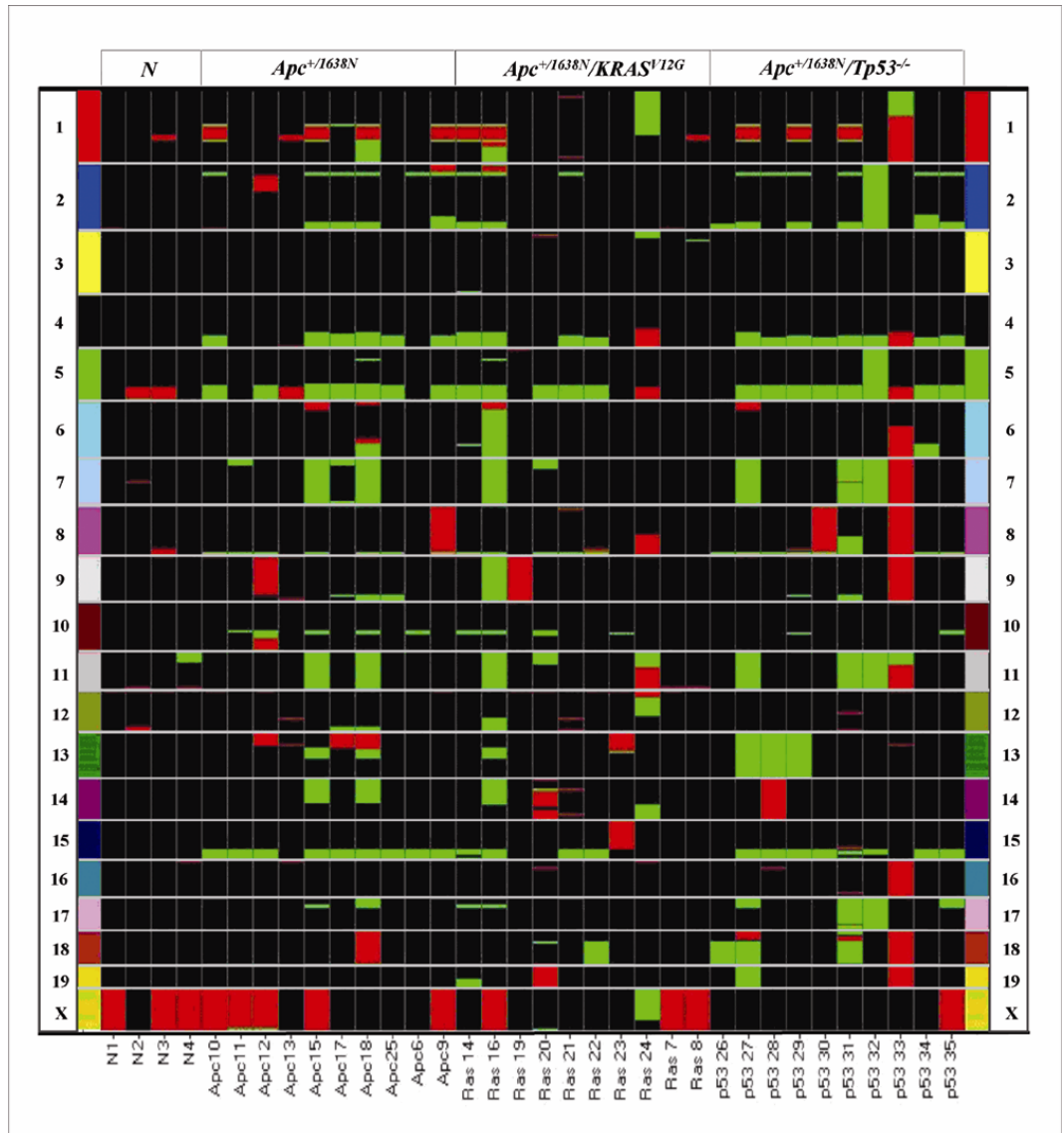


**Figure 1.** Heat map visualization of the CGH results for the three groups of tumors analyzed in the present study. After normalization and two-log smoothing of the array CGH ratios from the 30 tumor samples and four normal intestinal epithelia, the data were loaded onto SpotFire Decision Site 8.1 to obtain the heat map here represented. Data are ordered in the X bar according to the sample genotypes as normal (*N*), *Apc*<sup>+/<sub>1638N</sub> (*Apc*), *Apc*<sup>+/<sub>1638N</sub>/*KRAS*<sup>V12G</sup> (*Ras*), and *Apc*<sup>+/<sub>1638N</sub>/*TP53*<sup>-/-</sup> (*p53*), and in the Y bar according to the chromosome and Mb position of the BAC clones (color code at both sides of the heat map). The color code of the samples indicates BAC copy number changes: green, loss; red, gain; and black, no change.</sup></sup></sup>

From Chapter 4:

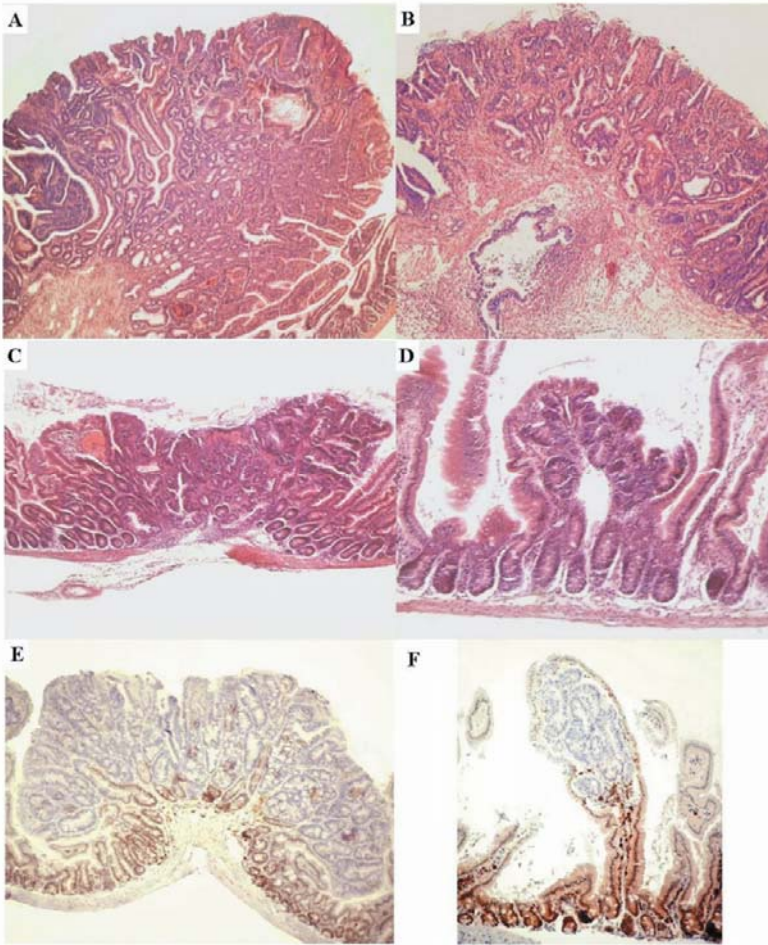


**Figure 1** Histopathology and immunohistochemical analysis of *Smad4*<sup>E6sad</sup> small intestinal polyps at different ages and progression stages. (a) Polyp originated in the gastric epithelium from 12-month-old *Smad4*<sup>+E6sad</sup> animal. Inset: higher magnification of hyperplastic region. Note the gastric epithelium (HE). (b) Advanced polyp from 15-month-old *Smad4*<sup>+E6sad</sup> mouse showing areas of frank dysplasia. Inset: higher magnification of dysplastic region (HE). (c) Smad4 IHC analysis of normal small intestinal epithelium from a *Smad4*<sup>+E6sad</sup> animal shows nuclear and cytoplasmatic staining with crypt-villus decreasing gradient of expression. The aspecific staining in the lamina propria is due to mouse IgG cross-reaction from the secondary antibody. (d) Smad4 IHC analysis of tumor from 12-month-old *Smad4*<sup>+E6sad</sup> mouse shows positive staining of tumor cells. Staining of stromal cells is due to mouse IgG cross-reaction from the secondary antibody. (e) Smad4 IHC analysis of tumor from 15-month-old *Smad4*<sup>+E6sad</sup> mouse shows an area of negatively stained parenchymal cells within an otherwise positive tumor. (f)  $\beta$  Catenin IHC analysis of tumor from 15-month-old *Smad4*<sup>+E6sad</sup> animal. The more dysplastic area of the lesion mainly shows membranous staining.

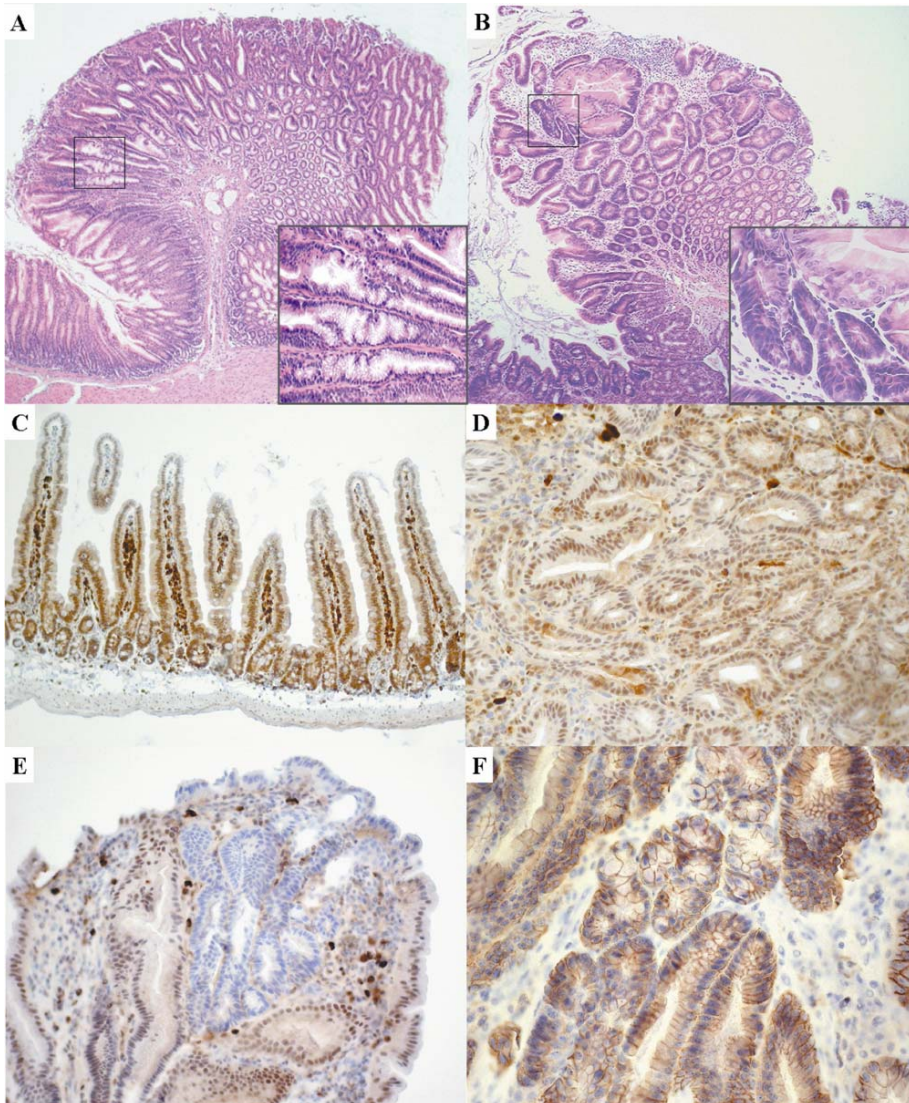


**Figure 3.** Histopathology and IHC analysis of intestinal tumors from compound  $Apc^{+/1638N}/Smad4^{+/E6sad}$ . (a) A typical dysplastic adenoma observed in TAS animals (HE staining). (b) An example of adenocarcinoma with extensive submucosal invasion from a TAS mouse (HE). (c) Sessile villous adenoma from a CAS mouse with areas of severe dysplasia and cystic formation (HE). (d) A nascent lesion or microadenoma observed in the duodenum of a CAS animal (HE). (e) Smad4 IHC analysis of a CAS tumor shows negative staining, thus indicating LOH of the wild-type allele. (f) Smad4 IHC analysis of a small microadenoma from the same CAS mouse also reveals LOH of the wild-type allele in the nascent lesion. Note the positively stained cells of the normal epithelial lining surrounding the dysplastic area.

From Chapter 5:

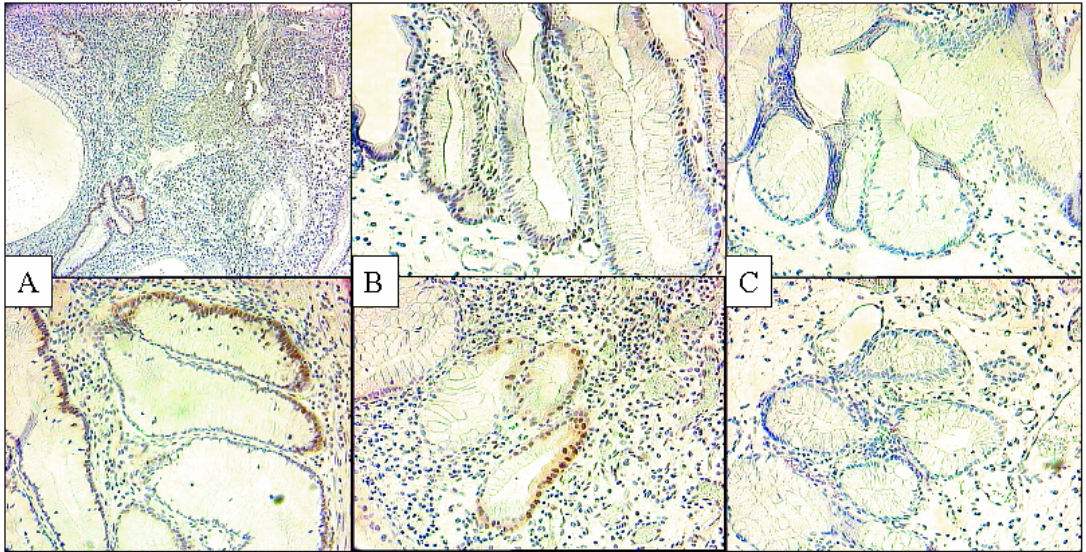


**Figure 3.** Immunohistochemical analysis of SMAD4 protein expression performed on polyps from three unrelated Familial Juvenile Polyposis patients with established SMAD4 germline mutation. A. Polyp with SMAD4 nuclear staining. B. Polyp with heterogeneous SMAD4 expression pattern with patches of positively and negatively staining tumor cells. C. SMAD4 negative juvenile polyp.

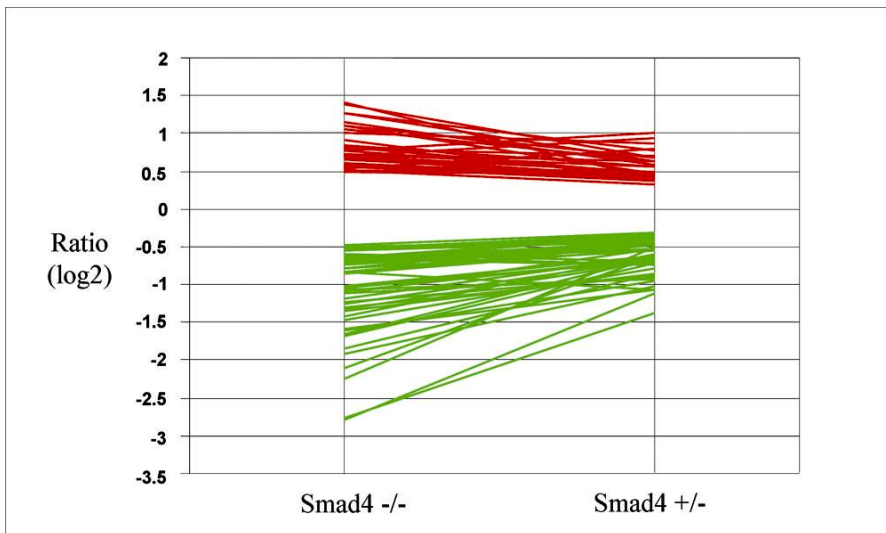


**Figure 4.** Expression profiling analysis of the subset of 79 genes (corresponding to 88 Affymetrix probes) found to be differentially expressed in both *Smad4*<sup>+/E6sad</sup> and *Smad4*<sup>E6sad/E6sad</sup> ES cells. The fold changes are represented as (log<sub>2</sub>) ratio values.

## From Chapter 6 Discussion:

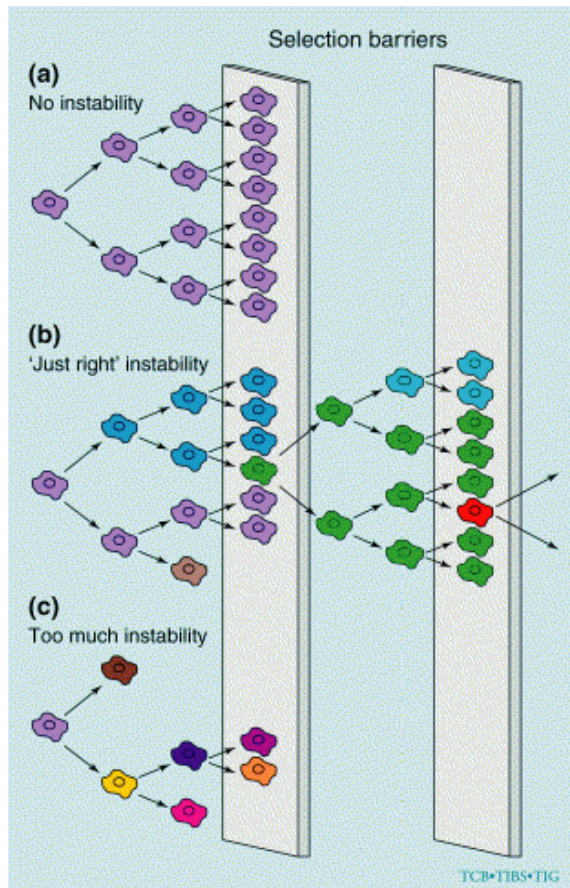


**Figure 1.** Overcoming selection barriers during tumor formation and progression. In normal cells (a), the intrinsic rate of instability is low. As none of the cells contains the genetic alteration required to overcome the selection barriers, tumour formation is prevented. Tumour cell precursors (b) are characterized by an increased level of genetic instability. In this case, the broad cellular heterogeneity virtually guarantees that at least one of the cells contains the requisite genetic alteration to overcome the selection barrier and proceed in tumour progression. If the level of genetic instability is too high (c), the damage accumulated from cell division rapidly rises above the threshold for viability – apoptotic pathways are activated and cell death ensues. At the level of the cellular population, this leads to extinction. Not enough cells reach the first selection barrier to select a malignant clone effectively.

Reprinted from "Genetic instability and darwinian selection" Trends in Cell Biology Vol 9 (Dec 12) 1999 Cahill DP, Kinzler KW, Vogelstein with permission from Elsevier.

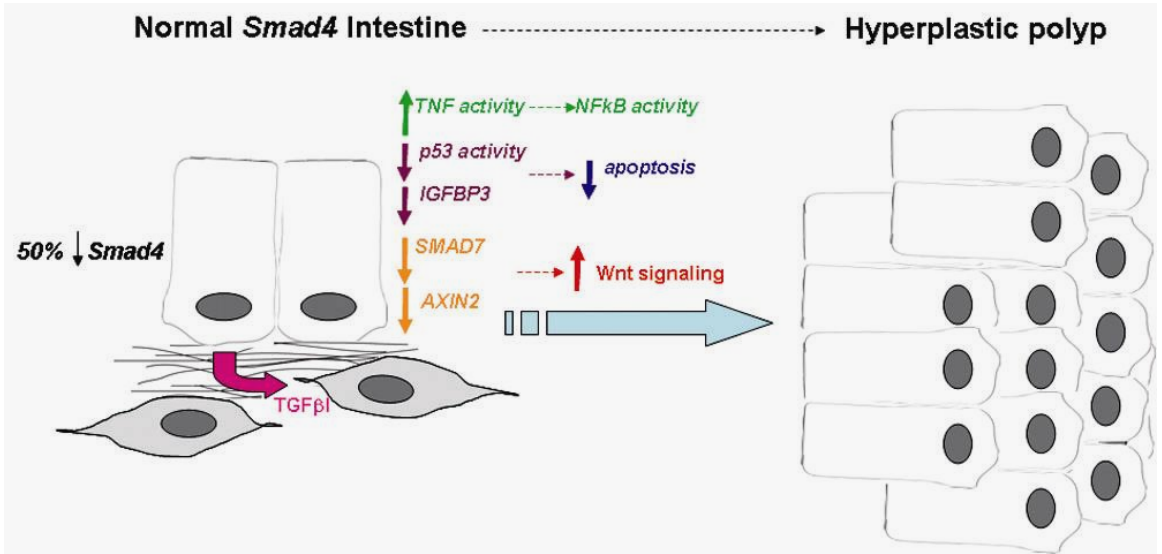


**Figure 3.** Hypothetical model for the molecular and cellular consequences of *Smad4* haploinsufficiency on intestinal homeostasis and cancer onset.

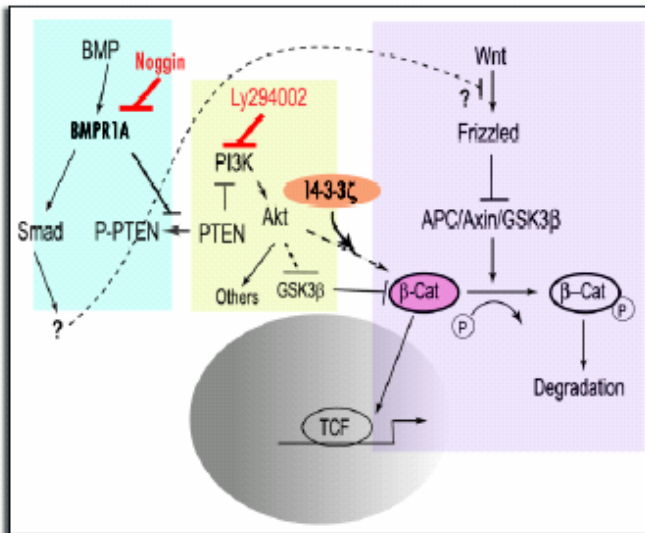


**Figure 6.** Illustration of the regulatory cross-talk network between BMP and Wnt signalings mediated by PTEN-PI3K pathway that controls the stem cell behaviour and the transition between quiescent and activated states. This network allows a balanced control of stem cell-renewal through a convergent downstream component. From Bridging the BMP and Wnt pathways by PI3 kinase/Akt and 14-3-3ζ. By Qian T. et al Cell Cycle. 2005 Feb;4(2):215-6. Reproduced with permission.